Initiation Of Excitation Waves

Thesis submitted in accordance with the requirements of the
University of Liverpool for the degree of Doctor in Philosophy

by

Ibrahim Idris

March 2008

Abstract

The thesis considers analytical approaches to the problem of initiation of excitation waves. An excitation wave is a threshold phenomenon. If the initial perturbation is below the threshold, it decays; if it is large enough, it triggers propagation of a wave, and then the parameters of the generated wave do not depend on the details of the initial conditions.

The problem of initiation of excitation waves is by necessity nonlinear, non-stationary and spatially extended with at least one spatial dimension. These factors make the problem very complicated. There are no known exact analytical, or even good asymptotic solutions to this kind of problem in any model, and the practical studies rely on numerical simulations.

In this thesis, we develop approaches to this problem based on some asymptotic ideas, but applied in the situation where the "small parameters" of those methods are not very small. Although results obtained by such methods are not very accurate, they still can be useful if they give qualitatively correct answers in a compact analytical form; such answers can give analytical insights which are impossible or very difficult to gain from numerical simulations.

We develop the approaches using, as examples, two simplified models describing fast stages of excitation process:

- Zeldovich-Frank-Kamenetskii (ZFK) equation, which is the fast (activator) subsystem of the FitzHugh-Nagumo (FHN) "base model" of excitable media, and

- Biktashev (2002) [8] front model, which is a caricature simplification of the fast subsystem of a typical detailed ionic model of cardiac excitation waves.

For these models, we consider two different approaches:

- Galerkin-style approximation, where the solution is sought for in a pre-determined analytical form ("ansatz") depending on a few parameters, and then the evolution equation for these parameters are obtained by minimizing the norm of a residual of the partial differential equation (PDE) system,

- linearization of the threshold hyper-surface in the functional space, described via linearization of the PDE system on an appropriately chosen solution on that surface (a "critical solution").

Publications and Presentations

Some of the materials in Chapter 2 and most of the materials in Chapter 3 are based on the following publications:

1. I. Idris, R. D. Simitev and V. N. Biktashev. "Using novel simplified models of excitation for analytic description of initiation propagation and blockage of excitation waves". In *IEEE Computers in Cardiology*, volume 33, pages 213 - 217, Valencia, Spain, 2006.

2. I. Idris and V. N. Biktashev. "Critical fronts in initiation of excitation waves". *Phys. Rev. E.*, 76(2): 021906-1 - 021906-6, 2007.

The following presentations have been given based on some of the materials in this thesis:

1. "Modelling initiation of propagation in excitable media", I. Idris, Annual Applied Maths. PhD symposium, University of Liverpool, May 23rd, 2006.

2. "Initiation and Block Excitation Waves: Some Analytical Insights", V. N. Biktashev and the Liverpool Cardiology group, Cardiac Dynamics miniprogram, Kavli Institute of Theoretical Physics, University of California in Santa Barbara, California, USA, July 17th, 2006.

3. "Simplified Models for Initiation and Block of Excitation Waves", V. N. Biktashev, I. Idris and R. D. Simitev, Computers in Cardiology, Valencia, Spain, Sept. 19th, 2006.

4. "Modelling excitation waves in heart muscle", V. N. Biktashev, the Liverpool Maths. Cardiology group, Liverpool Biocomplexity workshop, Liverpool, Nov. 16th, 2006.

5. "Asymptotic approaches to cardiac excitation models", V. N. Biktashev, I. V. Biktasheva, I. Idris, R. D. Simitev and R. Suckley, "Complex nonlinear processes in chemistry and biology", Institute of Theoretical Physics at Berlin University of Technology, Berlin, Germany. Feb. 2nd, 2007.

6. "Asymptotic approaches to cardiac excitation models", V. N. Biktashev, I. V. Biktasheva, I. Idris, R. D. Simitev and R. Suckley, Applied Mathematics seminar, University of Leicester, Feb. 22nd, 2007.

7. "Liverpool mathematical cardiology group: work in progress", V. N. Biktashev, I. V. Biktasheva, I. Idris, A. J. Foulkes, S. W. Morgan, B. N. Vasiev and G. V. Bordyugov, BIOSIM: Engineering Virtual Cardiac Tissues, Manchester University, March 16th, 2007.

8. "Non-standard asymptotics and analytical approaches to excitation waves in heart", V. N. Biktashev and the Liverpool Mathematical Cardiology Group, workshop, "Nonlinear dynamics in excitable media", Ghent, Belgium, April 16th, 2007.

9. "Critical fronts in initiation of excitation waves", I. Idris and V. N. Biktashev, The 49th BAMC, Bristol, April 17th-19th, 2007.

10. "Critical fronts and initiation of waves in ionic models of excitation", V. N. Biktashev and I. Idris, ESF Exploratory Workshop on European Heart Modelling and Supporting Technology, Oxford University, May 17th, 2007.

11. "Critical fronts in initiation of excitation waves", I. Idris and V. N. Biktashev, Annual Applied Maths. PhD symposium, University of Liverpool, May 22nd, 2007.

12. "Asymptotics of cardiac excitability equations", V. N. Biktashev, I. V. Biktasheva, I. Idris, R. D. Simitev and R. Suckley, Oxford Maths. Biology and Ecology seminar, Oxford university, Feb. 1st, 2008.

13. "Initiation of excitation waves", V. N. Biktashev and I. Idris, Liverpool Applied Maths. seminar, April 9th, 2008.

Contents

List of Tables

List of Figures

Declaration

No part of the work referred to in this thesis have been submitted in support of an application for another degree or qualification of this or any other institution of learning. However, some part of the materials contained herein have been previously published.

Acknowledgment

I wish to express my deep and sincere gratitude and appreciation to my supervisor Prof. V. N. Biktashev for the sustained guidance and motivation throughout the course of my study here in University of Liverpool, U. K. This work would not have been possible without his extraordinary degree of understanding, patience and support. I will forever remain grateful to him for introducing and leading me into the world of programming (C, Perl, Unix, Maple, Gnuplot, LATEX, Far).

I acknowledge all the support accorded me by my sponsor, Bayero University, Kano. I cannot thank you enough for offering me this rare and privileged opportunity. In particular, my special appreciation goes to Prof. M. Y. Bello for all his support and encouragement. I must express my deep appreciation to The John D. and Catherine T. MacArthur Foundation for the grant. I also have to acknowledge some partial support that I received from EPSRC and for that I am indeed very grateful.

I have to thank Dr Irina for all her words of advice and encouragement especially her unique, interesting and helpful ways of explaining difficult concepts. I can never forget the consultations I enjoyed from Dr Radostin, Dr Grigory and Dr Bakhti. They have been very helpful and accommodating personalities and so they will always be remembered. To Andy and Stuart I very much appreciated and enjoyed their friendly and very accommodating company. It is interesting having such wonderful pals.

Special thanks must go to all the staff members of the department for their friendliness and for providing a conducive atmosphere for learning and research. In particular, I am very grateful to my second supervisor, Prof. Bowers for all his advice and guidance. Many special thanks and appreciation go to Prof. Movchan (Sasha) whose Modules I quite enjoyed and immensely benefited from. I must also acknowledge all the support received from Prof. Giblin, especially for the software (Micrografx Designer) that I used for some of the sketches in this thesis. I appreciated the informal discussions I had with Dr Andre in the course of this work.

The indirect support that I enjoyed from Prof. Starmer via his web page in the early stages of my research work and later through his Scholarpedia articles, have played a significant role in the direction of this work. I am also grateful for the nice pictures on the match head chemistry he sent to me.

Finally, I wish to thank my family, friends and colleagues for all their support, messages of good will and prayers.

Dedication

This work is dedicated to my mum *Hajara Muhammad Tabi* (of blessed memory) and my dad *Idris Ibrahim*. This great achievement culminated several years of your efforts and support and is as well a testimony to your much cherished foresight.

Chapter 1

Introduction

1.1 Overview

In this work, we seek to study systems of partial differential equations (PDEs) that describe the electrical behaviour in nerve cells and cardiac tissues. In general, it is not always easy to obtain explicit analytical solutions to problems that involve PDEs. We will resort to numerical or qualitative techniques as appropriate where analytical ones are not possible or where they are going to be extremely difficult to obtain. Even where analytical solutions are found we will use numerical simulations to validate them.

In this chapter, we present an overview of the whole work, then give a brief exposition on excitable media and follow it up with some definitions and descriptions of some concepts and terminologies to be used throughout the entire work. We will end the chapter by stating the main objective of our work.

Chapter two is where we review the literature which starts with the continuation of the description of some concepts and terminologies. We then present, by way of exposition, some works, procedures which are used to tackle the problems we seek to address. Here, we analyse the excitability properties of the celebrated Hodgkin-Huxley (HH) model [44] and that of its descendants, the FitzHugh-Nagumo (FHN) system [33, 67, 74] and the simplified front model due to Biktashev [8]. The chapter is then closed with a review of some analytical approaches used to describe initiation of propagation waves: the projected dynamics to class of Gaussian ansatz by Neu and his co-workers [68] and the Biot-Mornev procedure [64] which is a variational method of computation of non-stationary processes of heat and diffusion mass transfer in regions of complex shape.

The major aspect of our work starts in chapter three where we formulate, solve and analyse the initiation problem for the three types of equations that we consider. That is, the Zeldovich-Frank-Kamenetskii (ZFK) equation, FHN system and the simplified

cardiac front model. We present and discuss some important numerical results which are crucial to initiation of propagation waves in excitable media.

In chapter four some variational approximation procedures are used to solve and analyse initiation problem in the ZFK equation and the front equations, and some numerical as well as qualitative results are then presented.

Chapter five is where we present the ignition criteria for both the ZFK equation and the front equations by deriving explicit analytical expressions for the threshold curves which then serve as the analytical initiation criteria for the two types of equations.

Finally, in chapter six we draw conclusions for our work and outline directions for future studies.

1.2   Background

Historically, in its original sense, *excitability* (i.e., the magnitude of perturbation required to initiate a propagating wave [48, 90]) refers to the property of living organisms (or of their constituent cells) to respond strongly to the action of a relatively weak external stimulus [103, 90, 92, 102]. A typical example of excitability is the formation of spike of transmembrane potential (action potential) by a cardiac cell, induced by a short depolarizing (becoming less negative) electrical perturbation (disturbance) of a resting state. Normally, the shape of the generated action potential does not depend on the perturbation strength provided that the perturbation exceeds a certain threshold value (all-or-nothing principle as is generally known in the literature). After the generation of this strong response, the system returns to its initial resting state. A subsequent excitation can be generated after the passage of a suitable length of time, called the *refractory period*. For another explanation of the concept of excitability, see [93, 18].

An *excitable medium*, by definition is a dynamical system distributed continuously in space, each elementary segment of which possesses the property of excitability [103, 94, 60, 59, 27]. The neighbouring segments of an excitable medium interact with each other via diffusion-like local transport processes. It is possible for excitation to be passed from one segment to another by means of local coupling. Thus, an excitable medium is able to support propagation of undamped solitary excitation waves, as well as wave trains.

Many cells such as neurons and muscle cells make use of the membrane potential as a signal, and thus, the operation of the nervous system and the contraction of a muscle

(just two of the numerous examples that abound) are dependent on the formation and propagation of electrical signals. The division of all cell types into two broad classes, *excitable* and *non-excitable*, aids in the understanding and the analysis of electrical signaling in cells.

Many cells maintain a stable equilibrium potential; for some, if a current is applied to the cell for a short time period, the potential returns directly to its equilibrium value after the removal of the applied current. The cells with this behavior are called *non-excitable*. For example, the epithelial cells that line the wall of the gut and the photoreceptor (a photosensitive cell) found in the retina of vertebrate eyes. Meanwhile, there are cells for which, if the applied current is strong enough, the membrane potential undergoes a large excursion, called an *action potential*, before eventually returning to rest. Such type of cells are called *excitable*. Examples for excitable cells include cardiac cells, smooth and skeletal muscle cells, secretory cells and most neurons [49]. Excitable media, in other words, are active (*nonlinear*) media as compared to passive (*linear*) media (for example, electromagnetic waves in a vacuum or sound waves [85]).

There are many examples of excitability that occur in nature and an example of one of the simplest of such *excitable systems* is a household match. The chemical components of the match head are stable to small fluctuations in temperature, but a sufficiently large temperature change due to the friction between the head and an abrasive surface, triggers the abrupt oxidation of these chemicals with a dramatic release of heat and light. In other words, the amount of pressure exerted during the striking of the match head against a rough surface plays a significant role, where a gentle pressure results in little friction and therefore occasionally the small spark generated is self-extinguished. In contrast, greater pressure causes more friction which produces a propagating flame as a result [49, 87].

(a)   (b)   (c)

Figure 1.1: The match head chemistry, ©: [87] (a) Preparing to strike the match head against the abrasive surface (b) Ignition after the strike (c) Stable propagating flame.

The most prominent examples of excitable media [61, 4, 37, 14, 102] are propagation of electrical excitation in various biological tissues, including nerve fibre and myocardium, concentration waves in the bromate-malonic acid reagent (the Belousov-Zhabotinsky reaction), propagating waves during the aggregation of social amoeba

(Dictyostelium), plankton's population explosion as described in [93], waves of spreading depression in the retina of the eye, concentrations waves in yeast extract during glycosis, calcium waves within frog eggs and the Mexican wave (or La Ola) [31].

The fuse of a dynamite is an example of one-dimensional continuous version of an excitable medium, while a field of dry grass is its two-dimensional counterpart. These two spatially extended systems admit the possibility of (excitation) wave propagation. The field of dry grass has an additional property that both the match head and the dynamite fuse fail to have, the recovery property. Though not very rapid by physiological standards, after a few months, a burnt-over field of grass still has the chance of regrowing enough fuel for another fire to spread across it [49].

Excitation waves play key roles in living organisms and they are observed in chemical and physical systems, e.g. nerves, heart muscle, catalytic redox reactions, large aspect lasers and star formation in galaxies [52]. Understanding conditions of successful initiation is particularly important for excitation waves in the heart where they trigger coordinated contraction of the muscle and where failure of initiation can cause or contribute to serious or fatal medical conditions, or render inefficient the work of pacemakers or defibrillators [101].

The ability of a stimulus to initiate a wave depends on its spatial extent. Rushton [81, 71], considering an early mathematical model of nerve excitation, introduced the concept of the "liminal length", the minimal spatial extent of the stimulus necessary to initiate an excitation wave. A more modern and detailed concept is that of the "critical curve" in the stimulus strength-spatial extent plane. A stimulus generates an excitation wave if its parameters are above this curve; otherwise the wave is either not created or collapses after a while. For a stimulus of nonzero time duration, the concept of a critical "strength-duration" curve is relevant [71].

Mathematically, after the stimulus has finished, the problem is in any case reduced to classification of initial conditions that will or will not lead to a propagating wave solution. The key question is the nature of the boundary between the two classes. A detailed analysis of this boundary has been done for simplified models of excitable media such as the FHN system and its variations. This has led to the concept of a *critical nucleus*, briefly reviewed below. Numerical simulations of the cardiac excitation models reveal significant qualitative differences in the way initiation occurs in such models, compared to the FHN-style systems [89]. In order to understand these differences, we analyse a recently proposed simplified model of cardiac excitation in this work, and demonstrate that for this model the concept of critical nucleus should be replaced with a new concept of *critical front*.

4

1.3   Problem statement

The mathematical models of excitable systems, specifically the detailed ionic models of propagation of excitation in the heart, are complicated and so are to a larger extent not analytically tractable. Therefore, they are mostly studied numerically and more often than not, these purely numerical studies provide limited insights into the mechanisms of the phenomena under investigation. In general, the parameter dependence of the models are sometimes not entirely known reliably. Therefore, simplified caricature-type models become subjects of intense studies. In particular, the study of front propagation is one of the fundamental problems in nonlinear dynamics. Our knowledge and understanding of the experimental and numerical studies of these nonlinear excitable systems are enhanced and deepened by analytical approaches which as a result help to reveal some qualitative properties of the underlying PDEs formed.

The central theme of this thesis is therefore the exploration and exposition of the nature of the critical solutions in some simplified models of excitable media. These models are namely, the ZFK equation which is a fast subsystem of the FHN equations and the Biktashev (2002) [8] model, a fast subsystem of the detailed ionic cardiac tissue models. We are not aware of any analytical approach pertaining to initiation of excitation wave propagation regarding the derivation of expression for the threshold curves in a compact form for the ZFK equation and most especially that of the front equations (Biktashev (2002) model). Therefore, one of the main goals of this work is to develop some analytical approaches to solve the nonlinear initiation problem for the two subsystems by deriving in a compact form, the analytical expression of their numerically obtained critical curves. This then serves as analytical ignition criteria for these subsystems in particular, and hopefully for excitable systems in general.

Initiation of excitation waves is a threshold phenomenon [19, 28] and therefore, these problems are about classification of initial conditions that will or will not lead to a traveling-wave solution (i.e., *excitation wave*). Basically, the key question is about the nature of the boundary between these two classes (i.e., *excitation* and *decay*). Mathematically, this can be formulated as follows: Given

$$\frac{\partial \bar{u}}{\partial t} = \bar{f}(\bar{u}) + \bar{D}\frac{\partial^2 \bar{u}}{\partial X^2}, \quad (X, t) \in [0, +\infty) \times [0, +\infty),$$

$$\bar{u}(X, 0) = \bar{U}_r + U_{\text{stim}}\,\bar{H}(X, X_{\text{stim}}),$$

where $\bar{U}_r$ is the resting state, $\bar{H}$ describes the shape of the initial perturbation, say $\bar{H}(X, X_{\text{stim}}) = \bar{c}\,\Theta(X_{\text{stim}} - X)$, X_{stim} and U_{stim} are the width and amplitude of that perturbation respectively; $\bar{c}$ is a constant vector, $\bar{u} \in \mathbb{R}^n$ is an n-dimensional vector of dynamic variables, $\bar{D}$ a diagonal diffusion coefficients matrix and $\bar{f}(\bar{u})$ a vector of

nonlinear functions that specify the local dynamics. A typical picture observed in numerical simulations is that if initial conditions satisfy $U_{\text{stim}} < U^*_{\text{stim}}(X_{\text{stim}})$, $X \in [0, \infty)$ then $\bar{u}(X, t)$ decays as $t \to \infty$, and if $U_{\text{stim}} > U^*_{\text{stim}}(X_{\text{stim}})$, $X \in [0, \infty)$ then $\bar{u}(X, t)$ approaches a stable propagating front solution as $t \to \infty$. Hence, the goal is to find such $U^*_{\text{stim}}(X_{\text{stim}})$.

Chapter 2

Literature Review

2.1 Mathematical definitions and concepts

In this section we present definitions and description of some mathematical concepts used in the study.

Mathematical models

The description of the dynamical processes in excitable media are represented in many applications in the generic form [103]

$$\frac{\partial E_i}{\partial t} = \nabla(D_i \nabla E_i) + F_i(\nabla E_i, \bar{E}) + I_i(\bar{r}, t), \tag{2.1}$$

where E_i are the field variables of the active medium, $\bar{E}$ determines the state of the system, F_i are nonlinear functions of $\bar{E}$ and perhaps ∇E_i, D_i are diffusion coefficients, I_i are external actions varying in space $(\bar{r})$ and time (t) used for initiation of excitation waves. The system in (2.1) is a generic form of nonlinear reaction-diffusion equations which are used widely to describe various phenomena in neurobiology, electrophysiology, biophysics, chemical physics, population genetics, mathematical ecology and in other areas [21, 103].

Reaction-diffusion systems [78, 69] are mathematical equations which describe how the concentration of one or more substances distributed in space changes under the influences of two processes: (1) *local* (chemical) *reactions* in which substances are transformed into each other and, (2) *diffusion* that causes the substances to spread out in space. Originally, as the name suggests, reaction diffusion systems are naturally applied in chemistry. However, later these equations have been used to describe dynamical processes of non-chemical nature. Example of such processes are found in biology, physics, geology, ecology.

The solutions of reaction-diffusion equations exhibit a broad range of behaviours, for example, formation of traveling waves and wave-like phenomena and other self-

organized patterns like spiral waves and stripes, and intricate structures as solitons.

The simplest type of reaction-diffusion equation is the one which is concern with the concentration of a single substance in one spatial dimension which is of the form

$$\frac{\partial u}{\partial t} = D\,\frac{\partial^2 u}{\partial x^2} + f(u), \tag{2.2}$$

and is also referred to as the KPP (Kolmogorov-Petrovsky-Piscounov) equation; $f(u)$ is the reaction part which takes on various forms. If the reaction part vanishes, then the equation represent a pure diffusion process which is known as the *heat equation*. The choice of $f(u)$ in (2.2) gives the following well known equations which were named after their founders [97, 69]:

- $f(u) = u(1-u)$: Fishers's equation [20], originally used to describe the spreading of biological populations;

- $f(u) = u(1-u^2)$: Newell-Whitehead-Segel equation, to describe Rayleigh-Benard convection;

- $f(u) = u(1-u)(u-\alpha)$, $0 < \alpha < 1$: the general Zeldovich equation that arises in combustion theory, and its particular degenerate case $f(u) = u^2 - u^3$.

In contrast, the basic features of self-sustained dynamics in excitable media can be describe by the relatively simple two-component *activator-inhibitor* (or propagator-controller) system

$$\begin{aligned}
\frac{\partial u}{\partial t} &= \nabla^2 u + f(u,v),\\
\frac{\partial v}{\partial t} &= \sigma\,\nabla^2 v + \varepsilon\,g(u,v),
\end{aligned} \tag{2.3}$$

where $u(\mathbf{r},t)$ and $v(\mathbf{r},t)$ describe the state of the system, $f(u,v)$ and $g(u,v)$ specify the local dynamics, σ determines the ratio between two diffusion constants and ε is the ratio of the reaction rates. For parameter $\varepsilon \ll 1$, the reaction-diffusion system exhibit relaxational dynamics with interval of fast and slow motions. The system is referred to as the Brusselator, FitzHugh-Nagumo [33, 28], Rinzel-Keller, [80], Barkley [5] depending on the nature of the nonlinear functions f, g.

The space-clamped version of (2.3) reduces to

$$\begin{aligned}
\frac{\mathrm{d}u}{\mathrm{d}t} &= f(u,v),\\
\frac{\mathrm{d}v}{\mathrm{d}t} &= \varepsilon\,g(u,v),
\end{aligned} \tag{2.4}$$

which is known as FitzHugh-Nagumo equations (also often called Bonhoeffer Van der Pol (oscillator) equations).

Classifications of the reaction-diffusion systems

Based on the nature of nullclines which emanate as a result of the type of nonlinearity of the functions f, g, [26, 41, 65, 66], the systems (2.2, 2.3, 2.4) can roughly be classified into three groups (i) monostable (ii) bistable and (iii) oscillatory.

The monostable systems have only one stable fixed point (stationary state or resting state). A small (subthreshold) perturbation of the stationary state returns immediately to it, while a sufficiently large (superthreshold) perturbation induces a long excursion in the phase space and eventually the system relaxes again to its rest state.

For the bistable system, it nullclines intersect at three fixed points, two of which are stable, sometimes referred to as rest and excited states and the one remaining is unstable (saddle point). Meanwhile, in the oscillatory system there is one unstable fixed point and a stable limit cycle.

2.2 Hodgkin-Huxley (HH) model

In 1952, Alan Hodgkin and Andrew Huxley in their Noble Prize winning work developed a model from the popularly known *cable equation* which describes the electrical behaviour and properties of the surface membrane of a giant squid axon [44, 84, 72].

Later this system of equations became a prototype of a large family of mathematical models quantitatively describing electrophysiology of various living cells and tissues. These cells and tissues are specialized electric circuits that carry vital signals from one part of either animals or human system to another. Therefore, an understanding of the structures of the equations in this model is indispensable as it serves as the spring board from which many researches in the field of biophysical sciences take off.

Before giving a brief description of this model there is the need for an acquaintance with some terminologies as found in the literature.

2.2.1 Definitions and description of some technical terms

Membrane potential Also called *transmembrane potential difference* or *transmembrane potential* or *transmembrane potential gradient* is the electrical potential difference across a plasma membrane. In physical terms it is described as the voltage *drop* or the difference in voltage between one face of a bilayer and its immediate opposite face.

Resting membrane potential In biological cells that are electrically *at rest*, the *cytosol* (the internal fluid of the cell) posses a uniform *electrical potential* or voltage compared to the extracellular solution. This voltage is the resting cell potential, also called the *resting potential*. In other words, the constant potential

difference observed when an electrode is inserted into the interior of a cell. E.g. -70mV (in Nuerons) and -90mV (in skeletal muscle).

Equilibrium potential The membrane potential at equilibrium (an equilibrium point is when influx and efflux of ions are equal).

Action potential The rapid change in electric potential that part of a cell or tissue undergoes when it is stimulated (depolarized), especially by the transmission of an impulse. It is also called *electrical excitation* or *propagated signal*. Minimally, an action potential involves a *depolarization*, a *repolarization* and finally a *hyperpolarization*.

Depolarization In biology this refers to the event a cell undergoes when its *membrane potential* grows more *positive* with respect to the extracellular solution. It typically results from the influx of *positively charged ions* (such as sodium or calcium) into the cell. Alternatively, depolarization can also happen if potassium channels are closed.

Repolarization In neuroscience, this refers to the change in membrane potential that returns the membrane potential to a negative value after the *depolarization phase* of an action potential has just previously changed it (i.e. the membrane potential) to a positive value.

Repolarization results from the movement of positively charged potassium ions out of the cell. Typically the repolarization phase of an action potential results in *hyperpolarization*, attainment of a membrane potential that is more *negative* than the resting potential.

Hyperpolarization In neuroscience, this is the event a *neuron* (nerve cell) undergoes when it membrane potential grows more *negative* with respect to the extracellular solution. It can be caused by the flow of *positively charged ions* (such as potassium) out of the cell, or by the influx of *negatively charged ions* (such as chloride). In other words, hyperpolarization is said to occur when a cell's membrane potential dips below it's *resting level*.

Absolute refractory period (ARP) This is a period during an action potential when a second stimulus will not produce a second action potential (no matter how strong that stimulus is). This corresponds to the period when the sodium channels are open (typically just a millisecond or less).

Relative refractory period (RRP) This is a period when another action potential can be produced, but only if the stimulus is greater than the *threshold stimulus*. This corresponds to the period when the potassium channels are open (several

milliseconds). In this case nerve cell membrane becomes progressively more 'sensitive' (easier to stimulate) as the relative refractory period proceeds. Therefore it takes a very strong stimulus to cause an action potential at the beginning of the relative refractory period, but only a slightly above threshold stimulus to cause an action potential near the end of the relative refractory period.

Threshold(stimulus/potential) The minimum stimulus needed to achieve an action potential is called *threshold stimulus* and the resultant potential change is called the *threshold potential*. Thus, if the membrane potential reaches the threshold potential (generally $5 - 15$ mV less negative than the resting potential), the voltage-regulated sodium channels all open and sodium ions rapidly diffuse inward and depolarization occurs.

2.2.2 Equations

In their paper [44], Hodgkin and Huxley formulated a complete mathematical model via nonlinear PDE popularly known as the cable equation. The equation gives the total membrane current (I_m) at any point along the axon as the sum of the displacement current of the membrane capacitance ($C\dfrac{\partial v}{\partial t}$) and the current resulting from the movement of ions through the membrane (I_i) [24, 23]

$$\frac{a}{2R}\frac{\partial^2 v}{\partial x^2} = I_m = C\frac{\partial v}{\partial t} + I_i, \tag{2.5}$$

where a is the axon radius (cm), R the specific resistance (ohm cm) of the axoplasm, C the specific membrane capacitance ($\mu F/\text{cm}^2$), v the departure from the resting voltage of the membrane (mV), x distance along the axon from the stimulating electrode (cm), t time (msec), I_i ionic current density ($\mu A/\text{cm}^2$) and I_m total membrane current density ($\mu A/\text{cm}^2$).

And by the appropriate experimental procedures, the membrane potential can be constrained to have the same value along a finite length of the of axon (i.e., space-clamp constraint). Therefore, equation (2.5) simplifies to the ordinary differential equation (ODE)

$$I_m = C\frac{\mathrm{d}v}{\mathrm{d}t} + I_i, \tag{2.6}$$

with $I_i = I_{\text{Na}} + I_{\text{K}} + I_{\text{L}}$ (sum of Na$^+$, K$^+$ and other ions's current),

$$I_{\text{Na}} = g_{\text{Na}}(v - v_{\text{Na}}),$$
$$I_{\text{K}} = g_{\text{K}}(v - v_{\text{K}}),$$
$$I_{\text{L}} = \bar{g}_{\text{L}}(v - v_{\text{L}}), \tag{2.7}$$

v_{Na}, v_{K}, v_L, the equilibrium potential for sodium, potassium and leakage current respectively and where

$$g_{\mathrm{Na}} = \bar{g}_{\mathrm{Na}} \, m^3 \, h,$$
$$g_{\mathrm{K}} = \bar{g}_{\mathrm{K}} \, n^4. \tag{2.8}$$

Note that g_{Na}, g_{K}, $\bar{g}_L$ are respectively the conductivities for Na^+, K^+, and other ions species and correspondingly $\bar{g}_{\mathrm{Na}}$, $\bar{g}_{\mathrm{K}}$ (constants) are the maximum attainable values for g_{Na}, g_{K}.

The dimensionless variables m, h, n, which varies from 0 to 1, are voltage-sensitive gate proteins (otherwise known as the *gating variables*). Specifically, m, h (for activation and inactivation of Na^+ gate) and n (for activation of K^+ gate) describe all the smoothly varying voltage and time dependence of the kinectics. These gating variables obey the ODEs

$$\frac{\mathrm{d}m}{\mathrm{d}t} = \alpha_m(v)(1 - m) - \beta_m(v)m,$$
$$\frac{\mathrm{d}h}{\mathrm{d}t} = \alpha_h(v)(1 - h) - \beta_h(v)h,$$
$$\frac{\mathrm{d}n}{\mathrm{d}t} = \alpha_n(v)(1 - n) - \beta_n(v)n, \tag{2.9}$$

where $\alpha_j(v)$, $\beta_j(v)$, $j = h$, m, n are gate's closing and opening rates in ms^{-1}. Hodgkin and Huxley empirically determined expressions for the gate rates as

$$\alpha_m(v) = \frac{0.1(v + 25)}{\exp\left[(v + 25)/10\right] - 1}, \qquad \beta_m(v) = 4.0 \, \exp\left(v/18\right),$$

$$\alpha_h(v) = 0.07 \, \exp\left(v/20\right), \qquad \beta_h(v) = \frac{1}{\exp\left[(v + 30)/10\right] + 1},$$

$$\alpha_n(v) = \frac{0.01(v + 10)}{\exp[(v + 10)/10] - 1}, \qquad \beta_n(v) = 0.125 \exp(v/80). \tag{2.10}$$

The values of other constants appearing in the equations are $\bar{g}_{\mathrm{Na}} = 120$, $\bar{g}_{\mathrm{K}} = 36$, $\bar{g}_{\mathrm{L}} = 0.3$ (m.mho/cm^2); $v_{\mathrm{Na}} = -115$, $v_{\mathrm{K}} = 12$, $v_L = -10.5989$ (mv). Hence, the Hodgkin-Huxley model consist of four coupled ordinary differential equations (ODEs), and thus, from (2.6) and (2.9) we obtain

$$\frac{\mathrm{d}v}{\mathrm{d}t} = -\frac{1}{C}\left(\bar{g}_{\mathrm{Na}} \, m^3 \, h \, (v - v_{\mathrm{Na}}) + \bar{g}_{\mathrm{K}} \, n^4 \, (v - v_{\mathrm{K}}) + \bar{g}_{\mathrm{L}} \, (v - v_L)\right),$$
$$\frac{\mathrm{d}m}{\mathrm{d}t} = \alpha_m(v)(1 - m) - \beta_m(v)m,$$
$$\frac{\mathrm{d}h}{\mathrm{d}t} = \alpha_h(v)(1 - h) - \beta_h(v)h,$$
$$\frac{\mathrm{d}n}{\mathrm{d}t} = \alpha_n(v)(1 - n) - \beta_n(v)n. \tag{2.11}$$

2.2.3 Action potentials (AP): Solutions and structure

By 'membrane' *action potential* is meant one in which the membrane potential is uniform, at each instant, over the whole of the length of fibre under consideration. There is no current along the axis cylinder and the net membrane current must therefore always be zero, except during the stimulus. If the stimulus is a short shock at $t = 0$, the form of the action potential should be given by solving equation (2.11) with the initial conditions that $v = v_0$ and m, n and h take on their resting steady state values $n_0 = 0.3177$, $m_0 = 0.0530$, $h_0 = 0.5961$, to four places of decimals.

The process by which an *action potential* signal is propagated can be understood when we look closely at the events happening in the immediate vicinity of the membrane [85, 30]. A certain *threshold voltage* is required to start the process: the potential difference must be raised to about -30 to -20 (mV) at some site on the membrane. Experimentally this can be achieved by a stimulating electrode that pierces a single neuron. Biologically this happens at the axon hillock in response to an integrated appraisal of excitatory inputs impinging on the soma. Consequently, when the *threshold voltage* is reached the following sequence of events occur:

- Sodium channels open, letting to the influx of Na^+ ions into the cell interior. This causes the membrane potential to *depolarize* further; that is, the inside becomes more positive with respect to the outside, the reverse of resting-state polarization.

- After a slight delay, the potassium channels open, letting to the eflux of K^+ ions to the cell exterior. This in essence restores the original *polarization* of the membrane, and further causes an overshoot of the negative rest potential (*hyperpolarization*).

- The sodium channels then close in response to a decrease in the potential difference.

- Adjacent to a site that has experienced these events the potential difference exceeds the threshold level necessary to set in motion the first event. The process repeats, leading to a spatial conduction of spike-like signal. The action potential can thus be transported down the length of the axon without attenuation or change in shape, mathematically, this makes it a *traveling wave.*

The system (2.11) and equations (2.10) are used to draw the graphs in Fig. 2.1. The red solid curve in the left top panel of Fig. 2.1 describes the complete stages of an *action potential* (i.e., *electrical excitability*) process: *depolarization, repolarization and hyperpolarization.*

Also shown in Fig. 2.1 are: The *absolute refractory* period (ARP) which is the period during which a second stimulus will not trigger a second action potential (however,
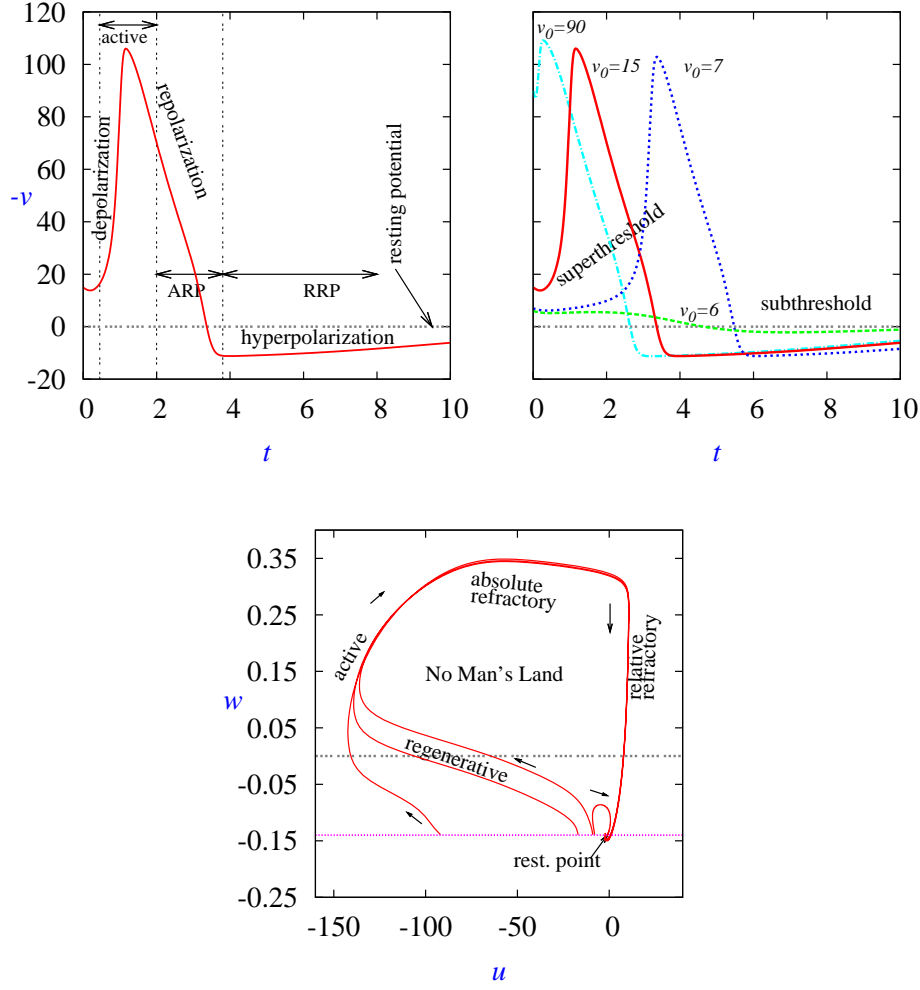
Figure 2.1: Numerical solution of system (2.11) [44, 63] for initial depolarization $v_0 = 15$ mV showing the complete stages of an action potential process: *depolarization, repolarization and hyperpolarization.*

strong the second stimulus might be). This corresponds to the period when the sodium channels are open (typically some millisecond or less);

The relative refractory period (RRP) which is the period when another action potential is possible if the stimulus is greater than the *threshold* stimulus. This corresponds to the period when the potassium channels are open (several milliseconds). In other words, the nerve cell membrane becomes progressively more 'sensitive' (easier to stimulate) as the relative refractory period proceeds. Therefore, it takes a very strong stimulus to produce an action potential at the beginning of the relative refractory period, but only a slightly above threshold stimulus to cause an action potential near the end of the relative refractory period.

In the top right panel of Fig. 2.1 are solutions of (2.11) for initial depolarizations, v_0,

of 90, 15, 7 and 6 (mV) illustrating excitability around the threshold and equilibrium. The HH model has only one equilibrium (resting point), therefore if a small shock (*subthreshold*) is applied to the resting state, then this shock cause small perturbation which is below the critical level (*threshold*) of the system, and it decays immediately back to the resting state (no excitation). However, if the shock exceeds the critical level of the system due to a large shock (*superthreshold*), then this cause *excitation* to occur and the cells are depolarized, meaning the membrane potential is moved away from its resting state for quite a while before eventually returning to the rest state. In other words, above threshold initial voltages lead to a rapid response with large changes in the state of the system.

In the bottom panel is the reduced 2-dimensional (u, w) phase portrait of the 4-dimensional (v, m, n, h) space of the HH model with $u = v - 36\,m$ and $w = (n - h)/2$ [33]. The regions marked on the trajectories (red solid curves) correspond to the physiological responses which are known as: *regenerative, active, absolute refractory, and relative refractory* phases. It also shows the only one equilibrium (resting point) of the HH system from which small, below threshold (subthreshold) stimulus do not lead to excitation, but rather a gradual return to it; while larger, above-threshold (superthreshold) stimulus result in a large excursion through the phase space before finally returning to it (the equilibrium). Such superthreshold trajectories are the phase-space representation of an *action potential*. The region marked 'no man's land', a non-physiological term is a region where rare trajectories could be obtained and so chosen to represent a state the nerve seldom reached in physiological experiments.

2.3   FitzHugh-Nagumo (FHN) model

2.3.1   Bonhoeffer-van der Pol (BVP) Model

Richard FitzHugh was the first investigator to apply mathematical analysis (phase plane analysis) to study the qualitative properties of HH system of equations. In his paper [33], FitzHugh suggested that a modified version of the Van der Pol system of equations which he called the Bonhoeffer-van der Pol (BVP) model [33, 39, 36, 74], has similar qualitative properties to the HH system. He suggested that the four-dimensional projection of HH space portrait to a two-dimensional subspace gives a phase portrait, (see Sec. 2.2), where the trajectories look similar to that of FitzHugh phase portrait. The BVP model is given by

$$\dot{x} = c\,(y + x - x^3/3 + z)$$
$$\dot{y} = -\,(x - a + by)/c \qquad\qquad (2.12)$$

where a and b are constants and satisfy the conditions $1 - 2b/3 < a < 1$, $0 < b < 1$, $b < c^2$ and x represents the *excitability* of the system (membrane potential,v), y represents
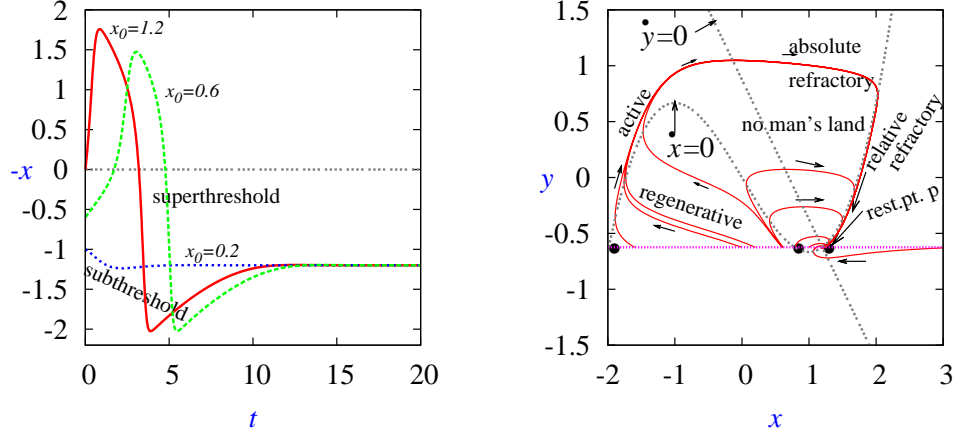
Figure 2.2: Solutions of equations (2.12) [33] having an equilibrium $(x_0, y_0) = (1.20, -0.625)$ with parameters $a = 0.7$, $b = 0.8$, $c = 3.0$ and $z = 0$ for stimuli 1.20, 0.6, 0.2. It shows the complete stages of an action potential process: depolarization, repolarization and hyperpolarization.

combined forces that tend to return the axonal membrane resting state, z represents the stimulus intensity which corresponds to the external current $I(t)$ in HH equations.

Action potentials and physiological states of BVP Model

In Fig. 2.2 the curves fairly resemble those of the HH model in Fig. 2.1 with small shock (*subthreshold*) of 0.2, and 0.6, 1.20 as superthreshold respectively. This illustrates the same excitability phenomenon of the HH model in that the small shock fails to excite as the action potential it elicits immediately goes back to the resting point of the system. The resting point (P) the only one as is the case with HH system is stable , therefore if a phase point displaced initially a short distance from the resting point will return toward its spontaneously. If a stimulus consisting of an instantaneous shock is applied to the system, the phase point jumps horizontally along the dotted line for a distance Δx proportional to the amplitude of the shock- to the left for a cathodal (-z) shock or to the right for an anodal one (+z) (see [33] for detailed explanations).

After a sufficiently large cathodal shock, the phase point travels along a path to the left through the regenerative zone, upward through the active, to the right through the absolute refractory, downward to the relatively refractory and finally back to P. This clockwise circuit represents a complete action potential (electrical excitability). If the shock is too small, no *impulse* (AP) results; instead, the phase point returns more directly to P through the small clockwise- circuits (representing subthresholds) as shown in the diagram Fig. 2.2.

The no-man's land (non-physiological term) is a region where rare trajectories could be obtained and is chosen to represent state the nerve seldom reached in physiological experiments. *The horizontal distance of a point from the separatrix is proportional to*

16

the **threshold** (magnitude of instantaneous z pulse). It should be noted that since excitation is the result of the phase point being displaced horizontally across the *threshold separatrix*, it follows that the system will be *absolutely refractory* when the phase point is above the separatrix, where such crossing is impossible. In the *relative refractory* zone, the phase point lies to the right of the separatrix and can be displaced across it, but the threshold stimulus required is greater than for the resting point [33].

In Fig. 2.2 we can see that we have a stable singular point (equilibrium point) with a trajectory that spirals toward its. FitzHugh used the BVP system of equations because it has qualitative properties similar to that of HH system. Thus, it can be argued that the pair (v, m) corresponds to x and they represent *excitability*. The pair (h, n) corresponds to y and represent *recovery*. As suggested by FitzHugh [33], the phase portraits of both HH and BVP look similar and hence exhibit the same excitability phenomenon.

2.3.2   FitzHugh-Nagumo (FHN) equations

The FHN model [33, 67] which is a generic model for excitable media and its numerous variants have served well as simple yet qualitatively reasonable models of the complicated processes of excitation and propagation in nerve fibre, heart muscle and other biological spatially-extended excitable systems. Among the variants, this is one of the format as used by Winfree [96]

$$\frac{\partial u}{\partial t} = \frac{1}{\varepsilon} f(u, v) + D \frac{\partial^2 u}{\partial x^2},$$
$$\frac{\partial v}{\partial t} = \varepsilon g(u, v) + \delta D \frac{\partial^2 v}{\partial x^2}, \tag{2.13}$$

where x, $t \in \mathrm{R}$ are measured respectively in "space units" and "time units", $f(u, v) = u - u^3/3 - v$, $g(u, v) = u + \beta - \gamma v$. The *propagation* variable u represents an *electric potential*, the *recovery* variable v represents *ion channels* (as those channels in HH model), D is the coefficient of diffusion in "space units/time unit" and δ the diffusion rate (it is usual in electrophysiological applications to take $\delta = 0$). Often for the sake of simplicity $D = 1$, $\delta = 0$ and the system reduced to

$$\frac{\partial u}{\partial t} = \frac{1}{\varepsilon} f(u, v) + \frac{\partial^2 u}{\partial x^2},$$
$$\frac{\partial v}{\partial t} = \varepsilon g(u, v). \tag{2.14}$$

The generic FHN system has been represented by various formats as discussed in [96, 28]. The form we are going to use in this work is the one due to Neu, Pressig and Krassowska [68] but with the notational change $v = u$, $y = v$, $\mu = \theta$

$$\frac{\partial u}{\partial t} = \frac{\partial^2 u}{\partial x^2} + f(u) - v,$$
$$\frac{\partial v}{\partial t} = \varepsilon(\alpha u - v), \tag{2.15}$$

where $f(u) = u(u - \theta)(1 - u)$, a cubic polynomial with the state variables, u and v representing respectively the transmembrane potential and inactivation variable; ε a small parameter, α a constant and θ corresponds to the threshold state of the system and must satisfy $0 < \theta < 1/2$ in order for the FHN system to give rise to a propagating wave [56, 57] as shown in Fig. 2.3
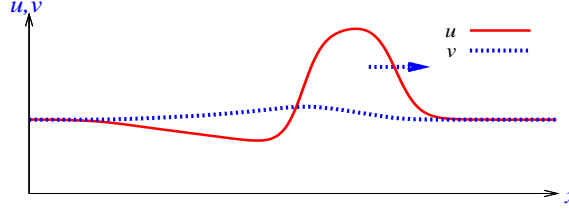
Figure 2.3: A propagating pulse profile solution to the FHN system (2.15).

2.3.3 Zeldovich-Frank-Kamenetskii (ZFK) equation

The fast subsystem of (2.15) coincides with the ZFK [99] equation, also known as the Nagumo equation [50, 6, 58]

$$\frac{\partial u}{\partial t} = \frac{\partial^2 u}{\partial x^2} + f(u), \tag{2.16}$$

where $f(u) = -(u - u_1)(u - u_2)(u - u_3)$; $u_1 < u_2 < u_3$, $u_2 < (u_1 + u_3)/2$ and u_1, u_2, u_3 are roots of $f(u)$. Note that u_1 corresponds to the resting state of the full FHN system. Meanwhile, u_2, u_3 are respectively the threshold and excited state (see [88] for details). The ZFK equation in (2.16) has as solution the propagating front which is a profile with two different asymptotic states, that is u_1 on the right and u_3 on the left as in Fig. 2.4.
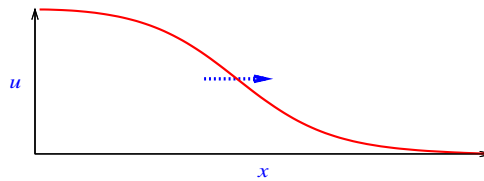
Figure 2.4: A propagating front profile solution to the ZFK equation in (2.16) which is a fast subsystem to the FHN system in (2.15).

2.4 Biktashev 2002 model (a front model)

The FHN model has indisputably and reputedly been one of the most widely studied excitable system in literature for almost five decades now. However, its role as a universal prototype of excitable system has in recent times become under intense and sustained pressures for reasons ranging from phenomenology to structure of the

model(s) it ought to caricature. As a results many alternative simplified models had been suggested [1, 32, 29, 7, 42, 8].

Here, we are presenting the simplified cardiac front model due to Biktashev [8], the main subject of our study. It is one of the direct descendants of the biophysically detailed models. The two-variable cardiac excitation front model which we shall be referring to as the front model is a simplified model based on the celebrated HH model [44], the more recent ionic models such as the Noble-1962 [70] and Courtmenche et al (CRN-1998) [25, 86] models. The human atrial tissue model (CRN-1998) is a homogenous and isotropic one-dimensional medium which satisfies the reaction-diffusion system (RDS)

$$\frac{\partial \mathbf{u}}{\partial T} = \hat{\mathbf{D}} \cdot \frac{\partial^2 \mathbf{u}}{\partial X^2} + \mathbf{F}(\mathbf{u}), \tag{2.17}$$

where $\mathbf{F}(\mathbf{u})$ is a vector defined according to the atrial single-cell realistic CRN-1998 model, $\mathbf{u} = (E, m, h, j, \dots,)^T \in \mathbb{R}^{21}$ is a vector of all dynamic variables of the model and $\hat{\mathbf{D}} = \mathrm{diag}\,(D, 0, 0, \dots,)$ is the tensor of diffusion in which only the coefficients of the voltage E is nonzero. Thus, the simplified description focuses on the excitation and propagation of impulses while ignoring the effects due to the geometry, anisotropy and heterogeneity of a real atrium [86].

After some non-standard asymptotic analysis [8, 9, 46] based on the smallness of certain quantities in the equations in (2.17), formalized with an explicit parameter ϵ it is re-written as

$$\frac{\partial E}{\partial T} = -C_M^{-1}\left(\frac{1}{\epsilon}I_{\mathrm{Na}}(E, m, h, j) + {\sum_I}'(E, \cdots)\right) + D\frac{\partial^2 E}{\partial X^2},$$

$$\frac{\partial m}{\partial T} = \frac{(\bar{m}(E; \epsilon) - m)}{\epsilon\,\tau_m(E)}, \quad \bar{m}(E; \epsilon) = \begin{cases} \bar{m}(E), & \epsilon = 1, \\ \Theta(E - E_m), & \epsilon = 0, \end{cases}$$

$$\frac{\partial h}{\partial T} = \frac{(\bar{h}(E; \epsilon) - h)}{\epsilon\,\tau_h(E)}, \quad \bar{h}(E; \epsilon) = \begin{cases} \bar{h}(E), & \epsilon = 1, \\ \Theta(E_h - E), & \epsilon = 0, \end{cases}$$

$$\frac{\partial y}{\partial T} = \frac{(\bar{y}(E; \epsilon) - y)}{\epsilon\,\tau_y(E)}, \quad y = u_a, w, o_a, d,$$

$$\frac{\partial \mathbf{U}}{\partial T} = \mathbf{W}(E, \cdots), \tag{2.18}$$

where $\Theta()$ is the Heaviside function. The dynamic variables E, m, h, u_a, w, o_a and d as defined in [25] are considered as "fast" variables and change significantly during the upstroke of a typical action potential (AP). $\mathbf{U} = (j, o_i, \cdots, Nai, Ki, \cdots)^T$ is the vector of all other slower variables and $\mathbf{W}$ is the vector of the corresponding right-hand sides. The sum ${\sum_I}'(E, \cdots)$, is for all other currents except the fast sodium current $I_{\mathrm{Na}} = \overline{I_{\mathrm{Na}}}\,m^3\,h\,j$, which is only large during the upstroke of the AP and not that large otherwise (the m or h gates are almost closed outside the upstroke since their quasistationary values $\bar{m}(E)$, $\bar{h}(E)$ are small there).

Thus, in the limit $\epsilon \to 0$, functions $\bar{m}(E)$ and $\bar{h}(E)$ have to be considered as zero in certain overlapping intervals $E \in (-\infty, E_m]$, $E \in [E_h, \infty)$ and $E_h \leq E_m$. Hence, the representations $\bar{m}(E; 0) = \Theta(E - E_m)$ and $\bar{h}(E; 0) = \Theta(E_h - E)$. Therefore, (2.18) in the limit $\epsilon \to 0$, in the fast time $t = T/\epsilon$, and with $x = (\epsilon D)^{-1/2} X$ gives a closed system of three equations

$$
\begin{aligned}
\frac{\partial E}{\partial t} &= -\overline{I_{\mathrm{Na}}}\, m^3\, h\, j/C_M + D\, \frac{\partial^2 E}{\partial x^2}, \\
\frac{\partial m}{\partial t} &= \left(\Theta(E - E_m) - m \right)/\tau_m(E), \\
\frac{\partial h}{\partial t} &= \left(\Theta(E_h - E) - h \right)/\tau_h(E).
\end{aligned}
\tag{2.19}
$$

Simplifying (2.19) further by replacing $\tau_h(E)$ and $\overline{I_{\mathrm{Na}}}(E)$ with constants and assuming additionally the limit of small $\tau_m(E)$ so that m always remains close to its quasi-stationary value $\Theta(E - E_m)$.

Hence, after suitable rescaling (so that $E_m = 1, E_h = 0$) (2.19) reduced to the system of two PDEs (2.20) that models the excitation fronts in cardiac tissue. It describes very well the *propagation block* phenomenon, a feature typical of realistic excitation models that the FHN failed to adequately capture [8, 9, 10]

$$
\begin{aligned}
\frac{\partial E}{\partial t} &= \frac{\partial^2 E}{\partial x^2} + F(E, h), \\
\frac{\partial h}{\partial t} &= G(E, h)/\tau,
\end{aligned}
\tag{2.20}
$$

with

$$
\begin{aligned}
F(E, h) &= \Theta(E - 1)\, h, \\
G(E, h) &= \Theta(-E) - h,
\end{aligned}
\tag{2.21}
$$

where E corresponds to the transmembrane potential, h is the probability density of the Na^+ channel gates being open and τ is a dimensionless parameter.

2.4.1 Traveling fronts solutions

The solutions to (2.20) are in the form of traveling front propagating rightward with speed $c > 0$, $z = x - ct$ and satisfying the system of ODEs

$$
\begin{aligned}
-c\, E' &= E'' + \Theta(E - 1)\, h, \\
-c\, h' &= \frac{1}{\tau}(\Theta(-E) - h),
\end{aligned}
\tag{2.22}
$$

where $(') = \dfrac{\mathrm{d}}{\mathrm{d}z}$ and with auxiliary conditions given by

$$
\begin{aligned}
E(+\infty) &= -\alpha < 0, & E(-\infty) &= \omega > 1, \\
h(+\infty) &= 1, & h(-\infty) &= 0.
\end{aligned}
\tag{2.23}
$$

The phase of the front solution is chosen so that the internal boundary conditions $E(0) = 0$ and $E(-\Delta) = 1$ at $z = 0, -\Delta$ are satisfied with the requirements that $E(z) \in C^1$ and $h(z) \in C^0$. The ODE problem along with its auxilliary conditions has a family of propagating front solutions that depends on one parameter, the *pre-front voltage* α which is fixed.

$$
E(z) = \begin{cases} \omega - \dfrac{\tau^2 c^2}{1 + \tau c^2} \, e^{z/\tau c}, & z \le -\Delta, \\[2mm] -\alpha + \alpha \, e^{-cz}, & z \ge -\Delta, \end{cases}
$$

$$
h(z) = \begin{cases} e^{z/\tau c}, & z \le 0, \\[2mm] 1, & z \ge 0, \end{cases}
$$

$$\tag{2.24}$$

where $z = x - ct$, $\omega = 1 + \tau c^2(\alpha + 1)$, $\Delta = \dfrac{1}{c} \ln(\dfrac{\alpha + 1}{\alpha})$ and c is an implicit function of τ and α as given by the following transcendental function,

$$
\tau c^2 \ln \left(\frac{(1 + \alpha)(1 + \tau c^2)}{\tau} \right) + \ln \left(\frac{\alpha + 1}{\alpha} \right) = 0. \tag{2.25}
$$

For a fixed α, there is a $\tau_*(\alpha)$ such that for $\tau > \tau_* \approx 7.6740$, equation (2.25) has two solutions for c: $c = c_\pm(\alpha, \tau)$, $c_+(\text{higher}) > c_-(\text{lower})$ [8]. There is numerical and analytical evidence that solutions (2.24) with $c = c_+$ are *stable* and those with $c = c_-$ are *unstable* with one positive eigenvalue [8, 43].
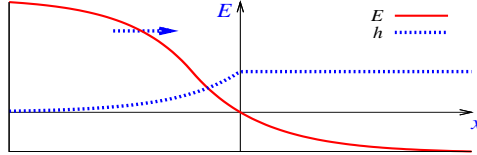
Figure 2.5: A typical propagating front profile for the unstable front solution to the ODE system (2.22) for the simplified cardiac equations in (2.20).

2.5 Approximations to initiation problem for the ZFK equation

2.5.1 The critical nucleus

There exist a well developed theory of *initiation* of *propagating waves* in the FitzHugh-Nagumo equations [34, 35, 68], in the singular limit when the activator (excitation) variable is much faster than the inhibitor (recovery) variable. The key role in this theory is played by the so called *critical nucleus*, $u_{cr}(x)$, which is an unstable, non-trivial stationary solution of

$$
\frac{\partial u}{\partial t} = \frac{\partial^2 u}{\partial x^2} + f(u), \tag{2.26}
$$

21

such that $u_{cr}(\pm\infty) = u_1$ where $f(u) = -(u-u_1)(u-u_2)(u-u_3)$ with u_1 corresponding to the resting state (see Sec. 2.3.3). The critical nucleus plays a key role in understanding the initiation processes for the FHN systems, such solution is unique as found in [68] for quadratic nonlinearity (i.e., when the limit of small θ is considered for the cubical $f(u)$ in (2.16)) as

$$u_{cr}(x) = \frac{3\theta}{2} \operatorname{sech}^2(\frac{\sqrt{\theta}}{2} x). \tag{2.27}$$

However, for the cubical nonlinearity $f(u)$ as in (2.16) we have reproduced the solution as found by Flores in [34] though in a slightly different form

$$u_{cr}^*(x) = 3\,\theta\sqrt{2}\left[(1+\theta)\sqrt{2} + \cosh(x\sqrt{\theta})\sqrt{2 - 5\theta + \theta^2}\right]^{-1}. \tag{2.28}$$

Its linearization spectrum has exactly one unstable eigenvalue, while all other eigenvalues are stable. So the center-stable manifold of this stationary solution has codimension one, and divides the phase space of (2.16) into two open sets. One of these sets corresponds to initial conditions leading to successful initiation, and the other to decay [58, 34, 62, 35, 68].

2.5.2 Variational approaches

One of the analytical approaches to the description of initiation of propagation as employed in [68] was the use of projected dynamics (a Galerkin-style approximation) to the class of Gaussian ansatz. Neu and co-workers derived this approximation after transforming the ZFK equation to gradient form. In general not every equation can be written in that form, so we have tried more generic approaches, for instance, we present some new results of approximations done on the ZFK equation for both smooth and piece-wise smooth ansatzes by minimizing the L_2-norm of the residual of the equation on one hand and on the other by using a modified Biot-Mornev procedure [64].

Variational approximation of initiation problem by Neu *et al*

An analytical approach to the description of initiation of propagation as used by Neu and co-workers, [68] is the used of projected dynamics (a Galerkin-style approximation) to the class of Gaussian ansatz

$$u(x,t) = a(t)\,\exp(-k(t)\,x)^2, \tag{2.29}$$

with varying amplitude $a(t)$ and inverse width $k(t)$. After rewriting the ZFK equation in terms of variational derivative they obtained ODE system in the limit of small θ. Not every equation can be written that form, so we tried a more generic approach, where we minimize the equation of the residuals using L_2-norm. To find the residue functional,

we express our approximate solution $u(x,t)$ in terms of the unknown parameters $a(t)$ and $k(t)$ by letting

$$u(x,t) \equiv V(x,a(t),k(t)) \tag{2.30}$$

and the residue functional is then

$$\mathcal{R} = \int_0^\infty \left(\frac{\partial u}{\partial t} - \frac{\partial^2 u}{\partial x^2} - f(u) \right)^2 \, \mathrm{d}x. \tag{2.31}$$

Now minimizing (2.31) w.r.t $\dot{a}$, $\dot{k}$ by using calculus we have the ODE system as obtained by Neu and co-workers [68] in terms of $\dot{a}$, $\dot{k}$

$$\dot{a} = -a(2k^2 + 1 - c_1 a),$$
$$\dot{k} = -k(2k^2 - c_2 a), \tag{2.32}$$

where

$$c_1 = \frac{7\sqrt{6}}{18}, \qquad c_2 = \frac{7\sqrt{6}}{9}. \tag{2.33}$$

We have approximated the stable separatrices (the center-stable manifold) of the critical nucleus with its eigenvector by using the transformation

$$a = 1.4697 + 1.2866\,s$$
$$k = 0.4472 + s, \tag{2.34}$$

where $s \in \mathbb{R}$ is a parameter, $(1.4697,\, 0.4472)$ is the critical nucleus and $(1.2866, 1)^{\mathrm{T}}$ its corresponding eigenvector.

With the knowledge that $x_{\text{stim}}^{-1} \propto k$ and $u_{\text{stim}} \propto a$, we obtain a relationship between the threshold curve and the center-stable manifold (the separatrix of our Galerkian ODE) as

$$x_{\text{stim}} = \frac{B}{k}, \qquad u_{\text{stim}} = A\,a. \tag{2.35}$$

Now using the ansatz

$$V = a\,e^{-(kx)^2} \approx u_{\text{stim}}\Theta(x_{\text{stim}} - x), \tag{2.36}$$

where Θ is a Heaviside function and the values of the parameters $A = 0.7506376700$ and $B = 0.9899390828$ numerically determined. The result shown in Fig. 2.6(b) is our contribution and therefore, not found in [68].
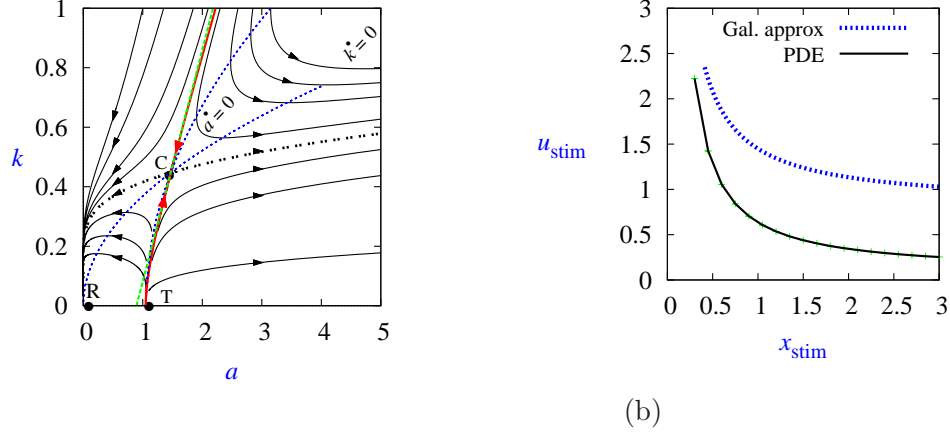
Figure 2.6: (a) The phase-portrait of the Galerkin ODE system reproduced from [68]. The eigenvector (dashed - green line) of the *center-stable manifold* (solid - red line) of the *critical nucleus* serving as the approximation of the center-stable manifold of the critical nucleus. The unstable manifold is the dotted - gray curve. (b) The threshold curves in the u_{stim} - x_{stim} plane, the result of our approximation (dotted - blue line) compared with that (solid - black line) obtained from simulations with the PDE system in [68].

The Biot-Mornev variational approximation

Mornev [64], devised a modified version of the Biot's variational method of computation of non-stationary processes of heat and diffusion mass transfer in regions of complex shape. The modification were necessary because Biot procedure according to Mornev [64] had some setbacks. One of the setbacks was the non invocation of any variational principle since no minimization functional that would yield the analytical relations obtained had been specified. There was also the usage of variables that had no physical meaning [13] which made it difficult for physical intuition to be used to construct *a priori* classes of functions via which approximate solutions could be sought for. In addition, the method was not applicable to the integration of diffusion or heat matter generation by chemical reaction. In fact, the method as suggested by Mornev did not even allow for the integration of the simplest reaction-diffusion with nonlinear reaction part of the form

$$\varphi_t = \operatorname{div}(D\,\nabla\,\varphi) + f(\varphi), \tag{2.37}$$

where $f(\varphi) = -\dfrac{\mathrm{d}\Pi}{\mathrm{d}\varphi}$, is a nonlinear function generated by the potential $\Pi(\varphi)$, $\operatorname{div}(D\,\nabla\,\varphi) = \nabla \bullet (D\,\nabla\varphi) = D\,\nabla^2\varphi$.[1] Therefore, Mornev suggested some modifications of the Biot method to take care of the outlined disadvantages by developing a direct method of integration of reaction-diffusion equations of type (2.37) and their generalization based on the minimum dissipation principle.

---

[1]For convenience and brevity we retain the original notations for the partial derivatives as used in [64].

The generalized versions of the the reaction-diffusion of type (2.37) given in continuous (2.38) format is

$$\varphi_t = v,$$

$$\gamma \, v = -\frac{\delta G}{\delta \varphi} = \operatorname{div} \frac{\partial g}{\partial(\nabla \varphi)} - \frac{\partial g}{\partial \varphi}, \tag{2.38}$$

where φ is an unknown function with arguments x, t; $\gamma = \gamma(\varphi, \nabla(\varphi), x)$ is a specified function and $G = G[\varphi] \equiv \int_W g(\varphi, \nabla(\varphi), x, t) \, d\tau$ is the energy functional, and $d\tau$ is the volume element of the physical space. The integration is performed via the spatial region W which can be finite or infinite. Equation (2.38) is supplemented with the boundary conditions

$$\mathbf{n} \frac{\partial g}{\partial(\nabla \varphi)} \, |_{\partial W} = 0, \tag{2.39}$$

where $\mathbf{n}$ is the outer normal to the ∂W. The dynamic principle of minimum dissipation for mechanical system suggested that the actual vector $v = \varphi$, as defined by the right-hand side of (2.38) and realized along the paths of the actual motion $\varphi(x, t)$ obtained by the integration of system (2.38) at boundary conditions (2.39), provided a stationarity for the local dissipative potential (2.40)

$$\sigma = \Gamma + \frac{dG}{dt}, \tag{2.40}$$

in which the functional (2.41) is substituted for G

$$G = G[\varphi] = \int_W g \, d\tau \equiv \frac{1}{2} \int_W D|\nabla \varphi|^2 \, d\tau + \int_W \Pi(\varphi) \, d\tau, \tag{2.41}$$

and the dissipation functional

$$\Gamma = \Gamma[\varphi, v] \equiv (1/2) \int_W \gamma(\varphi, \nabla(\varphi), x) \, v^2 \, d\tau, \tag{2.42}$$

for Γ. Therefore, the second equation in (2.38) is represented in the form of variational condition as

$$\delta_v \, \sigma|_{t, \varphi} \equiv \delta_v \left(\Gamma[\varphi, v] + \frac{dG[\varphi]}{dt} \right) |_{t, \varphi},$$

$$= \delta_v \Gamma[\varphi, v]|_{t, \varphi} + \delta_v \left(\frac{dG[\varphi]}{dt} \right) |_{t, \varphi} = 0. \tag{2.43}$$

Mornev method considered some *a priori* specified family of of functions ("ansatz"), $\hat{\varphi}(x, t, \mathbf{q})$ that satisfy conditions (2.39) at any time t, and where $\mathbf{q} \equiv \{q^\alpha\}_{\alpha=1}^n$ is a set of parameters which Biot termed as Lagrange variables. The main idea of the method is that the unknown solutions $\varphi(x, t)$ to (2.38) are approximated by the functions $\hat{\varphi}(x, t, \mathbf{q}(t))$ which at any time belong to a specified family, with functions $q^\alpha(t)$ found by integration of the ordinary differential equations derived from the variational condition (2.43).

The geometrical interpretations of the stated points in the previous paragraph as explained by Mornev are: The evolution of a physical system described by equations (2.38) occurs in an infinite-dimensional states space (φ-space) whose points are the functions $\varphi(x)$ which obey the boundary conditions (2.39).

The right-hand side of the the second/third equation in (2.38) specify in the φ-space, a time dependent vector field that provides the stationarity to the potential σ. Integration of this field with some initial conditions $\varphi(x, t_0) = \varphi_0(x)$ recovers in the φ-space the actual path, $\varphi(x, t)$ (i.e., solution) of the system passing through the point $\varphi_0(x)$ at $t = t_0$. Therefore, introducing an *a priori* ("ansatz") family of functions $\hat{\varphi}(x, t, \mathbf{q})$ that imaged the infinite-dimensional space into n-dimensional space of Lagrange functions constructed from q^α (q-space). Thus, the states of the system and its evolution is now approximated by the points of the q-space and by the paths in it. Finding the actual path $\mathbf{q}(t)$, necessitated the construction of the actual vector field in the q-space that would approximate the original field in (2.38) and then integrating the corresponding system of ordinary differential equations.

Construction of the vector field in the q-space

Mornev considered the velocity vector in (2.38) to be such that

$$\hat{\varphi}_t = \frac{\partial \hat{\varphi}}{\partial t} + \frac{\partial \hat{\varphi}}{\partial \mathbf{q}} \, \dot{\mathbf{q}} = \frac{\partial \hat{\varphi}}{\partial t} + \frac{\partial \hat{\varphi}}{\partial \mathbf{q}} \, \mathbf{u} \equiv \hat{v}(x, t, \mathbf{q}, \mathbf{u}), \tag{2.44}$$

where $\dot{\mathbf{q}} \equiv \{\dot{q}^\alpha\}_{\alpha=1}^n = \mathbf{u} \equiv \{u^\alpha\}_{\alpha=1}^n$; thus, the velocity vector is expressed in terms of the velocity vector $\mathbf{u}$ in the q-space. Then it is very clear from (2.44),

$$\frac{\partial \hat{\varphi}}{\partial \mathbf{q}} = \frac{\partial \hat{v}}{\partial \mathbf{u}} = \frac{\partial \hat{\varphi}_t}{\partial \dot{\mathbf{q}}},$$
$$\delta \hat{v} = \frac{\partial \hat{\varphi}}{\partial \mathbf{q}} \, \delta \mathbf{u} = \frac{\partial \hat{v}}{\partial \mathbf{u}} \, \delta \mathbf{u} = \frac{\partial \hat{\varphi}_t}{\partial \dot{\mathbf{q}}} \, \delta \mathbf{u}. \tag{2.45}$$

Using (2.42) and (2.43), expressions for Γ become

$$\Gamma[\hat{\varphi}, \hat{v}] \equiv \frac{1}{2} \int_W \gamma \, \hat{v}^2 \, \mathrm{d}\tau = \frac{1}{2} \int_W \gamma \, \hat{\varphi}_t^2 \, \mathrm{d}\tau \equiv \Gamma[\hat{\varphi}, \hat{\varphi}_t^2], \tag{2.46}$$

and $\delta_v \Gamma$

$$\delta_{\hat{v}} \, \Gamma[\hat{\varphi}, \hat{v}] \equiv \frac{1}{2} \int_W \gamma \, \hat{v} \, \delta \hat{v} \, \mathrm{d}\tau = \frac{1}{2} \int_W \gamma \, \hat{v} \, \frac{\partial \hat{v}}{\partial \mathbf{u}} \delta \mathbf{u} \, \mathrm{d}\tau,$$

$$= \int_W \gamma \, \hat{\varphi}_t \, \frac{\partial \hat{\varphi}_t}{\partial \dot{\mathbf{q}}} \delta \mathbf{u} \, \mathrm{d}\tau = \frac{\partial}{\partial \dot{q}^\alpha} \left(\frac{1}{2} \int_W \gamma \, \hat{\varphi}_t^2 \, \mathrm{d}\tau \right) \delta u^\alpha = \frac{\partial}{\partial \dot{q}^\alpha} \left(\Gamma[\hat{\varphi}, \hat{\varphi}_t] \right) \delta u^\alpha, \tag{2.47}$$

26

are obtained in terms of $\hat{\varphi}$. And for $\frac{\mathrm{d}G[\hat{\varphi}]}{\mathrm{d}t}$ in (2.43),

$$\frac{\mathrm{d}G[\hat{\varphi}]}{\mathrm{d}t} = \frac{\partial G[\hat{\varphi}]}{\partial t} + \frac{\partial G[\hat{\varphi}]}{\partial q^{\alpha}}\,\dot{q}^{\alpha} = \frac{\partial G[\hat{\varphi}]}{\partial t} + \frac{\partial G[\hat{\varphi}]}{\partial q^{\alpha}}\,u^{\alpha}, \tag{2.48}$$

and since $\delta_{\hat{v}}\left(\frac{\partial G[\hat{\varphi}]}{\partial t}\right) = 0$,

$$\delta_{\hat{v}}\left(\frac{\mathrm{d}G[\hat{\varphi}]}{\mathrm{d}t}\right) = \frac{\partial G[\hat{\varphi}]}{\partial q^{\alpha}}\delta u^{\alpha}. \tag{2.49}$$

Thus, substituting (2.48) and (2.49) in (2.43) and due to the arbitrariness of δu^{α}, the system of ordinary differential equations were obtained

$$\frac{\partial}{\partial \dot{q}^{\alpha}}\left(\Gamma[\hat{\varphi}, \hat{\varphi}_t]\right)\delta u^{\alpha} = -\frac{\partial G[\hat{\varphi}]}{\partial q^{\alpha}}, \quad (\alpha = 1, 2, \cdots, n). \tag{2.50}$$

Hence, the required vector field is determined by the right-hand sides of the resultant equations obtain when (2.50) is resolved with respect to $\dot{q}^{\alpha}$. Note that ODE system (2.50) is now a finite-dimensional approximation of the initial partial differential equations (PDEs) (2.38).

2.6   Summary

- We have reviewed models of excitable media of two classes: generic ones, including FitzHugh-Nagumo (FHN) system and fast subsystem known as Zeldovich-Frank-Kamenetskii (ZFK) equation, and biologically specific "ionic" models, such as the Hodgkin-Huxley model one of its descendants, including the simplified model of cardiac front due to Biktashev [8, 9].

- We have also reviewed existing analytical approaches to approximate description of excitation waves, such as Galerkin style (variational) approaches of Neu et al. and Mornev's modification of the Biot's variational method. Both approaches have been applied to the generic models (FHN and ZFK) but not to the ionic models.

- We note that in the analytical treatment of the initiation problem in the ZFK equation, the central role belongs to the concept of the critical nucleus, which is an unstable stationary and spatially inhomogeneous solution whose stable manifold is the threshold surface in the functional space, separating the initial conditions leading to successful initiation from those leading to decay.

Table 2.1: Glossary of notations for Chapter 2

Notation	Explanation(s): bf=before, af=after	Place introduced
α	pre-frontal voltage	af (2.2)
ω	post-frontal voltage	(2.23)
$\alpha_j(v)$, $\beta_j(v)$, $j = m, h, n$	Na$^+$; K$^+$ opening/closing gate rates	(2.9)
ε; ϵ	ratio of the reaction rates	(2.3); (2.18)
σ	ratio between diffusion constants	(2.3)
σ	minimization functional [64]	(2.40)
Γ	a component of σ [64]	(2.40)
γ	a specified function	(2.38)
Π	the potential in the Biot-Mornev formalism	af (2.37)
Θ	Heaviside step function	(2.18)
δ	diffusion rate	(2.13)
δ	variational derivative	(2.38)
φ	path of actual motion [64]	(2.37)
$\hat{\varphi}$	path of motion in the q-space [64]	af (2.43)
θ	threshold parameter	bf (2.15)
τ	parameter	(2.20)
Δ	constant	af (2.23)
τ_m, τ_h, τ_n	Na$^+$, K$^+$ time scales	(2.19)
$\mathrm{d}\tau$	volume element of the physical space [64]	af (2.38)
a	axon radius	(2.5)
A, B	constants	(2.35)
$c: c_-, c_+$	speed: lower, higher	af (2.21), af (2.25)
C, C_M	specific membrane capacitance	bf (2.5), (2.18)
D_i, D	diffusion coefficient	(2.1)
$\hat{\mathbf{D}}$	tensor of diffusion	(2.17)
		continued on the next page $\Rightarrow$

Notation	Explanation(s): bf=before, af=after	Place introduced
E_h, E_m	constants	(2.18)
E_i	field variable	(2.1)
$\bar{E}$	state of the system	(2.1)
E	Voltage	(2.18)
F_i, f, g	nonlinear function	(2.1), (2.2), (2.3)
F, G	nonlinear function	(2.20)
$\mathbf{F}$	nonlinear vector	(2.17)
G	energy functional [64]	(2.38)
g	energy density [64]	(2.38)
I_i	external actions	(2.1)
I_m	total membrane current density	bf (2.5)
I_{Na}, I_{K}, I_{L}	Na$^+$, K$^+$, other ions' current	af (2.6)
g_{Na}, g_{K}, $\bar{g}_{\mathrm{L}}$	Na$^+$, K$^+$, other ions' conductance	(2.7)
$\bar{g}_{\mathrm{Na}}$, $\bar{g}_{\mathrm{K}}$	Na$^+$, K$^+$ max. conductance	(2.7), (2.8)
v_{Na}, v_{K}, v_L	Na$^+$, K$^+$, other ions' equilibrium potential	(2.7)
m, h, n	Na$^+$, K$^+$ gates variables	(2.8)
$\bar{m}$, $\bar{h}$	Na$^+$, K$^+$ gate variables' quasi-stationary values	(2.18)
$\mathbf{n}$	outer normal to ∂W [64]	(2.39)
$\mathbf{q} : \dot{\mathbf{q}}$	vector of Lagrange variables: its velocity [64]	af (2.43): (2.44)
$\bar{r}$	space coordinate	(2.1)
R	specific resistance	(2.5)
$\mathcal{R}$	residue functional	(2.31)
s	parameter	(2.34)
u, v	dynamic variable	(2.2, 2.3)
u_{cr}	critical nucleus for the quadratic nonlinearity	bf (2.26)

Chapter 3

Numerical study of two nonlinear models

3.1 Introduction

Investigating initiation criteria is not possible without the knowledge and understanding of the nature of the critical solution. Therefore, we present some numerical results of initiation for the ZFK equation which is a reduced form of the FHN system when $\varepsilon = 0$. This equation is also known as the Nagumo equation that has the critical pulse (a.k.a. critical nucleus) as its non-constant solution which is stationary. Meanwhile, for the full FHN system the critical solution is in the form of critical pulse, an unstable propagating pulse solution [56, 57, 47]. As for the simplified front model [8] we present a numerically verified conjecture that the center-stable manifold of the unstable front solution is the threshold hypersurface separating initial conditions leading to excitation from those that lead to decay.

3.2 Numerical Methods

Our numerics are carried out on the three models that we consider in this work, that is, the ZFK, the FHN and the front equations. These equations are integrated via finite difference discretization techniques based on either explicit Euler forward difference in time or central difference in space or both as the case may be. We use C code for the implementation of all our discretization schemes. We however, sometimes use Maple and/or Matlab for some of our numerical computations, most especially, for verifying the evaluations of the integrals from our analytical studies.

3.2.1 Finite difference approximation schemes

We introduce a grid of equally spaced $x-$ and $t-$ coordinates for the rectangular domain, say, $0 \leq x \leq L$, $0 \leq t \leq T$. The goal is to approximate the *grid values* $Q(x_i, t_j)$. Therefore, we write Q_i^j as a shorthand notation for the numerical approximation of

$Q(x_i, t_j)$ with the *grid points* x_i, t_j chosen as

$$x_i = x_0 + i\,\Delta x,$$
$$t_j = t_0 + j\,\Delta t, \tag{3.1}$$

where Δx, Δt are the spatial and time grid sizes, otherwise known as the discretization steps and $i = 0, 1, \ldots, N$, $j = 0, 1, \ldots, M$ for N, $M > 0$, the *pre-determined numbers* of grid points.

We therefore, discretize our PDEs by replacing the time derivative with the explicit Euler forward difference approximation (a forward difference approximation for first order PDE with respect to time t)

$$\frac{\partial Q_i^j}{\partial t} \approx \frac{Q_i^{j+1} - Q_i^j}{\Delta t}, \quad Q = u,\, v,\, E,\, h, \tag{3.2}$$

and the spatial derivative with the explicit central difference approximation of the second order PDE with respect to x

$$\frac{\partial^2 Q_i^j}{\partial x^2} \approx \frac{Q_{i-1}^j - 2\,Q_i^j + Q_{i+1}^j}{(\Delta x)^2}, \quad Q = u,\, E. \tag{3.3}$$

The discretization schemes in (3.2)-(3.3) give the following discretization formulas:

FHN (ZFK) discretization formulas

The formulas for FHN equations are

$$u_i^{j+1} = u_i^j + \Delta t\, f(u_i^j, v_i^j) + \frac{\Delta t}{(\Delta x)^2}(u_{i-1}^j - 2u_i^j + u_{i+1}^j),$$
$$v_i^{j+1} = v_i^j + \Delta t\, \varepsilon\, g(u_i^j, v_i^j), \tag{3.4}$$

where

$$f(u_i^j, v_i^j) = u_i^j\, (u_i^j - \theta)(1 - u_i^j) - v_i^j \tag{3.5}$$
$$g(u_i^j, v_i^j) = \alpha\, u_i^j - v_i^j. \tag{3.6}$$

Meanwhile, for its initial conditions

$$u_i^0 = u_0 + u_{\text{stim}}\, \Theta(x_{\text{stim}} - x_i),$$
$$v_i^0 = v_0, \tag{3.7}$$

and boundary conditions

$$u_1^0 = u_0^0,$$
$$u_N^0 = u_{N-1}^0,$$
$$u_1^{j+1} = u_0^{j+1},$$
$$u_N^{j+1} = u_{N-1}^{j+1}, \tag{3.8}$$

for $i = 1, \ldots, N-1$, $j = 0, 1, \ldots, M-1$.

Front discretization formulas

The formulas for the front equations are

$$E_i^{j+1} = E_i^j + \Delta t\, F(E_i^j, h_i^j) + \frac{\Delta t}{(\Delta x)^2}(E_{i-1}^j - 2E_i^j + E_{i+1}^j),$$

$$h_i^{j+1} = h_i^j + \Delta t\, \frac{1}{\tau} G(E_i^j, h_i^j), \tag{3.9}$$

where

$$F(E_i^j, h_i^j) = \Theta(E_i^j - 1)\, h_i^j,$$

$$G(E_i^j, h_i^j) = \Theta(-E_i^j) - h_i^j. \tag{3.10}$$

While that of its initial conditions

$$E_i^0 = -\alpha + E_{\text{stim}}\, \Theta(x_{\text{stim}} - x_i),$$

$$h_i^0 = 1, \quad \forall\, x_i, \tag{3.11}$$

and boundary conditions

$$E_1^0 = E_0^0,$$

$$E_N^0 = E_{N-1}^0,$$

$$E_1^{j+1} = E_0^{j+1},$$

$$E_N^{j+1} = E_{N-1}^{j+1}, \tag{3.12}$$

for $i = 1, \ldots, N-1$, $j = 0, 1, \ldots, M-1$. Table (3.1) gives a summary of the parameters that we used for our numerics according to figures

Table 3.1: Parameters used for the numerical simulations

Figure	Parameter values
Fig. 3.1(a, b)	$\varepsilon = 0$, $\theta = 0.13$, $\Delta x = 0.15$, $\Delta t = 0.01$, $L = 120$, $x_{\text{stim}} = 2.10$
Fig. 3.1(c)	$\alpha = 0.37$, $\theta = 0.13$, $\varepsilon = 0(\text{ZFK}), \varepsilon = 0.02(\text{FHN})$, $\Delta x = 0.15$, $\Delta t = 0.01$, $L = 120$
Fig. 3.2	$\alpha = 0.37$, $\theta = 0.13$, $\varepsilon = 0$, $\Delta x = 0.15$, $\Delta t = 0.01$, $L = 15$
Fig. 3.3(a, b)	$\alpha = 0.37$, $\theta = 0.13$, $\varepsilon = 0$, $\Delta x = 0.15$, $\Delta t = 0.01$, $L = 15$
Fig. 3.4	$\alpha = 0.37$, $\theta = 0.13$, $\varepsilon = 0.02$, $\Delta x = 0.15$, $\Delta t = 0.01$, $L = 120$, $x_{\text{stim}} = 2.10(a, b)$, $x_{\text{stim}} = 10.05(c, d)$

Figure	Parameter values
Fig. 3.5	$\alpha = 0.37$, $\theta = 0.13$, $\varepsilon = 0.0094$, $\Delta x = 0.15$, $\Delta t = 0.01$, $L = 60$, $x_{\mathrm{stim}} = 2.10(a, b)$, $x_{\mathrm{stim}} = 10.05(c, d)$
Fig. 3.6(a)	$\alpha = 1, 0.75$, $\tau = 8$, $\Delta x = 0.075$, $\Delta t = 0.0025$, $L = 450$
Fig. 3.6(b)	$\alpha = 1, 0.5$, $\tau = 9$, $\Delta x = 0.075$, $\Delta t = 0.0025$, $L = 450$
Fig. 3.7(a)	$\alpha = 1, 1.5$, $\tau = 10$, $\Delta x = 0.075, 0.15$, $\Delta t = 0.0025, 0.01$, $L = 450$
Fig. 3.7(b)	$\alpha = 0.5, 1, 0.75, 1.5$, $\tau = 8, 9, 10$, $\Delta x = 0.075$, $\Delta t = 0.0025$, $L = 450$
Fig. 3.8	$\alpha = 1$, $\tau = 8.2$, $\Delta x = 0.075$, $\Delta t = 0.0025$, $L = 50$, $x_{\mathrm{stim}} = 0.3$(top panel), $x_{\mathrm{stim}} = 1.5$(bottom panel)
Fig. 3.9	$\alpha = 1$, $\tau = 8.2$, $\Delta x = 0.075$, $\Delta t = 0.0025$, $L = 450$, $x_{\mathrm{stim}} = 1.5$
Fig. 3.10	$\alpha = 1$, $\tau = 8.2$, $\Delta x = 0.075$, $\Delta t = 0.0025$, $L = 450$, $x_{\mathrm{stim}} = 0.3$
Fig. 3.11	$\Delta x = 0.2$, $\Delta t = 0.01$, $L = 40$, $x_{\mathrm{stim}} = 2$
Fig. 4.2	$\Delta t = 0.0025$, $T = 250$, $\alpha = 0.37$

3.2.2   Fitting methods

We have used an implementation of the nonlinear least-squares (NLLS) Marquardt-Levenberg algorithm in Gnuplot for the linear fit in Fig. 3.3(b) and for the nolinear fit in Fig. 4.8(a).

3.3   Initiation problem for the ZFK equation

3.3.1   The critical nucleus

As pointed out earlier in Chapter 2 the theoretical concept of initiation of excitation waves started with the initiation problem for the ZFK equation, which is the reduced form of the FHN system when $\varepsilon \to 0$, $v = 0$

$$\frac{\partial u}{\partial t} = \frac{\partial^2 u}{\partial x^2} + f(u), \quad (x, t) \in [0, +\infty) \times [0, +\infty), \tag{3.13}$$

where $f(u) = u\,(u - \theta)\,(1 - u)$.

The initiation problem consists of (3.13), the boundary and initial conditions

$$\frac{\partial u}{\partial x}(0, t) = 0, \quad t \in [0, +\infty),$$
$$u(x, 0) = u_{\mathrm{stim}} \Theta(x_{\mathrm{stim}} - x), \quad x \in [0, +\infty), \tag{3.14}$$

where Θ is a Heaviside step function, u_{stim} and x_{stim} are respectively the threshold potential (*excitation amplitude*) and *width* of the excited region.

Fig. 3.1 (a,b) shows two typical results for the ZFK initiation process: a successful initiation, leading to generation of a propagating front, and an unsuccessful initiation,
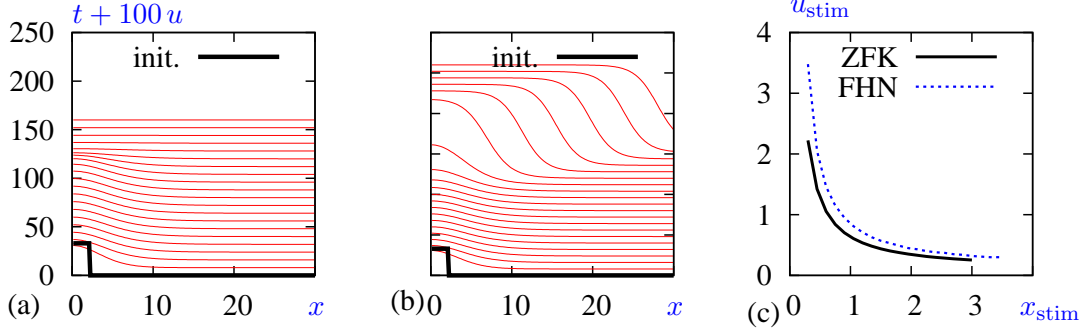
Figure 3.1: Initiation of excitation in ZFK equation. (a,b) Fast subsystem (3.13, 3.14) "ZFK" of "FHN" (2.15): for parameters values: $\alpha = 0.37$, $\theta = 0.13$, $\varepsilon = 0$. Stimulation parameters: $x_{\text{stim}} = 2.10$ for both, subthreshold $u_{\text{stim}} = 0.3304831$ for (a) and superthreshold $u_{\text{stim}} = 0.3304833$ for (b). Bold black lines: initial conditions. (c) The corresponding critical curves, separating initiation initial conditions from decay initial conditions.

leading to decay of excitation in the whole half-fibre into the resting state. The ZFK problem has a critical pulse as its non-constant solution which is stationary. Moreover, if a continuous one-parametric family of initial conditions contains some that initiate a wave and some that lead to decay, there is always at least one that does neither, but gives a solution that approaches the critical nucleus. This critical nucleus is the same for all such families, that is, it does not depend on the shape of the initial distribution $u(x, 0)$, as long as its amplitude is at the threshold corresponding to that shape. Initial conditions very close to the threshold generate solutions which approach the critical nucleus and then depart from it, either toward propagation or toward decay. This transient stationary state can be seen in Fig. 3.1(a,b) where the initial conditions are selected very close to the threshold.

The theoretical understanding of excitability stems from FitzHugh's simplified model of a nerve membrane [33]. One of his key concepts is "quasi-threshold", which gets precise in the limit of large time scale separation between the processes of excitation and recovery. Then the fast subsystem has unstable "threshold" equilibria; initial conditions below such an equilibrium lead to decay, and those above it to propagation (excitation).

In a spatially extended FHN system [33, 67, 71, 28, 27] the ability of a stimulus to initiate a wave depends on its spatial extent, the aspect summarized by Ruston's concept of "liminal length" [81, 71, 15]. A more generic concept is that of the "critical curve" in the stimulus-spatial extent plane (see Fig. 3.1(c)). A stimulus initiates a wave if its parameters are above this curve or decays if below.

Mathematically, the problem is about classification of initial conditions that will or will not lead to a traveling (excitation) wave solution. The key question is the nature

of the boundary between the two classes. A detailed analysis of which has been done for the FitzHugh-Nagumo system and its variations.

In particular, if initial condition $u(x, 0) < u_{cr}(x)$, $x \in [0, \infty)$ then $u(x, t)$ decays as $t \to \infty$, and if $u(x, 0) > u_{cr}(x)$, $x \in [0, \infty)$ then $u(x, t)$ approaches a stable propagating front solution. The center-stable manifold of the "critical nucleus" is the threshold surface separating initiation initial conditions and decay initial conditions. Roughly, this is a spatially extended analogue of a threshold equilibrium in the point system; critical nucleus is also a stationary but unstable solution, and its small perturbation lead to either initiation of excitation wave, for perturbations in one direction, or to decay, for perturbations in the opposite direction.

3.3.2 Numerical critical nuclei

The values of the parameters used for the numerics are $\theta = 0.13$, $\varepsilon = 0$ and $\alpha = 0.37$. The spatial distributions of the potential u are constructed based on a one-dimensional fibre model of length $L = 15$ and a predetermined value of time t given by $T = 200$ with no flux boundary conditions. The evolution of u is computed from (3.13) with the initial conditions $u_0(x)$ as given by (3.14). The PDE for u was solved using the method of forward differences in time and central differences in space with a time step $\Delta t = 0.01$ and the fibre discretized with $\Delta x = 0.15$.
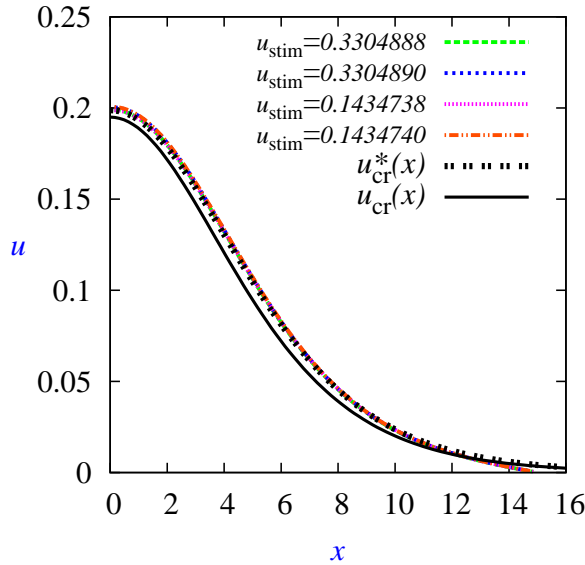
Figure 3.2: Plot of solutions (2.27, 2.28), the analytical critical nucleus $u_{cr}(x)$ due to Neu [68] shown as the black solid curve and $u_{cr}^*(x)$ represented by the black-dashed curve, the analytical critical nucleus for cubic nonlinearity compared with the four extracted numerical nuclei (shown in other colors).

Four numerical critical nuclei (shown in Fig. 3.2) were extracted by means of the minimal distance $\mathscr{D}(t)$ between two consecutive voltage profiles in L_2 norm. The min-

imal distance is an indicator for the slowest voltage profile $u(x, t)$ which approximates the critical nucleus. The computation of the minimal distance between consecutive voltage profiles is achieved using the following discretization formula

$$\mathscr{D}(t) = \sum_x |u(x, t + dt) - u(x, t)|^2, \tag{3.15}$$

where the right-hand side of (3.15) is equivalent to (3.16) as given in terms of continuous functions

$$\lim_{\substack{dt \to 0 \\ dx \to 0}} \int_0^\infty |\frac{\partial u(x, t)}{\partial t} \ dt|^2 \ dx = (dt)^2 \int_0^\infty |\frac{\partial u(x, t)}{\partial t}|^2 \ dx. \tag{3.16}$$

The computation is done by fixing x_{stim}, the excitation width, as the excitation amplitude u_{stim} is varied (see (3.14)). Two values, $x_{\text{stim}} = 2.10, \ 10.05$ which respectively represent subthreshold and superthreshold $u_0(x)$. In each case both the lower and upper bounds for u_{stim} are determined. The lower and upper bounds for the excitation amplitude u_{stim} that correspond to $x_{\text{stim}} = 2.10$ are respectively, 0.3304888, 0.3304890 and that of $x_{\text{stim}} = 10.05$ are 0.1434738, 0.1434740.

The original values for the excitation amplitude had four digits which were later extended to seven significant digits in order to improve the accuracy of the numerics. Such a high precision is needed as the solution we are looking for is unstable, in that the slightest change in initial conditions brings with it a significant change in the solution. When initial condition chosen is very close to the excitation threshold, we see a solution (with bell-shape) developing toward the critical nucleus and which after some time interval either decays to zero or propagates (i.e. excites). This critical nucleus corresponds to the saddle point which has a codimension-1 stable manifold and 1D-unstable manifold. The stable manifold of the saddle point acts as a separatrix that separates its two basins of attraction. In other words, the separatrix divides the phase plane into two regions, one of decay and the other of excitation (i.e. a region with *no excitation* and *excitation* respectively).

Initial pulses below the separatrix decay to zero with larger time and those pulses above the separatrix give rise to propagating wavefronts. The former are initial conditions that fail to start propagation while the latter are those that succeed in starting propagation.

In [34], it has been established that the Nagumo equation (3.13) has three relevant stationary solutions: 0, 1, and a standing wave $u(x)$. The constant states are stable, while the standing wave is a saddle of index 1 (i.e having a codimension 1 stable manifold) and thus corresponds to our critical nucleus. The stable manifold is sometimes called a nucleation manifold or ignition manifold [2, 3].

Excitation threshold curve for ZFK equation

The excitation threshold curve is a plot of the stimulus strength (excitation amplitude) and the width of excited region. It is the curve that separates the region when the wave just propagates (i.e. excites) and when it just diffuses (i.e. no propagation).

(a)   (b)
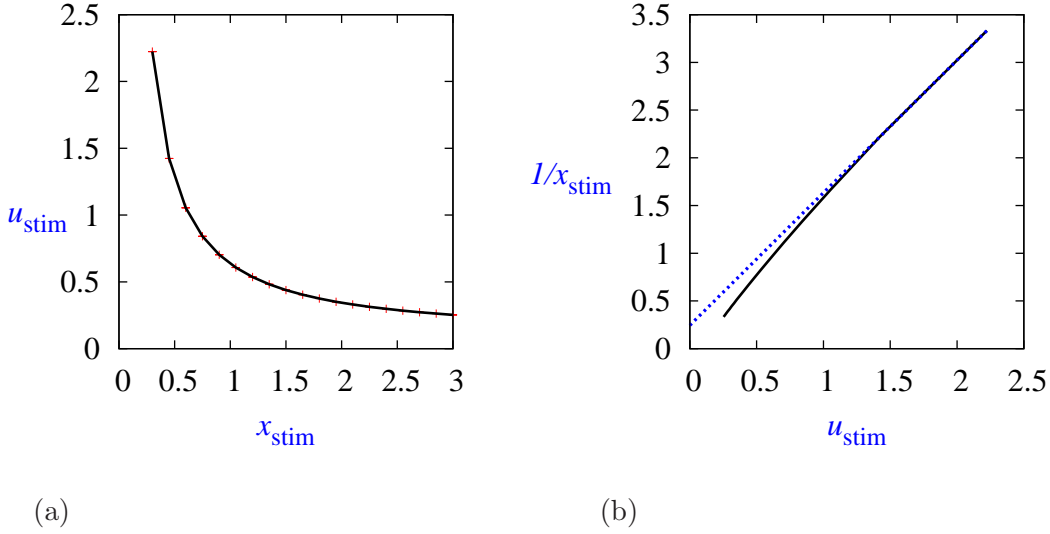
Figure 3.3: (a) The excitation amplitude u_{stim} as a function of the length of the excited region x_{stim} plotted using errorbars with 10^{-7} precision. (b) The excitation threshold curve (the separatrix of the critical nucleus) confirming that $u_{\text{stim}} \propto k$ as $k \to \infty$ [68], where $k = 1/x_{\text{stim}}$; that is, as $x_{\text{stim}} \to 0$ the separatrix can be fitted with a straight line.

Fig. 3.3 suggests that corresponding to certain excitation amplitude (chosen as initial conditions) a length of excited region is required in order to initiate propagation. This has confirmed the prediction by Neu and his co-workers [68] that for a specific pulse width, the separatrix determines the minimum amplitude necessary to start propagation and that infinitely broad pulses require amplitude equal to the membrane excitation threshold. In addition, as the width of the pulses decreases, the requirement on the amplitude grows.

Now plotting the inverse of the length of the excited region $1/x_{\text{stim}}$ which is given by k in [68] against the excitation amplitude u_{stim}, we obtain the excitation threshold curve as in Fig. 3.3 (b) where we see that despite the fact that rectangular initial conditions are used instead of the Gaussian one, yet we observe the same qualitative property as predicted in [68]: In the limit of very narrow pulses (very small excitation width), the pulse width and the amplitude are related by a linear relationship corresponding to a constant charge developed by the pulse (i.e $u_{\text{stim}} \propto k$ as $k \to \infty$, where $k = 1/x_{\text{stim}}$). In other words, in the limit of a very large k the separatrix as represented in the 2D-manifold of initial conditions looks like a straight line.

3.4 Initiation problem for the FHN system

3.4.1 The critical pulse

We consider the problem of initiation of propagating waves in a one-dimensional excitable fibre by considering the FHN system in the form

$$\frac{\partial u}{\partial t} = \frac{\partial^2 u}{\partial x^2} + f(u) - v,$$
$$\frac{\partial v}{\partial t} = \varepsilon\,(\alpha u - v), \tag{3.17}$$

where $(x, t) \in [0, \infty) \times [0, \infty)$ with no-flux boundary conditions

$$\frac{\partial u}{\partial x}(0, t) = 0, \quad t \in [0, \infty), \tag{3.18}$$

and a rectangular initial perturbation of width x_{stim} and amplitude u_{stim},

$$u(x, 0) = u_{\text{stim}}\Theta\,(x_{\text{stim}} - x),$$
$$v(x, 0) = 0, \quad x \in [0, \infty), \tag{3.19}$$

where $f(u) = u\,(u - \theta)\,(1 - u)$, $\varepsilon > 0$, $\alpha > 0$, $\theta \in (0, 1/2)$ and Θ a Heaviside step function.

For small $\varepsilon > 0$, system (3.17) does not have nontrivial stationary solutions, but has an unstable propagating pulse solution $\tilde{u}_{\text{cr}}(x - ct)$, $\tilde{v}_{\text{cr}}(x - ct)$ such that $\tilde{u}_{\text{cr}}(x) \to u_{\text{cr}}(x)$, $\tilde{v}_{\text{cr}}(x) \to 0$ and $c = \mathcal{O}\left(\varepsilon^{1/2}\right)$ as $\varepsilon \searrow 0$. This solution also has a single unstable eigenvalue [34, 35, 98, 2, 53, 3], and so its center-stable manifold is the threshold hypersurface (see [62] for a different treatment) dividing the phase space into the decay domain and the initiation domain. So, here we have a *critical pulse* solution, which is essentially a slowly traveling variant of the critical nucleus. Any solution with the initial condition at the threshold hypersurface asymptotically approaches this critical pulse (suitably shifted), and any solution starting close to the threshold approaches this critical pulse as a transient. This is illustrated in Fig. 3.4.

For much smaller value of the parameter ε, the results are shown in Fig. 3.5. With this understanding, the excitation condition in terms of $(x_{\text{stim}}, u_{\text{stim}})$ reduces to computing the intersection of the two-parametric manifold described by (3.19) with the codimension 1 stable (center-stable) manifold of the critical nucleus (critical pulse). This gives the curve on the $(x_{\text{stim}}, u_{\text{stim}})$ plane separating initial conditions leading to excitation propagation from those leading to decay. This can be done numerically or, with appropriate simplifications, analytically. An example of dealing with this problem in the ZFK equation, using Galerkin style approximations can be found in [68] (see also Sec. 2.5.2 and figure Fig. 2.6(b)). We present some further approaches below, in Sec. 4.1 and Sec. 5.2.
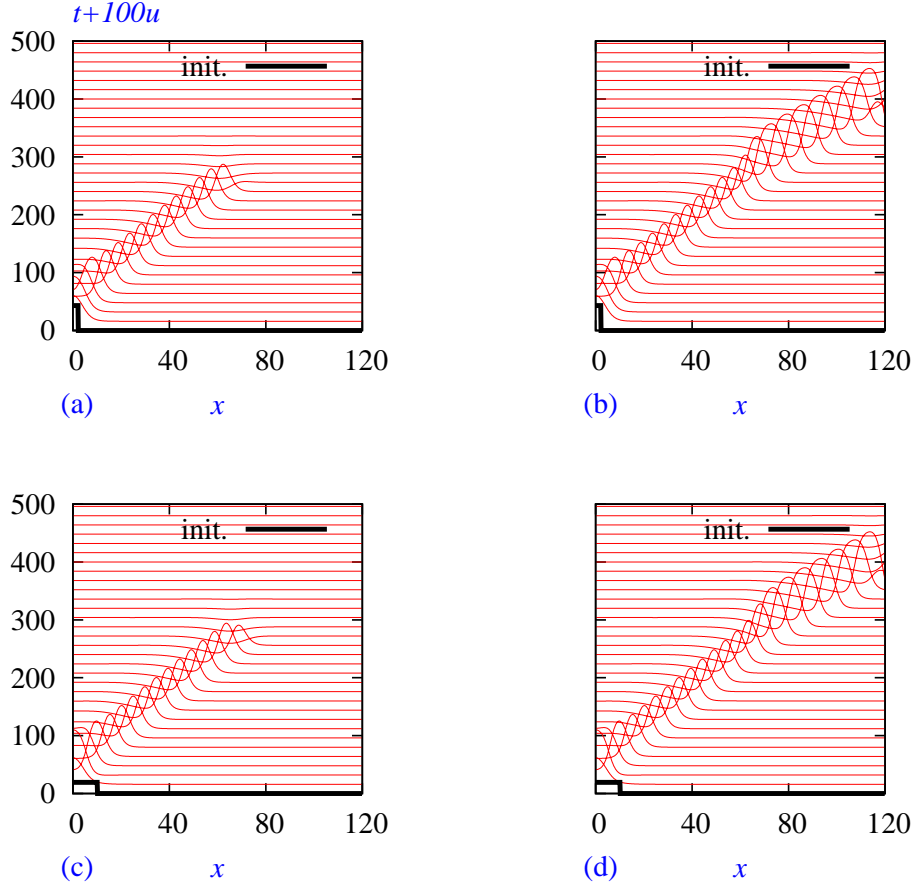
Figure 3.4: The critical pulse is a universal transient for any near-threshold initial condition. The solutions to (3.17) for slightly sub-threshold (a,c) and slightly super-threshold (b,d) amplitudes, for smaller stimulus width $x_{\text{stim}} = 2.10$ in (a,b) and larger $x_{\text{stim}} = 10.05$ in (c,d). Parameter values: $\varepsilon = 0.02$, $\alpha = 0.37$, $\Delta t = 0.01$, $\Delta x = 0.15$, $L = 120$. Bold black lines: initial conditions. In all cases we see a slow, low-amplitude unstable propagating pulse which subsequently either decays or evolves into a fast, high-amplitude stable propagating pulse [45].

3.5 Initiation problem for the front model

3.5.1 The critical front

Now consider the simplified model of I_{Na}-driven excitation fronts in typical cardiac excitation models [8]

$$\frac{\partial E}{\partial t} = \frac{\partial^2 E}{\partial x^2} + F(E, h),$$
$$\frac{\partial h}{\partial t} = (1/\tau)G(E, h), \quad (x, t) \in (-\infty, +\infty) \times [0, +\infty), \tag{3.20}$$

where

$$F(E, h) = \Theta(E - 1)h,$$
$$G(E, h) = \Theta(-E) - h, \tag{3.21}$$
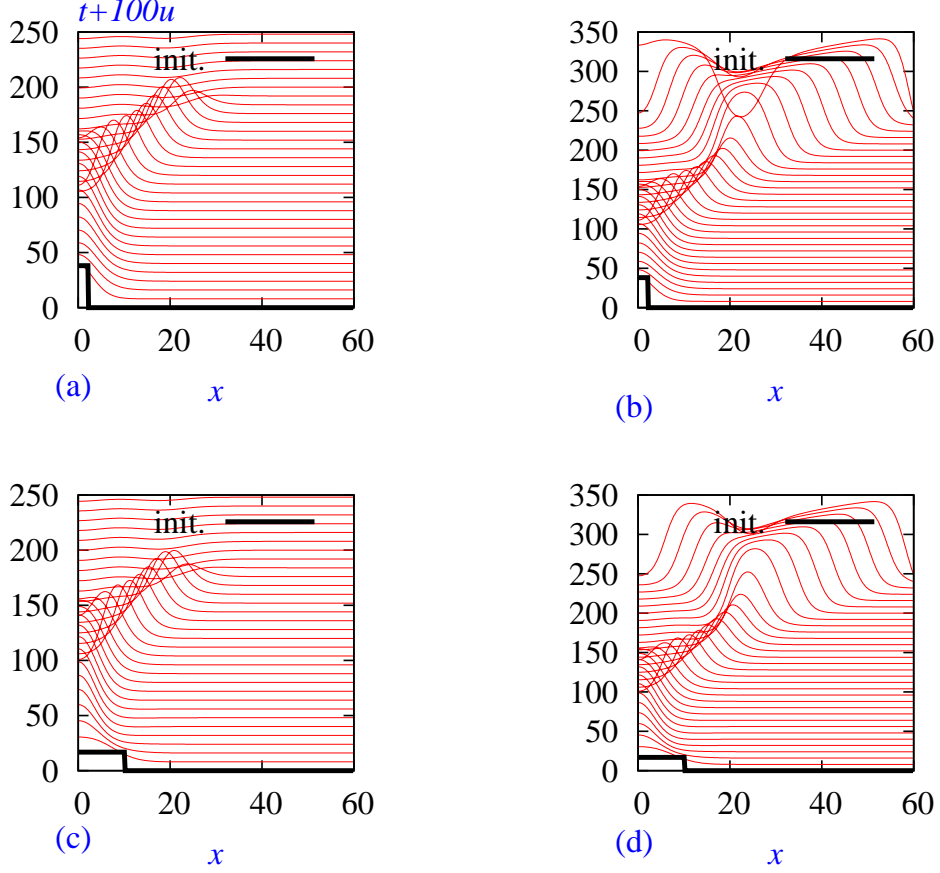
Figure 3.5: The *critical pulse* solutions to the FHN system (3.17) for parameter values: $\varepsilon = 0.0094, \alpha = 0.37, \Delta t = 0.01, \Delta x = 0.15$. Top panels: $x_{\mathrm{stim}} = 2.10$ (a) $u_{\mathrm{stim}} = 0.380723412971864$, (b) $u_{\mathrm{stim}} = 0.380723412971866$. Bottom panels: $x_{\mathrm{stim}} = 10.05$ (c) $u_{\mathrm{stim}} = 0.168543917244412$, (d) $u_{\mathrm{stim}} = 0.168543917244414$. (a) & (c) for slightly-below threshold initial conditions (b) & (d) for slightly-above threshold initial conditions [45].

and Θ is a Heaviside function with boundary condition

$$\frac{\partial E}{\partial x}(0, t) = 0, \quad t \in [0, +\infty), \tag{3.22}$$

and initial conditions

$$E(x, 0) = -\alpha + E_{\mathrm{stim}}\Theta(x_{\mathrm{stim}} - x),$$
$$h(x, 0) = 1, \quad x \in (-\infty, +\infty). \tag{3.23}$$

System (3.20) does not have nontrivial bounded stationary solutions: if $\dfrac{\partial E}{\partial t} = \dfrac{\partial h}{\partial t} = 0$ then any bounded solution has the form $E = a$, $h = \Theta(-a)$ for some $a = $ const. So, *there are no critical nuclei* in this system. Nevertheless, system (3.20) is known to develop stable propagating wave solutions from some initial conditions but not from others, and there should therefore be a threshold, i.e. a boundary in the phase space of (3.20, 3.23) between initial conditions leading to initiation and those leading to

decay. Hence the question, what happens when the initial conditions are exactly at the threshold? We answer this question shortly. Meanwhile, we note that system (3.20) has a family of propagating front solutions

$$
E(z) = \begin{cases} \omega - \dfrac{\tau^2 c^2}{1 + \tau c^2} \exp\left(\dfrac{z}{\tau c}\right), & (z \le -\Delta), \\ -\alpha + \alpha \exp(-cz), & (z \ge -\Delta), \end{cases}
$$

$$
h(z) = \begin{cases} \exp\left(\dfrac{z}{\tau c}\right), & (z \le 0), \\ 1, & (z \ge 0), \end{cases} \tag{3.24}
$$

where $z = x - ct$, $\omega = 1 + \tau c^2 (1 + \alpha)$, $\Delta = \dfrac{1}{c} \ln\left(\dfrac{1 + \alpha}{\alpha}\right)$.

3.5.2 Numerical Results for the front model

Our numerics were carried out via the finite differencing method using forward differences in time and central difference in space implemented using a C code. The time step and space steps for the numerical integration were $\Delta t = 0.0025, \Delta x = 0.075$ but only used $\Delta t = 0.01, \Delta x = 0.15$ once to check our discretization steps. In the simulations the model parameters were τ, α and the admissible values for the pair chosen so that propagation would be possible.

Threshold curves for the front model

The threshold curve that determines the parameter region for E_{stim}, x_{stim}, the parametric set of initial conditions, is the curve which sets conditions for the success or failure of propagation in the simplified cardiac front model. In our case we obtain threshold curves for different admissible pairs of the numerical parameters τ, α where the front model is simulated with the following pairs. The threshold curves for $\tau = 8$, $\alpha = 1$, 0.75; $\tau = 9$, $\alpha = 1$, 0.5; and $\tau = 10$, $\alpha = 1$, 1.5 are respectively given in Fig. 3.6 and Fig. 3.7. The solid black curves are for $\alpha = 1$ while the dashed blue are for other values of α. Note also that the asymptotic threshold value for the voltage, E_{asym} is $\alpha + 1$ which is represented by the dashed cyan line as shown in Fig. 3.7(b).

The threshold curves in Fig. 3.7 are calculated with the same values of parameters as used in Fig. 3.6 but only with different spatial and time steps, $\Delta t = 0.01, \Delta x = 0.15$ and different τ. The lack of any conspicuous error suggest that our discretization steps in space and time are not crude.

From the plot given in Fig. 3.7(b) we can easily deduce that the dependence of the asymptotic threshold (rheobase), E_{asym} on the pre-frontal voltage α is linear and is given by the relation $E_{\text{asym}} = \alpha + 1$ which is represented by the red solid line.
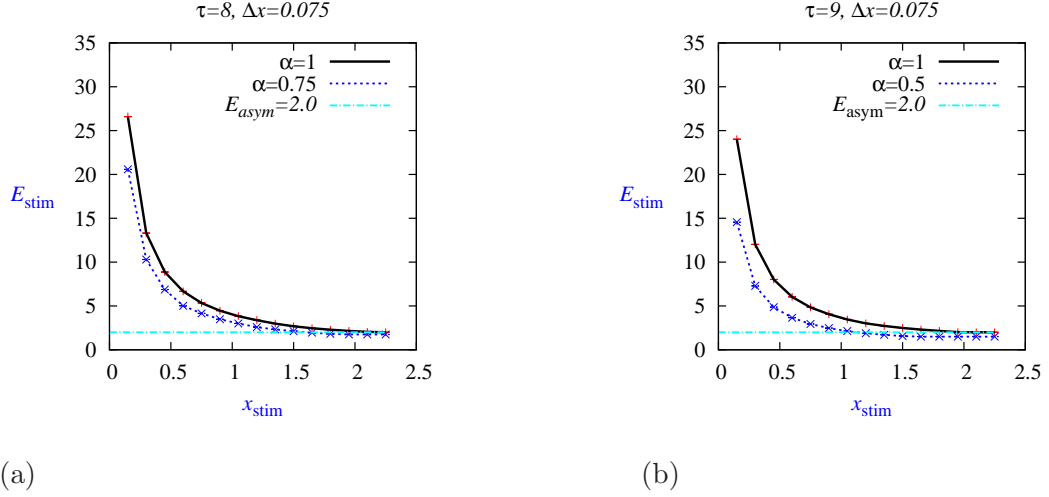
Figure 3.6: The threshold curves plotted with errorbars and represented by the solid black line and dashed blue line respectively for $\alpha = 1$ and $\alpha = 0.75,\ 0.5$: (a) $\tau = 8$ (b) $\tau = 9$. The dashed cyan represent the asymptotic threshold voltage for $\alpha = 1$.
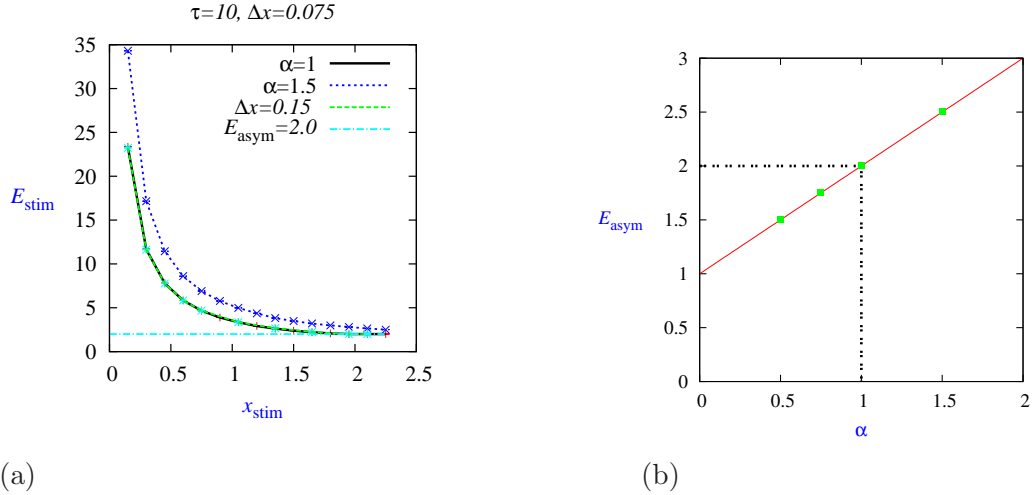
Figure 3.7: (a) The threshold curves for $\tau = 10$ plotted with errorbars and represented by the solid black line and dashed blue line respectively for $\alpha = 1$ and $\alpha = 1.5$. The dashed green line is for $\alpha = 1$ but with spatial discretization step reduced by two fold compared to that in Fig. 3.6. The dashed green line exactly coincide with the solid black curve indicative of the non crude nature of our discretization steps. (b) Asymptotic threshold E_{asym} (when $x_{\mathrm{stim}} \to \infty$) against pre-frontal voltage α: the large green dots are values from points simulation. The asymptotic threshold voltage (rheobase), $E_{\mathrm{asym}} = 2$ is for the pre-frontal voltage $\alpha = 1$.

There is numerical and analytical evidences that solutions with $c = c_+$ (higher speed) are stable and those with $c = c_-$ (lower speed) are unstable with one positive eigenvalue (see Sec. 2.4.1) [8, 43]. Hence by analogy with the FHN system, we propose the following:

***Conjecture:* 1** *The center-stable manifold of the unstable front solution (3.24) with $c = c_-(\alpha, \tau)$ is the threshold hypersurface, separating the initial conditions leading to*

initiation from the initial conditions leading to decay.

An "experimentally testable" consequence of this conjecture is that for any initial conditions exactly at the threshold, the solution will approaches the unstable front as $t \to +\infty$. For any initial condition near to the threshold, the solution comes close to the unstable front and stays in its vicinity for a long time: if the positive eigenvalue is λ and the initial condition is δ-close to the threshold, the transient front should be observed for the time $\propto \lambda^{-1}|\ln \delta|$. This transient front solution *does not depend on the initial condition*, as long as the initial condition is at the threshold.
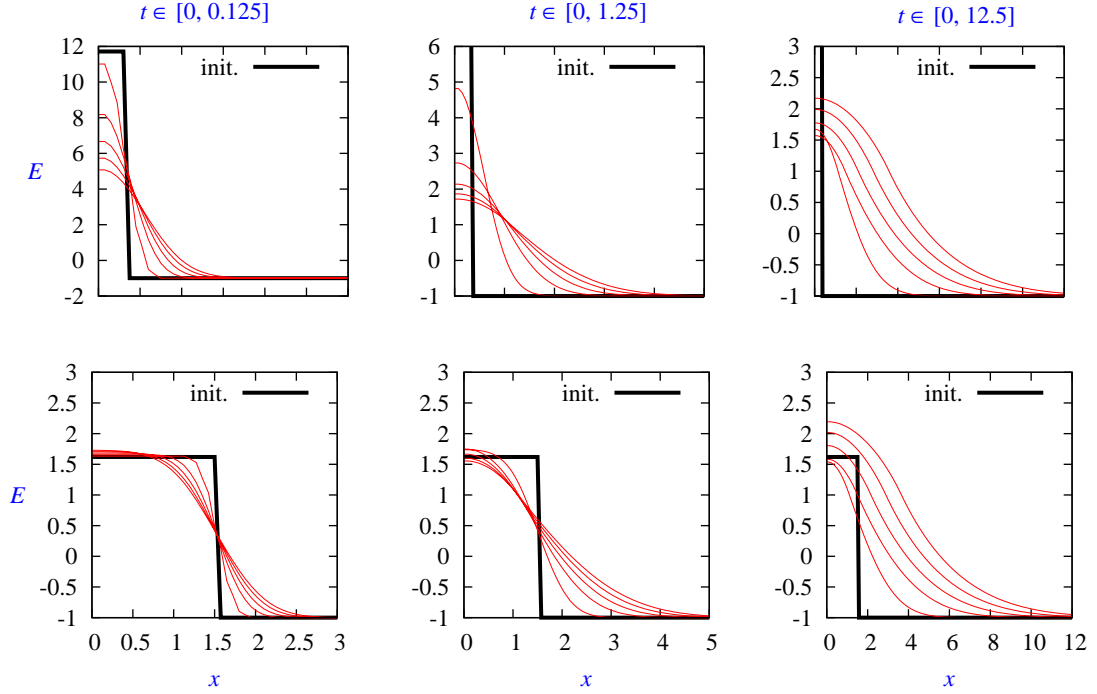
Figure 3.8: Evolution of two different near-threshold initial conditions toward the critical front solution in system (3.20). Initial stimuli: $x_{\text{stim}} = 0.3$, $E_{\text{stim}} = 12.716330706144868$ (upper row) and $x_{\text{stim}} = 1.5$, $E_{\text{stim}} = 2.619968799545055$ (lower row). Other parameters: $\tau = 8.2$, $\alpha = 1$, $\Delta x = 0.075$, $\Delta t = 0.0025$, $L = 50$ [45].

We have tested these predictions by numerical simulation of (3.20, 3.22, 3.23). The results are shown in Fig. 3.8 and Fig. 3.9. Fig. 3.8 illustrates two solutions starting from initial conditions with different x_{stim}. In both cases, E_{stim} values have been chosen close to the respective threshold with high precision. In both cases, the solutions evolve in the long run toward the same propagating front. Fig. 3.9 presents an analysis of a pair of solutions, one with slightly overthreshold and the other with slightly underthreshold initial conditions. To separate the evolution of the front shape from its movement, we employ the idea of symmetry group decomposition with explicit representation of the orbit manifold (see e.g. [11]). Practically, we define the front point $x_f = x_f(t)$ via

$$E(x_f(t), t) = E_*, \tag{3.25}$$

for some constant E_* which is guaranteed to be represented exactly once in the front at every instant of time (we have chosen $E_* = 0$). Then $E(x - x_f(t), t)$ gives the voltage profile "in the standard position", and $x_f(t)$ describes the movement of this profile.
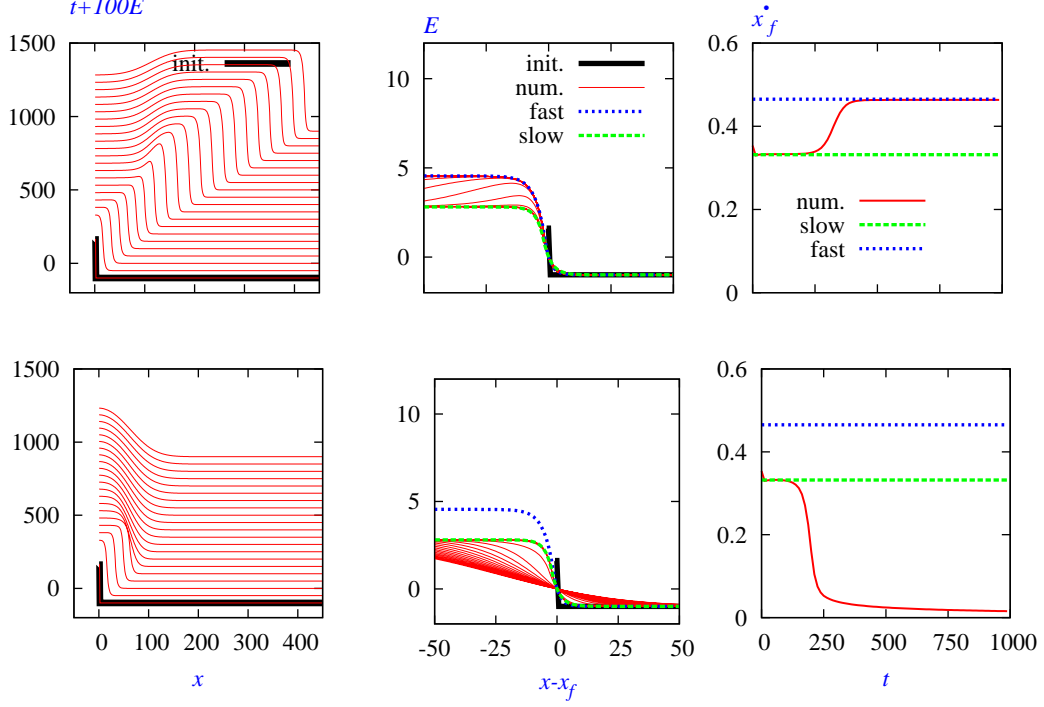
Figure 3.9: Transient "critical fronts" are close to the unstable front solution of (3.20). Initial conditions: $x_{\text{stim}} = 1.5$, with $E_{\text{stim}} = 2.619968799545055$ in the upper row and $E_{\text{stim}} = 2.619968799545054$ in the lower row, other parameters the same as in Fig. 3.8. Left column: evolution of the E profiles in the laboratory frame of reference. Middle column: same evolution, in the frame of reference comoving with the front. Right column: Speed of the front. Blue/green dashed lines in the middle and right columns correspond to the exact fast/slow front solutions of (3.20) [45].

The predictions based on the Conjecture are that the voltage profiles should, after an initial transient depending on the initial condition, approach the profile of the slow unstable front solution given by (3.24) with $c = c_-(\tau, \alpha)$ and stay close to it for some time, before either developing into the fast stable front (3.24) with $c = c_+(\tau, \alpha)$ or decaying. Likewise, the speed of the fronts should, after an initial transient, be close to the speed of the slow unstable front $c_-(\tau, \alpha)$, before either switching the speed of the fast stable front $c_+(\tau, \alpha)$ or dropping to zero. This is precisely what is seen on Fig. 3.9, where we have taken advantage of knowing the exact solutions $E(x - c_\pm t)$ and $c_\pm$ for both the fast and the slow fronts.

Initial conditions with different x_{stim} and E_{stim} close to the corresponding threshold, produce the same picture with the exception of the initial transient. We have also checked that length of the time period during which the solution stays close to the unstable front is, roughly, a linear function of the number of correct decimal figures in

E_{stim}, as it should be according to the Conjecture.
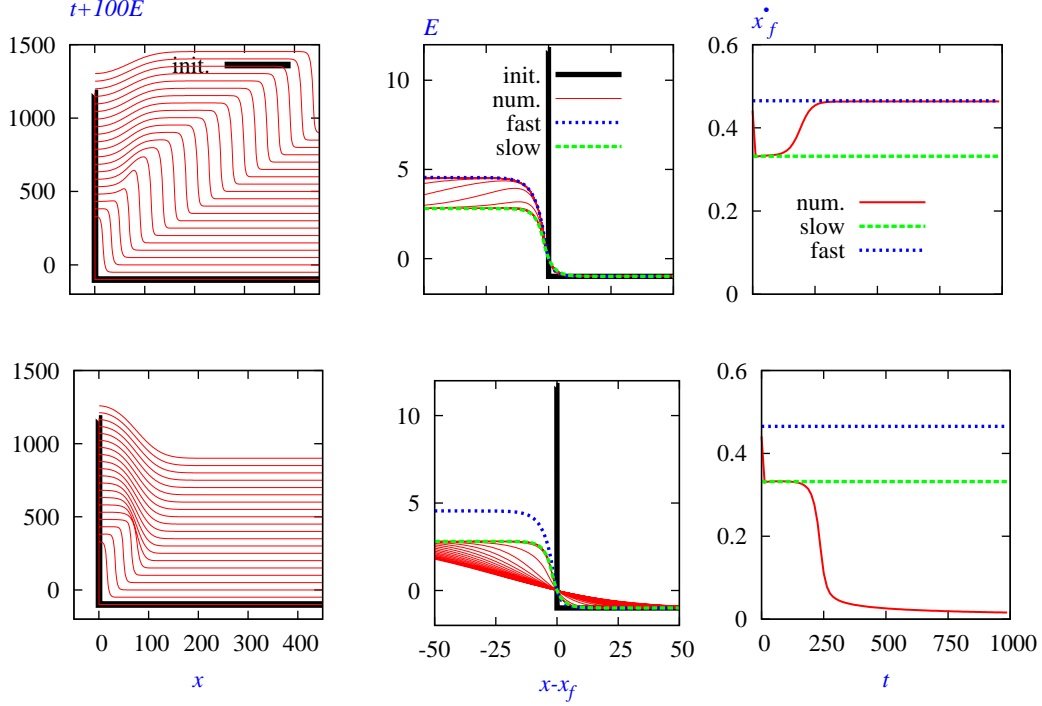
Figure 3.10: Transient "critical fronts" are close to the unstable front solution of (3.20). Initial conditions: $x_{\mathrm{stim}} = 0.3$, with $E_{\mathrm{stim}} = 12.716330706144868$ in the upper row and $E_{\mathrm{stim}} = 12.716330706144867$ in the lower row, other parameters the same as in Fig. 3.8. Left column: evolution of the E profiles in the laboratory frame of reference. Middle column: same evolution, in the frame of reference comoving with the front. Right column: Speed of the front. Blue/green dashed lines in the middle and right columns correspond to the exact fast/slow front solutions of (3.20) [45].

3.5.3 Detailed cardiac excitation model

The simplified front model (3.20, 3.21) has many peculiar qualitative features which stemmed from the nonstandard asymptotic embedding leading to it. Quantitatively, however, it is very far from any realistic ionic model of cardiac excitation. Hence, the newly described phenomena of *critical front* could be an artifact which might have been brought about by the simplifications.

To eliminate this possibility, we have tested the relevance of the critical concept in a full ionic model of cardiac excitation. We have chosen the model of human atrial tissue due to Courtmanche, Ramirez and Nattel (CRN) [25], which is less stiff than most stereotypical ventricular or Purkinje fibre model. It is well formulated in mathematical sense and is also popular among cardiac modelers. The model operates with 21 dynamic variables including the transmembrane voltage V. We have used the default parameters as described in [25] and supplemented the equation for V in the system of equations

with a diffusion term $D\dfrac{\partial^2 V}{\partial x^2}$. Noting that the spatial scale is not important to the question at hand, we assumed $D = 1$. Thus, the initial condition for V were taken in the form

$$V(x, 0) = V_r + V_{\text{stim}}\,\Theta(x_{\text{stim}} - x), \qquad (3.26)$$

where $V_r = -81.18$ mV is the standard resting potential, and for all other 20 variables at their resting values as described in [25].
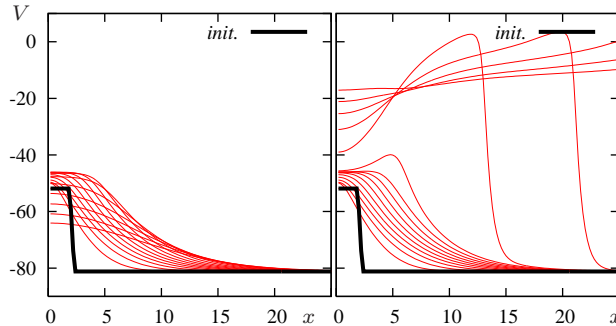
Figure 3.11: Critical fronts in CRN model [25]. Shown are voltage profiles in every 10 ms. Parameter values: $\Delta t = 0.01$ ms, $\Delta x = 0.2$, $L = 40$, the length unit chosen so that voltage diffusion coefficient equals 1. Stimulus witdh $x_{\text{stim}} = 2$, stimulus amplitudes: $V_{\text{stim}} = 29.31542299307152$ mV (left panel) and $V_{\text{stim}} = 29.31542299307153$ mV (right panel). The critical fronts are formed within first 10 ms and then are seen for subsequent 80 ms on both panels before exploding into an excitation wave of much bigger amplitude and speed on the right panel, and decaying on the left panel [45].

Fig. 3.11 illustrates a pair of solutions with initial conditions slightly above and slightly below the threshold. The critical front solution is clearly seen there: it has the upper voltage of about -46 mV and during 80 ms of its existence propagates with a speed approximately 0.06 space units per millisecond. Then for the above-critical case it develops into an excitation front with maximal voltage about +3 mV and speed 0.8 space units per millisecond, and decays for the below-critical case.

Mathematically, the post-front voltage of about -46 mV observed in Fig. 3.11 is not a true equilibrium of the full CRN model, so the critical front can only be an asymptotic concept in an appropriate asymptotic embedding, say as ones described in [12] or [77], and the observed critical front may well be the front of a critical pulse solution in the full model. However Fig. 3.11 demonstrates that the critical front is a practical and well-working concept even for the full model, unlike the critical pulse, which may be theoretically existing, but practically unobservable: notice the number of significant decimal digits in initial conditions required to produce only the critical front observed for 80 ms and recall that the number of decimals is roughly proportional to the duration of the observation of an unstable solution.

3.6   Summary

- We have developed a numerical procedure for identifying critical nucleus in an excitable model by means of finding the minimal value of the L_2-norm of the time derivative of a solution with near-threshold initial conditions. This has been tested on the ZFK equation for which the critical nucleus solution is known exactly.

- Our numerical critical curves confirm the prediction from the approximate analytical theory by Neu *et al.* [68] about inverse proportionality of critical stimulus amplitude to its width.

- We presented numerical evidence that the role of the "critical nucleus" as for ZFK equation is being played by its slowly moving variant, the "critical pulse" for FHN system, which is consistent with the theoretical results by Flores [35, 57]. The critical pulse is an unstable propagating pulse whose center-stable manifold is the threshold hypersurface dividing the phase space into excitation and decay regions. We showed that any solution with initial conditions at the threshold approach this "critical pulse" asymptotically as a transient. In other words, the critical pulse plays the role of an attractor on the critical manifold. This is found to be the case even with different nonzero values for the small parameter solution.

- In the case of the simplified front model, we have observed through numerics that the relationship between the asymptotic voltage (rheobase), E_{asym} and the pre-frontal voltage α is found to be $E_{\mathrm{asym}} = \alpha + 1$, which means that at very large stimulus width, the stimulus amplitude should be such that it opens the m-gates (see Sec. 2.4). This revelation will among other things assist us to check the analytical ignition criteria that we seek to find.

- We have demonstrated that neither critical nucleus nor critical pulse concepts are applicable to the front model. We have conjectured that the role of the critical solution is played by the unstable front solutions which were known to exist in this model. We have confirmed this "critical front" conjecture by numerical simulation. That is, we presented numerical evidence that the center-stable manifold of the unstable front solution in the simplified cardiac model is the threshold hypersurface that separate excitation initial conditions from decay initial conditions. This is found to be always true no matter the nature of the initial stimulus we consider provided it is chosen at the threshold.

Table 3.2: Glossary of notations for Chapter 3

Notation	Explanation(s): bf=before, af=after	Place introduced
α	constant	Fig. 3.1
α	pre-frontal voltage	(3.23)
ω	post-frontal voltage	(3.24)
ε	ratio of the reaction rates	Sec. 3.1
δ	distance between the initial condition and the threshold surface	af(Con. 1)
λ	positive eigenvalue of the unstable front	af(Con. 1)
Θ	Heaviside step function	(3.14)
θ	threshold parameter	af (3.13)
τ	parameter	(3.20)
$\mathscr{D}$	L_2-distance between consecutive voltage profiles	(3.15)
a	constant	af (3.23)
$c : c_-, c_+$	speed:lower, higher	af(3.25): bf(Con. 1)
D	diffusion coefficient	bf (3.26)
E_*	constant	(3.25)
E, h	dynamic variable: Voltage, gate variable	(3.20)
E_{asym}	rheobase	Sec. 3.5.2
E_{stim}	stimulus amplitude	(3.23)
f	nonlinear function	(3.13)
F, G	nonlinear function	(3.20)
I_{Na}	Na^+ current	bf (3.20)
u_{cr}	critical nucleus for the quadratic nonlinearity	Sec. 3.3.1
u_{cr}^*	critical nucleus for the cubic nonlinearity	Fig. 3.2
$\tilde{u}_{\mathrm{cr}}, \tilde{v}_{\mathrm{cr}}$	critical pulse	af (3.19)
V	transmembrane voltage [25]	bf/in (3.26)
V_r	resting potential [25]	bf/in (3.26)
u, v	dynamic variable	(3.13, 3.17)
$x_{\mathrm{stim}}, u_{\mathrm{stim}}$	stimulus: width, amplitude	(3.14)
x_f	front position	(3.25)

Chapter 4

Analysis of variational approximations to initiation problems

4.1 ZFK equation

4.1.1 Piece-wise smooth ansatzes

In Sec. 2.5.2, we have reproduced results by Neu *et al.* [68] on a variational approximation to the initiation problem for the ZFK equation, using the method of minimization of the residual, which is close to that used by Neu *et al.* themselves but we did not require the equations to be written in the gradient form.

In this section, we apply the variational method of Biot-Mornev [64], which we briefly described (also see Sec. 2.5.2). An advantage of this method is that it requires from the ansatz to have only one spatial derivative and not necessarily the second, even though reaction-diffusion equation contains second spatial derivative.

We consider the functional σ as a function of u and $\dfrac{\partial u}{\partial t}$ as given by the formulation

$$\sigma = \Gamma + \frac{\mathrm{d}G}{\mathrm{d}t} = \sigma[u, \frac{\partial u}{\partial t}], \tag{4.1}$$

where

$$\Gamma = \frac{1}{2} \int_{-\infty}^{+\infty} \left(\frac{\partial u}{\partial t} - f(u)\right)^2 \mathrm{d}x = \Gamma[u, \frac{\partial u}{\partial t}], \tag{4.2}$$

and

$$G = \frac{1}{2} \int_{-\infty}^{+\infty} \left(\frac{\partial u}{\partial x}\right)^2 \mathrm{d}x = G[u]. \tag{4.3}$$

It can be easily verified that the variational equation (with u fixed)

$$\frac{\delta \sigma}{\delta(\frac{\partial u}{\partial t})} = 0, \tag{4.4}$$

is equivalent to the PDE for u,

$$\frac{\partial u}{\partial t} = f(u) + \frac{\partial^2 u}{\partial x^2}, \quad x \in [0, +\infty). \tag{4.5}$$

We consider (4.5) and the boundary condition $\dfrac{\partial}{\partial x} u(0, t) = 0$, by applying the procedure to the piece-wise smooth ansatz

$$u = \begin{cases} a, & 0 \leq x \leq x_a, \\ a\dfrac{(x_0 - x)}{x_0 - x_a}, & x_a \leq x \leq x_0, \\ 0, & \text{otherwise,} \end{cases} \tag{4.6}$$

with the cubic nonlinearity $f(u) = u(u - \theta)(1 - u)$ and where $a \equiv a(t)$, $x_a \equiv x_a(t)$ and $x_0 \equiv x_0(t)$ are the dynamic variables. The sketch of the ansatz is as shown in Fig. 4.1.
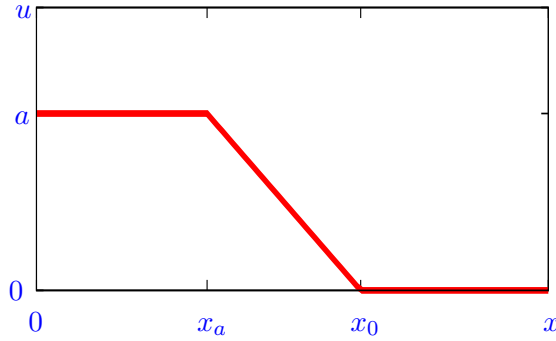
Figure 4.1: The sketch of the piece-wise smooth ansatz given in (4.6).

We use (4.6) and its temporal derivative $\dfrac{\partial u}{\partial t}$ (derived via formulation (4.7))

$$\frac{\partial u}{\partial t} = \sum_q \frac{\partial u}{\partial q} \dot{q}, \qquad q = a, \, x_a, \, x_0, \tag{4.7}$$

$\left(\dot{q} = \dfrac{\mathrm{d}q}{\mathrm{d}t}\right)$ in (4.2, 4.3) to minimize the resultant functional σ given in (4.1) with respect to $\dot{q}$. Then by considering $x_a = x_0/2$ due to translational invariant we obtain the ODE system

$$\dot{a} = -a\big(468a^2 - (1 + \theta)475a + 480\theta + 1920k^2\big)/480,$$
$$\dot{k} = -k\big(36a^2 - (1 + \theta)25a + 480k^2\big)/240, \tag{4.8}$$

where $k = 1/x_0$.

The phase portrait of the ODE system (4.8) is presented in Fig. 4.2. The equilibria of the ODE system are depicted with the thick blue dot, the null-clines by the dotted-blue and dotted-magenta lines. The saddle-point equilibrium with both a and k nonzero corresponds to the critical nucleus. Its stable separatrix is shown by the solid red line and its unstable separatrix is shown by the dashed black line. The stable separatrix serves as the boundary between excitation and decay. Initial conditions to the left of it correspond to decaying solutions, and initial conditions to the right of it give rise to excitation, i.e. propagating waves. The phase portrait is qualitatively similar to that obtained by Neu *et al.* in [68]. However, one major difference is that we have successful initiation represented by solutions with $a \to 1$, which corresponds to propagating waves, as opposed to those in [68] which have $a \to \infty$, blow up in finite time. This is because we have used the full cubic kinetics in the ZFK equation whereas Neu *et al.* used its quadratic approximation, which corresponds to the limit of very high values of the upper zero of the cubic.
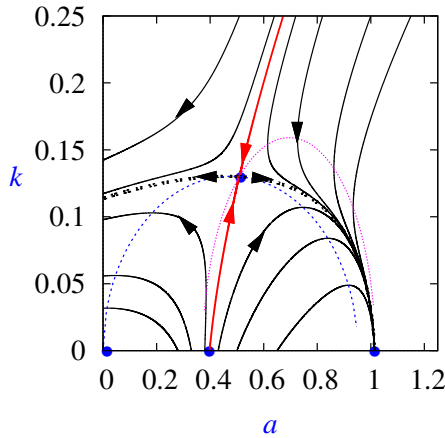
Figure 4.2: The equilibria of the ODE system are depicted with the thick blue dot, the null-clines by the dotted-blue and -magenta lines. The center-stable manifolds (solid - red lines) of the *critical nucleus* (i.e., point of intersection of the stable and unstable manifolds) serving as the boundary between excitation and decay. The unstable manifolds are the dotted - gray lines. Initial perturbations to the left of the stable manifolds decays to zero, and those to the right give rise to excitation. The phase portrait is qualitatively similar to that obtained by Neu and his co-workers [68] shown in Fig. 2.6 of Chapter 2
.

4.2 Front equations

4.2.1 Piece-wise smooth ansatzes

In this section, we consider a variational description of the rightward propagating front solution for the Biktashev model (2.20)-(2.21) [8] written in the form of piece-wise linear functions. Instead of using Biot-Mornev technique, we use the method of minimization

of the residual functional, re-written in the form which allows using C^1 but not C^2 approximate solutions. The technique is well known in principle but we are not aware of it being described in the literature in the very form that we need, so we explain it here in detail. The residual functional, after introducing a weighting parameter $\mu \in (0, \infty)$, becomes

$$S = \frac{1}{2} \int_{-\infty}^{+\infty} \left(\left(\frac{\partial E}{\partial t} - \frac{\partial^2 E}{\partial x^2} - F(E, h) \right)^2 + \mu^2 \left(\tau \frac{\partial h}{\partial t} - G(E, h) \right)^2 \right) \, dx, \qquad (4.9)$$

where $F(E, h) = \Theta(E-1)h$ and $G(E, h) = \Theta(-E) - h$ with Θ a Heaviside step function. Obviously, $S \geq 0$, and $S = 0$ only for the true solution of (2.20)-(2.21) (also (3.20)-(3.21) in Chapter 3). The strategy is that minimizing S for a given set of functions yields the "best"' approximate solution achievable with those functions. For brevity, we subsequently retain the subscript notations for partial derivatives where necessary.

Suppose in general the ansatzes are given by the functions

$$E = V((a_k(t)); \; x),$$
$$h = W((a_k(t)); \; x), \qquad (4.10)$$

where $k = 1, \, 2, \, 3$. By minimizing our residual functionals with respect to $a_k(t)$, that is, $\dfrac{\partial S}{\partial a_k} = 0$, we obtain the system of ODEs

$$\sum_k \dot{a}_k M_{jk} = Q_j + F_j + G_j \, , \quad j, k = 1, 2, 3. \qquad (4.11)$$

where

$$M_{jk} = \int_{-\infty}^{+\infty} V_{a_j} V_{a_k} \, dx + \mu^2 \tau^2 \int_{-\infty}^{+\infty} W_{a_j} W_{a_k} \, dx,$$
$$Q_j = -\frac{1}{2} \frac{\partial}{\partial a_j} \int_{-\infty}^{+\infty} V_x^2 \, dx \equiv \left(\int_{-\infty}^{+\infty} V_{a_j} V_{xx} \, dx \right),$$
$$F_j = \int_{-\infty}^{+\infty} V_{a_j} F(V, W) \, dx,$$
$$G_j = \mu^2 \tau \int_{-\infty}^{+\infty} W_{a_j} G(V, W) \, dx. \qquad (4.12)$$

In the equation for Q_j above, by using integration by parts, we obtain the form of this integral which contains only V_x but not V_{xx}. This is a standard trick in Galerkin-type approximations. Since none of the expressions in (4.12) contains second order derivatives with respect to x, we can use C^1 ansatzes rather than C^2. We consider as ansatzes the piece-wise linear functions V and W which respectively approximate the rightward propagating front and the profile of h that describes the dynamics of the

gating variable

$$
V = \begin{cases}
\tilde{V}(x,t), & x < x_\omega \\
-\alpha - \dfrac{\alpha + \omega}{x_\alpha - x_\omega}(x - x_\alpha), & x_\omega \leq x < x_\alpha \\
-\alpha, & x_\alpha \leq x,
\end{cases}
$$

$$
W = \begin{cases}
0, & x < x_\omega \\
\dfrac{\alpha + \omega}{\omega(x_\alpha - x_\omega)}(x - x_\omega), & x_\omega \leq x < x_0 \\
1, & x_0 \leq x.
\end{cases}
\tag{4.13}
$$

Here, $a_1(t) = \omega(t)$, $a_2(t) = x_0(t)$ and $a_3(t) = x_1(t)$. The sketch of the ansatzes, the red solid (V) and the blue dashed (W) lines are shown in Fig. 4.3(a).

(a)

(b)
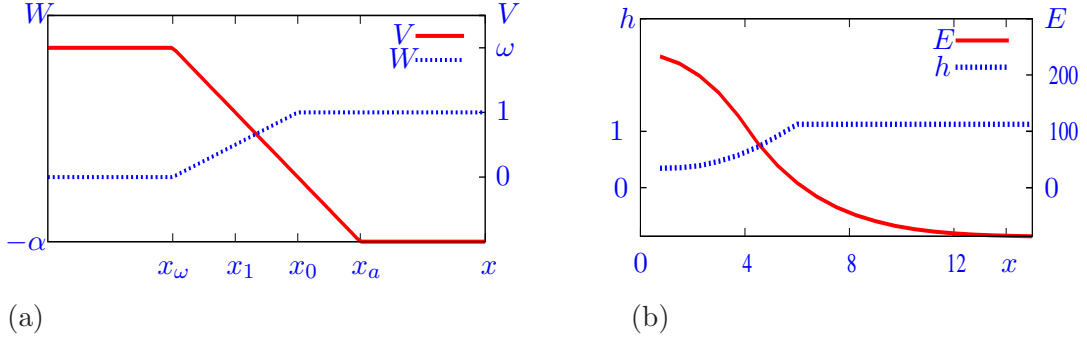
Figure 4.3: (a) The sketch of the piece-wise smooth ansatzes for the front model given in (4.13) and (b) the plot of a propagating front profile. The red solid (E) curve and blue-dashed (h) respectively correspond to solid red line (V) and dashed blue line (W) in (a).

We take the function $\tilde{V}(x,t)$ for $x < x_\omega(t)$ as the exact solution of the diffusion equation $\tilde{V}_t = \tilde{V}_{xx}$ with an appropriate initial condition and the boundary condition $\tilde{V}(x_\omega(t),t) = \omega(t)$. This exact solution can be written explicitly but it is complicated and we do not need it, so we omit it. Also $W = 0$ in the interval, $(-\infty, x_\omega)$. Thus, the terms,

$$
\int_{-\infty}^{x_\omega} \left(\frac{\partial E}{\partial t} - \frac{\partial^2 E}{\partial x^2} - F(E,h) \right)^2 \, dx, \quad \mu^2 \int_{-\infty}^{x_\omega} \left(\tau \frac{\partial h}{\partial t} - G(E,h) \right)^2 \, dx,
\tag{4.14}
$$

contribute nothing to the residuals $\mathcal{S}$. Consequently, we consider our integrals in the interval $[x_\omega(t), \infty)$.

From our knowledge of the internal boundary conditions $E(x_1) = 1$ and $E(x_0) = 0$, we derive the relationships between x_ω, x_α and our dynamic variables ω, x_1 and x_0 (whichever is suitable) as

$$
x_0 = \frac{\alpha x_\omega + \omega x_\alpha}{\alpha + \omega}, \qquad x_1 = \frac{(1+\alpha)x_\omega + (\omega - 1)x_\alpha}{\alpha + \omega},
\tag{4.15}
$$

$$
x_\omega = -(\omega - 1)x_0 + \omega x_1, \qquad x_\alpha = (1+\alpha)x_0 - \alpha x_1.
\tag{4.16}
$$

Also, to simplify the computations of the integrals M_{jk}, Q_j, F_j and G_j and their integrands, we take advantage of the equivalence relationships $\Theta(V-1) \equiv \Theta(x_1 - x)$ and $\Theta(-V) \equiv \Theta(x - x_0)$

$$F(V,W) = \Theta(V-1)W = \Theta(x_1 - x)W,$$
$$G(V,W) = \Theta(-V) - W = \Theta(x - x_0) - W. \tag{4.17}$$

For the computation of the integrands in (4.12) and subsequently the values of the integrals see Sec. A.1 in Appendix A.

The second order ODE system resulting from the approximation as derived in Appendix A is

$$
\begin{aligned}
\frac{d\omega}{dt} = &-\Big(\tau\,\mu^2\omega^6 + (4\,\alpha\,\tau\,\mu^2 - \tau^2\,\mu^2)\,\omega^5 + (6\,\alpha^2\,\tau\,\mu^2 + \tau^3\,\mu^4 - 4\,\alpha\,\tau^2\,\mu^2)\,\omega^4 \\
&+ (3\,\tau^2\,\mu^2 - \tau^4\,\mu^4 + 4\,\alpha^3\,\tau\,\mu^2 - 9\,\alpha^2\,\tau^2\,\mu^2)\,\omega^3 \\
&- (6\,\alpha^3\,\tau^2\,\mu^2 - 3\,\alpha^2\tau^3\,\mu^4 - 2\,\tau^2\,\mu^2 + 12\,\alpha^2\,\tau^2\,\mu^2 + \tau\,\alpha^4\,\mu^2 + 12\,\alpha\,\tau^2\,\mu^2)\,\omega^2 \\
&+ (12\,\alpha^3\,\tau^2\,\mu^2 + 3\,\alpha^2\tau^2\,\mu^2 - 8\,\alpha\,\tau^2\,\mu^2 + 3\,\tau^4\,\mu^4 - 2\,\alpha^3\,\tau^3\,\mu^4 - 2\,\alpha^3\,\tau^3\,\mu^4)\,\omega \\
&- 6\,\alpha^2\,\tau^2\,\mu^2 - 6\,\alpha^3\tau^2\,\mu^2 - 2\,\tau^4\,\mu^4\Big)\Big/\Big(2\,\tau^2\,\mu^2\Big(\omega^5 + 4\,\alpha\,\omega^4 + (6\,\alpha^2 + \tau^2\,\mu^2)\,\omega^3 \\
&+ 4\,\alpha^3\,\omega^2 + \alpha^4\,\omega - \alpha^3\,\tau^2\,\mu^2\Big)\Big) \\
&- \Big(3\,\omega^6 + 12\,\alpha\,\omega^5 + (9\,\tau^2\,\mu^2 + 18\,\alpha^2)\,\omega^4 + (27\,\alpha\,\tau^2\,\mu^2 + 12\,\alpha^3)\,\omega^3 \\
&+ (3\,\alpha^4 + 39\,\alpha^2\,\tau^2\mu^2 + 6\,\tau^4\,\mu^4)\,\omega^2 + (3\,\alpha\,\tau^4\,\mu^4 + 21\,\alpha^3\,\tau^2\,\mu^2)\,\omega\Big)\Big/\Big(2\,\tau^2\,\mu^2\,q^2 \\
&\Big(\omega^5 + 4\,\alpha\,\omega^4 + (6\,\alpha^2 + \tau^2\,\mu^2)\,\omega^3 + 4\,\alpha^3\,\omega^2 + \alpha^4\,\omega + \alpha^3\,\tau^2\,\mu^2\Big)\Big) = f(\omega, q),
\end{aligned}
$$

$$
\begin{aligned}
\frac{dq}{dt} = &\,q\,\Big(2\,\omega^5 + (-4\,\alpha + 3\,\tau\,\mu^2 - 12)\,\omega^4 + (-\tau^2\,\mu^2 - 6\,\alpha^2 + 18)\,\omega^3 \\
&+ (-3\,\alpha^2\,\tau\,\mu^2 + 12\alpha^2 - 8 + 12\,\alpha)\,\omega^2 + (-6\,\alpha^2 - 8\,\alpha + 3\,\tau^2\,\mu^2)\,\omega - 2\,\tau^2\,\mu^2\Big) \\
&\Big/\Big(2\,\omega\,(\omega + \alpha)\Big(\omega^4 + 3\,\alpha\,\omega^3 + (3\,\alpha^2 + \tau^2\,\mu^2)\,\omega^2 + (\alpha^3 - \alpha\,\tau^2\,\mu^2)\,\omega + \alpha^2\,\tau^2\,\mu^2\Big)\Big) \\
&+ \Big(15\,\omega^4 + 36\,\alpha\,\omega^3 + (21\,\alpha^2 + 6\,\tau^2\,\mu^2)\,\omega^2 + 3\,\alpha\,\tau^2\,\mu^2\,\omega\Big)\Big/\Big(2\,\omega\,(\omega + \alpha)\,q \\
&\Big(\omega^4 + 3\,\alpha\,\omega^3 + (3\,\alpha^2 + \tau^2\,\mu^2)\,\omega^2 + (\alpha^3 - \alpha\,\tau^2\,\mu^2)\,\omega + \alpha^2\,\tau^2\,\mu^2\Big)\Big) = g(\omega, q). \tag{4.18}
\end{aligned}
$$

Choice of parameter value for μ

In the above consideration, μ is an arbitrary positive constant, therefore, we need to choose a value for it. Let us choose it so that some parameters of propagating fronts in the approximation correspond to those in the exact solution. A steady front solution corresponds to an equilibrium of (4.18) given by

$$f(\omega, q) = 0, \qquad g(\omega, q) = 0. \tag{4.19}$$

The quest for suitable choice of parameter value for μ is simplified if we can reduce the 2D system (4.19) into a single equation. Therefore, resolving each of the equations with respect to q

$$q = f^\omega(\omega; \mu, \tau, \alpha), \qquad q = g^\omega(\omega; \mu, \tau, \alpha), \tag{4.20}$$

we obtain a single equation with $\mathcal{G} = 0$, where $\mathcal{G}$ is a function in terms of ω:

$$\mathcal{G}(\omega; \mu, \tau, \alpha) = f^\omega(\omega; \mu, \tau, \alpha) - g^\omega(\omega; \mu, \tau, \alpha) = 0. \tag{4.21}$$

The equation (4.21) can be written explicitly as

$$\mathcal{G} = \sqrt{\frac{\mathcal{G}_0}{\mathcal{G}_1}} - \sqrt{\tau}\,\mu\,\sqrt{\frac{\mathcal{G}_2}{\mathcal{G}_3}} = 0, \tag{4.22}$$

where

$$
\begin{aligned}
\mathcal{G}_0(\omega) &= \omega^5 + 4\,\alpha\,\omega^4 + \left(6\,\alpha^2 + 3\,\tau^2\mu^2\right)\omega^3 + \left(9\,\mu^2\tau^2\alpha + 4\,\alpha^3\right)\omega^2 \\
&\quad + \left(2\,\mu^4\tau^4 + \alpha^4 + 13\,\alpha^2\mu^2\tau^2\right)\omega + 7\,\alpha^3\tau^2\mu^2 + \mu^4\tau^4\alpha,
\end{aligned}
$$

$$
\begin{aligned}
\mathcal{G}_1(\omega) &= -\omega^6 - (4\,\alpha - \tau)\,\omega^5 + \left(4\,\tau\,\alpha - 6\,\alpha^2 - \tau^2\mu^2\right)\omega^4 \\
&\quad - \left(3\,\tau - 9\,\alpha^2\tau - \mu^2\tau^3 + 4\,\alpha^3\right)\omega^3 \\
&\quad + \left(3\,\alpha^2\mu^2\tau^2 + 2\,\tau - \alpha^4 + 6\,\alpha^3\tau - 12\,\alpha^2\tau - 12\,\tau\,\alpha\right)\omega^2 \\
&\quad + \left(2\,\alpha^3\tau^2\mu^2 - 3\,\alpha^2\tau - 12\,\alpha^3\tau + 8\,\tau\,\alpha - 3\,\mu^2\tau^3\right)\omega + 6\,\alpha^2\tau + 2\,\mu^2\tau^3 + 6\,\alpha^3\tau,
\end{aligned}
$$

$$\mathcal{G}_2(\omega) = 5\,\omega^3 + 12\,\alpha\,\omega^2 + \left(7\,\alpha^2 + 2\,\tau^2\mu^2\right)\omega + \mu^2\tau^2\alpha,$$

$$
\begin{aligned}
\mathcal{G}_3(\omega) &= -2\,\omega^5 + \left(12 + 4\,\alpha - 3\,\mu^2\tau\right)\omega^4 - \left(18 - 6\,\alpha^2 - \tau^2\mu^2\right)\omega^3 \\
&\quad + \left(8 - 12\,\alpha - 12\,\alpha^2 + 3\,\alpha^2\mu^2\tau\right)\omega^2 + \left(8\,\alpha + 6\,\alpha^2 - 3\,\tau^2\mu^2\right)\omega + 2\,\tau^2\mu^2. \tag{4.23}
\end{aligned}
$$

We choose μ using the following consideration: For the ODE system (4.18) to be a qualitatively adequate approximation of the original PDE system, it should have a saddle-point equilibrium corresponding to the unstable front solution of the original system. Ideally, we would like this ODE system to have equilibria corresponding to the stable and unstable front solutions. Hence, we choose μ to ensure the existence of such equilibria. Moreover, we can choose μ to ensure not only existence of two equilibria, but also their qualitative characteristics, say the value of ω of an equilibrium in (4.18) which corresponds to the post-front voltage of the stable front or the unstable front. It is clear that by varying only one parameter μ we can only arrange an exact value of only one characteristic.

From numerics, for $\tau = 8.2$ and $\alpha = 1.0$, we find that $c_- = 0.3318742892$ (unstable front speed) and $c_+ = 0.4650981666$ (stable front speed) [8, 9]. Therefore, using $\omega = 1 + \tau\,c^2(1 + \alpha)$, the corresponding values for ω are then $\omega_- = 2.8063049181$ and $\omega_+ = 4.547587396$ respectively.

If we demand that ω_- (ω_+) is a root of equation (4.22), this then becomes an equation for μ. For $\tau = 8.2$, $\alpha = 1.0$ and $\omega_- = 2.8063049181$ ($\omega_+ = 4.547587396$), corresponding to our unstable (stable) front solution we have from (4.22) an equation in terms of μ as

$$\mathcal{G} = \sqrt{\frac{c_0 + c_1\,\mu^2 + c_2\,\mu^4}{c_3 + c_4\,\mu^2}} - \sqrt{\tau}\,\mu\,\sqrt{\frac{c_5 + c_6\,\mu^2}{c_7 - c_8\,\mu^2}} = 0, \qquad (4.24)$$

where for ω_-

$$c_0 = 589.0459329, \quad c_1 = 12147.71067, \quad c_2 = 29897.04797, \quad c_3 = 1799.883593,$$

$$c_4 = 6442.102195, \quad c_5 = 224.6514311, \quad c_6 = 444.6318854, \quad c_7 = 292.3125140,$$

$$c_8 = 277.547141. \qquad (4.25)$$

We have found solutions to the equation (4.24) numerically, and there is only one positive real root for μ. Thus, for $\omega_- = 2.8063049181$ the root is $\mu_- = 0.3235887618$. Similarly for $\omega_+ = 4.547587396$ the only positive real root is $\mu_+ = 0.3115506093$.

Having determined μ and ω, we now need to ensure that the corresponding value of q represents a feasible equilibrium, that is, it is positive. To check this, we substitute the values $\tau = 8.2$, $\alpha = 1.0$, $\omega_- = 2.8063049181$ ($\omega_+ = 4.547587396$) into the two equations in (4.20) and find $q_- = 2.945066761$ ($q_+ = 3.148342385$) and which are positive in each case.

Equilibrium for the ODE system

Substituting $\tau = 8.2$, $\alpha = 1.0$, $\mu_- = 0.3235887618$ in (4.18), we obtain an ODE system in terms of ω, q with three real equilibria (w_*, q_*): (0.2187904350, 0.8244415445) represented by the magenta solid box, (2.806304866, 2.945066780) by the black solid diamond and (3.798043236, 2.878740670) by the red solid circle symbols, as shown in Fig. 4.4(a). And the corresponding eigenvalues λ_1, λ_2 from the Jacobian matrix of the ODE system are found to be -17.240, 0.116; -0.014, -0.625; and 0.007, -0.107 respectively. Thus, we have two saddle points, represented by the magenta solid box and red solid circle, meanwhile the stable equilibrium is represented by the small black solid diamond. This is not good enough as we need to have two stable equilibria with a saddle point in between them to exemplify excitability. Similarly for $\mu_+ = 0.3115506095$, the corresponding equilibria are: (0.2286427356, 0.8563359843) which is a saddle and represented by the magenta solid box, (2.054948934, 3.637802532) a node by the black solid diamond and (4.547587392, 3.148342384) a saddle point represented by the red solid circle symbols, as shown in Fig. 4.4(b).

Therefore, our analysis did not yield the desired result, perhaps the ansatz for the h variable does not exhibit the vital dissipation property as its slope remains constant in the interval $[x_\omega, x_0]$ where it ideally supposed to be changing. The reason for the
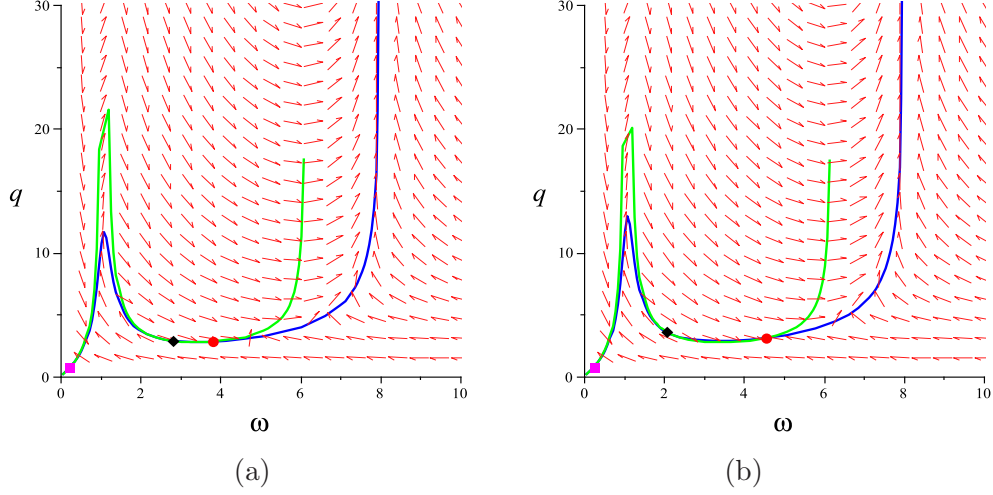
Figure 4.4: The Phase portrait from the approximation to the front using the piece-wise smooth ansatz corresponding to $\mu_- = 0.3235887617$ for (a) and $\mu_+ = 0.3115506093$ for (b) respectively. The blue and green lines are the null-clines, the magenta solid box and red solid circle represent the saddle points meanwhile the black solid diamond represent the stable equilibrium.

unexpected result is due to the absence of dissipation property in our chosen ansatz. To illustrate this, we plot the current profiles $I_{\text{Na}} \equiv F(E, h) = \Theta(E-1)\, h$ (see (2.20, 2.21)) together with their corresponding front profiles as shown in the top panel of Fig. 4.5. Meanwhile, in the bottom panel we emulate these profiles by estimating the parameters in our piecewise linear ansatz to correspond to the ones from our real numerics in the top panel. The I_{Na} profile in (d) can be seen to be a correct caricature of that in (b) and so its corresponding ansatz can be used in approximating successful propagation. However, in (c), we see a considerable I_{Na} profile as opposed to very small I_{Na} profile in (a). Thus, the two are very different. Therefore the ansatz is not good enough for approximating unsuccessful propagation. The results, as shown in the bottom panel of Fig. 4.5, (c) and (d), where we have non-changing I_{Na} profile for both successful and unsuccessful initiations, illustrate the absence of dissipation for this case.

4.2.2 Smooth ansatzes

We have seen that 2-parametric ansatzes are not flexible enough to represent the essential features (front dissipation) for our ignition procedure. Hence, we want to try 3-parametric ansatzes. In this section, we try smooth ansatzes akin to the ones used by Neu *et al* for the ZFK equation [68].

Galerkin residue functional to the front model

We consider the simplified ionic model (2.20)-(2.21) (also (3.20)-(3.21) in Chapter 3) We build a finite dimensional approximation to this front model in the following way.
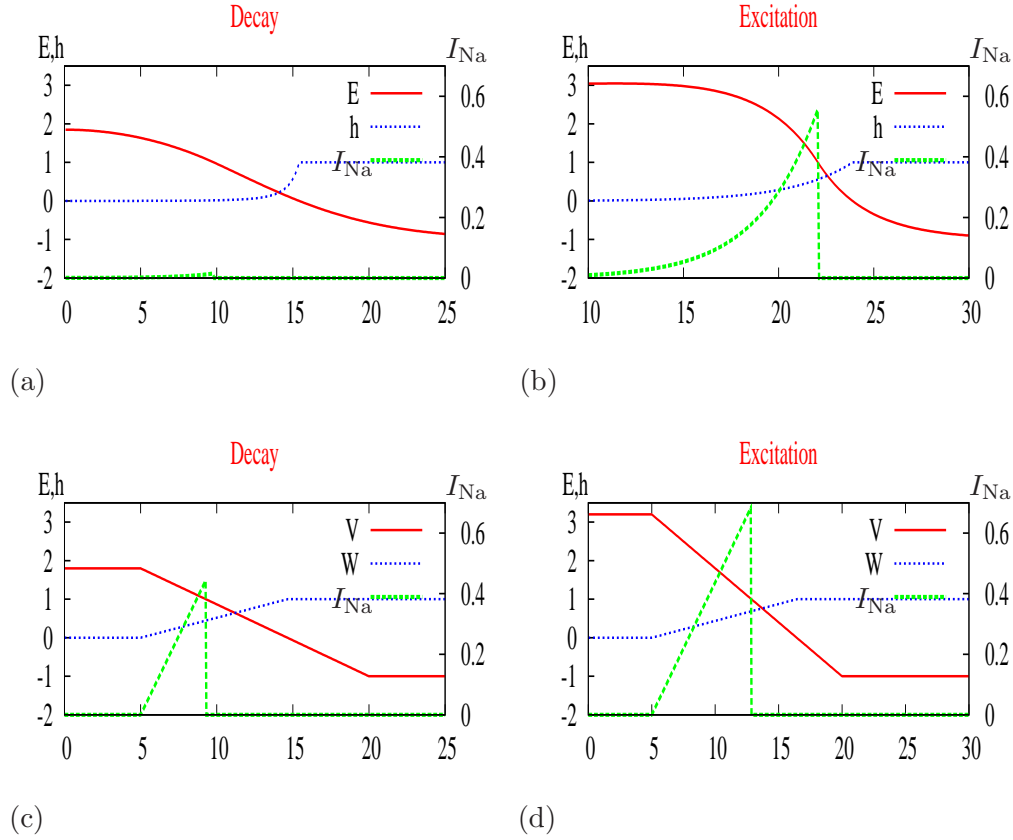
Figure 4.5: The plots of the current profile I_{Na} in (d) can be viewed as a correct caricature of that in (b), so the ansatz is in this case suitable for approximating successful propagation. However, in (c) the I_{Na} profile is very different from that in (a), the ansatz in (c) shows considerable I_{Na}, whereas the accurate numerical profile in (a) shows only very small I_{Na}. Thus, the ansatz is in this case not good for approximating failure (unsuccessful propagation).

We seek for approximations to $E(x,t)$ and $h(x,t)$ in the form of ansatzes V, W

$$E \approx V\big(x,\, a(t),\, b(t),\, x_1(t)\big),$$
$$h \approx W\big(x,\, a(t),\, b(t),\, x_1(t)\big), \qquad (4.26)$$

where the time dynamics is via the dynamics of three parameters a, b and x_1. Parameters $a(t)$ and $x_1(t)$ correspond to $a(t)$, $1/k(t)$, the *amplitude* and *width* of the Gaussian ansatz as in [68] (see also Sec. 2.5.2) and $b(t)$ is the new parameter introduced to describe the dynamics of gate h.

We substitute these approximations into (2.20) (also (3.20)) and minimize the residual, that is, a norm of the discrepancy between the left and right hand sides of the equations. We do the minimization locally in time, i.e. we vary $(\dot{a}, \dot{b}, \dot{x}_1)$ at given (fixed) values of (a, b, x_1) at every t. For the x-dependence, we choose the L_2 norm, with an equal weight for both equations, so the minimization function is

$$S = \int_{-\infty}^{+\infty} \left(\left(V_t - V_{xx} - F(V,W) \right)^2 + \left(W_t - \frac{1}{\tau} G(V,W) \right)^2 \right) \, \mathrm{d}x. \qquad (4.27)$$

As all time dependence is via the parameters (a, b, x_1), the minimization function becomes

$$S = \int_{-\infty}^{+\infty} \left(\dot{a} V_a + \dot{b} V_b + \dot{x}_1 V_{x_1} - V_{xx} - F(V,W) \right)^2 \, \mathrm{d}x,$$

$$+ \int_{-\infty}^{+\infty} \left(\dot{a} W_a + \dot{b} W_b + \dot{x}_1 W_{x_1} - \frac{1}{\tau} G(V,W) \right)^2 \, \mathrm{d}x. \qquad (4.28)$$

Using our ansatzes V, W, the functions in (3.21) become

$$F(V,W) = \Theta(V-1)\, W,$$

$$G(V,W) = \Theta(-V) - W. \qquad (4.29)$$

Now, by minimizing (4.28) with respect to $\dot{a}$, $\dot{b}$, $\dot{x}_1$ (using $\dfrac{\partial S}{\partial \dot{a}} = 0$, $\dfrac{\partial S}{\partial \dot{b}} = 0$, $\dfrac{\partial S}{\partial \dot{x}_1} = 0$), we obtain the integral system in terms of the unknown parameters $\dot{a}$, $\dot{b}$ and $\dot{x}_1$

$$\dot{a} \int_0^\infty V_a^2 \, \mathrm{d}x + W_a^2) \, \mathrm{d}x + \dot{b} \int_0^\infty (V_a V_b + W_a W_b) \, \mathrm{d}x + \dot{x}_1 \int_0^\infty (V_a V_{x_1} + W_a W_{x_1}) \, \mathrm{d}x$$

$$= \int_0^\infty V_a(V_{xx} + F(V,W)) \, \mathrm{d}x + \int_0^\infty \frac{1}{\tau} W_a\, G(V,W) \, \mathrm{d}x, \qquad (4.30)$$

$$\dot{a} \int_0^\infty (V_a V_b + W_a W_b) \, \mathrm{d}x + \dot{b} \int_0^\infty (V_b^2 + W_b^2) \, \mathrm{d}x + \dot{x}_1 \int_0^\infty (V_b V_{x_1} + W_b W_{x_1}) \, \mathrm{d}x$$

$$= \int_0^\infty V_b(V_{xx} + F(V,W)) \, \mathrm{d}x + \int_0^\infty \frac{1}{\tau} W_b\, G(V,W) \, \mathrm{d}x, \qquad (4.31)$$

$$\dot{a} \int_0^\infty (V_a V_{x_1} + W_a W_{x_1}) \, \mathrm{d}x + \dot{b} \int_0^\infty (V_b V_{x_1} + W_b W_{x_1}) \, \mathrm{d}x + \dot{x}_1 \int_0^\infty (V_{x_1}^2 + W_{x_1}^2) \, \mathrm{d}x$$

$$= \int_0^\infty V_{x_1}(V_{xx} + F(V,W)) \, \mathrm{d}x + \int_0^\infty \frac{1}{\tau} W_{x_1}\, G(V,W) \, \mathrm{d}x. \qquad (4.32)$$

The nature of the front model profiles as observed through numerics informed our decision to now choose the ansatzes for both the front and recovery variable as (see

Fig. 4.6)

$$
V = \begin{cases} -\alpha + a - \dfrac{a-1-\alpha}{1-\cosh(\frac{x_1}{p})}\left(1-\cosh(\frac{x}{p})\right) & , x < x_1, \\[3em] -\alpha + (1+\alpha)\exp\left(\dfrac{-c}{\tanh(\frac{x_1}{2p})}(x-x_1)\right) & , x > x_1, \end{cases}
$$

$$
W = \begin{cases} 1 - b + \dfrac{b}{x_0{}^2}\,x^2 & , x < x_0, \\[1.5em] 1 & , x > x_0, \end{cases} \tag{4.33}
$$

where

$$
\begin{aligned}
x_0 &= x_1 - \frac{1}{c}\ln(\frac{\alpha}{1+\alpha})\tanh(\frac{x_1}{2p}), \\
p &= \frac{a-1-\alpha}{c\,(1+\alpha)}.
\end{aligned} \tag{4.34}
$$

The sketch of the ansatzes (V, W) presented in Fig. 4.6(a) are shown respectively as the solid red and dashed blue lines and that of the front model profiles (E, h) are also shown respectively as the solid red and dashed blue lines as in Fig. 4.6(b).

(a)   (b)
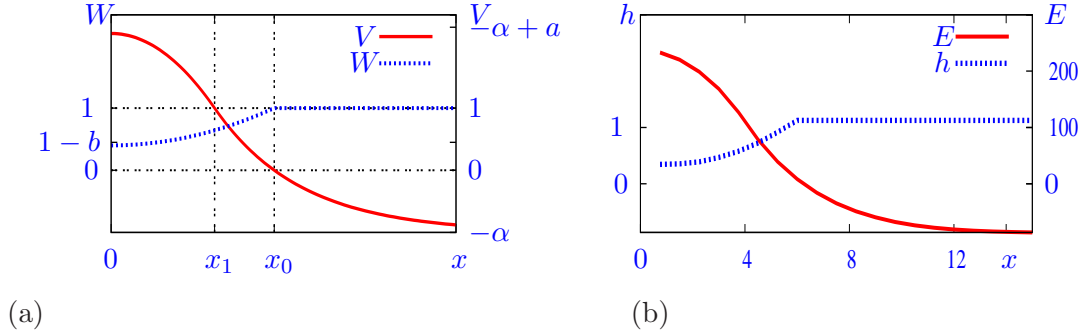
Figure 4.6: The sketch of (a) the smooth ansatzes (4.33) to the front model and that of its (b) profile which serves as the motivation that informed our choice of the ansatzes. The red solid (V) and blue dashed (W) lines in (a) respectively correspond to the red solid (E) and blue dashed (h) profiles to the front model in (b).

For computational convenience, we transform the ansatzes V and W in (4.33) using $x = \dfrac{\sigma}{\beta_1}\ln(\eta)$, $x_1 = \dfrac{\sigma}{\beta_1}\ln(\xi)$, $x_0 = \dfrac{\sigma}{\beta_1}\ln(\xi) - \beta\dfrac{\xi-1}{\xi+1}$ and after some simplifications to

the form

$$
V = \begin{cases} 1 + \sigma - \dfrac{\sigma\,\xi}{(\xi-1)^2}\,\dfrac{(\eta-1)^2}{\eta} & , \eta < \xi, \\[3mm] -\alpha + (1+\alpha)\,\xi^{k_1\sigma}\,\eta^{-k_1\sigma} & , \eta > \xi, \end{cases}
$$

$$
W = \begin{cases} 1 - b + \dfrac{b\,(\xi+1)^2\sigma^2}{\Big(\sigma(\xi+1)\,\ln(\xi) - \beta\beta_1(\xi-1)\Big)^2}\,\ln(\eta)^2 & , \eta < \eta_0, \\[4mm] 1 & , \eta > \eta_0, \end{cases} \tag{4.35}
$$

with

$$
k_1 = \frac{\xi+1}{(1+\alpha)(\xi-1)}, \qquad \sigma = a - 1 - \alpha, \qquad \xi = \mathrm{e}^{\frac{\beta_1 x_1}{\sigma}},
$$

$$
\beta = \frac{1}{c}\,\ln(\frac{\alpha}{1+\alpha}), \qquad \beta_1 = c(1+\alpha), \qquad x_0 = \frac{\sigma}{\beta_1}\ln(\xi) - \beta\frac{\xi-1}{\xi+1},
$$

$$
\eta_0 = \xi\,\mathrm{e}^{-\frac{\beta\beta_1}{\sigma}(\frac{\xi-1}{\xi+1})}, \qquad \eta = \mathrm{e}^{\frac{\beta_1 x}{\sigma}}. \tag{4.36}
$$

Galerkin ODE system for the front model

The evaluation of the integrals in (4.30, 4.31, 4.32) and resolving these equations with respect to $\dot{a}$, $\dot{b}$ and $\dot{x}_1$ give explicit but rather complicated equations of motion in the form

$$
\dot{a} = F_a(a, b, x_1), \quad \dot{b} = F_b(a, b, x_1), \quad \dot{x}_1 = F_{x_1}(a, b, x_1). \tag{4.37}
$$

The details of the calculations and description of the functions $F_a(a, b, x_1)$, $F_b(a, b, x_1)$ and $F_{x_1}(a, b, x_1)$ are given in Appendix B.

The 3D-phase portrait for the front model

We present the 3D - phase portrait of the ODE system (4.37) in stereo-pairs, as shown in Fig. 4.7. For visualization purposes, x_1 and $a - (1+\alpha)$ are in logarithmic scale. The two panels show the same 3D picture from slightly different angles so that the 3D image can be appreciated.

The trajectories are selected numerically by considering initial conditions to the initial value problem for the ODE system in (4.37) to be very close to the excitation threshold. The black and red bold lines result from the choice of initial conditions very close to the threshold. These two collections of lines are chosen such that they all lie on the critical surface. The bold blue and green trajectories, however, result when initial conditions are chosen slightly above and below threshold respectively.

The bold lines are the trajectories in the 3D space, and the thin lines are their projections onto the coordinate walls. The blue, green and brown lines represent superthreshold, subthreshold and near-critical trajectories respectively. The brown lines which are formed as a result of the superposition of the black (the slightly subthreshold) and the red (the slightly superthreshold) trajectories represent the critical, or threshold surface between excitation (i.e., initiation) and decay and its structure consists of initial segments that depend on initial conditions, all meeting at a set of common points (i.e., "highway") which corresponds to the unstable propagating front solution. These illustrate the idea that the critical surface is the center-stable manifold of the unstable propagating front solution.
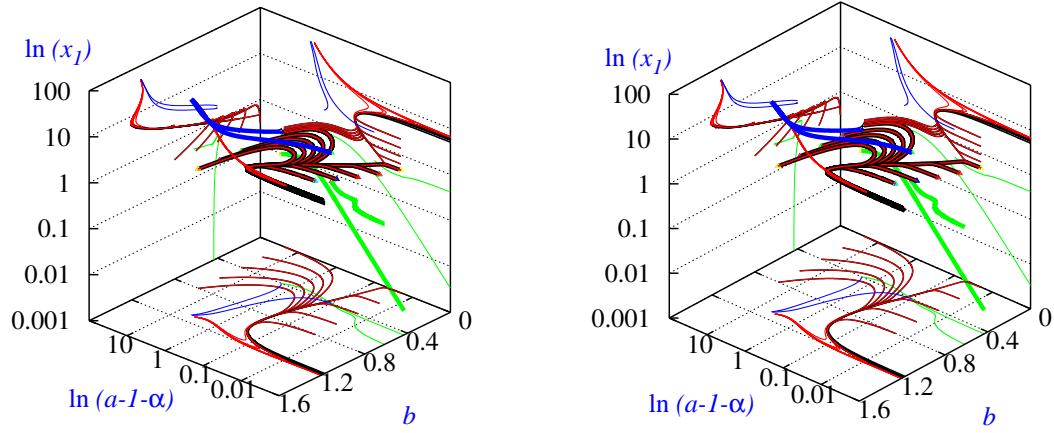
Figure 4.7: The 3D-phase portrait of the projected system (4.37). The bold lines are the trajectories in the 3D space, and the thin lines are their projections onto the coordinate walls. The blue, green and brown lines represent superthreshold, subthreshold and near-critical trajectories respectively. The brown lines represent the critical, or threshold surface between excitation (i.e., initiation) and decay and its structure consists of initial segments that depend on initial conditions, all meeting at a "highway" which corresponds to the unstable propagating front solution.

The critical surface fit for the front model

In order to derive the expression for the critical curve to the front model we fit a surface of the form $z = f(b, y)$ to the critical surface obtained through numerical simulations of the Galerkin approximation (4.37). The critical surface is taken to be represented by the near-critical trajectories (brown lines in Fig. 4.7). The fitting surface is chosen in the form of a cubic polynomial

$$f(b, y) = c_1 b^3 + c_2 y^3 + c_3 b^2 y + c_4 b y^2 + c_5 b y + c_6 b^2 + c_7 y^2 + c_8 b + c_9 y + c_{10}, \tag{4.38}$$

where $z = \ln(x_1)$, $y = \ln(a - 1 - \alpha)$ and c_j, $j = 1, 2, \cdots, 10$ are the fitting parameters. The c_j's are found to be

$$c_1 = 0.43158, \qquad c_2 = -0.0136067, \qquad c_3 = -0.0558982, \qquad c_4 = 0.0178415,$$

$$c_5 = -0.192341, \qquad c_6 = 0.18523, \qquad c_7 = -0.0852002, \qquad c_8 = 0.59912,$$

$$c_9 = 0.0402983, \qquad c_{10} = -0.22668. \tag{4.39}$$

The coordinates a, x_1 correspond respectively to the *amplitude* and *width* of the ansatz in our Galerkin approximation, while b describes the dynamics of the h-gate. The logarithmic scales as used for a, x_1 are purposely for visualizations.

The blue solid curves in Fig. 4.8(a) represent the fitting surface (4.38), while the red solid lines represent the trajectories we presume lie on the critical surface (that is, the threshold surface). The results from our fit are used to obtain the red solid line that is being compared with the numerical critical curve (black line) in Fig. 4.8(b). The red solid line in Fig. 4.8(b) is the plot of a against x_1 derived from the relation

$$z = f(0, y) \equiv \ln(x_1) = c_2 y^3 + c_7 y^2 + c_9 y + c_{10}. \tag{4.40}$$

It is evident from Fig. 4.8(b) that the approximation is not good enough. The fol-

(a)	(b)
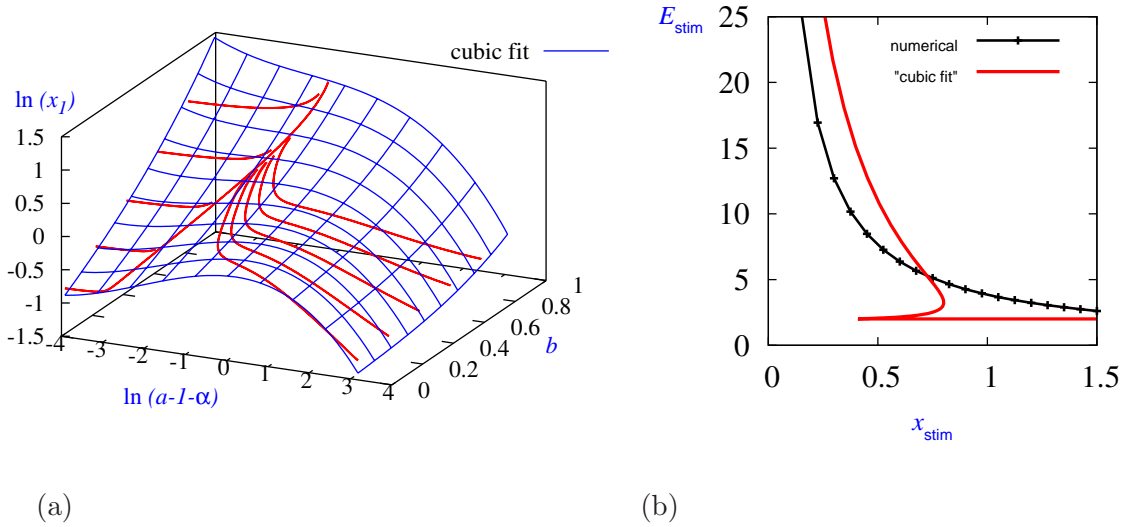
Figure 4.8: (a) The fitting of the critical surface (red-solid lines) with a cubic functional (blue-dashed lines). (b) The numerical critical curve for the simplified front model (black-solid line) compared with the approximated analytical critical curve (red-solid line).

lowing might be the possible reasons for the discrepancy in the approximation: the actual initial conditions are different from the ansatz profiles and the errors from the Galerkin approximation itself. Therefore, linear approximation in functional space (the eigenfunction expansion approach) is to be employed as we did for the ZFK equation (see Chapter 5).

4.3 Summary

- We have applied a modified version of Biot-Mornev approximation procedure to the ZFK equation, using a piece-wise linear ansatz. This has led to a phase portrait similar to that in [68]. However, we did not employ the quadratic approximation of the cubic nonlinearity in the ZFK equation, so our phase portrait is more realistic: trajectories representing successful initiation approach a finite equilibrium, $(a, k) \to (a_*, 0)$, $a_* \approx 1$, rather than blow up ($a \to \infty$) in finite time as in [68].

- We have applied the minimization of the residuals method with a two-parametric piece-wise linear ansatz to the front model. This has led to a phase portrait qualitatively different from the expected: no stable equilibrium representing the successful initiation and no saddle point corresponding to the critical front. The conclusion is that a two-parametric approximation is insufficient as it gives no possibility to account for decrease in the h gate distribution which is responsible for the propagation block.

- We have applied the minimization of the residuals method with a three-parametric ansatz which is smooth for the voltage. This has led to a three-dimensional phase portrait that is qualitatively correct, with an unstable trajectory representing the critical front, and its stable manifold as the critical surface. We have obtained an analytical fit of this critical surface. Intersection of this fit with the manifold of initial conditions produced an approximation of the critical curve, which is comparable with the exact curve, but the approximation is not very good.

Table 4.1: Glossary of notations for Chapter 4

Notation	Explanation(s): bf=before, af=after	Place introduced
α	pre-frontal voltage	(4.13)
ω	post-frontal voltage	(4.13)
σ	minimization functional	(4.1)
Γ	component of σ	(4.1)
μ	weighting variable	bf (4.9)
Θ	Heaviside step function	af (4.9)
		continued on the next page $\Rightarrow$

Notation	Explanation(s): bf=before, af=after	Place introduced
θ	threshold parameter	af (4.6)
$\mathcal{G}$	function of ω	bf (4.21)
$\mathcal{S}$	residue functional	(4.9)
τ	dimensionless paramter	(4.9)
η	independent variable	bf (4.35)
σ, β, β_1, ξ, η_0	auxiliary variable (combination of parameters)	bf (4.35),(4.35)
a, x_a, x_0	dynamic variables	(4.6)
a, b, x_1, k	Galerkin parameters	(4.26), af(4.26)
x_0, k_1	auxiliary variable (combination of parameters)	bf (4.35),(4.35)
c_i, $i = 1, 2, \cdots, 8$	constant	(4.24)
$c : c_-$, c_+	speed: lower, higher	bf (4.24)
C^1	space of continuously real valued functions	af (4.9)
C^2	space of functions whose second derivative exists & are continuous	af (4.9)
E	dynamic variable: voltage	(4.9)
f	nonlinear function	(4.2)
F, G	nonlinear function	(4.9)
G	energy functional	(4.1)
f, g	right hand side of the Galerkin ODEs	(4.18)
F_a, F_b, F_{x_1}	right hand side of the Galerkin ODEs	(4.37)
h	dynamic variable: Na$^+$ gate variable	(4.9)
M_{jk}, Q_j, F_j, G_j j, $k = 1, 2, 3$	Galerkin integral	(4.12)
k, q	indexing paramter	(4.7), (4.10)
u	dynamic variable: voltage	(4.1)
V, W	Galerkin ansatz	(4.10)

Chapter 5

Linear perturbation theory for the ZFK and the front equations

5.1 Introduction

We have established in Chapter 2 and Chapter 3 that the critical surface separating the basins of decay and excitation is a codimension-1 center-stable manifold of a critical solution: the critical nucleus for the ZFK, the critical pulse for the FHN and the critical front for the cardiac front models.

In the present chapter, we develop the method of approximating this center-stable manifold with its tangent, the corresponding center-stable space, i.e., the subspace spanned by the eigenfunctions corresponding to the eigenvalues with non-positive real parts [95, 54]. This can be achieved by linearizing our nonlinear equations around the critical solution, i.e. the critical nucleus for the ZFK and the critical front for the cardiac front model. The analysis of the behaviour of the linearized solutions allows us to classify the initial conditions, and this gives an analytical initiation criterion.

As an example, Fig. 5.1 shows a sketch of the stable manifold of a critical nucleus solution for the ZFK equation. It illustrates the idea of the threshold surface role played by the stable manifold of the critical solution (i.e. critical nuclues). The critical nucleus is represented by the black dot; the critical trajectories, constituting the stable manifold, are shown in black. Meanwhile, the family of initial conditions is represented by the dash-dotted line. The bold black line is the critical trajectory with initial condition in that family. The sub-threshold trajectories are represented by the blue line meanwhile the red lines represent the super-threshold trajectories.
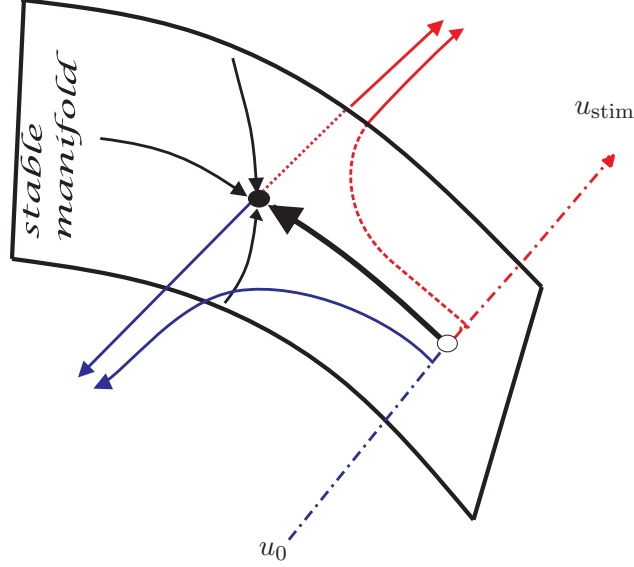
Figure 5.1: The sketch of a stable manifold of the critical solution for the ZFK equation. The critical nucleus is represented by the black dot; the critical trajectories, constituting the stable manifold, are shown in black. The family of initial conditions is represented by the dash-dotted line. The bold black line is the critical trajectory with initial condition in that family. The sub-threshold trajectories are represented by the blue line, while the red lines represent super-threshold trajectories. Note that the point where the initial condition intersect the stable manifold is shown as the empty circle.

5.2 Analytical initiation criterion for the ZFK equation

Recall the initiation problem for the ZFK equation (3.13, 3.14) in Sec. 3.3

$$\frac{\partial u}{\partial t} = \frac{\partial^2 u}{\partial x^2} + f(u), \quad x, t \geq 0$$

$$\frac{\partial u(0,t)}{\partial x} = 0, \quad t \geq 0$$

$$u(x,0) = u_{\text{stim}}\Theta(x_{\text{stim}} - x), \quad x \geq 0. \tag{5.1}$$

Let us consider an even extension of problem (5.1),

$$\frac{\partial u}{\partial t} = \frac{\partial^2 u}{\partial x^2} + f(u), \quad x \in (-\infty, \infty),$$

$$u(-x,0) = u(x,0) = u_{\text{stim}}\Theta(x_{\text{stim}} - x), \quad x \geq 0,$$

or, equivalently, $\quad u(x,0) = u_{\text{stim}}\Theta(x_{\text{stim}} - x)\Theta(x_{\text{stim}} + x). \tag{5.2}$

It is easy to see that if $u(x,t)$ satisfies (5.2), then its restriction to $x \geq 0$ satisfies (5.1), since the initial condition in (5.2) is even and the equation is equivariant with respect to inversion $x \to -x$; therefore its solution remains even for all $t > 0$ and as such satisfies the boundary condition of (5.1).

To obtain an analytical criterion of initiation, we linearize the first equation in (5.2)

about the critical nucleus solution, $u_{cr}(x)$ its steady state solution. Using

$$u(x, t) = u_{cr}(x) + w(x, t), \tag{5.3}$$

where $w(x, t)$ is a perturbation such that $|w| \ll 1$, this leads to the linearized problem

$$\frac{\partial w}{\partial t} = \frac{\partial^2 w}{\partial x^2} + q(x)\, w, \tag{5.4}$$

where $q(x) = \dfrac{\partial f(u_{cr})}{\partial u}$. The substitution

$$w(x, t) = e^{\lambda t} \varphi(x), \tag{5.5}$$

now leads to a self-adjoint (Sturm-Liouville) eigenvalue problem

$$\frac{d^2 \varphi(x)}{dx^2} + (q(x) - \lambda)\varphi(x) = 0. \tag{5.6}$$

Hence all eigenvalues $\lambda \in \mathbb{R}$. In linear operator format, (5.6) is written as

$$\mathcal{L}\,\varphi = 0, \tag{5.7}$$

where $\mathcal{L} \equiv \dfrac{d^2}{dx^2} + q(x) - \lambda$.

Flores in [34] proved using Sturm's Theorem that (5.6) has exactly one solution with positive λ.

Here, we look for solutions of the eigenvalue equation (5.6) with bounded $\varphi(x)$ and $\lambda > 0$, analytical if possible. Thus, our eigenvalue problem becomes for $\lambda > 0$

$$\frac{d^2 \varphi(x)}{dx^2} + (q(x) - \lambda)\varphi(x) = 0,$$

$$\varphi(\pm\infty) = 0 \quad (\text{ or in general } |\varphi| < \text{ Const}). \tag{5.8}$$

5.2.1 Solution to the eigenvalue problem

To solve (5.8), we suppose $\varphi(x) = \psi(z)$ where $z \equiv z(x)$ is to be chosen, and knowing the critical nucleus solution of the ZFK equation, using approximate $f(u) = u\,(u - \theta)$, is of the form

$$u_{cr}(x) = \frac{3\theta}{2}\text{sech}^2(kx), \tag{5.9}$$

where $k = \dfrac{\sqrt{\theta}}{2}$, we choose $z = \tanh(kx)$. Then $q(x) = \theta\left(3\text{sech}^2(kx) - 1\right)$ is transformed to

$$q(z) = \theta\left(3(1 - z^2) - 1\right). \tag{5.10}$$

69

The problem given by (5.8) can now be re-written in terms of the variable z as

$$\frac{\mathrm{d}}{\mathrm{d}z}\left((1-z^2)\frac{\mathrm{d}\psi}{\mathrm{d}z}\right) + \left(12 - \frac{4(1+\frac{\lambda}{\theta})}{(1-z^2)}\right)\psi = 0,$$

$$\psi(\pm 1) = 0. \tag{5.11}$$

Problem (5.8) is a Sturm-Liouville problem for a (time independent) Schrödinger equation [83]. The properties of eigenfunctions of this problem are well known [40, 16, 22, 73, 17]. The spectrum consists of a number of discrete real and simple eigenvalues and a continuous spectrum. If the eigenvalues λ_n are numbered in decreasing order,

$$\lambda_1 > \lambda_2 > \lambda_3 > \cdots \lambda_n > \cdots , \tag{5.12}$$

then eigenfunction $\phi_n(x)$ has exactly $(n-1)$ zeros in the interval $x \in (-\infty, \infty)$; correspondingly, $\psi_n(z)$ has exactly $(n-1)$ zeros in $z \in (-1, 1)$. We are however, after an *unstable eigenfunction* corresponding to a *positive* eigenvalue.

It is easy to show that $\dfrac{\partial}{\partial x}u_{\mathrm{cr}}(x)$ is a solution to (5.6) at $\lambda = 0$, therefore it is the same as the eigenfunction which corresponds to the zero eigenvalue. Thus, knowing $\dfrac{\partial}{\partial x}u_{\mathrm{cr}}(x)$ from (5.9) and using the transformation $z = \tanh(k\,x)$, the zero eigenfunction is then

$$\frac{\mathrm{d}u_{\mathrm{cr}}(x)}{\mathrm{d}x} = -\frac{3}{2}\theta^{3/2}\mathrm{sech}^2(k\,x)\,\tanh(k\,x),$$

$$\equiv C\,z\,(1-z^2), \tag{5.13}$$

where $C = -\dfrac{3}{2}$ is a multiplicative constant. It is obvious in (5.13) that our zero eigenfunction, $C\,z\,(1-z^2)$ has only one zero in the interval (-1, 1). Hence, we conclude that, according to Sturm-Liouville theory, $\lambda_2 = 0$ and $\psi_2(z) \propto z(1-z^2)$, and therefore there is a $\lambda_1 > 0$, exactly one positive eigenvalue, which corresponds to a $\psi_1(z)$ which has no zeros in $(-1, 1)$. Therefore, the unstable eigenvalue we are after corresponds to this one and only one positive eigenvalue.

Equation (5.11) is a special case of the differential equation

$$\frac{\mathrm{d}}{\mathrm{d}z}\left((1-z^2)\frac{\mathrm{d}W}{\mathrm{d}z}\right) + \left(\nu(\nu+1) - \frac{\mu^2}{(1-z^2)}\right)W = 0, \tag{5.14}$$

which has as its solutions the so-called **Associated Legendre Functions** [75, 38] in which ν and μ are arbitrary complex constants. The linearly independent functions

that are the associated Legendre functions are given by

$$P_\nu^\mu(z) = \frac{1}{\Gamma(1-\mu)} \left(\frac{z+1}{z-1}\right)^{\mu/2} F\left(-\nu, \nu+1; 1-\mu; \frac{1-z}{2}\right),$$

$$Q_\nu^\mu(z) = \frac{e^{\mu\pi i}\, \Gamma(\nu+\mu+1)\Gamma(1/2)}{2^{\nu+1}\Gamma(\nu+\frac{3}{2})} (z^2-1)^{\mu/2}\, z^{-\nu-\mu-1}$$

$$\times F\left(\frac{\nu+\mu+2}{2}, \frac{\nu+\mu+1}{2}; \nu+\frac{3}{2}; \frac{1}{z^2}\right), \tag{5.15}$$

where F is a hypergeometric function which by definition is of the form

$$F(\alpha, \beta; \gamma; z) = 1 + \frac{\alpha \cdot \beta}{\gamma \cdot 1}\, z + \frac{\alpha(\alpha+1)\beta(\beta+1)}{\gamma(\gamma+1) \cdot 1 \cdot 2}\, z^2$$

$$+ \frac{\alpha(\alpha+1)(\alpha+2)\beta(\beta+1)(\beta+2)}{\gamma(\gamma+1)(\gamma+2) \cdot 1 \cdot 2 \cdot 3}\, z^3 + \cdots. \tag{5.16}$$

The hypergeometric series terminates if α or β is a negative integer or zero as it is obvious from the definition. The functions $P_\nu^\mu(z)$ and $Q_\nu^\mu(z)$ are referred to as the associated **Legendre P** and **Legendre Q** respectively (see, for example [38]). Therefore, the general solution is

$$\psi(z) = C_1\, P_\nu^\mu(z) + C_2\, Q_\nu^\mu(z), \tag{5.17}$$

where C_1 and C_2 are undetermined constants. Comparing (5.11) and (5.14), we have $\nu = 3$ and $\mu = \pm\frac{2\sqrt{\lambda+\theta}}{\sqrt{\theta}}$. It happens that the solution we are after and which satisfies our boundary conditions is

$$P_3^{\frac{2\sqrt{\lambda+\theta}}{\sqrt{\theta}}}(z) = \frac{(z-1)^{\left(\frac{\sqrt{\theta+\lambda}}{\sqrt{\theta}}\right)} F\left(-3, 4; \frac{\sqrt{\theta}+2\sqrt{\theta+\lambda}}{\sqrt{\theta}}; \frac{1}{2} - \frac{z}{2}\right)}{(z+1)^{\left(\frac{\sqrt{\theta+\lambda}}{\sqrt{\theta}}\right)} \Gamma\left(\frac{\sqrt{\theta}+2\sqrt{\theta+\lambda}}{\sqrt{\theta}}\right)}. \tag{5.18}$$

Using (5.16), solution (5.18) simplifies to

$$\psi(z) = \left(\frac{z-1}{z+1}\right)^{\frac{\sqrt{\theta+\lambda}}{\sqrt{\theta}}} \frac{\left(15\theta^{\frac{3}{2}} z^3 + 30\theta\sqrt{\theta+\lambda}\, z^2 + (24\lambda\sqrt{\theta} + 15\theta^{\frac{3}{2}})z + 8\lambda\sqrt{\theta+\lambda}\right)}{\Gamma\left(\frac{\sqrt{\theta}+2\sqrt{\theta+\lambda}}{\sqrt{\theta}}\right)(\sqrt{\theta}+\sqrt{\theta+\lambda})(\sqrt{\theta}+2\sqrt{\theta+\lambda})(3\sqrt{\theta}+2\sqrt{\theta+\lambda})}. \tag{5.19}$$

The values of the eigenvalue λ which make our boundary conditions $\psi(\pm 1) = 0$ to be satisfied are the solutions to the equation

$$8\lambda\sqrt{\theta+\lambda} + 30\theta^{\frac{3}{2}} + 24\lambda\sqrt{\theta} + 30\theta\sqrt{\theta+\lambda} = 0, \tag{5.20}$$

71

and are found to be $\lambda_1 = \dfrac{5\theta}{4}$, $\lambda_2 = 0$, $\lambda_3 = \dfrac{-3\theta}{4}$. From (5.19), it follows that the corresponding eigenfunction to the eigenvalue $\lambda_2 = 0$ is

$$\psi_2(z) = -\frac{z(1-z^2)}{8}, \tag{5.21}$$

which is equivalent to our deduced zero eigenfunction in (5.13) and therefore confirms that our solution is correct.

We are interested in the *positive eigenvalue* λ which corresponds to the *unstable eigenfunction* that we are looking for. Thus, substituting $\lambda_1 = \dfrac{5\theta}{4}$ in (5.19) reduces it to

$$\psi_1(z) = \frac{1}{48}(1-z^2)^{(3/2)}. \tag{5.22}$$

From Sturm-Liouville's theory, $\lambda_1 = \dfrac{5\theta}{4}$ is the only positive eigenvalue and $\psi_1(z)$ does not change sign. The plots of ψ_1 and ψ_2 are shown in Fig. 5.2.
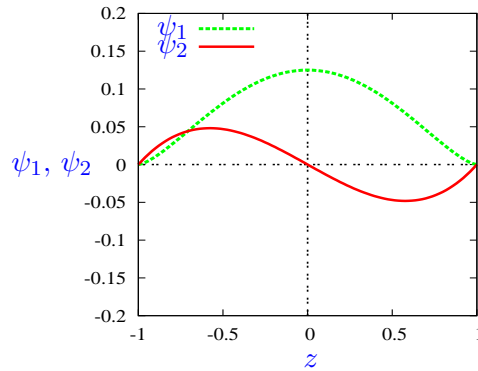
Figure 5.2: The plot of the unstable eigenmode ψ_1 (green curve) for the ZFK equation and the zero eigenmode ψ_2 (red curve) showing the only zero of ψ_2 in the interval $(-1, 1)$ confirming that λ_1 is the only positive eigenvalue.

Finally, rewriting the *unstable eigenfunction* in terms of the original variable x, we obtain after simplifications and neglecting of multiplicative constant

$$\varphi(x) = \mathrm{sech}^3(k\,x), \tag{5.23}$$

where $k = \dfrac{\sqrt{\theta}}{2}$.

5.2.2 Analytical critical (threshold) curve for the ZFK equation

A general solution to (5.4) satisfying appropriate conditions at $x \to \pm\infty$ can be described by

$$w(x,t) = \sum_j a_j\,\varphi_j(x)\,\mathrm{e}^{\lambda_j t} = \sum_j w_j(x,t), \tag{5.24}$$

where $\varphi_j(x)$, $j = 1, \ldots$ are the eigenfunctions, λ_j are the corresponding eigenvalues and a_j are constants depending on initial conditions, and summation includes integration for the continuous part of the spectrum. That is,

$$\sum_j a_j \, \varphi_j(x) \, \mathrm{e}^{\lambda_j t} = \sum_{j=1}^{N} a_j \, \varphi_j(x) \, \mathrm{e}^{\lambda_j t} + \int_{-\infty}^{-\theta} a(\lambda) \, \varphi_\lambda(x) \, \mathrm{e}^{\lambda t} \, \mathrm{d}\lambda. \tag{5.25}$$

Recall that $\lambda_j \leq 0$ for $j \geq 2$. Therefore, as $t \to \infty$, we have $w_j \to 0$ for any $j > 2$ and $w_2 \to a_2 \, \varphi_2(x)$. As to $w_1(x)$, it exponentially grows unless $a_1 = 0$: $w_1(x,t) \to -\infty$ if $a_1 < 0$ (decay: below the critical surface) and $w_1(x,t) \to \infty$ if $a_1 > 0$ (excitation: above the critical surface). If $a_1 = 0$, then the solution is on the critical surface. Note that $a_2 \, \varphi_2(x)$ accounts for a shift of the perturbation by the distance a_2.

The coefficients a_j are determined from initial conditions, as a_j are the projections of initial conditions onto the eigenfunctions (see for example [22]). Initially, that is, at $t = 0$

$$w_0(x) = u_0(x) - u_{\mathrm{cr}}(x) = \sum_j a_j \, \varphi_j(x), \tag{5.26}$$

where $w_0(x) = w(x,0)$, $u_0(x) = u(x,0)$. Now if we take the scalar product of both sides of (5.26) by φ_k, and since the operator $\mathcal{L}$ in (5.7) is self-adjoint [55], then the eigenfunctions can be normalized so that

$$\langle \varphi_j, \varphi_k \rangle \equiv \int_{-\infty}^{+\infty} \varphi_j \, \varphi_k \, \mathrm{d}x = \delta_{jk} = \begin{cases} 1 & j = k \\ 0 & j \neq k \end{cases} \tag{5.27}$$

(δ_{jk}, the *Kronecker delta* symbol), we have

$$a_j = \langle w_0(x), \varphi_j(x) \rangle = \langle u_0(x) - u_{\mathrm{cr}}(x), \varphi_j \rangle. \tag{5.28}$$

Thus, to obtain the expression for our *critical surface* (and by implication our critical curve) we consider the *unstable eigenmode* φ_1. For any family of initial perturbations rewritten as

$$w_0(x) = u_0(x) - u_{\mathrm{cr}}(x) = \sum_j a_j \, \varphi_j(x), \tag{5.29}$$

we compute $a_1 = \langle w_0(x), \varphi_1 \rangle$. If $a_1 > 0$, then the initial condition leads to initiation; and if $a_1 < 0$, it leads to decay and if $a_1 = 0$, it is on the critical surface (i.e. the center-stable manifold). Therefore, our ignition criterion then becomes

$$a_1 = \int_0^{+\infty} \big(u_0(x) - u_{\mathrm{cr}}(x)\big)\varphi_1 \, \mathrm{d}x = 0,$$

$$= \int_0^{x_{\mathrm{stim}}} u_{\mathrm{stim}} \, \varphi_1(x) \, \mathrm{d}x - \int_0^{+\infty} u_{\mathrm{cr}}(x) \, \varphi_1(x) \, \mathrm{d}x = 0, \tag{5.30}$$

after substituting in it $u_0(x) = u_{\text{stim}}\Theta(x_{\text{stim}} - x)$. Now by using

$$u_{\text{cr}}(x) \approx \frac{3\theta}{2}\text{sech}^2\left(\frac{x\sqrt{\theta}}{2}\right), \quad \varphi_1(x) \approx \text{sech}^3\left(\frac{x\sqrt{\theta}}{2}\right), \tag{5.31}$$

we obtain after resolving in terms of u_{stim}, the explicit expression for the threshold (critical) curve

$$u_{\text{stim}} = \frac{9\theta}{8}\left(\frac{2}{\pi}\tanh\left(\frac{x_{\text{stim}}\sqrt{\theta}}{2}\right)\text{sech}\left(\frac{x_{\text{stim}}\sqrt{\theta}}{2}\right) + \frac{4}{\pi}\arctan\left(\exp(\frac{x_{\text{stim}}\sqrt{\theta}}{2})\right) - 1\right)^{-1}.$$
$$\tag{5.32}$$

The plot of our analytical critical curve is compared with other numerical critical curves as shown in the Fig. 5.3. It shows the graphs of the analytical threshold curve for the quadratic nonlinearity (red-solid) compared with the numerical ones for the ZFK (blue-dashed: cubic nonlinearity; light green-cross: quadratic nonlinearity) and the FHN (black-solid) equations. The value of θ for both quadratic and cubic nonlinearity is 0.13 in both numerical and analytic computations. From the plot, one can see some agreement between the analytical threshold curve for the quadratic nonlinearity and the numerical for the ZFK (with cubic nonlinearity). The vital question of how far
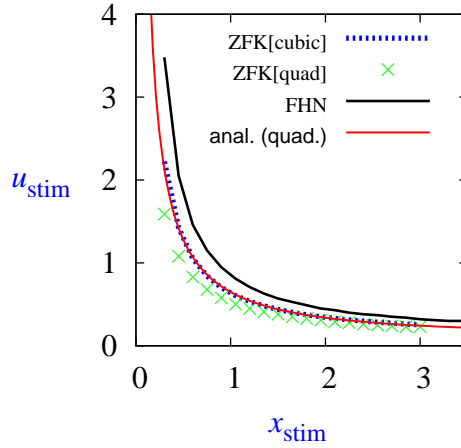
Figure 5.3: The plot of the analytical threshold curves for the quadratic nonlinearity (red-solid) versus the numerical ones for the ZFK (blue-dashed: cubic, light green - cross: quadratic) and the FHN (black-solid) equations. The value of θ for both quadratic and cubic nonlinearity is 0.13 in both numerical and analytic computations.

the critical nucleus should be from initial perturbations is to be addressed in the next section.

5.2.3 Generalized threshold criterion for the ZFK equation

The above consideration has avoided one delicate issue. Equation (5.2) has not just one unstable spatially nonuniform solution (critical nucleus) $u_{cr}(x)$ but a whole one-parametric family of such solutions $u_{cr}(x - \delta)$, obtained by shifts by arbitrary distance δ from the original critical nucleus $u_{cr}(x)$. It is easy to show that $\varphi_2(x) = \dfrac{\partial}{\partial x} u_{cr}(x)$ and that a small shift in $u_{cr}(x)$ is equivalent to adding/subtracting a bit of $\varphi_2(x)$ to $u_{cr}(x)$ for some small δ. This is derived via Taylor expansion as

$$u_{cr}(x - \delta) = u_{cr}(x) - \delta \frac{\partial}{\partial x} u_{cr}(x) = u_{cr}(x) - \delta \, \varphi_2(x). \qquad (5.33)$$

When the additional constraint of $u(-x, t) = u(x, t)$ is imposed, only $u_{cr}(x)$ is admissible. However, if we want to generalize the method for arbitrary, not necessarily even initial conditions, then this constraint has to be lifted. We thus have infinitely many critical nuclei which could be used to linearize our equation, and correspondingly, infinitely many initiation criteria which have the form

$$a_1(\delta) = \int_{-\infty}^{+\infty} \big(u_0(x) - u_{cr}(x - \delta) \big) \varphi_1(x - \delta) \ \mathrm{d}x = 0, \qquad (5.34)$$

for arbitrary δ. The question then arises, which of these infinitely many criteria to prefer that gives a more accurate result? In the light of the foregoing reasons, we have a *center-stable manifold* instead of a *stable manifold* as illustrated by the sketch in Fig. 5.4

5.2.4 The value for δ in the generalized criterion

There is the important question of the value of δ to be used in the formulation (5.34). We have considered two approaches on how to determine the appropriate value of δ that should be used for our threshold criterion. One approach is through minimization of u_{stim}, that is, we choose δ such that u_{stim} is minimum. The second is minimization of the amplitude of the initial perturbation where we exploit the linearization requirement that the perturbation w_0 should be small.

First, we consider the minimization of u_{stim} by taking a general initial condition of the form

$$u_0 = u_{stim} H(x), \qquad (5.35)$$

where $H(x)$ is some function of x. Equation (5.34) can then be written as

$$a_1(\delta) \equiv u_{stim} D_1(x_{stim}, \delta) - N_1 = 0, \qquad (5.36)$$
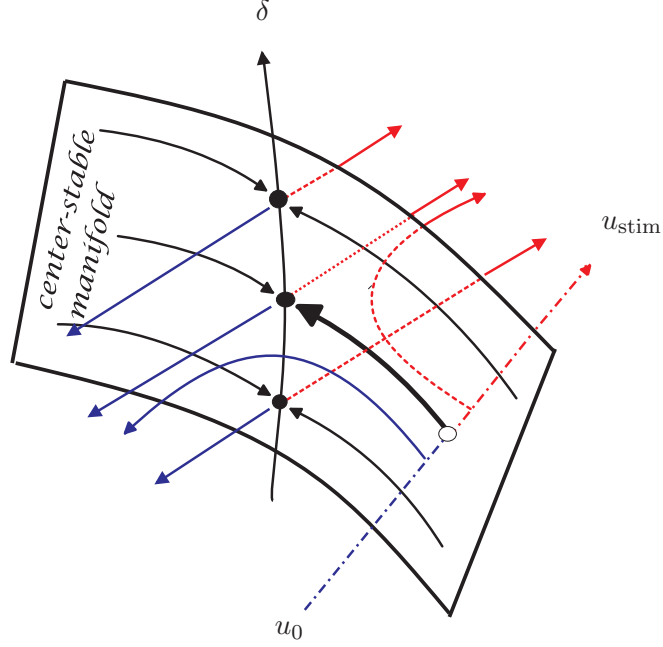
Figure 5.4: The sketch of a center-stable manifold of the critical solution for the ZFK equation. The line δ is a 1-parametric family of equilibria corresponding to translations of the "standard" critical solution (i.e. critical nucleus). Otherwise, notations are the same as in Fig. 5.1.

where

$$D_1(x_{\text{stim}}, \delta) = \int_{-\infty}^{+\infty} H(x)\, \varphi_1(x - \delta)\, \mathrm{d}x,$$

$$N_1 = \int_{-\infty}^{+\infty} u_{\text{cr}}(x - \delta)\, \varphi_1(x - \delta)\, \mathrm{d}x. \tag{5.37}$$

Thus, from (5.36)

$$u_{\text{stim}} = \frac{N_1}{D_1(x_{\text{stim}}, \delta)}, \tag{5.38}$$

and therefore to minimize u_{stim}, we maximize $D_1(x_{\text{stim}}, \delta)$ with respect to δ using $\dfrac{\partial D_1}{\partial \delta} = 0$ which then leads to

$$\int_{-\infty}^{+\infty} H(x)\, \varphi_1'(x - \delta)\, \mathrm{d}x = 0. \tag{5.39}$$

Now integrating (5.39) by parts, we obtain

$$\int_{-\infty}^{+\infty} H'(x)\, \varphi_1(x - \delta)\, \mathrm{d}x = 0, \tag{5.40}$$

which then becomes the equation for determining δ such that u_{stim} in (5.38) is minimum. Hence, our threshold criterion is then given by (5.38) after substituting the δ value we get from (5.40).

For the second approach, we recall from equation (5.26) that

$$w_0(x) = u_0(x) - u_{\text{cr}}(x - \delta) = \sum_j a_j \, \varphi_j(x - \delta). \tag{5.41}$$

This is an initial condition for the linearized equation. Linearization assumes that perturbation is small, therefore our linearized approximation is the more accurate the smaller is the solution, that is, the smaller is the initial condition. We choose δ so as to minimize a norm Δ of the initial condition. That is, we choose an L_2 norm

$$\Delta(\delta) = \int_{-\infty}^{+\infty} w_0^2 \, \mathrm{d}x = \int_{-\infty}^{+\infty} \Big(u_0(x) - u_{\text{cr}}(x - \delta) \Big)^2 \, \mathrm{d}x. \tag{5.42}$$

Now minimizing (5.42) with respect to δ using $\dfrac{\partial \Delta(\delta)}{\partial \delta} = 0$ we have

$$a_2(\delta) = \int_{-\infty}^{+\infty} \Big(u_0(x) - u_{\text{cr}}(x - \delta) \Big) \, \varphi_2(x - \delta) \, \mathrm{d}x = 0, \tag{5.43}$$

since by chain rule $\dfrac{\partial}{\partial \delta} u_{\text{cr}}(x - \delta) = -\dfrac{\partial}{\partial x} u_{\text{cr}}(x - \delta)$ and $\varphi_2(x - \delta) = \dfrac{\partial}{\partial x} u_{\text{cr}}(x - \delta)$. Hence, using the initial condition $u_0 = u_{\text{stim}} H(x)$, as in the first approach, equation (5.43) then reduces to

$$a_2(\delta) \equiv \ u_{\text{stim}} \, D_2(x_{\text{stim}}, \delta) - N_2 = 0, \tag{5.44}$$

where

$$D_2(x_{\text{stim}}, \delta) = \int_{-\infty}^{+\infty} H(x) \, \varphi_2(x - \delta) \, \mathrm{d}x,$$

$$N_2 = \int_{-\infty}^{+\infty} u_{\text{cr}}(x - \delta) \, \varphi_2(x - \delta) \, \mathrm{d}x. \tag{5.45}$$

Considering N_2 from (5.45), integrating the right hand side by parts and also since $\varphi_2(x - \delta) = \dfrac{\partial}{\partial x} u_{\text{cr}}(x - \delta)$, we have

$$N_2 = \int_{-\infty}^{+\infty} u_{\text{cr}}(x - \delta) \, \varphi_2(x - \delta) \, \mathrm{d}x,$$

$$= \int_{-\infty}^{+\infty} u_{\text{cr}}(x - \delta) \frac{\partial}{\partial x} u_{\text{cr}}(x - \delta) \, \mathrm{d}x,$$

$$= 0, \tag{5.46}$$

but as $u_{\text{stim}} \neq 0$, it then implies from (5.44) that $D_2 = 0$.

Now, since $\varphi_2(x - \delta) = \dfrac{\partial}{\partial x} u_{\text{cr}}(x - \delta)$, and using integration by parts, D_2 can conveniently be written as

$$D_2(x_{\text{stim}}, \delta) = \int_{-\infty}^{+\infty} H^{'}(x) \, u_{\text{cr}}(x - \delta) \, \mathrm{d}x = 0. \tag{5.47}$$

The value of δ is computed from this equation and the threshold criterion is then obtained after substituting this δ in (5.38).

Symmetric initial condition

For symmetric initial condition $u_0 = u_{\text{stim}} H(x)$, where

$$H(x) = \Theta(x + x_{\text{stim}}) - \Theta(x - x_{\text{stim}}), \qquad (5.48)$$

we have

$$H'(x) = \delta(x + x_{\text{stim}}) - \delta(x - x_{\text{stim}}). \qquad (5.49)$$

Substituting (5.49) in (5.40) we get

$$\varphi_1(x_{\text{stim}} - \delta) - \varphi_1(-x_{\text{stim}} - \delta) = 0, \qquad (5.50)$$

from which δ is to be determined. In this case, because of the even nature of the function $\varphi_1(x)$ (see Fig. 5.5), the only possibility is $\delta = 0$. This means that the only possible real δ such that u_{stim} is minimum is $\delta = 0$.

In the alternative, substituting (5.49) in (5.47) we get

$$u_{\text{cr}}(x_{\text{stim}} - \delta) - u_{\text{cr}}(-x_{\text{stim}} - \delta) = 0, \qquad (5.51)$$

whose zero also gives the value of δ to be used in (5.38) for the threshold criterion. Here again, due to the even nature of the $u_{\text{cr}}(x)$ (see Fig. 5.5), the only value of δ such that u_{stim} is minimum is $\delta = 0$.
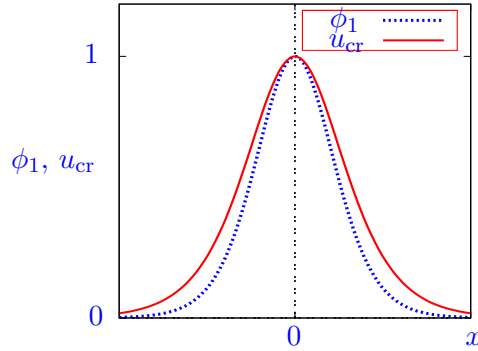
Figure 5.5: The plot of the unstable eigenmode $\phi_1(x)$ (blue-dashed curve) and the critical nucleus $u_{\text{cr}}(x)$ (red-solid curve) for ZFK equation (5.1).

Asymmetric initial condition

For an asymmetric initial condition in a form of a 2-step function $u_0 = u_{\text{stim}} H(x)$ where

$$H(x) = \Theta(x_{\text{stim}} + x)\,\Theta(-x) + 2\,\Theta(x_{\text{stim}} - x)\,\Theta(x), \qquad (5.52)$$

and then

$$H^{'}(x) = \left(2\,\Theta(x_{\text{stim}} - x) - \Theta(x + x_{\text{stim}})\right)\delta(x) + \Theta(-x)\,\delta(x + x_{\text{stim}})$$
$$- 2\,\Theta(x)\,\delta(x - x_{\text{stim}}). \tag{5.53}$$

Therefore, substituting (5.53) in (5.40) we get

$$2\,\varphi_1(x_{\text{stim}} - \delta) - \varphi_1(-\delta) - \varphi_1(-x_{\text{stim}} - \delta) = 0, \tag{5.54}$$

from which we determine the value of δ that can be used to achieve the minimum u_{stim} in (5.38). We can also use (5.47) from the second method to find the value of such δ from

$$2\,u_{\text{cr}}(x_{\text{stim}} - \delta) - u_{\text{cr}}(-\delta) - u_{\text{cr}}(-x_{\text{stim}} - \delta) = 0. \tag{5.55}$$

We observe that the value of δ such that u_{stim} is minimum is close to the zero of (5.55). In other words, the zero of $D_2(\delta) = 0$ is very close to the minimum of u_{stim} from (5.38). We have tested this observation numerically where we fixed x_{stim} at the values 0.3, 0.6, 0.9 and θ at 0.13 in both (5.38, 5.55) while plotting against δ the resultant u_{stim} in (5.38) and the resultant function of δ from (5.55). The results shown in Fig. 5.6 where in all the three cases (a), (b) and (c), the minimum of u_{stim} coincides exactly, with the accuracy allowed by the graph, with the zero of $D_2(\delta) = 0$, thus confirming our observation.

For the ZFK equation in (5.1) with quadratic nonlinearity, $f(u) = u\,(u - \theta)$ we find

$$u_{\text{cr}}(x - \delta) = \frac{3\theta}{2}\text{sech}^2\left(\frac{(x - \delta)\sqrt{\theta}}{2}\right), \tag{5.56}$$

$$\varphi_2(x - \delta) = \frac{-3}{2}\theta^{3/2}\text{sech}^2\left(\frac{(x - \delta)\sqrt{\theta}}{2}\right)\tanh\left(\frac{(x - \delta)\sqrt{\theta}}{2}\right), \tag{5.57}$$

$$\varphi_1(x - \delta) = \text{sech}^3\left(\frac{(x - \delta)\sqrt{\theta}}{2}\right). \tag{5.58}$$

By fixing x_{stim} at the values 0.3, 0.6, 0.9 and θ at 0.13 we obtain the results shown in Fig. 5.6 where in all the three cases (a), (b) and (c), the minimum of u_{stim} very closely coincides with the zero of $a_2(\delta) = 0$, thus again confirming our observation.

The two different approaches give the same result based on our tested observations. We explain this coincidence in this way. To determine optimal δ, one of the approaches uses equation (5.40), and the other uses equation (5.47). These two equations have very similar form, the difference is that, what is u_{cr} in one equation, is ϕ_1 in the other. However, as Fig. 5.5 shows, these two functions are rather close to each other, hence it is not surprising that the two equations give close results.

Clearly, this explanation depends on the details of this particular problem, so we do not expect this to be the case with other types of equations like the cardiac equations.
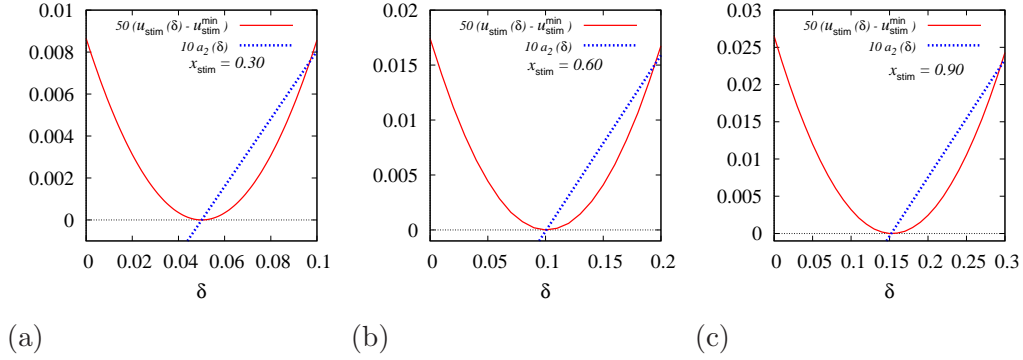
Figure 5.6: The plots of the minimum of u_{stim} and zeros of $D_2(\delta) = 0$ for fixed values (a) 0.3 (b) 0.6 and (c) 0.9 of x_{stim} and $\theta = 0.13$ for the quadratic nonlinearity $f(u) = u(u - \theta)$. In all the three cases the minimum of u_{stim} exactly coincides with the zero of $D_2(\delta) = 0$, thus confirming our prediction.

5.3 Analytical initiation criterion for the front model

5.3.1 Introduction

The simplified front model does not have "critical nucleus" or "critical pulse" solution. Instead, the role of the threshold is played by a "critical front", which is the unstable front solution with speed $c_-(\alpha, \tau)$ as explained in Chapter 2. Also we provide numerical evidence in Chapter 3 that the center-stable manifold of the unstable front solution is the threshold hypersurface separating initial conditions leading to excitation from initial conditions leading to decay.

We try to find the expression for the "critical curve" for a 2-parametric family of initial conditions with parameters x_{stim}, E_{stim} as the intersection of the codimension-1 unstable critical hypersurface, which is the centre-stable manifold of the critical front solution, with the 2-dimensional manifold of initial conditions. To do this analytically, as in the previous section for the ZFK equation, we approximate the center-stable manifold by a center-stable space which is a subspace spanned by eigenfunction corresponding to eigenvalues with nonpositive real parts (see [95, 54, 51]). This approximation is possible if we linearize our nonlinear system around the exact critical front solution which plays the same role as the critical nucleus solution in the ZFK equation. The sketch of the center-stable manifold of a non-stationary solution is shown in Fig. 5.7. When we consider the problem in a frame of reference comoving with the critical front then our critical front becomes a stationary solution (i.e. an equilibrium solution). Thus, we are dealing with a center-stable manifold of an equilibrium as in Fig. 5.4.
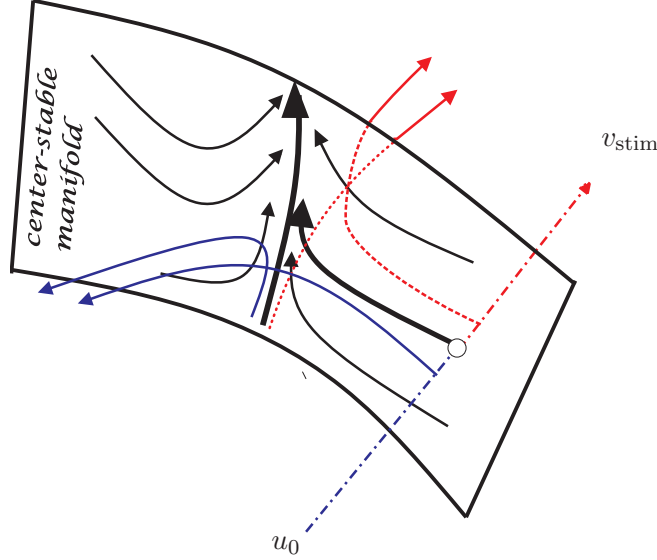
Figure 5.7: The sketch of a center-stable manifold of the critical solution for the front equations. Instead of the line of equilibria as in Fig. 5.4, we have a trajectory (bold black line) corresponding to the critical front. Otherwise, notations are the same as in in Fig. 5.4.

5.3.2 Eigenvalue problem to the Hinch (2004) model

Linearization of the system (2.20)-(2.21) is not straightforward, as the right-hand sides of it include Heaviside step functions and are discontinuous, thus linearization includes Dirac delta function and therefore is singular. A rigorous justification of this approach can be made by regularization, by considering our problem as a limit of a one-parametric, say depending on parameter ε, family of regular problems in which the step functions are replaced with smooth steps of width ε, and delta functions are replaced, correspondingly, by bell-shaped functions of width ε. Examples of using singular linearized equations for stability analysis with discontinuous right-hand sides are known in literature (see, for example, [79, 100]).

Another way to investigate stability of solutions in such equations is the free-boundary method, which considers, alongside with perturbations of the solutions, also perturbations of the matching points between the domains where the right-hand sides are continuous, thus avoiding any singularities in the linearized equations. This method has been used by Hinch [43] for a system similar to (2.20), (2.21) (see Appendix C for a detailed analysis establishing the equivalence of these two models with an appropriate choice of parameters).

However, for the purpose of developing an analytical initiation criterion, we need eigenfunctions of the adjoint linearized problem. We are not aware of any extensions of the free-boundary method to the adjoint problems. So we use linearization with the singular right-hand sides. We, first of all, find the eigenvalues and the eigenfunctions to

the linearized problem and compare the results with [43]. We accept this comparison as a justification of our method in lieu of the regularization proof, since this method has already been successfully used in literature for similar problems. Then we use the same method to find the eigenfunctions of the adjoint linearized problem which is used for the initiation criterion.

Linearization of the Hinch's equations

In a laboratory reference frame with $(\tilde{x}, \tilde{T})$ as coordinates, the front model [43] can be written in the form

$$\frac{\partial \tilde{v}}{\partial \tilde{T}} = \frac{\partial^2 \tilde{v}}{\partial \tilde{x}^2} + \tilde{F}(\tilde{v}, \tilde{h}),$$
$$\frac{\partial \tilde{h}}{\partial \tilde{T}} = \tilde{G}(\tilde{v}, \tilde{h}), \tag{5.59}$$

where $\tilde{F}(\tilde{v}, \tilde{h}) = \tilde{g}\,\Theta(\tilde{v})\tilde{h}$, $\tilde{G}(\tilde{v}, \tilde{h}) = \Theta(-\tilde{v} - \tilde{\Delta}) - \tilde{h}$ and Θ is a Heaviside step function. Meanwhile, in a moving frame of reference, the solutions to (5.59) for a right-ward moving front are of the form $\tilde{v}(\tilde{T} - \tilde{x}/\tilde{c}, \tilde{T})$, $\tilde{h}(\tilde{T} - \tilde{x}/\tilde{c}, \tilde{T})$. Introducing the coordinates $\tilde{\xi} = \tilde{T} - \tilde{x}/\tilde{c}$, $\tilde{t} = \tilde{T}$ with $\tilde{c} > 0$, we look for functions $\tilde{v}(\tilde{\xi}, \tilde{t})$, $\tilde{h}(\tilde{\xi}, \tilde{t})$ which satisfy (5.59) to give

$$\frac{\partial \tilde{v}}{\partial \tilde{t}} = \frac{1}{\tilde{c}^2} \frac{\partial^2 \tilde{v}}{\partial \tilde{\xi}^2} - \frac{\partial \tilde{v}}{\partial \tilde{\xi}} + \tilde{F}(\tilde{v}, \tilde{h}),$$
$$\frac{\partial \tilde{h}}{\partial \tilde{t}} = -\frac{\partial \tilde{h}}{\partial \tilde{\xi}} + \tilde{G}(\tilde{v}, \tilde{h}). \tag{5.60}$$

Traveling wave solutions of (5.59) correspond to stationary solutions of (5.60), (see, for example, [82]). Suppose $(\tilde{v}_0(\tilde{\xi}), \tilde{h}_0(\tilde{\xi}))$ is a stationary solution of (5.60), then

$$\frac{1}{\tilde{c}^2} \frac{\mathrm{d}^2 \tilde{v}_0}{\mathrm{d}\tilde{\xi}^2} - \frac{\mathrm{d}\tilde{v}_0}{\mathrm{d}\tilde{\xi}} + \tilde{F}(\tilde{v}_0, \tilde{h}_0) = 0,$$
$$\frac{\mathrm{d}\tilde{h}_0}{\mathrm{d}\tilde{\xi}} - \tilde{G}(\tilde{v}_0, \tilde{h}_0) = 0. \tag{5.61}$$

The linearized version of (5.60) about $\left(\tilde{v}_0(\tilde{\xi}), h_0(\tilde{\xi})\right)$ is obtained by neglecting higher order terms as

$$\frac{\partial \tilde{v}_1}{\partial \tilde{t}} = \frac{1}{\tilde{c}^2} \frac{\partial^2 \tilde{v}_1}{\partial \tilde{\xi}^2} - \frac{\partial \tilde{v}_1}{\partial \tilde{\xi}} + \tilde{g}\,\delta(\tilde{v}_0)\,\tilde{h}_0\,\tilde{v}_1 + \tilde{g}\,\Theta(\tilde{v}_0)\,\tilde{h}_1,$$
$$\frac{\partial \tilde{h}_1}{\partial \tilde{t}} = -\frac{\partial \tilde{h}_1}{\partial \tilde{\xi}} - \delta(\tilde{v}_0 + \tilde{\Delta})\,\tilde{v}_1 - \tilde{h}_1. \tag{5.62}$$

82

Let the linearized equations (5.62) support solutions of the form $\tilde{v}_1(\tilde{\xi}, \tilde{t}) = e^{\tilde{\lambda} \tilde{t}} \tilde{\phi}(\tilde{\xi})$ and $\tilde{h}_1(\tilde{\xi}, \tilde{t}) = e^{\tilde{\lambda} \tilde{t}} \tilde{\psi}(\tilde{\xi})$. This leads to the (*temporal*) eigenvalue problem

$$\tilde{\lambda} \tilde{\phi} = \frac{1}{\tilde{c}^2} \frac{\mathrm{d}^2 \tilde{\phi}}{\mathrm{d}\tilde{\xi}^2} - \frac{\mathrm{d}\tilde{\phi}}{\mathrm{d}\tilde{\xi}} + \tilde{g}\, \delta(\tilde{v}_0)\, \tilde{h}_0\, \tilde{\phi} + \tilde{g}\, \Theta(\tilde{v}_0)\, \tilde{\psi},$$

$$\tilde{\lambda} \tilde{\psi} = -\frac{\mathrm{d}\tilde{\psi}}{\mathrm{d}\tilde{\xi}} - \delta(\tilde{v}_0 + \tilde{\Delta})\, \tilde{\phi} - \tilde{\psi}, \tag{5.63}$$

where $\tilde{\phi}(\tilde{\xi})$ and $\tilde{\psi}(\tilde{\xi})$ are eigenfunctions. The eigenvalue equation (5.63) is then casted into a three first-order ODEs by letting $\dfrac{\mathrm{d}\tilde{\phi}}{\mathrm{d}\tilde{\xi}} = \tilde{\eta}$ and $\tilde{\Xi} = (\tilde{\phi},\, \tilde{\eta},\, \tilde{\psi})^{\mathrm{T}}$, thus, obtaining a linear system in $\mathbb{R}^3$

$$\tilde{\Xi}' = \tilde{A}\, \tilde{\Xi}, \tag{5.64}$$

where prime $(')$ denotes $\dfrac{\mathrm{d}}{\mathrm{d}\tilde{\xi}}$,

$$\tilde{A} = \begin{pmatrix} 0 & 1 & 0 \\ \tilde{c}^2 \left(\tilde{\lambda} - \tilde{g}\, \delta(\tilde{v}_0)\, \tilde{h}_0 \right) & \tilde{c}^2 & -\tilde{c}^2\, \tilde{g}\, \Theta(\tilde{v}_0) \\ -\delta(\tilde{v}_0 + \tilde{\Delta}) & 0 & -(1 + \tilde{\lambda}) \end{pmatrix}, \tag{5.65}$$

$$\tilde{v}_0(\tilde{\xi}) = \begin{cases} -1 + e^{\beta \tilde{\xi}}, & \tilde{\xi} \le 0, \\ \dfrac{\beta\, \tilde{g}\, H_0}{1 + \beta} (1 - e^{-\tilde{\xi}}), & \tilde{\xi} \ge 0, \end{cases}$$

$$\tilde{h}_0(\tilde{\xi}) = \begin{cases} 1, & \tilde{\xi} \le \tilde{\xi}_1, \\ H_0 e^{-\tilde{\xi}}, & \tilde{\xi} \ge \tilde{\xi}_1, \end{cases}$$

$$\tag{5.66}$$

and

$$\tilde{\xi}_1 = -\delta/\beta, \quad H_0 = e^{-\delta/\beta}, \quad \tilde{g} = (1 + \beta)\, e^{\delta/\beta}. \tag{5.67}$$

The general solution to (5.64) is (see Appendix C for details)

$$\begin{pmatrix} \tilde{\phi}_a \\ \tilde{\eta}_a \\ \tilde{\psi}_a \end{pmatrix} = \tilde{a}_2 \begin{pmatrix} 1 \\ \tilde{\nu}_2 \\ 0 \end{pmatrix} e^{\tilde{\nu}_2 \tilde{\xi}},$$

$$\begin{pmatrix} \tilde{\phi}_b \\ \tilde{\eta}_b \\ \tilde{\psi}_b \end{pmatrix} = \tilde{b}_1 \begin{pmatrix} 0 \\ 0 \\ 1 \end{pmatrix} e^{-\tilde{\nu}_1 \tilde{\xi}} + \tilde{b}_2 \begin{pmatrix} 1 \\ \tilde{\nu}_2 \\ 0 \end{pmatrix} e^{\tilde{\nu}_2 \tilde{\xi}} + \tilde{b}_3 \begin{pmatrix} 1 \\ \tilde{\nu}_2 \\ 0 \end{pmatrix} e^{\tilde{\nu}_2 \tilde{\xi}},$$

$$\begin{pmatrix} \tilde{\phi}_c \\ \tilde{\eta}_c \\ \tilde{\psi}_c \end{pmatrix} = \tilde{c}_1 \begin{pmatrix} 1 \\ -\tilde{\nu}_1 \\ -\tilde{\nu}_s \end{pmatrix} e^{-\tilde{\nu}_1 \tilde{\xi}} + \tilde{c}_3 \begin{pmatrix} 1 \\ \tilde{\nu}_2 \\ 0 \end{pmatrix} e^{\tilde{\nu}_2 \tilde{\xi}}, \tag{5.68}$$

where

$$\tilde{\nu}_1 = 1 + \tilde{\lambda}, \quad \tilde{\nu}_2 = \frac{\beta + \sqrt{\beta^2 + 4\tilde{\lambda}\beta}}{2}, \quad \tilde{\bar{\nu}}_2 = \frac{\beta - \sqrt{\beta^2 + 4\tilde{\lambda}\beta}}{2}. \tag{5.69}$$

The arbitrary constants $\tilde{a}_2$, $\tilde{b}_1$, $\tilde{b}_2$, $\tilde{b}_3$, $\tilde{c}_1$ and $\tilde{c}_3$ are to be determined from matching conditions of the solutions in the three intervals, which give the system of equations

$$\tilde{b}_2 \left(\tilde{g} H_0 - \tilde{\nu}_2\right) + \tilde{b}_3 \left(\tilde{g} H_0 - \tilde{\bar{\nu}}_2\right) - \tilde{c}_1 \tilde{\nu}_1 + \tilde{c}_3 \tilde{\bar{\nu}}_2 = 0,$$

$$\tilde{b}_2 + \tilde{b}_3 - \tilde{c}_1 - \tilde{c}_3 = 0,$$

$$\tilde{b}_1 \beta \tilde{g} + \tilde{c}_1 \left((1 + \tilde{\lambda})^2 + \beta\right) = 0,$$

$$\tilde{a}_2 \, e^{\tilde{\nu}_2 \tilde{\xi}_1} + \tilde{b}_1 \beta \, e^{(\beta - \tilde{\nu}_1)\tilde{\xi}_1} = 0,$$

$$\tilde{a}_2 \, e^{\tilde{\nu}_2 \tilde{\xi}_1} - \tilde{b}_2 \, e^{\tilde{\nu}_2 \tilde{\xi}_1} - \tilde{b}_3 \, e^{\tilde{\bar{\nu}}_2 \tilde{\xi}_1} = 0,$$

$$\tilde{a}_2 \tilde{\nu}_2 \, e^{\tilde{\nu}_2 \tilde{\xi}_1} - \tilde{b}_2 \tilde{\nu}_2 \, e^{\tilde{\nu}_2 \tilde{\xi}_1} - \tilde{b}_3 \tilde{\bar{\nu}}_2 \, e^{\tilde{\bar{\nu}}_2 \tilde{\xi}_1} = 0. \tag{5.70}$$

The solvability condition of this system leads to the characteristic equation

$$\tilde{f}_e(\tilde{\lambda}, \beta, \delta) = \beta \left(\sigma - \mu - 1\right) - 1 + \frac{(1 + \beta)(\beta \mu + 1 + \tilde{\lambda})}{(1 + \tilde{\lambda})^2 + \beta} \, e^{-\delta \left(\tilde{\lambda}/\beta + \sigma - 1\right)} = 0. \tag{5.71}$$

The characteristic equation (5.71) is exactly the same as that obtained in [43] when $\varepsilon_{k_1} = 0$ which is the case of interest to us in this work. For selected parameter values, which correspond to other numerical illustrations in this thesis, the graph of the function $\tilde{f}_e$ against $\tilde{\lambda}$ is shown in Fig. 5.8. This also confirms the existence of only one positive eigenvalue as reported in [8, 43].
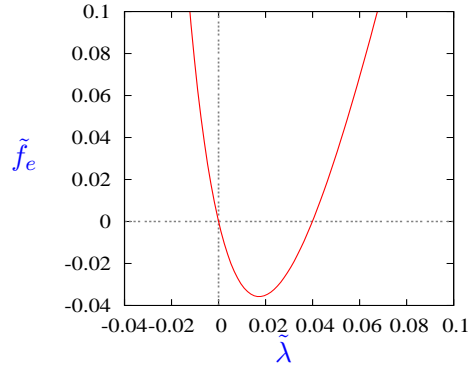
Figure 5.8: The plot of the characteristic function from (5.71) for the front in Hinch's model [43] for parameter values $\varepsilon_{k1} = 0$, $c = 0.3318742892$, $\tau = 8.2$, $\alpha = 1.0$.

5.3.3 Eigenvalue problem to the Biktashev (2002) model

Linearization of the front equations

Let us consider the front model in laboratory frame of reference (x, T) (see (C.69) in Appendix C)

$$
\begin{aligned}
\frac{\partial E}{\partial T} &= \frac{\partial^2 E}{\partial x^2} + F(E, h), \\
\frac{\partial h}{\partial T} &= G(E, h)/\tau,
\end{aligned}
\tag{5.72}
$$

where $F(E, h) = \Theta(E - 1)h$, $G(E, h) = \Theta(-E) - h$ and Θ is a Heaviside step function.

In a comoving frame of reference, (ξ, t), the solutions to (5.72) for a right-ward moving front can be represented in the form $E(\xi, t)$, $h(\xi, t)$. Using the transformations $\xi = x - cT$, $t = T$, with $c > 0$, (5.72) becomes

$$
\begin{aligned}
\frac{\partial E}{\partial t} &= \frac{\partial^2 E}{\partial \xi^2} + c \frac{\partial E}{\partial \xi} + F(E, h), \\
\frac{\partial h}{\partial t} &= c \frac{\partial h}{\partial \xi} + G(E, h)/\tau.
\end{aligned}
\tag{5.73}
$$

The traveling waves of (5.72) correspond to the stationary solution of (5.73). Suppose we take the exact unstable front solution as stationary to (5.73) and designate it by $\bar{U}_0 = \begin{pmatrix} v_0(\xi) \\ h_0(\xi) \end{pmatrix}$,

$$
\begin{aligned}
v_0(\xi) &= \begin{cases} \omega - \dfrac{\tau^2 c^2}{1 + \tau c^2}\, e^{\xi/\tau c}, & \xi \leq -\Delta, \\[2mm] -\alpha + \alpha\, e^{-c\xi}, & \xi \geq -\Delta, \end{cases} \\[3mm]
h_0(\xi) &= \begin{cases} e^{\xi/\tau c}, & \xi \leq 0, \\[1mm] 1, & \xi \geq 0, \end{cases}
\end{aligned}
\tag{5.74}
$$

where

$$
\xi = x - ct,\ \omega = 1 + \tau c^2 (1 + \alpha), \Delta = \frac{1}{c} \ln(\frac{1 + \alpha}{\alpha}).
\tag{5.75}
$$

Therefore, we linearize (5.73) around $(v_0(\xi), h_0(\xi))$ using

$$
\begin{aligned}
E &= v_0(\xi) + \varepsilon\, v_1(\xi, t), \\
h &= h_0(\xi) + \varepsilon\, h_1(\xi, t).
\end{aligned}
\tag{5.76}
$$

Now using Taylor expansion, $\Theta(-v_0) \equiv \Theta(\xi)$, $\Theta(v_0 - 1) \equiv \Theta(-\xi - \Delta)$ and the fact that $\delta(u) = \dfrac{d\Theta(u)}{du}$, then by chain rule $\delta(-v_0) = \delta(v_0) = \dfrac{1}{v_0'}\delta(\xi)$, $\delta(v_0 - 1) = \dfrac{-1}{v_0'}\delta(\xi + \Delta)$.

Thus, we obtain (see Sec. C.3 in Appendix C)

$$\frac{\partial v_1}{\partial t} = \frac{\partial^2 v_1}{\partial \xi^2} + c \frac{\partial v_1}{\partial \xi} - \frac{1}{v_0'} \delta(\xi + \Delta) \, h_0 \, v_1 + \Theta(-\xi - \Delta) \, h_1,$$

$$\frac{\partial h_1}{\partial t} = c \frac{\partial h_1}{\partial \xi} + \left(\frac{1}{v_0'} \delta(\xi) \, v_1 - h_1 \right)/\tau. \tag{5.77}$$

Let the linearized equation (5.77) support solutions of the form $\bar{U}_1 = \begin{pmatrix} v_1(\xi, t) \\ h_1(\xi, t) \end{pmatrix}$ where $v_1(\xi, t) = e^{\lambda t} \, \phi(\xi)$ and $h_1(\xi, t) = e^{\lambda t} \, \psi(\xi)$. This leads to a (*temporal*) eigenvalue problem with λ, φ as eigenpairs

$$\mathcal{L} \, \bar{V} = \lambda \, \bar{V}, \tag{5.78}$$

where

$$\mathcal{L} \equiv \bar{D} \frac{d^2}{d\xi^2} + \bar{C} \frac{d}{d\xi} + \bar{F}, \qquad \bar{V} = \begin{pmatrix} \phi \\ \psi \end{pmatrix}, \qquad \bar{D} = \begin{pmatrix} 1 & 0 \\ 0 & 0 \end{pmatrix},$$

$$\bar{C} = \begin{pmatrix} c & 0 \\ 0 & c \end{pmatrix}, \qquad \bar{F} = \begin{pmatrix} \frac{-1}{v_0'} \delta(\xi + \Delta) \, h_0 & \Theta(-\xi - \Delta) \\ \frac{1}{\tau v_0'} \delta(\xi) & -1/\tau \end{pmatrix}. \tag{5.79}$$

We now cast (5.78) into a three ODE system

$$\frac{d\phi}{d\xi} = \eta,$$

$$\frac{d\eta}{d\xi} = \left(\lambda + \frac{1}{v_0'} \delta(\xi + \Delta) \, h_0 \right) \phi - c \, \eta - \Theta(-\xi - \Delta) \, \psi,$$

$$\frac{d\psi}{d\xi} = -\frac{1}{\tau \, c \, v_0'} \delta(\xi) \phi + \frac{(1 + \lambda \tau)}{\tau \, c} \psi, \tag{5.80}$$

which can be written in matrix form as

$$\Xi' = A \, \Xi, \tag{5.81}$$

where

$$A = \begin{pmatrix} 0 & 1 & 0 \\ \lambda + \frac{1}{v_0'} \delta(\xi + \Delta) \, h_0 & -c & -\Theta(-\xi - \Delta) \\ \frac{-1}{\tau \, c \, v_0'} \delta(\xi) & 0 & \frac{1 + \lambda \tau}{\tau \, c} \end{pmatrix}. \tag{5.82}$$

The general solution to (5.81) is therefore,

$$\begin{pmatrix} \phi_a \\ \eta_a \\ \psi_a \end{pmatrix} = a_1 \begin{pmatrix} 1 \\ \nu_1 \\ -\nu_q \end{pmatrix} e^{\nu_1 \xi} + a_3 \begin{pmatrix} 1 \\ -\bar{\nu}_2 \\ 0 \end{pmatrix} e^{-\bar{\nu}_2 \xi},$$

$$\begin{pmatrix} \phi_b \\ \eta_b \\ \psi_b \end{pmatrix} = b_1 \begin{pmatrix} 0 \\ 0 \\ 1 \end{pmatrix} e^{\nu_1 \xi} + b_2 \begin{pmatrix} 1 \\ -\nu_2 \\ 0 \end{pmatrix} e^{-\nu_2 \xi} + b_3 \begin{pmatrix} 1 \\ -\bar{\nu}_2 \\ 0 \end{pmatrix} e^{-\bar{\nu}_2 \xi},$$

$$\begin{pmatrix} \phi_c \\ \eta_c \\ \psi_c \end{pmatrix} = c_2 \begin{pmatrix} 1 \\ -\nu_2 \\ 0 \end{pmatrix} e^{-\nu_2 \xi}, \tag{5.83}$$

where

$$\nu_1 = \frac{1 + \lambda \tau}{\tau c}, \quad \nu_2 = \frac{c + \sqrt{c^2 + 4\lambda}}{2}, \quad \bar{\nu}_2 = \frac{c - \sqrt{c^2 + 4\lambda}}{2}. \tag{5.84}$$

The arbitrary constants a_1, a_3, b_1, b_2, b_3, and c_2 are to be determined from matching conditions of the solutions in the three intervals, which gives a system of six equations

$$a_1 \alpha c \nu_1 e^{-\nu_1 \Delta} - a_3 \alpha c \bar{\nu}_2 e^{\bar{\nu}_2 \Delta} + b_2 e^{\nu_2 \Delta}\left(\alpha c \nu_2 - e^{-\nu \Delta}\right),$$

$$+ b_3 e^{\bar{\nu}_2 \Delta}\left(\alpha c \bar{\nu}_2 - e^{-\nu \Delta}\right) = 0,$$

$$a_1 e^{-\nu_1 \Delta} + a_3 e^{\bar{\nu}_2 \Delta} - b_2 e^{\nu_2 \Delta} - b_3 e^{\bar{\nu}_2 \Delta} = 0,$$

$$a_1 \nu_q + b_1 = 0,$$

$$b_1 \alpha \tau c^2 + c_2 = 0,$$

$$b_2 + b_3 - c_2 = 0,$$

$$b_2 \nu_2 + b_3 \bar{\nu}_2 - c_2 \nu_2 = 0. \tag{5.85}$$

The solvability condition for this system gives a characteristic equation

$$f_e(\lambda; c, \alpha, \tau) = \alpha c (\nu_2 - \bar{\nu}_2) e^{\nu \Delta} - 1 + \frac{\tau c (\nu_1 + \bar{\nu}_2)}{(1 + \lambda \tau)^2 + \tau c^2} e^{-(\nu_1 + \nu_2 - \nu)\Delta} = 0, \tag{5.86}$$

where

$$\nu = \frac{1 + \tau c^2}{\tau c}, \qquad \nu_1 = \frac{1 + \lambda \tau}{\tau c},$$

$$\nu_2 = \frac{c + \sqrt{c^2 + 4\lambda}}{2}, \qquad \bar{\nu}_2 = \frac{c - \sqrt{c^2 + 4\lambda}}{2},$$

$$\Delta = \frac{1}{c} \ln\left(\frac{1 + \alpha}{\alpha}\right). \tag{5.87}$$

It is easy to check using (C.147, C.148) that the characteristic equations (5.71, 5.86) are equivalent. This further confirm the validity of our linearization procedure. For selected parameter values, which correspond to other numerical illustrations in this thesis, the graph of the function f_e against λ is shown in Fig. 5.9.

Figure 5.9: The plot of the characteristic function from (5.86) for the front model [8] for parameter values $c = 0.3318742892$, $\tau = 8.2$, $\alpha = 1.0$.

Adjoint eigenvalue problem for the front model

The nature of the problem we try to solve, that is, approximation of the center-stable manifold requires that we deal instead with the adjoint eigenvalue problem. Thus, the *adjoint* eigenvalue problem to (5.78) is

$$\mathcal{L}^{+} \bar{W} = \mu \bar{W}, \tag{5.88}$$

where

$$\mathcal{L}^{+} = \bar{D}^{T} \frac{\mathrm{d}^{2}}{\mathrm{d}\xi^{2}} - \bar{C} \frac{\mathrm{d}}{\mathrm{d}\xi} + \bar{F}^{T}, \quad \bar{D}^{T} = \bar{D}, \quad \bar{W} = \begin{pmatrix} \phi^{*} \\ \psi^{*} \end{pmatrix}, \tag{5.89}$$

and

$$\bar{F}^{T} = \begin{pmatrix} \dfrac{-1}{v_{0}'} \delta(\xi + \Delta) \, h_{0} & \dfrac{1}{\tau \, v_{0}'} \delta(\xi) \\ \Theta(-\xi - \Delta) & -1/\tau \end{pmatrix}. \tag{5.90}$$

We cast (5.88) into three ODEs

$$\begin{aligned}
\frac{\mathrm{d}\phi^{*}}{\mathrm{d}\xi} &= \eta^{*}, \\
\frac{\mathrm{d}\eta^{*}}{\mathrm{d}\xi} &= \left(\mu + \frac{1}{v_{0}'} \delta(\xi + \Delta) \, h_{0} \right) \phi^{*} + c \, \eta^{*} - \frac{1}{\tau \, v_{0}'} \delta(\xi) \psi^{*}, \\
\frac{\mathrm{d}\psi^{*}}{\mathrm{d}\xi} &= \frac{1}{c} \Theta(-\xi - \Delta) \, \phi^{*} - \frac{(1 + \mu \, \tau)}{\tau \, c} \phi^{*},
\end{aligned} \tag{5.91}$$

and which is then written in matrix format as

$$\Xi^{*\prime} = B \, \Xi^{*}, \tag{5.92}$$

88

where $\Xi^* = (\phi^*, \eta^*, \psi^*)^T$, $\eta^* = \phi^{*\,\prime}$ and

$$B = \begin{pmatrix} 0 & 1 & 0 \\ \mu + \dfrac{1}{v_0'}\delta(\xi+\Delta)\,h_0 & c & \dfrac{-1}{\tau\,c\,v_0'}\delta(\xi) \\ \dfrac{1}{c}\Theta(-\xi-\Delta) & 0 & -\dfrac{(1+\mu\,\tau)}{\tau\,c} \end{pmatrix}. \tag{5.93}$$

The general solution to the eigenvalue problem (5.92) (see Sec. C.3 in Appendix C) is

$$\phi^*(\xi) = \begin{cases} \phi_a^*(\xi) = a_2^*\,e^{\gamma_2\,\xi}, & \xi < -\Delta, \\ \phi_b^*(\xi) = b_2^*\,e^{\gamma_2\,\xi} + b_3^*\,e^{\bar{\gamma}_2\,\xi}, & -\Delta \le \xi < 0, \\ \phi_c^*(\xi) = c_3^*\,e^{\bar{\gamma}_2\,\xi}, & \xi \ge 0, \end{cases}$$

$$\psi^*(\xi) = \begin{cases} \psi_a^*(\xi) = a_2^*\,\gamma_3\,e^{\gamma_2\,\xi}, & \xi < -\Delta, \\ \psi_b^*(\xi) = b_1^*\,e^{-\gamma_1\,\xi}, & -\Delta \le \xi < 0, \\ \psi_c^*(\xi) = c_1^*\,e^{-\gamma_1\,\xi}, & \xi \ge 0, \end{cases} \tag{5.94}$$

$$\eta^*(\xi) = \begin{cases} \eta_a^*(\xi) = a_2^*\,\gamma_2\,e^{\gamma_2\,\xi}, & \xi < -\Delta, \\ \eta_b^*(\xi) = b_2^*\,\gamma_2\,e^{\gamma_2\,\xi} + b_3^*\,\bar{\gamma}_2\,e^{\bar{\gamma}_2\,\xi}, & -\Delta \le \xi < 0, \\ \eta_c^*(\xi) = c_3^*\,\bar{\gamma}_2\,e^{\bar{\gamma}_2\,\xi}, & \xi \ge 0, \end{cases}$$

where

$$\gamma_1 = \frac{1+\mu\,\tau}{\tau\,c}, \qquad\qquad \gamma_2 = \frac{c+\sqrt{c^2+4\,\mu}}{2},$$

$$\bar{\gamma}_2 = \frac{c-\sqrt{c^2+4\,\mu}}{2}, \qquad\qquad \gamma_3 = \frac{1}{c\,(\gamma_1+\gamma_2)},$$

$$\gamma = \frac{1+\tau\,c^2}{\tau\,c}, \qquad\qquad \Delta = \frac{1}{c}\,\ln(\frac{1+\alpha}{\alpha}). \tag{5.95}$$

The arbitrary constants a_2^*, b_1^*, b_2^*, b_3^*, c_1^*, c_3^* are to be determined from the matching conditions which give a system of six equations for six unknowns

$$a_2^*\,\alpha\,c\,\gamma_2\,e^{-\gamma_2\Delta} - b_2^*\,e^{-\gamma_2\Delta}\left(\alpha\,c\,\gamma_2 + e^{-\gamma\Delta}\right) - b_3^*\,e^{-\bar{\gamma}_2\Delta}\left(\alpha\,c\,\bar{\gamma}_2 + e^{-\gamma\Delta}\right) = 0,$$

$$a_2^*\,e^{-\gamma_2\,\Delta} - b_2^*\,e^{-\gamma_2\,\Delta} - b_3^*\,e^{-\bar{\gamma}_2\,\Delta} = 0,$$

$$a_2^*\,\gamma_3\,e^{-\gamma_2\,\Delta} - b_1^*\,e^{\gamma_1\,\Delta} = 0,$$

$$b_2^*\,\alpha\,\tau\,c\,\gamma_2 + b_3^*\,\alpha\,\tau\,c\,\bar{\gamma}_2 + c_1^* - c_3^*\,\alpha\,\tau\,c\,\bar{\gamma}_2 = 0,$$

$$b_2^* + b_3^* - c_3^* = 0,$$

$$b_1^* - c_1^* = 0. \tag{5.96}$$

System (5.96) has nontrivial solutions only if the determinant of its coefficient matrix is zero which consequently leads to the following characteristic equation (see Appendix C)

$$f_e^* = \alpha\,c\,(\gamma_2 - \bar{\gamma}_2)\,e^{\gamma\Delta} - 1 + \frac{\tau\,c\,(\gamma_1 + \bar{\gamma}_2)}{(1+\mu\,\tau)^2 + \tau\,c^2}\,e^{-(\gamma_1+\gamma_2-\gamma)\Delta} = 0. \tag{5.97}$$

89

We note that this characteristic equation (5.97) is exactly equivalent to (5.86), the characteristic equation of the direct problem with $\gamma \equiv \nu$, $\lambda \equiv \mu$.

For the same selected parameter values which correspond to numerical illustrations in this work, the Fig. 5.10 shows the graph of f_e^* as a function of μ.
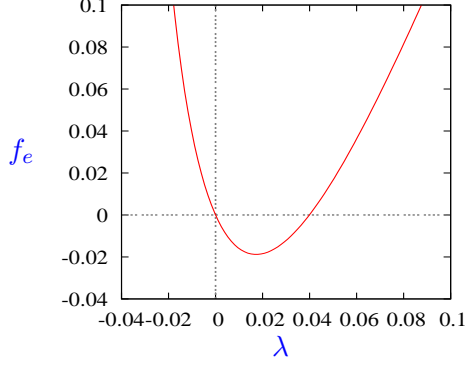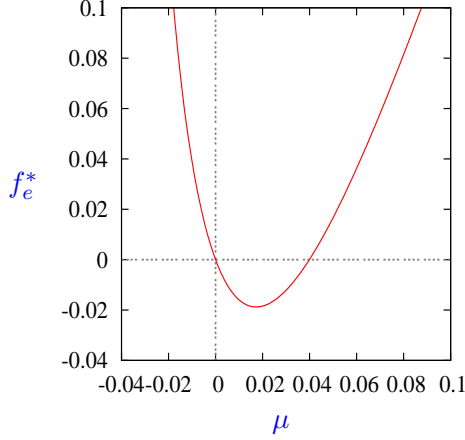

Figure 5.10: The plot of the adjoint characteristic function from (5.97) for the front model in [8] for parameter values $c = 0.3318742892$, $\tau = 8.2$, $\alpha = 1.0$.

5.3.4 Analytical threshold curve for the front: Projection onto the unstable mode

Now we use the adjoint eigenfunctions to obtain analytical ignition criteria, using the same two methods as we developed for the ZFK equation in sections Sec. 5.2.

We illustrate the method for particular values of parameters, as used in Fig. 5.8, Fig. 5.9 and Fig. 5.10. For $c = 0.3318742892$, $\alpha = 1.0$, $\tau = 8.2$, the linearized equation at the unstable front and its adjoint have one positive eigenvalue $\lambda = 0.03990255031$ which guarantees that the center-stable manifold is a codimension-1 hypersurface in the functional space, which separates the decay and ignition initial conditions, as we have shown in Sec. 4.2.2.

To derive the ignition criterion, we consider, as in ZFK equation, linearization at the unstable front solution. We look for a solution in the form

$$\bar{U} = \bar{U}_0 + \sum_{k=1}^{\infty} a_k \bar{V}_k(\xi)\, \mathrm{e}^{\lambda_k t}, \tag{5.98}$$

where $\bar{U} = \begin{pmatrix} E(\xi, t) \\ h(\xi, t) \end{pmatrix}$ is the solution to (5.73) of Sec. 5.3.3, $\bar{U}_0 = \begin{pmatrix} v_0(\xi) \\ h_0(\xi) \end{pmatrix}$ is a stationary solution to the nonlinear system (5.73) (see (5.74) in Sec. 5.3.3) and the second term on the right hand side of (5.98) represents the solution to the linearized problem (5.78). Specifically, $\bar{V}_k = \begin{pmatrix} \phi_k(\xi) \\ \psi_k(\xi) \end{pmatrix}$ and λ_k are eigenpairs to the linearized problem.

We know $\lambda_1 > 0$ is the positive eigenvalue mentioned above, $\lambda_2 = 0$ corresponds to the translational symmetry, and $\mathrm{Re}(\lambda_k) < 0$ for $k > 2$. Note that since the linearized problem is now not self-adjoint, we cannot apply Sturm theorem about eigenvalues (but rely on Hinch's results [43] about an equivalent problem), and also cannot guarantee that all eigenvalues are real.

As before, the equation of the critical surface in this linear approximation is $a_1 = 0$: with one sign of a_1, solutions depart from the critical front in one direction, toward decay, and with the opposite sign of a_1, they depart toward ignition. Since the problem is not self-adjoint, to determine a_1, we project the initial conditions of the linearized problem by taking scalar product with the corresponding adjoint eigenfunctions $\bar{W}_k^* = \begin{pmatrix} \phi_k^*(\xi) \\ \psi_k^*(\xi) \end{pmatrix}$. Hence, we come to the following equation

$$a_1(\delta) = \int_{-\infty}^{\infty} \left[\left(-\alpha + v_{\mathrm{stim}} \, H(\xi - \delta) - v_0(\xi) \right) \phi_1^*(\xi) + \left(1 - h_0(\xi) \right) \psi_1^*(\xi) \right] \, \mathrm{d}\xi = 0,$$

(5.99)

with δ as the shift along the spatial coordinate and

$$H(\xi - \delta) = \begin{cases} 1, & \xi \in [\xi_{\mathrm{b}}, \, \xi_{\mathrm{f}}], \\ 0, & \text{otherwise,} \end{cases}$$

where

$$\begin{aligned} \xi_{\mathrm{f}} &= \xi_{\mathrm{stim}} + \delta, \\ \xi_{\mathrm{b}} &= -\xi_{\mathrm{stim}} + \delta. \end{aligned}$$

(5.100)

The exact analytical solutions $(v_0(\xi), h_0(\xi))$ to our nonlinear system (5.73) are given as

$$v_0(\xi) = \begin{cases} v_{0a}(\xi) = \omega - \theta_1 \, \mathrm{e}^{\xi/\tau c}, & \xi \leq -\Delta, \\ v_{0b}(\xi) = -\alpha + \alpha \, \mathrm{e}^{-c\xi}, & \xi \geq -\Delta, \end{cases}$$

$$h_0(\xi) = \begin{cases} h_{0a}(\xi) = \mathrm{e}^{\xi/\tau c}, & \xi \leq 0, \\ h_{0b}(\xi) = 1, & \xi \geq 0, \end{cases}$$

where $\omega = 1 + \tau \, c^2 (1 + \alpha)$, $\theta_1 = \dfrac{\tau^2 \, c^2}{1 + \tau \, c^2}$ and $\Delta = \dfrac{1}{c} \ln\left(\dfrac{1 + \alpha}{\alpha} \right)$.

The unstable eigenmodes, ϕ_1^*, ψ_1^* which correspond to the positive eigenvalue are [1]

$$\phi_1^*(\xi) = \begin{cases} \phi_a^*(\xi) = a_{12}^* \, e^{\gamma_2 \xi}, & \xi < -\Delta, \\ \phi_b^*(\xi) = b_{12}^* \, e^{\gamma_2 \xi} + b_{13}^* \, e^{\bar{\gamma}_2 \xi}, & -\Delta \leq \xi < 0, \\ \phi_c^*(\xi) = c_{13}^* \, e^{\bar{\gamma}_2 \xi}, & \xi \geq 0, \end{cases}$$

$$\psi_1^*(\xi) = \begin{cases} \psi_a^*(\xi) = a_{12}^* \gamma_3 \, e^{\gamma_2 \xi}, & \xi < -\Delta, \\ \psi_b^*(\xi) = b_{11}^* \, e^{-\gamma_1 \xi}, & -\Delta \leq \xi < 0, \\ \psi_c^*(\xi) = c_{11}^* \, e^{-\gamma_1 \xi}, & \xi \geq 0, \end{cases}$$

where

$$\gamma_1 = \frac{1 + \mu\,\tau}{\tau\,c}, \qquad\qquad\qquad \gamma_2 = \frac{c + \sqrt{c^2 + 4\,\mu}}{2},$$

$$\bar{\gamma}_2 = \frac{c - \sqrt{c^2 + 4\,\mu}}{2}, \qquad\qquad \gamma_3 = \frac{1}{c\,(\gamma_1 + \gamma_2)}. \qquad (5.101)$$

The formulation in (5.99) can be compactly expressed in the form

$$D_1(\xi_{\text{stim}}, \delta)\, v_{\text{stim}} + N_1 = 0, \qquad (5.102)$$

where

$$D_1 = \int_{\xi_b}^{\xi_f} \phi_1^* \, \mathrm{d}\xi,$$

$$N_1 = \int_{-\infty}^{\infty} \Big((-\alpha - v_0)\, \phi_1^* + (1 - h_0)\, \psi_1^* \Big) \, \mathrm{d}\xi. \qquad (5.103)$$

Due to the nature of the unstable eigenmode as shown in Fig. 5.11 the integrals in (5.103) now become

$$D_1 = \int_{\xi_b}^{-\Delta} \phi_a^*(\xi) \, \mathrm{d}\xi + \int_{-\Delta}^{\xi_f} \phi_b^*(\xi) \, \mathrm{d}\xi,$$

$$N_1 = \int_{-\infty}^{-\Delta} \Big((-\alpha - v_{0a})\, \phi_a^*(\xi) + (1 - h_{0a})\psi_a^*(\xi) \Big) \, \mathrm{d}\xi$$

$$+ \int_{-\Delta}^{0} \Big((-\alpha - v_{0b})\, \phi_b^*(\xi) + (1 - h_{0a})\psi_b^*(\xi) \Big) \, \mathrm{d}\xi$$

$$+ \int_{0}^{\infty} (-\alpha - v_{0b})\, \phi_c^*(\xi) \, \mathrm{d}\xi. \qquad (5.104)$$

Therefore,

$$D_1 = \frac{a_{12}^*}{\gamma_2}\big(e^{-\gamma_2 \Delta} - e^{\gamma_2 \xi_b}\big) + \frac{b_{12}^*}{\gamma_2}\big(e^{\gamma_2 \xi_f} - e^{-\gamma_2 \Delta}\big) + \frac{b_{13}^*}{\bar{\gamma}_2}\big(e^{\bar{\gamma}_2 \xi_f} - e^{-\bar{\gamma}_2 \Delta}\big), \quad (5.105)$$

---

[1]Note that we use a_{1j}^*, b_{1j}^*, c_{1j}^*, $j = 1, 2, 3$ in place of a_j^*, b_j^*, c_j^*, $j = 1, 2, 3$ if the eigenvalue for unstable eigenmode applies. Meanwhile, we use a_{2j}^*, b_{2j}^*, c_{2j}^*, $j = 1, 2, 3$ whenever the zero eigenvalue that corresponds to zero eigenmode applies.
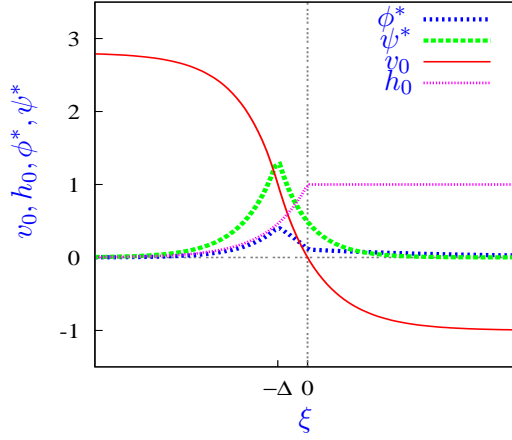
Figure 5.11: The plot of the unstable eigenmode for the front obtained from Biktashev's model [8] for parameter values $c = 0.3318742892$, $\tau = 8.2$, $\alpha = 1.0$. The red solid line, the magenta, blue and green dashed lines are respectively for v, h, ϕ^*, ψ^*.

and

$$
\begin{aligned}
N_1 = a_{12}^* &\left(\frac{\theta_1 - \gamma_3}{\gamma_2 + \frac{1}{\tau c}} \, e^{-(\gamma_2 + \frac{1}{\tau c})\Delta} + \frac{\gamma_3 - \alpha - \omega}{\gamma_2} \, e^{-\gamma_2 \Delta} \right) \\
&+ b_{11}^* \left(\frac{1}{\gamma_1 - \frac{1}{\tau c}} (1 - e^{(\gamma_1 - \frac{1}{\tau c})\Delta}) - \frac{1}{\gamma_1}(1 - e^{\gamma_1 \Delta}) \right) \\
&- \frac{b_{12}^* \alpha}{\gamma_2 - c} \left(1 - e^{-(\gamma_2 - c)\Delta} \right) - \frac{b_{13}^* \alpha}{\bar{\gamma}_2 - c} \left(1 - e^{-(\bar{\gamma}_2 - c)\Delta} \right) + \frac{c_{13}^* \alpha}{\bar{\gamma}_2 - c}.
\end{aligned} \tag{5.106}
$$

Hence,

$$
v_{\text{stim}} = -\frac{N_1}{D_1(\xi_{\text{stim}}, \delta)}. \tag{5.107}
$$

5.3.5 Analytical threshold curve for the front: threshold minimization method (Method 1)

As with the ZFK equation, we explore two methods for choosing the arbitrary constant δ in (5.107): minimization of the threshold and minimization of the norm of the initial condition.

The minimum value of v_{stim} is attained if D_1 is at maximum, therefore, maximizing D_1 with respect to δ, we get

$$
b_{12}^* \, e^{\gamma_2(\xi_{\text{stim}} + \delta)} + b_{13}^* \, e^{\bar{\gamma}_2(\xi_{\text{stim}} + \delta)} - a_{12}^* \, e^{-\gamma_2(\xi_{\text{stim}} - \delta)} = 0, \tag{5.108}
$$

and correspondingly the expression for δ at this minimum v_{stim} is

$$
\delta = \delta^* = -\frac{1}{D} \ln \left(\frac{-b_{12}^*}{b_{13}^*} \right) - \xi_{\text{stim}} - \frac{1}{D} \left(1 - \frac{a_{12}^*}{b_{12}^*} \, e^{-2\gamma_2 \xi_{\text{stim}}} \right), \tag{5.109}
$$

where $D = \sqrt{c^2 + 4\mu}$.

93

We now use the known values of our parameters $c = 0.3318742892$, $\alpha = 1.0$, $\tau = 8.2$ for the unstable front solution and $\mu = 0.03990255031$ found from the adjoint characteristic equation (5.97), to determine the arbitrary constants a_{12}^*, b_{11}^*, b_{12}^*, b_{13}^*, c_{11}^*, c_{13}^* in system (5.96). For these parameter values, $\omega = 2.806304918$, $\theta_1 = 3.891359376$. Therefore, by arbitrarily choosing $a_{12}^* = 1$ we find $b_{11}^* = 0.4897404175$, $b_{12}^* = -0.3464951502$, $b_{13}^* = 0.4550928743$, $c_{11}^* = 0.4897404175$ and $c_{13}^* = 0.1085977241$. Consequently, (5.106) evaluates to $N_1 = -0.8630528410$ and thus,

$$\delta^*(\xi_{\text{stim}}) = 0.5249242192 - \xi_{\text{stim}} - 1.925389830 \ln\left(1 + 2.886043281 \ e^{-0.8512496304 \, \xi_{\text{stim}}}\right). \tag{5.110}$$

We then substitute $\delta = \delta^*$ in (5.107) to obtain

$$v_{\text{stim}}(\xi_{\text{stim}}) = \frac{-k_0 \left(1 + k_2 \ e^{-k_8 \, \xi_{\text{stim}}}\right)^{k_3}}{k_5 + k_1 \ e^{-k_8 \, \xi_{\text{stim}}} + k_4 \left(1 + k_2 \ e^{-k_8 \, \xi_{\text{stim}}}\right)^{k_3} \left(k_6 \left(1 + k_2 \ e^{-k_8 \, \xi_{\text{stim}}}\right)^{k_7} - 1\right)}, \tag{5.111}$$

where

$$
\begin{array}{lll}
k_0 = 0.03443800972, & k_1 = 0.1172206492, & k_2 = 2.886043281, \\
k_3 = 0.8194936906, & k_4 = 0.2874873522, & k_5 = 0.04061638645, \\
k_6 = 0.6414100599, & k_7 = 0.1805063093, & k_8 = 0.8512496304. \quad (5.112)
\end{array}
$$

Alternatively, we can find the maximum of D_1 by analysing equation (5.103). We observe that $D_1 = \int_{\xi_{\text{b}}}^{\xi_{\text{f}}} \phi_1^*(\xi) \ d\xi$ and therefore

$$
\begin{aligned}
\frac{\partial D_1}{\partial \delta} &= \phi_1^*(\xi_{\text{f}}) \frac{\partial \xi_{\text{f}}}{\partial \delta} - \phi_1^*(\xi_{\text{b}}) \frac{\partial \xi_{\text{b}}}{\partial \delta}, \\
&= \phi_1^*(\xi_{\text{f}}) - \phi_1^*(\xi_{\text{b}}), \tag{5.113}
\end{aligned}
$$

and thus the maximum of D_1 is achieved when $\phi_1^*(\xi_{\text{b}}) = \phi_1^*(\xi_{\text{f}})$. Hence a *graphical* method of solution: we need to find two points on the graph of $\phi_1^*(x)$ (see Fig. 5.11) which have the same ordinate ϕ^{**} and whose abscissas are at the distance $2\xi_{\text{stim}}$ from each other. As evident from Fig. 5.11, graph of $\phi_1^*(x)$ is unimodal so the solution to such a problem is unique, and $\xi_{\text{f}} > -\Delta$ and $\xi_{\text{b}} < -\Delta$, and for smaller values of ξ_{stim}, we have $\xi_{\text{f}} < 0$. Therefore,

$$\phi_a^*(\xi_{\text{b}}) = \phi^{**} = \phi_b^*(\xi_{\text{f}}), \tag{5.114}$$

which leads to

$$\xi_{\text{b}}(\xi_{\text{f}}) = \frac{1}{\gamma_2} \ln\left(\frac{b_{12}^* \ e^{\gamma_2 \, \xi_{\text{f}}} + b_{13}^* \ e^{\bar{\gamma}_2 \, \xi_{\text{f}}}}{a_{12}^*}\right). \tag{5.115}$$

Note that from (5.115), since $\xi_b = -\xi_{stim} + \delta$ and $\xi_f = \xi_{stim} + \delta$, we can derive an exact expression for δ as given in (5.109). Equation (5.115) can further be simplified to become, depending on the sign of the ratio b_{12}^*/a_{12}^*

$$\xi_b(\xi_f) = \begin{cases} \xi_f + \dfrac{1}{\gamma_2} \ln\left(\dfrac{b_{12}^*}{a_{12}^*}\right) + \dfrac{1}{\gamma_2} \ln\left(1 + \dfrac{b_{13}^*}{b_{12}^*} e^{-D\xi_f}\right), & b_{12}^*/a_{12}^* > 0, \\[3mm] \xi_f + \dfrac{1}{\gamma_2} \ln\left(\dfrac{-b_{12}^*}{a_{12}^*}\right) + \dfrac{1}{\gamma_2} \ln\left(-1 - \dfrac{b_{13}^*}{b_{12}^*} e^{-D\xi_f}\right), & b_{12}^*/a_{12}^* < 0, \end{cases} \tag{5.116}$$

where $D = \sqrt{c^2 + 4\mu}$. Now using the same set of parameter values c, τ, α, μ and the same values for the constants a_{12}^*, b_{11}^*, b_{12}^*, b_{13}^*, c_{11}^*, c_{13}^*, as used in the first approach and after substituting $\xi_b(\xi_f)$ from (5.116) in (5.107), we now have expression for v_{stim} in terms of ξ_f

$$v_{stim}(\xi_f) = 0.1197896555 \left(1 - 0.8221718799 \ e^{-0.09375052600\,\xi_f}\right)^{-1}. \tag{5.117}$$

Since $\xi_{stim} = 0.5\,(\xi_f - \xi_b)$ and using the expression for ξ_b from (5.116), we can rewrite the expression for ξ_{stim} in terms of ξ_f

$$\xi_{stim}(\xi_f) = 1.245094763 - 1.174743535 \ln\left(-1 + 1.313417732 \ e^{-0.5193753412\,\xi_f}\right). \tag{5.118}$$

The pictures in Fig. 5.12 show the threshold curves (blue dashed curves) from our analytical ignition criterion being compared with the one (solid-red curve) obtained from numerics. And it also shows that the two approaches for determining v_{stim} from the first method yield the same result.
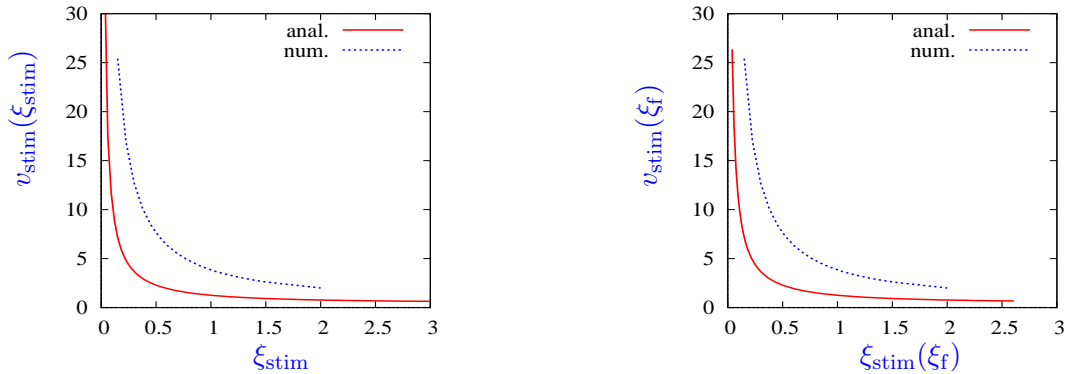
Figure 5.12: The plot of the threshold curves (analytical and numerical) for the front obtained from Biktashev's model [8] for parameter values $c = 0.3318742892$, $\tau = 8.2$, $\alpha = 1.0$: The red solid line is the threshold curve from analytical formulations (5.111, 5.117), while the blue dashed line is the threshold curve from numerical simulations. The plot of v_{stim} against ξ_{stim} on the right is a parametric plot when ξ_f is treated as parameter.

5.3.6 Analytical threshold curve for the front: initial condition minimization method (Method 2)

The threshold criteria are given by

$$a_1(\delta) = \int_{-\infty}^{\infty} \left[\left(-\alpha + v_{\text{stim}} H(\xi - \delta) - v_0(\xi) \right) \phi_1^*(\xi) + \left(1 - h_0(\xi) \right) \psi_1^*(\xi) \right] \, d\xi = 0,$$

$$a_2(\delta) = \int_{-\infty}^{\infty} \left[\left(-\alpha + v_{\text{stim}} H(\xi - \delta) - v_0(\xi) \right) \phi_2^*(\xi) + \left(1 - h_0(\xi) \right) \psi_2^*(\xi) \right] \, d\xi = 0,$$

$$(5.119)$$

where the first is the projection onto the positive eigenmodes and the second can be derived from the condition of minimum of the L_2 norm of the initial condition for the linearized problem as in ZFK equation. Note that the second equation can be considered as corresponding to projection onto the zero eigenmodes in a similar fashion to the first equation. Here, H is given by

$$H(\xi - \delta) = \begin{cases} 1, & \xi \in [\xi_{\text{b}}, \xi_{\text{f}}], \\ 0, & \text{Otherwise,} \end{cases} \qquad (5.120)$$

where

$$\begin{aligned} \xi_{\text{f}} &= \xi_{\text{stim}} + \delta, \\ \xi_{\text{b}} &= -\xi_{\text{stim}} + \delta. \end{aligned} \qquad (5.121)$$

The exact analytical solutions to the nonlinear system are

$$v_0(\xi) = \begin{cases} v_{0a}(\xi) = \omega - \theta_1 \, e^{\frac{\xi}{\tau c}}, & \xi \leq -\Delta, \\ +v_{0b}(\xi) = -\alpha + \alpha \, e^{-c\xi}, & \xi \geq -\Delta, \end{cases}$$

$$h_0(\xi) = \begin{cases} h_{0a}(\xi) = e^{\frac{\xi}{\tau c}}, & \xi \leq 0, \\ h_{0b}(\xi) = 1, & \xi \geq 0, \end{cases} \qquad (5.122)$$

where $\omega = 1 + \tau c^2(1 + \alpha)$, $\theta_1 = \dfrac{\tau^2 c^2}{1 + \tau c^2}$ and $\Delta = \dfrac{1}{c} \ln\left(\dfrac{1 + \alpha}{\alpha} \right)$.

Meanwhile, ϕ_1^*, ψ_1^*, the unstable eigenmodes corresponding to the positive eigenvalue are

$$\phi_1^*(\xi) = \begin{cases} \phi_{1a}^*(\xi) = a_{12}^* \, e^{\gamma_2 \xi}, & \xi < -\Delta, \\ \phi_{1b}^*(\xi) = b_{12}^* \, e^{\gamma_2 \xi} + b_{13}^* \, e^{\bar{\gamma}_2 \xi}, & -\Delta \leq \xi < 0, \\ \phi_{1c}^*(\xi) = c_{13}^* \, e^{\bar{\gamma}_2 \xi}, & \xi \geq 0, \end{cases}$$

$$\psi_1^*(\xi) = \begin{cases} \psi_{1a}^*(\xi) = a_{12}^* \gamma_3 \, e^{\gamma_2 \xi}, & \xi < -\Delta, \\ \psi_{1b}^*(\xi) = b_{11}^* \, e^{-\gamma_1 \xi}, & -\Delta \leq \xi < 0, \\ \psi_{1c}^*(\xi) = c_{11}^* \, e^{-\gamma_1 \xi}, & \xi \geq 0, \end{cases} \qquad (5.123)$$

where

$$\gamma_1 = \frac{1 + \mu\,\tau}{\tau\,c}, \qquad\qquad \gamma_2 = \frac{c + \sqrt{c^2 + 4\,\mu}}{2},$$

$$\bar{\gamma}_2 = \frac{c - \sqrt{c^2 + 4\,\mu}}{2}, \qquad\qquad \gamma_3 = \frac{1}{c\,(\gamma_1 + \gamma_2)}. \qquad (5.124)$$

The eigenmodes ϕ_2^*, ψ_2^* correspond to zero eigenvalue

$$\phi_2^*(\xi) = \begin{cases} \phi_{2a}^*(\xi) = a_{22}^*\;e^{c\xi}, & \xi < -\Delta, \\ \phi_{2b}^*(\xi) = b_{22}^*\;e^{c\xi} + b_{23}^*, & -\Delta \le \xi < 0, \\ \phi_{2c}^*(\xi) = c_{23}^*, & \xi \ge 0, \end{cases}$$

$$\psi_2^*(\xi) = \begin{cases} \psi_{2a}^*(\xi) = a_{22}^*\,\dfrac{\tau}{1 + \tau\,c^2}\;e^{c\xi}, & \xi < -\Delta, \\[2mm] \psi_{2b}^*(\xi) = b_{21}^*\;e^{-\dfrac{\xi}{\tau\,c}}, & -\Delta \le \xi < 0, \\[2mm] \psi_{2c}^*(\xi) = c_{21}^*\;e^{-\dfrac{\xi}{\tau\,c}}, & \xi \ge 0. \end{cases} \qquad (5.125)$$

The equations in (5.119) can be rewritten as

$$v_{\text{stim}}\,D_1(\xi,\delta) = N_1,$$

$$v_{\text{stim}}\,D_2(\xi,\delta) = N_2, \qquad (5.126)$$

where

$$D_1 = \int_{-\infty}^{\infty} H(\xi - \delta)\,\phi_1^*(\xi)\;\mathrm{d}\xi,$$

$$D_2 = \int_{-\infty}^{\infty} H(\xi - \delta)\,\phi_2^*(\xi)\;\mathrm{d}\xi,$$

$$N_1 = \int_{-\infty}^{\infty} \Big(\alpha + v_0(\xi)\Big)\,\phi_1^*(\xi)\;\mathrm{d}\xi - \int_{-\infty}^{\infty} \Big(1 - h_0(\xi)\Big)\psi_1^*(\xi)\;\mathrm{d}\xi,$$

$$N_2 = \int_{-\infty}^{\infty} \Big(\alpha + v_0(\xi)\Big)\,\phi_2^*(\xi)\;\mathrm{d}\xi - \int_{-\infty}^{\infty} \Big(1 - h_0(\xi)\Big)\psi_2^*(\xi)\;\mathrm{d}\xi. \qquad (5.127)$$

From (5.126, 5.127) we have

$$\int_{-\infty}^{\infty} H(\xi - \delta)\Phi(\xi)\;\mathrm{d}\xi = 0, \qquad (5.128)$$

where

$$\Phi(\xi) = N_1\,\phi_2^*(\xi) - N_2\,\phi_1^*(\xi). \qquad (5.129)$$

Let us look for $\eta(x)$ such that $\Phi(x) = [\eta(x)]'$, that is,

$$\eta(x) = \int_{-\infty}^{x} \Big(N_1\,\phi_2^*(\xi) - N_2\,\phi_1^*(\xi)\Big)\;\mathrm{d}\xi. \qquad (5.130)$$

Then we can apply here the same graphical method of solution as we applied in our first method in the previous subsection, with function $\eta(x)$ in place of $\phi_1^*(x)$.

For $x < -\Delta$,

$$\eta_L(x) = N_1\, a_{22}^* \int_{-\infty}^{x} \mathrm{e}^{c\xi}\, \mathrm{d}\xi - N_2\, a_{12}^* \int_{-\infty}^{x} \mathrm{e}^{\gamma_2 \xi}\, \mathrm{d}\xi,$$

$$= \frac{N_1\, a_{22}^*}{c}\, \mathrm{e}^{cx} - \frac{N_2\, a_{12}^*}{\gamma_2}\, \mathrm{e}^{\gamma_2 x}, \tag{5.131}$$

and for $x > -\Delta$ and $x \leq 0$,

$$\eta_{R_1}(x) = \int_{-\infty}^{-\Delta} \Big(N_1\, \phi_2^*(\xi) - N_2\, \phi_1^*(\xi)\Big)\, \mathrm{d}\xi + \int_{-\Delta}^{x} \Big(N_1\, \phi_2^*(\xi) - N_2\, \phi_1^*(\xi)\Big)\, \mathrm{d}\xi,$$

$$= N_1\, a_{22}^* \int_{-\infty}^{-\Delta} \mathrm{e}^{c\xi}\, \mathrm{d}\xi - N_2\, a_{12}^* \int_{-\infty}^{-\Delta} \mathrm{e}^{\gamma_2 \xi}\, \mathrm{d}\xi$$

$$+ N_1 \int_{-\Delta}^{x} \Big(b_{22}^*\, \mathrm{e}^{c\xi} + b_{23}^*\Big)\, \mathrm{d}\xi - N_2 \int_{-\Delta}^{x} \Big(b_{12}^*\, \mathrm{e}^{\gamma_2 \xi} + b_{13}^*\, \mathrm{e}^{\bar{\gamma}_2 \xi}\Big)\, \mathrm{d}\xi,$$

$$= \frac{N_1\, a_{22}^*}{c}\, \mathrm{e}^{-c\Delta} - \frac{N_2\, a_{12}^*}{\gamma_2}\, \mathrm{e}^{-\gamma_2 \Delta} + \frac{N_1\, b_{22}^*}{c}\, \mathrm{e}^{cx} - \frac{N_1\, b_{22}^*}{c}\, \mathrm{e}^{-c\Delta} + N_1\, b_{23}^* (x + \Delta)$$

$$- \frac{N_2\, b_{12}^*}{\gamma_2}\, \mathrm{e}^{\gamma_2 x} + \frac{N_2\, b_{12}^*}{\gamma_2}\, \mathrm{e}^{-\gamma_2 \Delta} - \frac{N_2\, b_{13}^*}{\bar{\gamma}_2}\, \mathrm{e}^{\bar{\gamma}_2 x} + \frac{N_2\, b_{13}^*}{\bar{\gamma}_2}\, \mathrm{e}^{-\bar{\gamma}_2 \Delta}. \tag{5.132}$$

We note that $\eta_L(-\Delta) = \int_{-\infty}^{-\Delta} \Big(N_1\, \phi_2^*(\xi) - N_2\, \phi_1^*(\xi)\Big)\, \mathrm{d}\xi$.

Thus,

$$\eta_L(x) = \frac{N_1\, a_{22}^*}{c}\, \mathrm{e}^{cx} - \frac{N_2\, a_{12}^*}{\gamma_2}\, \mathrm{e}^{\gamma_2 x}, \tag{5.133}$$

and

$$\eta_{R_1}(x) = \frac{N_1\, b_{22}^*}{c}\, \mathrm{e}^{cx} - \frac{N_2\, b_{12}^*}{\gamma_2}\, \mathrm{e}^{\gamma_2 x} - \frac{N_2\, b_{13}^*}{\bar{\gamma}_2}\, \mathrm{e}^{\bar{\gamma}_2 x} + N_1\, b_{23}^* (x + \Delta)$$

$$+ \frac{N_1}{c}(a_{22}^* - b_{22}^*)\, \mathrm{e}^{-c\Delta} + \frac{N_2}{\gamma_2}(b_{12}^* - a_{12}^*)\, \mathrm{e}^{-\gamma_2 \Delta} + \frac{N_2\, b_{13}^*}{\bar{\gamma}_2}\, \mathrm{e}^{-\bar{\gamma}_2 \Delta}. \tag{5.134}$$

For $x \geq 0$,

$$\eta_{R_2}(x) = \eta_{R_1}(0) + \int_{0}^{x} \Big(N_1\, \phi_2^*(\xi) - N_2\, \phi_1^*(\xi)\Big)\, \mathrm{d}\xi,$$

$$= \eta_{R_1}(0) + N_1\, c_{23}^* \int_{0}^{x} \mathrm{d}\xi - N_2\, c_{23}^* \int_{0}^{x} \mathrm{e}^{\bar{\gamma}_2 \xi}\, \mathrm{d}\xi,$$

$$= \eta_{R_1}(0) + \overbrace{N_1\, c_{23}^*\, x - \frac{N_2\, c_{13}^*}{\bar{\gamma}_2}\Big(\mathrm{e}^{\bar{\gamma}_2 x} - 1\Big)}^{\eta_{R_{2a}}(x)}. \tag{5.135}$$

where

$$\eta_{R_1}(0) = \frac{N_1\, b_{22}^*}{c} - \frac{N_2\, b_{12}^*}{\gamma_2} - \frac{N_2\, b_{13}^*}{\bar{\gamma}_2} + N_1\, b_{23}^*\, \Delta + \frac{N_1}{c}(a_{22}^* - b_{22}^*)\, \mathrm{e}^{-c\Delta}$$

$$+ \frac{N_2}{\gamma_2}(b_{12}^* - a_{12}^*)\, \mathrm{e}^{-\gamma_2 \Delta} + \frac{N_2\, b_{13}^*}{\bar{\gamma}_2}\, \mathrm{e}^{-\bar{\gamma}_2 \Delta}. \tag{5.136}$$

We also note that $\eta_{R_1}(0) = \int_{-\infty}^{0} \Big(N_1\, \phi_2^*(\xi) - N_2\, \phi_1^*(\xi)\Big)\, \mathrm{d}\xi$.

Thus, $\eta_{R_2}(x) = \eta_{R_1}(0) + \eta_{R_{2a}}(x)$ and hence, our $\eta(x)$ function is written as

$$\eta(x) = \begin{cases} \eta_L(x), & x < -\Delta, \\ \eta_{R_1}(x), & -\Delta \le x < 0, \\ \eta_{R_2}(x), & x \ge 0. \end{cases}$$

(5.137)

The values of our parameters for the unstable front solution are $c = 0.3318742892$, $\tau = 8.2$, $\alpha = 1.0$ (for this value, $\Delta = 2.088583549$) and $\mu = 0.03990255031$ is found to be the only positive zero of the characteristic function from (5.97). For an arbitrary chosen value of one of the arbitrary constants, $a_{12}^* = 1$, we find from system (5.96) [2] the values of the other constants to be $b_{11}^* = 0.4897404175$, $b_{12}^* = -0.3464951502$, $b_{13}^* = 0.4550928743$, $c_{11}^* = 0.4897404175$ and $c_{13}^* = 0.1085977241$.

Similarly for $\mu = 0$ the eigenvalue corresponding to the zero eigenmode of the adjoint and for arbitrarily chosen value $a_{22}^* = 1$, we find from system (5.96) the other constants, $b_{21}^* = 1.0$, $b_{22}^* = -1.107232771$, $b_{23}^* = 1.053616385$, $c_{21}^* = 1.0$ and $c_{23}^* = -0.05361638563$.

And for these values, the integrals in (5.127) evaluate to $N_1 = 0.863052923$, $N_2 = -0.970438513$,

$$D_1 = 1.158369225 \; e^{-0.0937505260\,\xi_b} - 1.158369225 \; e^{-0.0937505260\,\xi_f},$$

(5.138)

and the η functions in (5.137) then become

$$\eta_L(x) = 2.600541684 \; e^{0.3318742892\,x} + 2.280032739 \; e^{0.4256248152\,x},$$

$$\eta_{R_1}(x) = 11.63093169 - 2.879404976 \; e^{0.3318742892\,x} + 0.9093267008\,x$$
$$- 0.7900202861 \; e^{0.4256248152\,x} - 4.710796526 \; e^{-0.0937505260\,x},$$

$$\eta_{R_2}(x) = 4.374836009 - 0.04627377834\,x - 1.124126108 \; e^{-0.0937505260\,x}. \quad (5.139)$$

The plot of the $\eta(x)$ function (see Fig. 5.13) shows that it has a unique maximum in the interval $x > 0$. Applying the same reasoning as in our first method, we need to find two points ξ_b and ξ_f such that $\xi_f - \xi_b = 2\,\xi_{\text{stim}}$ and $\eta(\xi_b) = \eta(\xi_f)$. Hence ξ_b and ξ_f are at different sides of the maximum of $\eta(x)$, and close to it, if δ is small.

The maximum of $\eta_{R_2}(x)$ is found to be located at $x = 8.779341309$ and has value $\eta_{\text{max}} = 3.474998428$. We consider

$$\eta_{R_2}(x) = 4.374836009 - 0.04627377834\,x - 1.124126108 \; e^{-0.0937505260\,x} = \eta_s, \quad (5.140)$$

---

[2]Note that we use a_{1j}^*, b_{1j}^*, c_{1j}^*, $j = 1, 2, 3$ in place of a_j^*, b_j^*, c_j^*, $j = 1, 2, 3$ for unstable eigenvalue and a_{2j}^*, b_{2j}^*, c_{2j}^*, $j = 1, 2, 3$ for the zero eigenvalue.
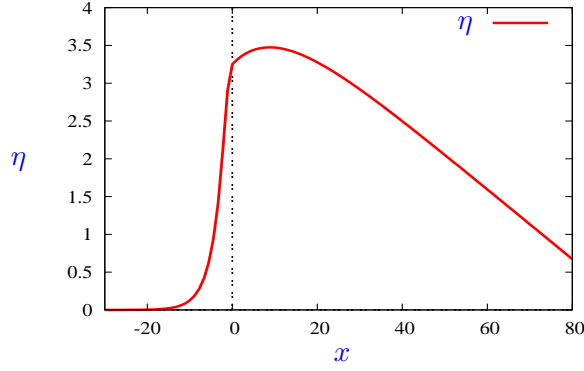
Figure 5.13: The plot of the η function, (5.137) showing the unique maximum when $x > 0$.

and then numerically, fix some constant values for η_s starting at some value, say $\eta_0 = 3.250709716$ to $\eta_{\max} = 3.474998428$ increasing by a constant step of approximately 0.0002. Each time we calculate the zeros of the resultant equation, the smaller of the two zeros we assign as ξ_b and the bigger as ξ_f. We substitute these values of ξ_b and ξ_f in (5.138) and then from the first equation in (5.126), we get our v_{stim} and the corresponding $\xi_{\mathrm{stim}} = \dfrac{\xi_b - \xi_f}{2}$. Plotting the pair of numerical values for $\xi_{\mathrm{stim}}, v_{\mathrm{stim}}$ should hopefully give us the threshold curve for the front model. The resultant plot is shown in Fig. 5.14, where the dashed-blue curve is the threshold curve obtained from numerical simulations and the solid-red one is from our analytical approximation.
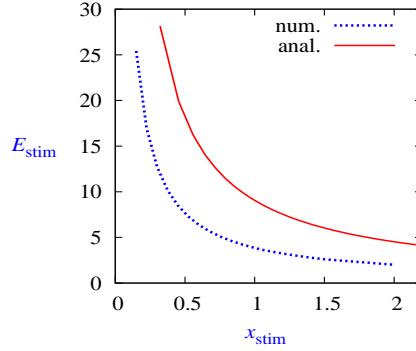
Figure 5.14: The plot of the threshold curves for the front equations from numerical simulations of our nonlinear PDEs (5.72) (dashed-blue curve) and the one (solid-red curve) from our analytical approximation using the second approach, that is projection onto the zero eigenmodes.

5.4   Summary

- We have developed a method of obtaining analytical criterion of ignition, by linear approximation of the center-stable manifold of the critical solution. This method depends on an arbitrary parameter δ, due to translational invariance of the prob-

lem. This arbitrary parameter is to be determined from further considerations, independent of the linear approximation.

- We have proposed two methods of determining parameter δ. Method 1 is about finding minimal u_{stim} at the given stimulus profile, and therefore provides a lower estimate of the threshold of all possible δ. Method 2 is about finding minimal L_2 norm of the initial condition for the linearized problem.

- We have applied the two methods for the ZFK equation. Both methods gave very close results, which agree very well with critical curve obtained by direct numerical simulations.

- We have applied the two methods for the front model. They gave qualitatively correct shape of the critical curve and correct order of magnitude of the quantities. Method 1 gave a noticeable underestimation of the threshold stimulus amplitude, whereas Method 2 gave a noticeable overestimation of this amplitude.

We conclude that a good approximation for the critical curve in the front model can be obtained for an appropriately chosen method of determining δ. This method remains a question for further study.

Table 5.1: Glossary of notations for Chapter 5

Notation	Explanation(s): bf=before, af=after	Place introduced
α	constant	(5.16)
α, ω	voltage: pre-frontal, post-frontal	(5.74)
β	constant	(5.16),(5.66)
$\tilde{\xi}_1$	constant parameter	(5.66)
Δ	norm	(5.42)
$\tilde{\Delta}$	constant	af(5.59)
ε_{k_1}	parameter	af(5.71)
ε	parameter	Sec. 5.3.2
δ	parameter (Hinch's equations)	bf(5.67)
δ	distance	bf(5.33)
τ	parameter	Fig. 5.8
θ	threshold parameter	bf(5.9)
θ_1	constant	af(5.100)
$\eta_{\max}$	constant	bf(5.140)
η_s	constant	(5.140)
Γ	Gamma function	(5.15)
$\tilde{\lambda}$	temporal eigenvalue (Hinch's problem)	af(5.62)
$\lambda_1, \lambda_2, \lambda_3$	eigenvalue: unstable, translation, stable (ZFK problem)	(5.12)
λ	temporal eigenvalue (direct front problem)	(5.5)
μ	parameter (Hinch's equation)	(5.71)
μ	temporal eigenvalue (adjoint to the direct front problem)	bf(5.88)
$\tilde{\nu}_1, \tilde{\nu}_2, \tilde{\bar{\nu}}_2$	spatial eigenvalue (Hinch's problem)	(5.68)
$\nu_1, \nu_2, \bar{\nu}_2$	spatial eigenvalue (direct front problem)	(5.83)
$\gamma_1, \gamma_2, \bar{\gamma}_2$	spatial eigenvalue (adjoint to the direct front problem)	(5.94)
		continued on the next page $\Rightarrow$

Notation	Explanation(s): bf=before, af=after	Place introduced
$\mu,\ \nu$	complex constant	(5.14)
ϕ	eigenfunction (ZFK)	(5.5)
$\varphi,\ \psi,\ \eta$	eigenfunction (direct front problem)	bf(5.78),(5.80)
$\varphi^*,\ \psi^*,\ \eta^*$	eigenfunction (adjoint to the direct front problem)	(5.89),(5.91)
$\psi_1,\ \psi_2;$ $\phi_1,\ \phi_2$	eigenfunction (ZFK): unstable, translation	(5.22), (5.21); bf(5.29), af(5.25)
$\phi_j,\ \phi_k$	the j'th, k'th eigenfunction (ZFK)	(5.24),(5.25),bf(5.27)
$\phi_1^*,\ \psi_1^*$	unstable eigenfunction for the adjoint front problem	(5.99)
$\phi_2^*,\ \psi_2^*$	translation (zero) eigenfunction for the adjoint front problem	(5.119)
Φ,η	function	(5.128), af(5.129)
$\eta_L,\ \eta_{R_1},\ \eta_{R_2}$	function	(5.131), (5.132), (5.135)
$\xi_{\text{stim}} : \xi_{\text{b}},\ \xi_{\text{f}}$	stimulus width: back, front	(5.100), bf(5.100)
Θ	Heaviside step function	(5.1)
$\tilde{\Xi},\ \Xi,\ \Xi^*$	vector of eigenfunctions	bf(5.64),(5.81),(5.92)
$\tilde{A},\ A,\ B$	coefficients matrix	(5.64),(5.81),(5.92)
$a_1(\delta)$	projection onto the unstable eigenfunction	(5.34)
$a_2(\delta)$	projection onto the translational eigenfunction	(5.43)
$c : c_-$	speed in the front equations: lower	bf(5.73), Sec. 5.3.1
$\tilde{c}$	speed in Hinch's model [43]	bf(5.60)
C	constant	(5.13)
$\bar{C}$	matrix	(5.79)
$D,\ \bar{D}$	diffusion: coefficient, matrix	(5.109), (5.79)
D	parameter dependent on $c,\ \mu$	(5.109)
$D_1,\ N_1,\ D_2,\ N_2$	integral	(5.36), (5.126)

Notation	Explanation(s): bf=before, af=after	Place introduced
E, h	dynamic variables: voltage, gate	(5.72)
F	hypergeometric function	(5.15)
f; F, G	nonlinear function	(5.1), (5.72)
$\tilde{F}$, $\tilde{G}$	nonlinear function	(5.59)
$\bar{F}$	matrix	(5.79)
$\tilde{f}_e$, f_e, f_e^*	characteristics function	(5.71),(5.86),(5.97)
H	function	(5.35), (5.119)
$\tilde{g}$, H_0	parameter in Hinch's equations	af (5.59), (5.66)
k	parameter	(5.9)
q	functions of x or z	(5.4),(5.10)
P_ν^μ, Q_ν^μ	Legendre P, Legendre Q	(5.15)
u_{cr}	critical nucleus for quadratic nolinearity	bf(5.3)
u	dynamic variable: voltage	(5.1)
v_0, h_0	exact solution (stationary) to the front	bf (5.74)
v_1, h_1	perturbation for the front equations	bf (5.76)
$\tilde{v}$, $\tilde{h}$	dynamic variable: voltage, gate	(5.59)
$\tilde{v}_0$, $\tilde{h}_0$	stationary solution	bf (5.61)
$\tilde{v}_1$, $\tilde{h}_1$	perturbation for the Hinch equations	(5.62)
w	perturbation	(5.3)
W	dynamic variable	(5.14)
$\bar{U}$, $\bar{U}_0$	solution: nonlinear, unstable	af (5.73), af(5.77), (5.98)
$\bar{V}$, $\bar{W}$	vector of eigenfunctions	(5.78), (5.88)
v_{stim}	stimulus amplitude	Fig. 5.7
x_{stim}, u_{stim}	stimulus: width, amplitude	(5.1)

Chapter 6

Conclusions

6.1 Results

In this thesis, the following results have been obtained:

- We have developed a numerical procedure for identifying critical nucleus and validated for the ZFK equation for which the critical nucleus solution is known exactly.

- Our numerical critical curves confirm the prediction from the approximate analytical theory by Neu *et al.* about inverse proportionality of the critical stimulus amplitude to its width.

- We presented numerical evidence that the role of the "critical nucleus" as for the ZFK equation is being played by its slowly moving variant, the "critical pulse" for the FHN system, which is consistent with the theoretical results by Flores. In the case of the simplified front model, we have observed through numerics that the relationship between the asymptotic voltage (rheobase) E_{asym} and the pre-frontal voltage α is found to be $E_{\text{asym}} = \alpha + 1$, which means that at very large stimulus width, the stimulus amplitude should be such that it opens the m-gates. This revelation will among other things assist in checking the analytical ignition criteria that we seek to find.

- We have established the role of unstable fronts as critical solutions in the cardiac front models, whose center-stable manifolds serve as threshold hyper-surfaces in the functional space between decay and ignition initial conditions.

- We have extended the variational description by Neu *et al.* of ignition in the ZFK equation, by using two-parametric piecewise linear ansatzes and avoiding blow-up solutions.

- We have developed a variational description of ignition in the front model using 2-parametric piece-wise linear ansatz, and established that a 2-parametric ap-

proximation is insufficient to describe the front dissipation mechanism essential for ignition failure in this model.

- We have developed a variational description of ignition in the front model using 3-parametric piece-wise smooth ansatz. This leads to a qualitatively correct critical curve approximation.

- We have developed a method of obtaining analytical criterion of ignition, by linear approximation of the center-stable manifold of the critical solution. This method depends on an arbitrary parameter δ, due to translational invariance of the problem. This arbitrary parameter is to be determined from further considerations, independent of the linear approximation.

- We have proposed two methods of determining parameter δ, one based on minimization of the threshold amplitude and the other based on minimization of the perturbation initial condition.

- We have applied the two linearized methods for the ZFK equation. Both methods gave very close results, which agree very well quantitatively with critical curve obtained by direct numerical simulations.

- We have applied the two methods for the front model. They gave qualitatively correct shape of the critical curve and correct order of magnitude of the quantities, with one of the method giving an overestimation and the other giving an underestimation of the threshold amplitude.

6.2   Further Directions

- Sequel to the unexpected result from our piece-wise linear variational approximation to the front model, we will revisit the problem adopting now a new approach by considering $t(x)$ rather than $x(t)$ description of the front motion, which hopefully will produce the unstable front solution.

- A good approximation for the critical curve in the front model can be obtained for an appropriately chosen method of determining the parameter δ. This method remains a question for further study.

- The propagation of excitation in cardiac muscle for example, generally have been treated as though it occurred in a continuous structure (medium). However, new evidences are emerging that suggest propagation in cardiac muscle often displays a discontinuous nature, "ectopic nexus" as it is popularly referred to (see [76]). We will therefore extend our initiation criterion to other applications and phenomena such as the ectopic nexus where initiation thresholds are crucial.

106

- We will consider other different initiation protocols, for example, initiation by current, where currents are used as stimulus, popularly used in physiology and experiment (see [88, 91]).

- It will also be interesting and quite challenging as well to try and explore how our initiation criteria are going to be molded appropriately so as to investigate initiation processes in models of higher dimensions, for example, 2D and 3D.

Appendix A

Derivation of the variational approximation of the front equations using piecewise smooth ansatz

A.1 Integrands for the ODE system

The integrands in (4.12) from Sec. 4.2.1 can be derived via chain rule using the formulas

$$
\begin{aligned}
[V_\omega]_{x_0,x_1} &= V_{x_\alpha}\,(x_\alpha)_\omega + V_{x_\omega}\,(x_\omega)_\omega + [V_\omega]_{x_\alpha,x_\omega}\,, \\
[V_{x_0}]_{\omega,x_1} &= V_{x_\alpha}\,(x_\alpha)_{x_0} + V_{x_\omega}\,(x_\omega)_{x_0} + [V_{x_0}]_{x_\alpha,x_\omega}\,, \\
[V_{x_1}]_{\omega,x_0} &= V_{x_\alpha}\,(x_\alpha)_{x_1} + V_{x_\omega}\,(x_\omega)_{x_1} + [V_{x_1}]_{x_\alpha,x_\omega}\,, \\
[V_x]_{\omega,x_0,x_1} &= V_{x_\alpha}\,(x_\alpha)_x + V_{x_\omega}\,(x_\omega)_x + [V_x]_{\omega,x_\alpha,x_\omega}\,.
\end{aligned}
$$

$$\text{(A.1)}$$

where the subscripts (except for x_ω, x_α, x_0) denote partial derivatives. After after some tedious calculations and simplification we get

$$
V_{x_0} = \begin{cases} 0, & x < x_\omega \\[2mm] \dfrac{(\alpha+\omega)\Big((\alpha+\omega)x + x_\alpha - x_\omega - (\alpha x_\omega + \omega x_\alpha)\Big)}{(x_\alpha - x_\omega)^2} \\ & x_\omega \le x < x_\alpha \\[2mm] 0, & x_\alpha \le x. \end{cases}
\qquad
V_\omega = \begin{cases} 1, & x < x_\omega \\ 0, & x_\omega \le x < x_\alpha\,, \\ 0, & x_\alpha \le x. \end{cases}
$$

$$
V_{x_1} = \begin{cases} 0, & x < x_\omega \\[2mm] \dfrac{-(\alpha+\omega)\Big((\alpha+\omega)x - (\alpha x_\omega + \omega x_\alpha)\Big)}{(x_\alpha - x_\omega)^2}, & x_\omega \le x < x_\alpha \\[2mm] 0, & x_\alpha \le x. \end{cases}
\qquad
V_x = \begin{cases} 0, & x < x_\omega \\[1mm] -\dfrac{(\alpha+\omega)}{x_\alpha - x_\omega}, & x_\omega \le x < x_\alpha \\[1mm] 0, & x_\alpha \le x. \end{cases}
$$

$$\text{(A.2)}$$

Similarly, the integrands in terms of W are obtained using the chain rule formulas in (A.1)

$$W_\omega = \begin{cases} 0, & x < x_\omega \\ -\frac{(\alpha+\omega)x - (\alpha x_\omega + \omega x_\alpha)}{\omega^2 (x_\alpha - x_\omega)}, & x_\omega \leq x < x_0 \ , \\ 0, & x_0 \leq x. \end{cases}$$

$$W_{x_0} = \begin{cases} 0, & x < x_\omega \\ -\frac{(\alpha+\omega)\Big((\alpha+\omega)x + x_\alpha - x_\omega - (\alpha x_\omega + \omega x_\alpha)\Big)}{\omega(x_\alpha - x_\omega)^2}, & \\ & x_\omega \leq x < x_0 \\ 0, & x_0 \leq x. \end{cases}$$

$$W_{x_1} = \begin{cases} 0, & x < x_\omega \\ -\frac{(\alpha+\omega)\Big((\alpha+\omega)x - (\alpha x_\omega + \omega x_\alpha)\Big)}{\omega(x_\alpha - x_\omega)^2}, & x_\omega \leq x < x_0 \\ 0, & x_0 \leq x. \end{cases} \tag{A.3}$$

A.2 Alternative representation of the integrands

Alternatively, we could express the integrands (4.12) directly in terms the dynamic variables $(\omega,\ x_0,\ x_1)$. Therefore, using the same formulas (A.1) we get

$$V = \begin{cases} \tilde{V}(x,t), & x < x_\omega \\ -\frac{x - x_0}{x_0 - x_1}, & x_\omega \leq x < x_\alpha \\ -\alpha, & x_\alpha \leq x. \end{cases} \tag{A.4}$$

$$V_\omega = \begin{cases} 1, & x < x_\omega \\ 0, & x_\omega \leq x < x_\alpha \ , \\ 0, & x_\alpha \leq x. \end{cases} \qquad V_{x_0} = \begin{cases} 0, & x < x_\omega \\ \frac{x - x_1}{(x_0 - x_1)^2}, & x_\omega \leq x < x_\alpha \\ 0, & x_\alpha \leq x. \end{cases}$$

$$V_{x_1} = \begin{cases} 0, & x < x_\omega \\ -\frac{x - x_0}{(x_0 - x_1)^2}, & x_\omega \leq x < x_\alpha \ , \\ 0, & x_\alpha \leq x. \end{cases} \qquad V_x = \begin{cases} 0, & x < x_\omega \\ -\frac{1}{x_0 - x_1}, & x_\omega \leq x < x_\alpha \\ 0, & x_\alpha \leq x. \end{cases} \tag{A.5}$$

$$W = \begin{cases} 0, & x < x_\omega \\ 1 + \frac{x - x_0}{\omega(x_0 - x_1)}, & x_\omega \leq x < x_0 \\ 1, & x_0 \leq x. \end{cases} \tag{A.6}$$

$$W_\omega = \begin{cases} 0, & x < x_\omega \\ -\frac{x - x_0}{\omega^2(x_0 - x_1)}, & x_\omega \leq x < x_0 \ , \\ 0, & x_0 \leq x. \end{cases} \qquad W_{x_0} = \begin{cases} 0, & x < x_\omega \\ -\frac{x - x_1}{\omega(x_0 - x_1)^2}, & x_\omega \leq x < x_0 \\ 0, & x_0 \leq x. \end{cases}$$

$$W_{x_1} = \begin{cases} 0, & x < x_\omega \\ \frac{x - x_0}{\omega(x_0 - x_1)^2}, & x_\omega \leq x < x_0 \\ 0, & x_0 \leq x. \end{cases} \tag{A.7}$$

A.3   The ODE system

Substituting the integrands (A.2, A.3) in (4.12) and from (4.11) we have

$$
\begin{pmatrix}
M_{\omega\omega} & M_{\omega x_0} & M_{\omega x_1} \\
M_{x_0\omega} & M_{x_0 x_0} & M_{x_0 x_1} \\
M_{x_1\omega} & M_{x_1 x_0} & M_{x_1 x_1}
\end{pmatrix}
\begin{pmatrix}
\dot{\omega} \\
\dot{x}_0 \\
\dot{x}_1
\end{pmatrix}
=
\begin{pmatrix}
Q_\omega + F_\omega + G_\omega \\
Q_{x_0} + F_{x_0} + G_{x_0} \\
Q_{x_1} + F_{x_1} + G_{x_1}
\end{pmatrix}
\tag{A.8}
$$

where (after some tedious computations)

$$
M_{\omega\omega} = \frac{(x_0 - x_1)\mu^2\tau^2}{3\omega}, \quad M_{\omega x_0} = \frac{(2\omega - 3)\mu^2\tau^2}{6\omega}, \quad M_{\omega x_1} = -\frac{\mu^2\tau^2}{3},
$$

$$
M_{x_0 x_0} = \frac{\omega^4 - 3\omega^3 + (\mu^2\tau^2 + 3)\omega^2 - (3\mu^2\tau^2 - \alpha^3 - 3\alpha^2 - 3\alpha)\omega + 3\mu^2\tau^2}{3\omega(x_0 - x_1)},
$$

$$
M_{x_0 x_1} = \frac{2\omega^3 - 3\omega^2 + 2\mu^2\tau^2\omega + 2\alpha^3 + 3\alpha^2 - 3\mu^2\tau^2}{-6(x_0 - x_1)}, \quad M_{x_0\omega} = M_{\omega x_0},
$$

$$
M_{x_1 x_1} = \frac{\omega^3 + \mu^2\tau^2\omega + \alpha^3}{3(x_0 - x_1)}, \quad M_{x_1 x_0} = M_{x_0 x_1}, \quad M_{x_1\omega} = M_{\omega x_1}
\tag{A.9}
$$

$$
Q_\omega = \frac{-1}{2(x_0 - x_1)}, \qquad Q_{x_0} = \frac{\alpha + \omega}{2(x_0 - x_1)^2}, \qquad Q_{x_1} = -\frac{\alpha + \omega}{2(x_0 - x_1)^2},
$$

$$
F_\omega = 0, \qquad F_{x_0} = -\frac{(\omega - 1)^3}{6\omega}, \qquad F_{x_1} = \frac{(\omega + 2)(\omega - 1)^2}{6\omega},
$$

$$
G_\omega = -\frac{(x_0 - x_1)\mu^2\tau}{6}, \qquad G_{x_0} = -\frac{(\omega - 3)\mu^2\tau}{6}, \qquad G_{x_1} = \frac{\omega\mu^2\tau}{6}.
\tag{A.10}
$$

Thus, we obtained the following system

$$
\tau^2\mu^2(2\omega - 3)(x_0 - x_1)\dot{x}_0 - 2\tau^2\mu^2\omega(x_0 - x_1)\dot{x}_1 + 2\tau^2\mu^2(x_0 - x_1)^2\dot{\omega}
$$
$$
+ \left(\tau\mu^2(x_0 - x_1)^2 + 3\right)\omega = 0,
$$

$$
2(x_0 - x_1)\left(\omega^4 - 3\omega^3 + (3 + \tau^2\mu^2)\omega^2 + (\alpha^3 + 3\alpha^2 + 3\alpha - 3\tau^2\mu^2)\omega + 3\tau^2\mu^2\right)\dot{x}_0
$$
$$
- (x_0 - x_1)\left(2\omega^4 - 3\omega^3 + 2\tau^2\mu^2\omega^2 + (2\alpha^3 + 3\alpha^2 + 3\alpha - 3\tau^2\mu^2)\omega\right)\dot{x}_1
$$
$$
+ (x_0 - x_1)^2\tau^2\mu^2(2\omega - 3)\dot{\omega} + (x_0 - x_1)^2\omega^3 - \left((x_0 - x_1)^2(3 - \tau\mu^2) + 3\right)\omega^2
$$
$$
- 3\left((1 + \tau^2\mu^2)(x_0 - x_1)^2 - \alpha\right)\omega - (x_0 - x_1)^2 = 0,
$$

$$
(x_0 - x_1)\left(-2\omega^4 + 3\omega^3 - 2\tau^2\mu^2\omega^2 - (2\alpha^3 + 3\alpha^2 - 3\tau^2\mu^2)\omega\right)\dot{x}_0
$$
$$
+ (x_0 - x_1)\left(2\omega^4 + 2\tau^2\mu^2\omega^2 + 2\alpha^3\omega\right)\dot{x}_1 - 2\tau^2\mu^2(x_0 - x_1)^2\omega\dot{\omega}
$$
$$
- (x_0 - x_1)^2\omega^3 - \left(\tau\mu^2(x_0 - x_1)^2 - 3\right)\omega^2 + 3\left((x_0 - x_1)^2 + \alpha\right)\omega - 2(x_0 - x_1)^2 = 0.
\tag{A.11}
$$

We solve (A.11) for $\dot{\omega}$, $\dot{x}_0$, $\dot{x}_1$ to obtain the third order ODE system and because of translation invariance we use $x_0 = x_1 + q$ to get the second order ODE system involving

only ω, q

$$\frac{d\omega}{dt} = -\Big(\tau\,\mu^2\omega^6 + (4\,\alpha\,\tau\,\mu^2 - \tau^2\,\mu^2)\,\omega^5 + (6\,\alpha^2\,\tau\,\mu^2 + \tau^3\,\mu^4 - 4\,\alpha\,\tau^2\,\mu^2)\,\omega^4$$
$$+\,(3\,\tau^2\,\mu^2 - \tau^4\,\mu^4 + 4\alpha^3\,\tau\,\mu^2 - 9\,\alpha^2\,\tau^2\,\mu^2)\,\omega^3$$
$$-\,(6\,\alpha^3\,\tau^2\,\mu^2 - 3\,\alpha^2\tau^3\,\mu^4 - 2\,\tau^2\,\mu^2 + 12\,\alpha^2\,\tau^2\,\mu^2 + \tau\,\alpha^4\,\mu^2 + 12\,\alpha\,\tau^2\,\mu^2)\,\omega^2$$
$$+\,(12\,\alpha^3\,\tau^2\,\mu^2 + 3\,\alpha^2\tau^2\,\mu^2 - 8\,\alpha\,\tau^2\,\mu^2 + 3\,\tau^4\,\mu^4 - 2\,\alpha^3\,\tau^3\,\mu^4 - 2\,\alpha^3\,\tau^3\,\mu^4)\,\omega$$
$$-\,6\,\alpha^2\,\tau^2\,\mu^2 - 6\,\alpha^3\tau^2\,\mu^2 - 2\,\tau^4\,\mu^4\Big)\Big/\Big(2\,\tau^2\,\mu^2\Big(\omega^5 + 4\,\alpha\,\omega^4 + (6\,\alpha^2 + \tau^2\,\mu^2)\,\omega^3$$
$$+\,4\,\alpha^3\,\omega^2 + \alpha^4\,\omega - \alpha^3\,\tau^2\,\mu^2\Big)\Big)$$

$$-\,\Big(3\,\omega^6 + 12\,\alpha\,\omega^5 + (9\,\tau^2\,\mu^2 + 18\,\alpha^2)\,\omega^4 + (27\,\alpha\,\tau^2\,\mu^2 + 12\,\alpha^3)\,\omega^3$$
$$+\,(3\,\alpha^4 + 39\,\alpha^2\,\tau^2\mu^2 + 6\,\tau^4\,\mu^4)\,\omega^2 + (3\,\alpha\,\tau^4\,\mu^4 + 21\,\alpha^3\,\tau^2\,\mu^2)\,\omega\Big)\Big/\Big(2\,\tau^2\,\mu^2\,q^2$$
$$\Big(\omega^5 + 4\,\alpha\,\omega^4 + (6\,\alpha^2 + \tau^2\,\mu^2)\,\omega^3 + 4\,\alpha^3\,\omega^2 + \alpha^4\,\omega + \alpha^3\,\tau^2\,\mu^2\Big)\Big) = f(\omega,q),$$

$$\frac{dq}{dt} = q\,\Big(2\,\omega^5 + (-4\,\alpha + 3\,\tau\,\mu^2 - 12)\,\omega^4 + (-\tau^2\,\mu^2 - 6\,\alpha^2 + 18)\,\omega^3$$
$$+\,(-3\,\alpha^2\,\tau\,\mu^2 + 12\alpha^2 - 8 + 12\,\alpha)\,\omega^2 + (-6\,\alpha^2 - 8\,\alpha + 3\,\tau^2\,\mu^2)\,\omega - 2\,\tau^2\,\mu^2\Big)$$
$$\Big/\Big(2\,\omega\,(\omega + \alpha)\Big(\omega^4 + 3\,\alpha\,\omega^3 + (3\,\alpha^2 + \tau^2\,\mu^2)\,\omega^2 + (\alpha^3 - \alpha\,\tau^2\,\mu^2)\,\omega + \alpha^2\,\tau^2\,\mu^2\Big)\Big)$$

$$+\,\Big(15\,\omega^4 + 36\,\alpha\,\omega^3 + (21\,\alpha^2 + 6\,\tau^2\,\mu^2)\,\omega^2 + 3\,\alpha\,\tau^2\,\mu^2\,\omega\Big)\Big/\Big(2\,\omega\,(\omega + \alpha)\,q$$
$$\Big(\omega^4 + 3\,\alpha\,\omega^3 + (3\,\alpha^2 + \tau^2\,\mu^2)\,\omega^2 + (\alpha^3 - \alpha\,\tau^2\,\mu^2)\,\omega + \alpha^2\,\tau^2\,\mu^2\Big)\Big) = g(\omega,q).$$
$$\tag{A.12}$$

Appendix B

Integrals for the variational approximation of the front equations using smooth ansatz

B.1   Derivation of the integrals

The integrals in (4.30, 4.31, 4.32) in Chapter 4 can respectively be further split so as to facilitate their computations

$$
\begin{aligned}
& \dot{a} \quad \left(\int_0^{x_1} V_a^2 \ \mathrm{d}x + \int_{x_1}^\infty V_a^2 \ \mathrm{d}x + \int_0^{x_0} W_a^2 \ \mathrm{d}x + \int_{x_0}^\infty W_a^2 \ \mathrm{d}x \right) \\
+ \ & \dot{b} \quad \left(\int_0^{x_1} V_a V_b \ \mathrm{d}x + \int_{x_1}^\infty V_a V_b \ \mathrm{d}x + \int_0^{x_0} W_a W_b \ \mathrm{d}x + \int_{x_0}^\infty W_a W_b \ \mathrm{d}x \right) \\
+ \ & \dot{x}_1 \quad \left(\int_0^{x_1} V_a V_{x_1} \ \mathrm{d}x + \int_{x_1}^\infty V_a V_{x_1} \ \mathrm{d}x + \int_0^{x_0} W_a W_{x_1} \ \mathrm{d}x + \int_{x_0}^\infty W_a W_{x_1} \ \mathrm{d}x \right) \\
= \ & \int_0^{x_1} V_a (V_{xx} + f(V, W)) \ \mathrm{d}x + \int_{x_1}^\infty V_a (V_{xx} + f(V, W)) \ \mathrm{d}x \\
+ \ & \int_0^{x_0} \frac{1}{\tau} W_a \, g(V, W) \ \mathrm{d}x + \int_{x_0}^\infty \frac{1}{\tau} W_a \, g(V, W) \ \mathrm{d}x,
\end{aligned}
\tag{B.1}
$$

$$
\begin{aligned}
& \dot{a} \quad \left(\int_0^{x_1} V_a V_b \ \mathrm{d}x + \int_{x_1}^\infty V_a V_b \ \mathrm{d}x + \int_0^{x_0} W_a W_b \ \mathrm{d}x + \int_{x_0}^\infty W_a W_b \ \mathrm{d}x \right) \\
+ \ & \dot{b} \quad \left(\int_0^{x_1} V_b^2 \ \mathrm{d}x + \int_{x_1}^\infty V_b^2 \ \mathrm{d}x + \int_0^{x_0} W_b^2 \ \mathrm{d}x + \int_{x_0}^\infty W_b^2 \ \mathrm{d}x \right) \\
+ \ & \dot{x}_1 \quad \left(\int_0^{x_1} V_b V_{x_1} \ \mathrm{d}x + \int_{x_1}^\infty V_b V_{x_1} \ \mathrm{d}x + \int_0^{x_0} W_b W_{x_1} \ \mathrm{d}x + \int_{x_0}^\infty W_b W_{x_1} \ \mathrm{d}x \right) \\
= \ & \int_0^{x_1} V_b (V_{xx} + f(V, W)) \ \mathrm{d}x + \int_{x_1}^\infty V_b (V_{xx} + f(V, W)) \ \mathrm{d}x \\
+ \ & \int_0^{x_0} \frac{1}{\tau} W_b \, g(V, W) \ \mathrm{d}x + \int_{x_0}^\infty \frac{1}{\tau} W_b \, g(V, W) \ \mathrm{d}x,
\end{aligned}
\tag{B.2}
$$

$$\dot{a} \left(\int_0^{x_1} V_a V_{x_1} \ dx + \int_{x_1}^{\infty} V_a V_{x_1} \ dx + \int_0^{x_0} W_a W_{x_1} \ dx + \int_{x_0}^{\infty} W_a W_{x_1} \ dx \right)$$

$$+ \ \dot{b} \left(\int_0^{x_1} V_b V_{x_1} \ dx + \int_{x_1}^{\infty} V_b V_{x_1} \ dx + \int_0^{x_0} W_b W_{x_1} \ dx + \int_{x_0}^{\infty} W_b W_{x_1} \ dx \right)$$

$$+ \ \dot{x}_1 \left(\int_0^{x_1} V_{x_1}^2 \ dx + \int_{x_1}^{\infty} V_{x_1}^2 \ dx + \int_0^{x_0} W_{x_1}^2 \ dx + \int_{x_0}^{\infty} W_{x_1}^2 \ dx \right)$$

$$= \ \int_0^{x_1} V_{x_1}(V_{xx} + f(V,W)) \ dx + \int_{x_1}^{\infty} V_{x_1}(V_{xx} + f(V,W)) \ dx$$

$$+ \ \int_0^{x_0} \frac{1}{\tau} W_{x_1} \, g(V,W) \ dx + \int_{x_0}^{\infty} \frac{1}{\tau} W_{x_1} \, g(V,W) \ dx. \tag{B.3}$$

The definitions in (B.4, B.5) and the Table (B.1) are used to help simplify and trim down the integrals in (B.1, B.2, B.3). Let $f(V,W)$ and $g(V,W)$ be define by

$$f(V,W) = f_V \cdot f_W, \quad g(V,W) = g_V - g_W, \tag{B.4}$$

where

$$f_V = \Theta(V-1), \qquad\qquad f_W = W,$$
$$g_V = \Theta(-V), \qquad\qquad g_W = W, \tag{B.5}$$

and let the table of the functional values of $f(V,W)$ and $g(V,W)$ in the specified intervals be:

Table B.1: Functions value in specified intervals

Interval	Functional value
$[0, x_1]$	$f_V = 1, \ f_W = W, \ g_V = 0, \ g_W = W$
$[x_1, x_0]$	$f_V = 0, \ f_W = W, \ g_V = 0, \ g_W = W$
$[x_0, \infty)$	$f_V = 0, \ f_W = 1, \ g_V = 1, \ g_W = 1$

Thus, the integrals in (B.1, B.2, B.3) simplify to

$$\dot{a} \left(\int_0^{x_1} V_a^2 \ dx + \int_{x_1}^{\infty} V_a^2 \ dx + \int_0^{x_0} W_a^2 \ dx \right)$$

$$+ \ \dot{b} \ \int_0^{x_0} W_a W_b \ dx$$

$$+ \ \dot{x}_1 \left(\int_0^{x_1} V_a V_{x_1} \ dx + \int_{x_1}^{\infty} V_a V_{x_1} + \int_0^{x_0} W_a W_{x_1} \ dx \right)$$

$$= \ \int_0^{x_1} V_a(V_{xx} + W) \ dx + \int_{x_1}^{\infty} V_a V_{xx} \ dx + \int_0^{x_0} \frac{1}{\tau} W_a(-W) \ dx, \tag{B.6}$$

$$\dot{a} \int_0^{x_0} W_a W_b \ dx + \dot{b} \int_0^{x_0} W_b^2 \ dx + \dot{x}_1 \int_0^{x_0} W_b W_{x_1} \ dx = \int_0^{x_0} \frac{1}{\tau} W_b(-W) \ dx, \tag{B.7}$$

$$\dot{a} \quad \left(\int_0^{x_1} V_a V_{x_1} \ \mathrm{d}x + \int_{x_1}^{\infty} V_a V_{x_1} \ \mathrm{d}x + \int_0^{x_0} W_a W_{x_1} \ \mathrm{d}x \right)$$

$$+ \quad \dot{b} \quad \int_0^{x_0} W_b W_{x_1} \ \mathrm{d}x$$

$$+ \quad \dot{x}_1 \quad \left(\int_0^{x_1} V_{x_1}^2 \ \mathrm{d}x + \int_{x_1}^{\infty} V_{x_1}^2 \ \mathrm{d}x + \int_0^{x_0} W_{x_1}^2 \ \mathrm{d}x \right)$$

$$= \quad \int_0^{x_1} V_{x_1}(V_{xx} + W) \ \mathrm{d}x + \int_{x_1}^{\infty} V_{x_1} V_{xx} \ \mathrm{d}x + \int_0^{x_0} \frac{1}{\tau} W_{x_1}(-W) \ \mathrm{d}x. \quad \text{(B.8)}$$

B.2 Values of the integrals

Let denote the values of integrals in (B.6) by $I_1^1, \cdots, I_{10}^1$, those in (B.7), by $I_1^2, \cdots, I_4^2$ and those in (B.8) by $I_1^3, \cdots, I_{10}^3$ respectively. Using (4.35), (4.36) from Chapter 4 and letting $\phi = \xi^{-1} = \mathrm{e}^{-\frac{\beta_1 x_1}{\sigma}}$, we obtain the values to the integrals in (B.6, B.7, B.8) as follows:

$$
\begin{aligned}
I_1^1 \quad = \quad & 8\sigma(2\phi^4 + 5\phi^3 + 2\phi^2)\ln(\xi)^3/(3\beta_1(1-\phi)^6) \\
+ \quad & 2\sigma(-2\phi^5 + \phi^4 - \phi^2 + 2\phi)\ln(\xi)^2/(\beta_1(1-\phi)^6) \\
+ \quad & \sigma(\phi^6 - 11\phi^5 + 10\phi^4 + 10\phi^2 - 11\phi + 1)\ln(\xi)/(\beta_1(1-\phi)^6) \\
+ \quad & 11\sigma(\phi^6 - 2\phi^5 + \phi^4 - \phi^2 + 2\phi - 1)/(4\beta_1(1-\phi)^6), \quad \text{(B.9)}
\end{aligned}
$$

$$I_2^1 \quad = \quad (\phi^2(1+\alpha)^3\ln(\xi)^2)/(\beta_1\sigma^2(1-\phi^2)(1+\phi)^2), \quad \text{(B.10)}$$

$$I_3^1 \quad = \quad 16b^2\beta^2\beta_1\ln(\xi)^2\phi^2)/((5\sigma^2(1+\phi)^3)(\sigma(1+\phi)\ln(\xi) - \beta\beta_1(1-\phi)), \quad \text{(B.11)}$$

$$I_4^1 \quad = \quad (8b\beta\ln(\xi)\phi)/(15\sigma(1+\phi)^2), \quad \text{(B.12)}$$

$$
\begin{aligned}
I_5^1 \quad = \quad & \sigma(1+\phi)(1 - 2\ln(\xi)\phi - \phi^2)/((1-\phi)^3) \\
- \quad & \sigma(1+\phi)((\ln(\xi)+1) + \phi(\ln(\xi)-1))(1 - 8\phi + 12\ln(\xi)\phi^2 + 8\phi^3 - \phi^4)/(2(1-\phi)^6) \\
+ \quad & \sigma(1+\phi)(2\ln(\xi)(1 - 4\phi - 4\phi^3 + \phi^4) - (1 - 8\phi + 8\phi^3 - \phi^4))/(4(1-\phi)^5), \quad \text{(B.13)}
\end{aligned}
$$

$$I_6^1 \quad = \quad (-(1+\alpha)^3\ln(\xi)\phi^2)/(\sigma^2(1+\phi)^2(1-\phi^2)) - ((1+\alpha)^2\ln(\xi)\phi)/(2\sigma(1-\phi^2)), \quad \text{(B.14)}$$

$$I_7^1 \quad = \quad (8b^2\beta\beta_1(\sigma(1+\phi)^2 - 2\beta\beta_1\phi)\ln(\xi)\phi)/(5\sigma^2(1+\phi)^3(\sigma(1+\phi)\ln(\xi) - \beta\beta_1(1-\phi))), \quad \text{(B.15)}$$

$$I_8^1 = \sigma(1-b)\ln(\xi)/\beta_1 - \beta_1(1+\phi)/(1-\phi) - \sigma(1-b)((\ln(\xi)+1)$$
$$+ \ (\ln(\xi)-1)\phi)(1-2\ln(\xi)\phi-\phi^2)/(\beta_1(1-\phi)^3)$$
$$+ \ \beta_1((\ln(\xi)+1) + (\ln(\xi)-1)\phi)(1-4\phi+4\ln(\xi)\phi^2+4\phi^3-\phi^4)/(2(1-\phi)^5)$$
$$+ \ b\sigma^3(1+\phi)^2\ln(\xi)^3/(3\beta_1(\sigma(1+\phi)\ln(\xi)-\beta\beta_1(1-\phi))^2)$$
$$+ \ \sigma(1-b)((\ln(\xi)-1)+(\ln(\xi)+1)\phi^2)/(\beta_1(1-\phi)^2)$$
$$- \ \beta_1((2\ln(\xi)-1)+(2\ln(\xi)+1)\phi^4)/(4(1-\phi)^4)$$
$$+ \ b\sigma^3(1+\phi)^2((\ln(\xi)+1)+(\ln(\xi)-1)\phi)(2\ln(\xi)^3\phi-3\ln(\xi)^2(1-\phi^2)+6\ln(\xi)(1+\phi^2)$$
$$- \ 6(1-\phi^2))/(3\beta_1(1-\phi)^3(\sigma(1+\phi)\ln(\xi)-\beta\beta_1(1-\phi))^2)$$
$$+ \ b\sigma^3(1+\phi)^2(\ln(\xi)^3(1+\phi^2)-3\ln(\xi)^2(1-\phi^2)+6\ln(\xi)(1+\phi^2)$$
$$- \ 6(1-\phi^2))/(\beta_1(1-\phi)^2(\sigma(1+\phi)\ln(\xi)-\beta\beta_1(1-\phi))^2), \tag{B.16}$$

$$I_9^1 = (-(1+\alpha)\beta_1\ln(\xi)\phi)/(2\sigma(1-\phi)^2), \tag{B.17}$$

$$I_{10}^1 = (-4b(2b-5)\beta\ln(\xi)\phi)/(15\sigma\tau(1+\phi)^2), \tag{B.18}$$

$$I_1^2 = (8b\beta\ln(\xi)\phi)/(15\sigma(1+\phi)^2), \tag{B.19}$$

$$I_2^2 = 8(\sigma(1+\phi)\ln(\xi)-\beta\beta_1(1-\phi))/(15\beta_1(1+\phi)), \tag{B.20}$$

$$I_3^2 = 4b(\sigma(1+\phi)^2-2\beta\beta_1\phi)/(15\sigma(1+\phi)^2), \tag{B.21}$$

$$I_4^2 = -2(4b-5)(\sigma(1+\phi)\ln(\xi)-\beta\beta_1(1-\phi))/(15\tau\beta_1(1+\phi)), \tag{B.22}$$

$$I_1^3 = \sigma(1+\phi)(1-2\ln(\xi)\phi-\phi^2)/((1-\phi)^3)$$
$$- \ \sigma(1+\phi)((\ln(\xi)+1)+\phi(\ln(\xi)-1))(1-8\phi+12\ln(\xi)\phi^2+8\phi^3-\phi^4)/(2(1-\phi)^6)$$
$$+ \ \sigma(1+\phi)(2\ln(\xi)(1-4\phi-4\phi^3+\phi^4)-(1-8\phi+8\phi^3-\phi^4))/(4(1-\phi)^5), \tag{B.23}$$

$$I_2^3 = (-(1+\alpha)^3\ln(\xi)\phi^2)/(\sigma^2(1+\phi)^2(1-\phi^2)) - ((1+\alpha)^2\ln(\xi)\phi)/(2\sigma(1-\phi^2)), \tag{B.24}$$

$$I_3^3 = (8b^2\beta\beta_1(\sigma(1+\phi)^2-2\beta\beta_1\phi)\ln(\xi)\phi)/(5\sigma^2(1+\phi)^3(\sigma(1+\phi)\ln(\xi)-\beta\beta_1(1-\phi))), \tag{B.25}$$

$$I_4^3 = 4b(\sigma(1+\phi)^2-2\beta\beta_1\phi)/(15\sigma(1+\phi)^2), \tag{B.26}$$

$$I_5^3 = \sigma\beta_1(1+\phi)^2(1-8\phi+12\ln(\xi)\phi^2+8\phi^3-\phi^4)/(2(1-\phi)^6), \tag{B.27}$$

$$I_6^3 = (1+\alpha)\beta_1(1+\phi)/(2(1-\phi)) + ((1+\alpha)^2\beta_1\phi)/(\sigma(1-\phi^2))$$
$$+ ((1+\alpha)^3\beta_1\phi^2)/(\sigma^2(1+\phi)^2(1-\phi^2)), \tag{B.28}$$

$$I_7^3 = 4b^2\beta_1(\sigma(1+\phi)^2 - 2\beta\beta_1\phi)^2/(5\sigma^2(1+\phi)^3(\sigma(1+\phi)\ln(\xi) - \beta\beta_1(1-\phi))), \tag{B.29}$$

$$I_8^3 = (\sigma(1-b)(1+\phi)(1-2\ln(\xi)\phi - \phi^2))/((1-\phi)^3)$$
$$- (\beta_1^2(1+\phi)(1-4\phi+4\ln(\xi)\phi^2+4\phi^3-\phi^4))/(2(1-\phi)^5)$$
$$- (b\sigma^3(1+\phi)^3(2\ln(\xi)^3\phi - 3\ln(\xi)^2(1-\phi^2)+6\ln(\xi)(1+\phi^2)-6(1-\phi^2)))$$
$$/ (3(1-\phi)^3(\sigma(1+\phi)\ln(\xi) - \beta\beta_1(1-\phi))^2), \tag{B.30}$$

$$I_9^3 = ((1+\alpha)\beta_1^2\phi)/(2\sigma(1-\phi)^2) + (\beta_1^2(1+\phi)^2)/(2(1-\phi)^2), \tag{B.31}$$

$$I_{10}^3 = (-2b(2b-5)(\sigma(1+\phi)^2 - 2\beta\beta_1\phi))/(15\tau\sigma(1+\phi)^2). \tag{B.32}$$

Thus, from integrals (B.6, B.7, B.8) and equations (B.9) to (B.32)

$$\begin{pmatrix} a_{11} & a_{12} & a_{13} \\ a_{21} & a_{22} & a_{23} \\ a_{31} & a_{32} & a_{33} \end{pmatrix} \begin{pmatrix} \dot{a} \\ \dot{b} \\ \dot{x}_1 \end{pmatrix} = \begin{pmatrix} b_1 \\ b_2 \\ b_3 \end{pmatrix}, \tag{B.33}$$

where

$$\begin{aligned} a_{11} &= I_1^1 + I_2^1 + I_3^1, \\ a_{12} &= I_4^1, \\ a_{13} &= I_5^1 + I_6^1 + I_7^1, \\ a_{21} &= I_1^2, \\ a_{22} &= I_2^2, \\ a_{23} &= I_3^2, \\ a_{31} &= I_1^3 + I_2^3 + I_3^3, \\ a_{32} &= I_4^3, \\ a_{33} &= I_5^3 + I_6^3 + I_7^3, \\ b_1 &= I_8^1 + I_9^1 + I_{10}^1, \\ b_2 &= I_4^2, \\ b_3 &= I_8^3 + I_9^3 + I_{10}^3. \end{aligned} \tag{B.34}$$

Let

$$\Delta = \begin{vmatrix} a_{11} & a_{12} & a_{13} \\ a_{21} & a_{22} & a_{23} \\ a_{31} & a_{32} & a_{33} \end{vmatrix},$$

$$\Delta_1 = \begin{vmatrix} b_1 & a_{12} & a_{13} \\ b_2 & a_{22} & a_{23} \\ b_3 & a_{32} & a_{33} \end{vmatrix},$$

$$\Delta_2 = \begin{vmatrix} a_{11} & b_1 & a_{13} \\ a_{21} & b_2 & a_{23} \\ a_{31} & b_3 & a_{33} \end{vmatrix},$$

$$\Delta_3 = \begin{vmatrix} a_{11} & a_{12} & b_1 \\ a_{21} & a_{22} & b_2 \\ a_{31} & a_{32} & b_3 \end{vmatrix}. \tag{B.35}$$

Now using Cramer's method we obtain the ODE system

$$\dot{a} = \frac{\Delta_1}{\Delta} \equiv F_a(a, b, x_1),$$

$$\dot{b} = \frac{\Delta_2}{\Delta} \equiv F_b(a, b, x_1),$$

$$\dot{x}_1 = \frac{\Delta_3}{\Delta} \equiv F_{x_1}(a, b, x_1). \tag{B.36}$$

Appendix C

Linear approximations of the front equations

C.1 Correspondence between Biktashev (2002) and Hinch (2004) models

The Hinch (2004) model [43] is given as

$$\frac{\partial \tilde{v}}{\partial \tilde{t}} = \frac{\partial^2 \tilde{v}}{\partial \tilde{x}^2} + g\,\Theta(\tilde{v})\,\tilde{h} - \varepsilon_{k1}\Theta(-\tilde{v})(1+\tilde{v}),$$
$$\frac{\partial \tilde{h}}{\partial \tilde{t}} = \Theta(-\tilde{v} - \tilde{\Delta}) - \tilde{h}, \tag{C.1}$$

meanwhile, Biktashev (2002) model [8] can be express as

$$\frac{\partial E}{\partial t} = \frac{\partial^2 E}{\partial x^2} + \Theta(E - 1)\,h,$$
$$\frac{\partial h}{\partial t} = (\Theta(-E) - h)/\tau, \tag{C.2}$$

where Θ is the Heaviside step function. The Bikatashev model (C.1) can be recovered from the HR (C.1) model when $\varepsilon_{k1} = 0$,

$$\frac{\partial \tilde{v}}{\partial \tilde{t}} = \frac{\partial^2 \tilde{v}}{\partial \tilde{x}^2} + g\,\Theta(\tilde{v})\,\tilde{h},$$
$$\frac{\partial \tilde{h}}{\partial \tilde{t}} = \Theta(-\tilde{v} - \tilde{\Delta}) - \tilde{h}. \tag{C.3}$$

We establish that (C.2) and (C.3) are equivalent by using the Affine transformation formulas

$$E = \mathrm{p} + \mathrm{q}\,\tilde{v}, \quad h = \mathrm{r} + \mathrm{s}\,\tilde{h},$$
$$t = \mathrm{k}^{-1}\,\tilde{t}, \quad x = \mathrm{w}^{-1}\,\tilde{x}, \tag{C.4}$$

where p, q, r, s, k and w are parameters to be determined. Using (C.4)

$$\frac{\partial E}{\partial t} = \mathrm{k}\,\mathrm{q}\,\frac{\partial \tilde{v}}{\partial \tilde{t}}, \quad \frac{\partial^2 E}{\partial x^2} = \mathrm{q}\,\mathrm{w}^2\,\frac{\partial^2 \tilde{v}}{\partial \tilde{x}^2}, \quad \frac{\partial h}{\partial t} = \mathrm{k}\,\mathrm{s}\,\frac{\partial \tilde{h}}{\partial \tilde{t}}. \tag{C.5}$$

Substituting (C.4) and (C.5) in (C.2) we obtain

$$\frac{\partial \tilde{v}}{\partial \tilde{t}} = (w^2/k)\,\frac{\partial^2 \tilde{v}}{\partial \tilde{x}^2} + (1/(k\,q))\,\Theta(p - 1 + q\,\tilde{v})\,\tilde{h},$$

$$\frac{\partial \tilde{h}}{\partial \tilde{t}} = (1/(k\,s\,\tau))\left(\Theta(-p - q\,\tilde{v}) - (r + s\,\tilde{h})\right). \tag{C.6}$$

Now by comparing (C.3) and (C.6) and since $\Theta(C\,E) \equiv \Theta(E)$ for some scalar C, we get

$$w^2/k = 1, \quad r = 0, \quad s/(k\,q) = g, \quad p = 1,$$

$$\tau k s = 1, \quad s = 1, \quad p/q = \tilde{\Delta}, \tag{C.7}$$

from which we have

$$p = 1, \quad q = \tau/g \ (\equiv 1/\tilde{\Delta}), \quad r = 0, \quad s = 1,$$

$$k = 1/\tau \ \text{(i.e., } k = \tau^{-1}), \quad w^2 = 1/\tau \ \text{(i.e., } w = \tau^{-1/2}), \tag{C.8}$$

and from (C.8), $g = \tau\,\tilde{\Delta}$. Hence,

$$E = 1 + (1/\tilde{\Delta})\,\tilde{v}, \qquad\qquad h = \tilde{h},$$

$$t = \tau\,\tilde{t}, \qquad\qquad x = \tau^{1/2}\,\tilde{x}. \tag{C.9}$$

And from the boundary conditions, $E(-\infty) = -\alpha$ [8] and $\tilde{v}(-\infty) = -1$ [43]

$$\tilde{\Delta} = 1/(1 + \alpha). \tag{C.10}$$

The speeds are related via $c = x/t$, $\tilde{c} = \tilde{x}/\tilde{t}$ and which lead from (C.9) to

$$\tilde{c} = c\,\tau^{1/2}, \quad \beta = \tilde{c}^2 = \tau\,c^2. \tag{C.11}$$

Here, we check our transformation formulas using

$$\frac{\partial}{\partial t} = \tau^{-1}\,\frac{\partial}{\partial \tilde{t}}, \quad \frac{\partial}{\partial x} = \tau^{-1/2}\,\frac{\partial}{\partial \tilde{x}}, \tag{C.12}$$

and thus,

$$\frac{\partial E}{\partial t} = \frac{1}{\tau\,\tilde{\Delta}}\frac{\partial \tilde{v}}{\partial \tilde{t}} = \frac{1}{g}\frac{\partial \tilde{v}}{\partial \tilde{t}}, \qquad\qquad \frac{\partial h}{\partial t} = \frac{1}{\tau}\frac{\partial \tilde{h}}{\partial \tilde{t}},$$

$$\frac{\partial^2 E}{\partial x^2} = \frac{1}{\tau\,\tilde{\Delta}}\frac{\partial^2 \tilde{v}}{\partial \tilde{x}^2} = \frac{1}{g}\frac{\partial^2 \tilde{v}}{\partial \tilde{x}^2}. \tag{C.13}$$

But since $\Theta(\tilde{v}/\tilde{\Delta}) = \Theta(\tilde{v})$, $\Theta\left(-(\tilde{v} + \tilde{\Delta})/\tilde{\Delta}\right) = \Theta(-(\tilde{v} + \tilde{\Delta}))$ and (C.13) we have

$$\frac{\partial \tilde{v}}{\partial \tilde{t}} = \frac{\partial^2 \tilde{v}}{\partial \tilde{x}^2} + g\,\Theta(\tilde{v})\,\tilde{h},$$

$$\frac{\partial \tilde{h}}{\partial \tilde{t}} = \Theta(-\tilde{v} - \tilde{\Delta}) - \tilde{h}, \tag{C.14}$$

which is exactly the same as (C.3).

C.1.1 Linearized equations

We linearize both the models in their comoving frame of reference to obtain

$$\frac{\partial v_1}{\partial t} = \frac{\partial^2 v_1}{\partial \xi^2} + c\,\frac{\partial v_1}{\partial \xi} + \delta(v_0 - 1)\,h_0\,v_1 + \Theta(v_0 - 1)\,h_1,$$

$$\frac{\partial h_1}{\partial t} = c\,\frac{\partial h_1}{\partial \xi} - \delta(v_0)\,v_1/\tau - h_1/\tau, \tag{C.15}$$

$$\frac{\partial \tilde{v}_1}{\partial \tilde{t}} = (1/\tilde{c}^2)\,\frac{\partial^2 \tilde{v}_1}{\partial \tilde{\xi}^2} - \frac{\partial \tilde{v}_1}{\partial \tilde{\xi}} + g\,\delta(\tilde{v}_0)\,\tilde{h}_0\,\tilde{v}_1 + g\,\Theta(\tilde{v}_0)\,\tilde{h}_1,$$

$$\frac{\partial \tilde{h}_1}{\partial \tilde{t}} = -\frac{\partial \tilde{h}_1}{\partial \tilde{\xi}} - \delta(\tilde{v}_0 + \tilde{\Delta})\,\tilde{v}_1 - \tilde{h}_1, \tag{C.16}$$

where

$$\xi = x - c\,t, \quad \tilde{\xi} = \tilde{t} - \tilde{x}/\tilde{c}. \tag{C.17}$$

From (C.9), (C.11) and (C.17) we deduce that

$$v_0 = 1 + (1/\tilde{\Delta})\,\tilde{v}_0, \quad h_0 = \tilde{h}_0, \quad \xi = -c\,\tau\,\tilde{\xi}. \tag{C.18}$$

As yet another check on our transformation formulas, we derive one of our linearized equations (C.15, C.16) from the other. Therefore, using the relations

$$\frac{\partial}{\partial t} = \tau^{-1}\,\frac{\partial}{\partial \tilde{t}}, \quad \frac{\partial}{\partial \xi} = -\tau^{-1}\,c^{-1}\,\frac{\partial}{\partial \tilde{\xi}}, \tag{C.19}$$

and

$$\frac{\partial v_1}{\partial t} = \frac{1}{\tau\,\tilde{\Delta}}\,\frac{\partial \tilde{v}_1}{\partial \tilde{t}} = \frac{1}{g}\,\frac{\partial \tilde{v}_1}{\partial \tilde{t}}, \qquad \frac{\partial h_1}{\partial t} = \frac{1}{\tau}\,\frac{\partial \tilde{h}_1}{\partial \tilde{t}}, \quad \frac{\partial h_1}{\partial \xi} = -\frac{1}{c\,\tau}\,\frac{\partial \tilde{h}_1}{\partial \tilde{\xi}},$$

$$\frac{\partial v_1}{\partial \xi} = -\frac{1}{c\,\tau\,\tilde{\Delta}}\,\frac{\partial \tilde{v}_1}{\partial \tilde{\xi}} = -\frac{1}{c\,g}\,\frac{\partial \tilde{v}_1}{\partial \tilde{\xi}}, \qquad \frac{\partial^2 v_1}{\partial \tilde{\xi}^2} = \frac{1}{\tau c^2 g}\,\frac{\partial^2 \tilde{v}_1}{\partial \tilde{\xi}^2} = \frac{1}{\tilde{c}^2\,g}\,\frac{\partial^2 \tilde{v}_1}{\partial \tilde{\xi}^2}. \tag{C.20}$$

Thus,

$$\frac{\partial \tilde{v}_1}{\partial \tilde{t}} = (1/\tilde{c}^2)\,\frac{\partial^2 \tilde{v}_1}{\partial \tilde{\xi}^2} - \frac{\partial \tilde{v}_1}{\partial \tilde{\xi}} + g\,\delta(\tilde{v}_0/\tilde{\Delta})\,\tilde{h}_0\,(\tilde{v}_1/\tilde{\Delta}) + g\,\Theta(\tilde{v}_0/\tilde{\Delta})\,\tilde{h}_1 + \underline{g\,\delta(\tilde{v}_0/\tilde{\Delta})\,\tilde{h}_0}, \tag{C.21}$$

and since $\Theta(\tilde{v}_1/\tilde{\Delta}) = \Theta(\tilde{v}_1)$, $\delta(\tilde{v}_1/\tilde{\Delta}) = \tilde{\Delta}\,\delta(\tilde{v}_1)$

$$\frac{\partial \tilde{v}_1}{\partial \tilde{t}} = (1/\tilde{c}^2)\,\frac{\partial^2 \tilde{v}_1}{\partial \tilde{\xi}^2} - \frac{\partial \tilde{v}_1}{\partial \tilde{\xi}} + g\,\delta(\tilde{v}_0)\,\tilde{h}_0\,\tilde{v}_1 + g\,\Theta(\tilde{v}_0)\,\tilde{h}_1 + \underline{g\,\delta(\tilde{v}_0)\,\tilde{h}_0\,\tilde{\Delta}}. \tag{C.22}$$

Meanwhile

$$\frac{\partial \tilde{h}_1}{\partial \tilde{t}} = -\frac{\partial \tilde{h}_1}{\partial \tilde{\xi}} - \delta((\tilde{v}_0 + \tilde{\Delta})/\tilde{\Delta})\,(\tilde{v}_1/\tilde{\Delta}) - \tilde{h}_1 - \underline{\delta((\tilde{v}_0 + \tilde{\Delta})/\tilde{\Delta})}, \tag{C.23}$$

120

reduces to

$$\frac{\partial \tilde{h}_1}{\partial \tilde{t}} = -\frac{\partial \tilde{h}_1}{\partial \tilde{\xi}} - \delta(\tilde{v}_0 + \tilde{\Delta})\, \tilde{v}_1 - \tilde{h}_1 - \underline{\delta(\tilde{v}_0 + \tilde{\Delta})\, \tilde{\Delta}}. \tag{C.24}$$

Hence,

$$\frac{\partial \tilde{v}_1}{\partial \tilde{t}} = (1/\tilde{c}^2)\frac{\partial^2 \tilde{v}_1}{\partial \tilde{\xi}^2} - \frac{\partial \tilde{v}_1}{\partial \tilde{\xi}} + g\,\delta(\tilde{v}_0)\,\tilde{h}_0\,\tilde{v}_1 + g\,\Theta(\tilde{v}_0)\,\tilde{h}_1 + \underline{g\,\delta(\tilde{v}_0)\,\tilde{h}_0\,\tilde{\Delta}},$$

$$\frac{\partial \tilde{h}_1}{\partial \tilde{t}} = -\frac{\partial \tilde{h}_1}{\partial \tilde{\xi}} - \delta(\tilde{v}_0 + \tilde{\Delta})\,\tilde{v}_1 - \tilde{h}_1 - \underline{\delta(\tilde{v}_0 + \tilde{\Delta})\,\tilde{\Delta}}. \tag{C.25}$$

NB: System (C.16) and (C.25) are equivalent only when the underlined extra terms in (C.25) become zero.

C.2 Linearization of Hinch (2004) equations

In a laboratory reference frame with $(\tilde{x}, \tilde{T})$ as coordinates, the front model ([43]), can be written in the form

$$\frac{\partial \tilde{v}}{\partial \tilde{T}} = \frac{\partial^2 \tilde{v}}{\partial \tilde{x}^2} + \tilde{F}(\tilde{v}, \tilde{h}),$$

$$\frac{\partial \tilde{h}}{\partial \tilde{T}} = \tilde{G}(\tilde{v}, \tilde{h}), \tag{C.26}$$

where $\tilde{F}(\tilde{v}, \tilde{h}) = \tilde{g}\,\Theta(\tilde{v})\tilde{h}$, $\tilde{G}(\tilde{v}, \tilde{h}) = \Theta(-\tilde{v} - \tilde{\Delta}) - \tilde{h}$ and Θ is a Heaviside step function. In a moving frame of reference, the solutions to (C.26) for a right-ward moving front are of the form $\tilde{v}(\tilde{T} - \tilde{x}/\tilde{c}, \tilde{T})$, $\tilde{h}(\tilde{T} - \tilde{x}/\tilde{c}, \tilde{T})$. Introducing the coordinates $\tilde{\xi} = \tilde{T} - \tilde{x}/\tilde{c}$, $\tilde{t} = \tilde{T}$ with $\tilde{c} > 0$, we look for functions $\tilde{v}(\tilde{\xi}, \tilde{t})$, $\tilde{h}(\tilde{\xi}, \tilde{t})$ which satisfy (C.26) to give

$$\frac{\partial \tilde{v}}{\partial \tilde{t}} = \frac{1}{\tilde{c}^2}\frac{\partial^2 \tilde{v}}{\partial \tilde{\xi}^2} - \frac{\partial \tilde{v}}{\partial \tilde{\xi}} + \tilde{F}(\tilde{v}, \tilde{h}),$$

$$\frac{\partial \tilde{h}}{\partial \tilde{t}} = -\frac{\partial \tilde{h}}{\partial \tilde{\xi}} + \tilde{G}(\tilde{v}, \tilde{h}). \tag{C.27}$$

NB: Traveling waves of (C.26) corresponds to stationary solutions of (C.27). Suppose $\tilde{v}_0(\tilde{\xi})$, $\tilde{h}_0(\tilde{\xi})$, is a stationary solution of (C.27), then

$$\frac{1}{\tilde{c}^2}\frac{\mathrm{d}^2 \tilde{v}_0}{\mathrm{d}\tilde{\xi}^2} - \frac{\mathrm{d}\tilde{v}_0}{\mathrm{d}\tilde{\xi}} + \tilde{F}(\tilde{v}_0, \tilde{h}_0) = 0,$$

$$\frac{\mathrm{d}\tilde{h}_0}{\mathrm{d}\tilde{\xi}} - \tilde{G}(\tilde{v}_0, \tilde{h}_0) = 0. \tag{C.28}$$

The linearized version of (C.27) about $\left(\tilde{v}_0(\tilde{\xi}), \tilde{h}_0(\tilde{\xi})\right)$ is neglecting higher order terms)

$$\frac{\partial \tilde{v}_1}{\partial \tilde{t}} = \frac{1}{\tilde{c}^2}\frac{\partial^2 \tilde{v}_1}{\partial \tilde{\xi}^2} - \frac{\partial \tilde{v}_1}{\partial \tilde{\xi}} + \tilde{g}\,\delta(\tilde{v}_0)\,\tilde{h}_0\,\tilde{v}_1 + \tilde{g}\,\Theta(\tilde{v}_0)\,\tilde{h}_1,$$

$$\frac{\partial \tilde{h}_1}{\partial \tilde{t}} = -\frac{\partial \tilde{h}_1}{\partial \tilde{\xi}} - \delta(\tilde{v}_0 + \tilde{\Delta})\,\tilde{v}_1 - \tilde{h}_1. \tag{C.29}$$

C.2.1 Eigenvalue problem

Let the linearized eqtn (C.29) support solutions of the form $\tilde{h}_1(\tilde{\xi}, \tilde{t}) = e^{\tilde{\lambda}\tilde{t}}\,\tilde{\phi}(\tilde{\xi})$ and $\tilde{h}_1(\tilde{\xi}, \tilde{t}) = e^{\tilde{\lambda}\tilde{t}}\,\tilde{\psi}(\tilde{\xi})$. This lead to the (*temporal* eigenvalue) problem

$$\tilde{\lambda}\,\tilde{\phi} = \frac{1}{\tilde{c}^2}\frac{\mathrm{d}^2\tilde{\phi}}{\mathrm{d}\tilde{\xi}^2} - \frac{\mathrm{d}\tilde{\phi}}{\mathrm{d}\tilde{\xi}} + \tilde{g}\,\delta(\tilde{v}_0)\,\tilde{h}_0\,\tilde{\phi} + \tilde{g}\,\Theta(\tilde{v}_0)\,\tilde{\psi},$$

$$\tilde{\lambda}\,\tilde{\psi} = -\frac{\mathrm{d}\tilde{\psi}}{\mathrm{d}\tilde{\xi}} - \delta(\tilde{v}_0 + \tilde{\Delta})\,\tilde{\phi} - \tilde{\psi}, \tag{C.30}$$

where $\tilde{\phi}(\tilde{\xi})$ and $\tilde{\psi}(\tilde{\xi})$ are some eigenfunctions. The eigenvalue eqtn (C.30) is then casted into a three first-order (ODE) equations by letting $\dfrac{\mathrm{d}\tilde{\phi}}{\mathrm{d}\tilde{\xi}} = \tilde{\eta}$ and $\tilde{\Xi} = (\tilde{\phi},\,\tilde{\eta},\,\tilde{\psi})^{\mathrm{T}}$. Thus, we obtain a linear system in $\mathbb{C}^3$

$$\tilde{\Xi}' = \tilde{A}\,\tilde{\Xi}, \tag{C.31}$$

where $(') = \dfrac{\mathrm{d}}{\mathrm{d}\tilde{\xi}}$,

$$\tilde{A} = \begin{pmatrix} 0 & 1 & 0 \\ \tilde{c}^2\left(\tilde{\lambda} - \tilde{g}\,\delta(\tilde{v}_0)\,\tilde{h}_0\right) & \tilde{c}^2 & -\tilde{c}^2\,\tilde{g}\,\Theta(\tilde{v}_0) \\ -\delta(\tilde{v}_0 + \tilde{\Delta}) & 0 & -(1 + \tilde{\lambda}) \end{pmatrix}, \tag{C.32}$$

$$\tilde{v}_0(\tilde{\xi}) = \begin{cases} -1 + e^{\beta\tilde{\xi}}, & \tilde{\xi} \le 0, \\[2mm] \dfrac{\beta\,\tilde{g}\,H_0}{1 + \beta}\,(1 - e^{-\tilde{\xi}}), & \tilde{\xi} \ge 0, \end{cases}$$

$$\tilde{h}_0(\tilde{\xi}) = \begin{cases} 1, & \tilde{\xi} \le \tilde{\xi}_1, \\ H_0 e^{-\tilde{\xi}}, & \tilde{\xi} \ge \tilde{\xi}_1, \end{cases}$$

$$\tag{C.33}$$

and

$$\tilde{\xi}_1 = -\delta/\beta, \quad H_0 = e^{-\delta/\beta}, \quad \tilde{g} = (1 + \beta)\,e^{\delta/\beta}. \tag{C.34}$$

Solution to the linearized equations We have three intervals (cases $i = a,\,b,\,c$) to consider. For case $i = a$, $\tilde{\xi} \in (-\infty, \tilde{\xi}_1)$, therefore in this interval, $\Theta(\tilde{v}_0) = 0$, $\delta(\tilde{v}_0) = 0$, $\delta(\tilde{v}_0 + \tilde{\Delta}) = \delta(\xi - \tilde{\xi}_1) = 0$, $\tilde{h}_0 = 1$. Thus, the solution is

$$\begin{pmatrix} \tilde{\phi}_a \\ \tilde{\eta}_a \\ \tilde{\psi}_a \end{pmatrix} = \tilde{a}_1\,\tilde{\vec{v}}^a_1\,e^{-\tilde{\nu}_1\tilde{\xi}} + \tilde{a}_2\,\tilde{\vec{v}}^a_2\,e^{-\tilde{\nu}_2\tilde{\xi}} + \tilde{a}_3\,\tilde{\vec{v}}^a_3\,e^{\tilde{\nu}_2\tilde{\xi}},$$

$$= \tilde{a}_1\begin{pmatrix} 0 \\ 0 \\ 1 \end{pmatrix}e^{-\tilde{\nu}_1\tilde{\xi}} + \tilde{a}_2\begin{pmatrix} 1 \\ \tilde{\nu}_2 \\ 0 \end{pmatrix}e^{\tilde{\nu}_2\tilde{\xi}} + \tilde{a}_3\begin{pmatrix} 1 \\ \tilde{\nu}_2 \\ 0 \end{pmatrix}e^{\tilde{\nu}_2\tilde{\xi}}, \tag{C.35}$$

where

$$\tilde{\nu}_1 = 1 + \tilde{\lambda}, \quad \tilde{\nu}_2 = \frac{\beta + \sqrt{\beta^2 + 4\,\tilde{\lambda}\,\beta}}{2}, \quad \bar{\tilde{\nu}}_2 = \frac{\beta - \sqrt{\beta^2 + 4\,\tilde{\lambda}\,\beta}}{2}. \tag{C.36}$$

For case $i = b$, $\tilde{\xi} \in (\tilde{\xi}_1, \tilde{\xi}_0)$, therefore in this interval, $\Theta(\tilde{v}_0) = 0$, $\delta(\tilde{v}_0) = 0$, $\delta(\tilde{v}_0 + \tilde{\Delta}) = \delta(\xi - \tilde{\xi}_1) = 0$, $\tilde{h}_0 = H_0 e^{-\tilde{\xi}}$. Thus, the solution is

$$\begin{pmatrix} \tilde{\phi}_b \\ \tilde{\eta}_b \\ \tilde{\psi}_b \end{pmatrix} = \tilde{b}_1 \, \tilde{\vec{v}}_1^{\,b} \, e^{-\tilde{\nu}_1 \tilde{\xi}} + \tilde{b}_2 \, \tilde{\vec{v}}_2^{\,b} \, e^{-\tilde{\nu}_2 \tilde{\xi}} + \tilde{b}_3 \, \tilde{\vec{v}}_3^{\,b} \, e^{\bar{\tilde{\nu}}_2 \tilde{\xi}},$$

$$= \tilde{b}_1 \begin{pmatrix} 0 \\ 0 \\ 1 \end{pmatrix} e^{-\tilde{\nu}_1 \tilde{\xi}} + \tilde{b}_2 \begin{pmatrix} 1 \\ \tilde{\nu}_2 \\ 0 \end{pmatrix} e^{\tilde{\nu}_2 \tilde{\xi}} + \tilde{b}_3 \begin{pmatrix} 1 \\ \tilde{\nu}_2 \\ 0 \end{pmatrix} e^{\bar{\tilde{\nu}}_2 \tilde{\xi}}, \tag{C.37}$$

and lastly, for case $i = c$, $\tilde{\xi} \in (\tilde{\xi}_0, \infty)$, therefore in this interval, $\Theta(\tilde{v}_0) = 1$, $\delta(\tilde{v}_0) = 0$, $\delta(\tilde{v}_0 + \tilde{\Delta}) = \delta(\xi - \tilde{\xi}_1) = 0$, $\tilde{h}_0 = H_0 e^{-\tilde{\xi}}$. Thus, the solution is

$$\begin{pmatrix} \tilde{\phi}_c \\ \tilde{\eta}_c \\ \tilde{\psi}_c \end{pmatrix} = \tilde{c}_1 \, \tilde{\vec{v}}_1^{\,c} \, e^{-\tilde{\nu}_1 \tilde{\xi}} + \tilde{c}_2 \, \tilde{\vec{v}}_2^{\,c} \, e^{-\tilde{\nu}_2 \tilde{\xi}} + \tilde{c}_3 \, \tilde{\vec{v}}_3^{\,c} \, e^{\bar{\tilde{\nu}}_2 \tilde{\xi}},$$

$$= \tilde{c}_1 \begin{pmatrix} 1 \\ -\tilde{\nu}_1 \\ -\tilde{\nu}_s \end{pmatrix} e^{-\tilde{\nu}_1 \tilde{\xi}} + \tilde{c}_2 \begin{pmatrix} 1 \\ \tilde{\nu}_2 \\ 0 \end{pmatrix} e^{\tilde{\nu}_2 \tilde{\xi}} + \tilde{c}_3 \begin{pmatrix} 1 \\ \tilde{\nu}_2 \\ 0 \end{pmatrix} e^{\bar{\tilde{\nu}}_2 \tilde{\xi}}, \tag{C.38}$$

where

$$\tilde{\nu}_s = \frac{(1 + \tilde{\lambda})^2 + \beta}{\beta \, \tilde{g}}. \tag{C.39}$$

C.2.2 Characteristic equation

Now to determine the characteristic equation for Hinch (2004) equations we consider the conditions at the boundaries:

Boundary conditions at $\pm\infty$: With $\tilde{\lambda} \geq 0$: $\tilde{\nu}_1 > 0$, $\tilde{\nu}_2 > 0$, $\bar{\tilde{\nu}}_2 < 0$, for the case $i = a$

$$\lim_{\tilde{\xi} \to -\infty} \begin{pmatrix} \tilde{\phi}_a \\ \tilde{\eta}_a \\ \tilde{\psi}_a \end{pmatrix}, \tag{C.40}$$

123

must be bounded and therefore $\tilde{a}_1 = 0$, $\tilde{a}_3 = 0$. Hence,

$$\begin{pmatrix} \tilde{\phi}_a \\ \tilde{\eta}_a \\ \tilde{\psi}_a \end{pmatrix} = \tilde{a}_2 \begin{pmatrix} 1 \\ \tilde{\nu}_2 \\ 0 \end{pmatrix} e^{\tilde{\nu}_2 \tilde{\xi}}. \qquad (C.41)$$

For the case $i = b$, we can only consider the internal boundary conditions and so the solution is

$$\begin{pmatrix} \tilde{\phi}_b \\ \tilde{\eta}_b \\ \tilde{\psi}_b \end{pmatrix} = \tilde{b}_1 \begin{pmatrix} 0 \\ 0 \\ 1 \end{pmatrix} e^{-\tilde{\nu}_1 \tilde{\xi}} + \tilde{b}_2 \begin{pmatrix} 1 \\ \tilde{\nu}_2 \\ 0 \end{pmatrix} e^{\tilde{\nu}_2 \tilde{\xi}} + \tilde{b}_3 \begin{pmatrix} 1 \\ \tilde{\nu}_2 \\ 0 \end{pmatrix} e^{\bar{\nu}_2 \tilde{\xi}}. \qquad (C.42)$$

However, for the case $i = c$

$$\lim_{\tilde{\xi} \to +\infty} \begin{pmatrix} \tilde{\phi}_c \\ \tilde{\eta}_c \\ \tilde{\psi}_c \end{pmatrix}, \qquad (C.43)$$

must be bounded and therefore, $\tilde{c}_2 = 0$. Hence,

$$\begin{pmatrix} \tilde{\phi}_c \\ \tilde{\eta}_c \\ \tilde{\psi}_c \end{pmatrix} = \tilde{c}_1 \begin{pmatrix} 1 \\ -\tilde{\nu}_1 \\ -\tilde{\nu}_s \end{pmatrix} e^{-\tilde{\nu}_1 \tilde{\xi}} + \tilde{c}_3 \begin{pmatrix} 1 \\ \tilde{\nu}_2 \\ 0 \end{pmatrix} e^{\bar{\nu}_2 \tilde{\xi}}. \qquad (C.44)$$

Internal boundary conditions (IBCS): Let (C.31) be rewritten in terms of regular $(R1, R2)$ and singular $(S1, S2)$ functions

$$\frac{d\tilde{\phi}}{d\tilde{\xi}} = \tilde{\eta},$$

$$\frac{d\tilde{\eta}}{d\tilde{\xi}} = \overbrace{\tilde{c}^2 \left(\tilde{\lambda}\tilde{\phi} + \tilde{\eta} - \tilde{g}\,\Theta(\tilde{v}_0)\,\tilde{\psi} \right)}^{R1(\tilde{\xi})} - \overbrace{\tilde{c}^2\,\tilde{g}\,\tilde{h}_0\,\delta(\tilde{v}_0)\,\tilde{\phi}}^{S1(\tilde{\xi})},$$

$$\frac{d\tilde{\psi}}{d\tilde{\xi}} = -\overbrace{(1 + \tilde{\lambda})\,\tilde{\psi}}^{R2(\tilde{\xi})} - \overbrace{\delta(\tilde{v}_0 + \tilde{\Delta})\,\tilde{\phi}}^{S2(\tilde{\xi})}. \qquad (C.45)$$

IBCS at $\tilde{\xi}_0 = 0$: Here, we integrate the second equation from (C.45) around $\tilde{\xi} = \tilde{\xi}_0$ over a small range, $(\tilde{\xi}_0 - \varepsilon, \tilde{\xi}_0 + \varepsilon)$ in the limit $\varepsilon \to 0$. But $\delta(\tilde{v}_0) = \delta(\tilde{\xi})/\tilde{v}_0'(\tilde{\xi})$ and the integral becomes

$$\lim_{\varepsilon \to 0} \int_{\tilde{\xi}_0 - \varepsilon}^{\tilde{\xi}_0 + \varepsilon} \frac{d\tilde{\eta}}{d\tilde{\xi}}\,d\tilde{\xi} = \lim_{\varepsilon \to 0} \int_{\tilde{\xi}_0 - \varepsilon}^{\tilde{\xi}_0 + \varepsilon} R1(\tilde{\xi})\,d\tilde{\xi} - \lim_{\varepsilon \to 0} \int_{\tilde{\xi}_0 - \varepsilon}^{\tilde{\xi}_0 + \varepsilon} \frac{\beta\,\tilde{g}\,\tilde{h}_0(\tilde{\xi})\,\tilde{\phi}(\tilde{\xi})}{\tilde{v}_0'(\tilde{\xi})}\,\delta(\tilde{\xi})\,d\tilde{\xi}. \qquad (C.46)$$

124

Its solution is

$$\lim_{\varepsilon \to 0} \left[\tilde{\eta}_c(\tilde{\xi}_0 + \varepsilon) - \tilde{\eta}_b(\tilde{\xi}_0 - \varepsilon) \right] \leq \lim_{\varepsilon \to 0} M1\, \varepsilon - \lim_{\varepsilon \to 0} \frac{\beta\, \tilde{g}\, \tilde{h}_0(\tilde{\xi}_0)\, \tilde{\phi}(\tilde{\xi}_0)}{\tilde{v}_0'(\tilde{\xi}_0)}, \qquad (C.47)$$

for some bounded function $M1$. Hence,

$$\tilde{\eta}_c(\tilde{\xi}_0) - \tilde{\eta}_b(\tilde{\xi}_0) = -\frac{\beta\, \tilde{g}\, \tilde{h}_0(\tilde{\xi}_0)\, \tilde{\phi}(\tilde{\xi}_0)}{\tilde{v}_0'(\tilde{\xi}_0)}. \qquad (C.48)$$

But from (C.37) and (C.38),

$$\tilde{\eta}_c(\tilde{\xi}_0) - \tilde{\eta}_b(\tilde{\xi}_0) = -\tilde{b}_2\, \tilde{\nu}_2 - \tilde{b}_3\, \tilde{\bar{\nu}}_2 - \tilde{c}_1\, \tilde{\nu}_1 + \tilde{c}_3\, \tilde{\bar{\nu}}_2, \qquad (C.49)$$

while from (C.33), (C.42),

$$\begin{aligned} \tilde{h}_0(\tilde{\xi}_0) &= H_0\, e^{-\tilde{\xi}_0} = H_0, \\ \tilde{v}_0'(\tilde{\xi}_0) &= \beta\, e^{\beta\, \tilde{\xi}_0} = \beta, \\ \tilde{\phi}(\tilde{\xi}_0) &= \tilde{\phi}_b(\tilde{\xi}_0) = \tilde{b}_2\, e^{\tilde{\nu}_2\, \tilde{\xi}_0} + \tilde{b}_3\, e^{\tilde{\bar{\nu}}_2\, \tilde{\xi}_0} = \tilde{b}_2 + \tilde{b}_3. \end{aligned} \qquad (C.50)$$

Hence,

$$\tilde{b}_2 \left(\tilde{g}\, H_0 - \tilde{\nu}_2 \right) + \tilde{b}_3 \left(\tilde{g}\, H_0 - \tilde{\bar{\nu}}_2 \right) - \tilde{c}_1\, \tilde{\nu}_1 + \tilde{c}_3\, \tilde{\bar{\nu}}_2 = 0. \qquad (C.51)$$

The IBCS at $\tilde{\xi} = \tilde{\xi}_0 = 0$ for regular functions are derived using the continuity conditions

$$\begin{aligned} \lim_{\tilde{\xi} \to \tilde{\xi}_0-} \tilde{\phi}_b &= \lim_{\tilde{\xi} \to \tilde{\xi}_0+} \tilde{\phi}_c, \\ \lim_{\tilde{\xi} \to \tilde{\xi}_0-} \tilde{\psi}_b &= \lim_{\tilde{\xi} \to \tilde{\xi}_0+} \tilde{\psi}_c, \end{aligned} \qquad (C.52)$$

which respectively give

$$\tilde{b}_2 + \tilde{b}_3 - \tilde{c}_1 - \tilde{c}_3 = 0, \qquad (C.53)$$

$$\tilde{b}_1\, \beta\, \tilde{g} + \tilde{c}_1 \left((1 + \tilde{\lambda})^2 + \beta \right) = 0. \qquad (C.54)$$

IBCS at $\xi = \tilde{\xi}_1$: Here we integrate the third equation from (C.45) around $\xi = \tilde{\xi}_1$ over a small range, $(\tilde{\xi}_1 - \varepsilon, \tilde{\xi}_1 + \varepsilon)$ in the limit $\varepsilon \to 0$. But, $\delta(\tilde{v}_0 + \tilde{\Delta}) = \delta(\tilde{\xi} - \tilde{\xi}_1)/\tilde{v}_0'(\tilde{\xi})$ and the integral becomes

$$\lim_{\varepsilon \to 0} \int_{\tilde{\xi}_1 - \varepsilon}^{\tilde{\xi}_1 + \varepsilon} \frac{d\tilde{\psi}}{d\tilde{\xi}}\, d\tilde{\xi} = \lim_{\varepsilon \to 0} \int_{\tilde{\xi}_1 - \varepsilon}^{\tilde{\xi}_1 + \varepsilon} R2(\tilde{\xi})\, d\tilde{\xi} - \lim_{\varepsilon \to 0} \int_{\tilde{\xi}_1 - \varepsilon}^{\tilde{\xi}_1 + \varepsilon} \frac{\tilde{\phi}(\tilde{\xi})}{\tilde{v}_0'(\tilde{\xi})}\, \delta(\tilde{\xi} - \tilde{\xi}_1)\, d\tilde{\xi}. \qquad (C.55)$$

Its solution is

$$\lim_{\varepsilon \to 0} \left[\tilde{\psi}_b(\tilde{\xi} + \varepsilon) - \tilde{\psi}_a(\tilde{\xi} - \varepsilon) \right] \leq \lim_{\varepsilon \to 0} M2\, \varepsilon - \lim_{\varepsilon \to 0} \frac{\phi(\tilde{\xi}_1)}{\tilde{v}_0'(\tilde{\xi}_1)}, \qquad (C.56)$$

for some bounded function $M2$. Hence,

$$\tilde{\psi}_b(\tilde{\xi}_1) - \tilde{\psi}_a(\tilde{\xi}_1) = -\frac{\phi(\tilde{\xi}_1)}{\tilde{v}_0'(\tilde{\xi}_1)}. \tag{C.57}$$

Now from (C.35) and (C.37),

$$\tilde{\psi}_b(\tilde{\xi}_1) - \tilde{\psi}_a(\tilde{\xi}_1) = b_1 \ e^{-\tilde{\nu}_1 \tilde{\xi}_1}, \tag{C.58}$$

while from (C.33), (C.41),

$$\tilde{v}_0'(\tilde{\xi}_1) = \beta \ e^{\beta \tilde{\xi}_1},$$
$$\tilde{\phi}(\tilde{\xi}_1) = \tilde{\phi}_a(\tilde{\xi}_1) = \tilde{a}_2 \ e^{\tilde{\nu}_2 \tilde{\xi}_1}. \tag{C.59}$$

Hence,

$$\tilde{a}_2 \ e^{\tilde{\nu}_2 \tilde{\xi}_1} + \tilde{b}_1 \ \beta \ e^{(\beta - \tilde{\nu}_1) \tilde{\xi}_1} = 0. \tag{C.60}$$

The IBCS at $\tilde{\xi} = \tilde{\xi}_1$ for regular functions are derived using the continuity conditions

$$\lim_{\tilde{\xi} \to \tilde{\xi}_1-} \tilde{\phi}_a = \lim_{\tilde{\xi} \to \tilde{\xi}_1+} \tilde{\phi}_b,$$
$$\lim_{\tilde{\xi} \to \tilde{\xi}_1-} \tilde{\eta}_a = \lim_{\tilde{\xi} \to \tilde{\xi}_1+} \tilde{\eta}_b, \tag{C.61}$$

which respectively give

$$\tilde{a}_2 \ e^{\tilde{\nu}_2 \tilde{\xi}_1} - \tilde{b}_2 \ e^{\tilde{\nu}_2 \tilde{\xi}_1} - \tilde{b}_3 \ e^{\tilde{\nu}_2 \tilde{\xi}_1} = 0, \tag{C.62}$$
$$\tilde{a}_2 \ \tilde{\nu}_2 \ e^{\tilde{\nu}_2 \tilde{\xi}_1} - \tilde{b}_2 \ \tilde{\nu}_2 \ e^{\tilde{\nu}_2 \tilde{\xi}_1} - \tilde{b}_3 \ \tilde{\nu}_2 \ e^{\tilde{\nu}_2 \tilde{\xi}_1} = 0. \tag{C.63}$$

Eigenvalues and Hinch's parameters The relationship between the eigenvalues and the parameters in Hinch's model can be establish as follows

$$\tilde{\nu}_1 = 1 + \tilde{\lambda}, \quad \tilde{\nu}_2 = \frac{\beta + \sqrt{\beta^2 + 4\beta\tilde{\lambda}}}{2} = \beta\sigma, \quad \tilde{\tilde{\nu}}_2 = \frac{\beta - \sqrt{\beta^2 + 4\beta\tilde{\lambda}}}{2} = \beta\mu,$$
$$\tilde{\xi}_1 = -\tilde{x}_1 = -\delta/\beta, \quad H_0 = e^{-\delta/\beta}, \quad \tilde{g} = (1 + \beta) \ e^{\delta/\beta}, \tag{C.64}$$

where

$$\sigma = \frac{1}{2} + \frac{1}{2}\sqrt{1 + \frac{4\tilde{\lambda}}{\beta}}, \qquad \mu = \frac{1}{2} - \frac{1}{2}\sqrt{1 + \frac{4\tilde{\lambda}}{\beta}},$$
$$\delta = -\ln\left(1 - \tilde{\Delta}\right). \tag{C.65}$$

Therefore, from (C.51), (C.54), (C.60), (C.63), and (C.64) we have a system of six equations in terms of the undetermined arbitrary constants

$$\tilde{b}_2\,(\tilde{g}\,H_0 - \tilde{\nu}_2) + \tilde{b}_3\,(\tilde{g}\,H_0 - \tilde{\bar{\nu}}_2) - \tilde{c}_1\,\tilde{\nu}_1 + \tilde{c}_3\,\tilde{\nu}_2 = 0,$$

$$\tilde{b}_2 + \tilde{b}_3 - \tilde{c}_1 - \tilde{c}_3 = 0,$$

$$\tilde{b}_1\,\beta\,\tilde{g} + \tilde{c}_1\left((1+\tilde{\lambda})^2 + \beta\right) = 0,$$

$$\tilde{a}_2\,\mathrm{e}^{\tilde{\nu}_2\,\tilde{\xi}_1} + \tilde{b}_1\,\beta\,\mathrm{e}^{(\beta - \tilde{\nu}_1)\,\tilde{\xi}_1} = 0,$$

$$\tilde{a}_2\,\mathrm{e}^{\tilde{\nu}_2\,\tilde{\xi}_1} - \tilde{b}_2\,\mathrm{e}^{\tilde{\nu}_2\,\tilde{\xi}_1} - \tilde{b}_3\,\mathrm{e}^{\tilde{\bar{\nu}}_2\,\tilde{\xi}_1} = 0,$$

$$\tilde{a}_2\,\tilde{\nu}_2\,\mathrm{e}^{\tilde{\nu}_2\,\tilde{\xi}_1} - \tilde{b}_2\,\tilde{\nu}_2\,\mathrm{e}^{\tilde{\nu}_2\,\tilde{\xi}_1} - \tilde{b}_3\,\tilde{\bar{\nu}}_2\,\mathrm{e}^{\tilde{\bar{\nu}}_2\,\tilde{\xi}_1} = 0. \tag{C.66}$$

System (C.66), has non-trivial solutions only if the determinant of the coefficient matrix is zero.

$$\begin{vmatrix} 0 & 0 & 1+\beta-\beta\,\sigma & 1+\beta-\beta\,\mu & -(1+\tilde{\lambda}) & \beta\,\mu \\ 0 & 0 & 1 & 1 & -1 & -1 \\ 0 & \beta\,(1+\beta)\,\mathrm{e}^{\delta/\beta} & 0 & 0 & (1+\tilde{\lambda})^2 + \beta & 0 \\ \mathrm{e}^{-\delta\,\sigma} & \beta\,\mathrm{e}^{-\frac{\delta}{\beta}(\beta-1-\tilde{\lambda})} & 0 & 0 & 0 & 0 \\ \mathrm{e}^{-\delta\,\sigma} & 0 & -\,\mathrm{e}^{-\delta\,\sigma} & -\,\mathrm{e}^{-\delta\,\mu} & 0 & 0 \\ \beta\,\sigma\,\mathrm{e}^{-\delta\,\sigma} & 0 & -\beta\,\sigma\,\mathrm{e}^{-\delta\,\sigma} & -\beta\,\mu\,\mathrm{e}^{-\delta\,\mu} & 0 & 0 \end{vmatrix} = 0. \tag{C.67}$$

This lead to a characteristic equation

$$\tilde{f}_e(\tilde{\lambda},\,\beta,\,\delta) = \beta\,(\sigma - \mu - 1) - 1 + \frac{(1+\beta)(\beta\,\mu + 1 + \tilde{\lambda})}{(1+\tilde{\lambda})^2 + \beta}\,\mathrm{e}^{-\delta\left(\tilde{\lambda}/\beta + \sigma - 1\right)} = 0. \tag{C.68}$$

C.3   Linearization of the Biktashev (2002) equations

In a laboratory reference frame with (x, T) as coordinates, the front model [8], is written in the form

$$\frac{\partial E}{\partial T} = \frac{\partial^2 E}{\partial x^2} + F(E, h),$$

$$\frac{\partial h}{\partial T} = G(E, h)/\tau, \tag{C.69}$$

where $F(E, h) = \Theta(E - 1)h$, $G(E, h) = \Theta(-E) - h$ and Θ is a Heaviside step function. In a moving frame of reference, the solutions to (C.69) for a right-ward moving front are of the form $E(x - c\,T, T)$, $h(x - c\,T, T)$. Introducing the coordinates $\xi = x - c\,T$, $t = T$, and with $c > 0$, we look for functions $E(\xi, t)$, $h(\xi, t)$ that satisfy (C.69) thereby getting

$$\frac{\partial E}{\partial t} = \frac{\partial^2 E}{\partial \xi^2} + c\,\frac{\partial E}{\partial \xi} + F(E, h),$$

$$\frac{\partial h}{\partial t} = c\,\frac{\partial h}{\partial \xi} + G(E, h)/\tau. \tag{C.70}$$

NB: Traveling waves of (C.69) corresponds to stationary solutions of (C.70). Suppose $v_0(\xi)$, $h_0(\xi)$, is a stationary solution of (C.70), then

$$\frac{d^2 v_0}{d\xi^2} + c\,\frac{dv_0}{d\xi} + F(v_0, h_0) = 0,$$

$$c\,\frac{dh_0}{d\xi} + G(v_0, h_0)/\tau = 0. \tag{C.71}$$

Now linearizing (C.70) about $\left(v_0(\xi),\, h_0(\xi)\right)$ using

$$E = v_0(\xi) + \varepsilon\, v_1(\xi, t),$$

$$h = h_0(\xi) + \varepsilon\, h_1(\xi, t), \tag{C.72}$$

where $\varepsilon \ll 1$, $|v_1(\xi, t)| \ll 1$ and $|h_1(\xi, t)| \ll 1$. Thus, (C.70) becomes

$$\varepsilon\,\frac{\partial v_1}{\partial t} = \frac{d^2 v_0}{d\xi^2} + c\,\frac{dv_0}{d\xi} + \varepsilon\,\frac{\partial^2 v_1}{\partial \xi^2} + \varepsilon\,c\,\frac{\partial v_1}{\partial \xi} + F(v_0 + \varepsilon\, v_1, h_0 + \varepsilon\, h_1),$$

$$\varepsilon\,\frac{\partial h_1}{\partial t} = c\,\frac{dh_0}{d\xi} + \varepsilon\,c\,\frac{\partial h_1}{\partial \xi} + G(v_0 + \varepsilon\, v_1, h_0 + \varepsilon\, h_1)/\tau. \tag{C.73}$$

Using Taylor expansion we express $F(v_0 + \varepsilon\, v_1, h_0 + \varepsilon\, h_1)$ and $G(v_0 + \varepsilon\, v_1, h_0 + \varepsilon\, h_1)$ as

$$F(v_0 + \varepsilon\, v_1, h_0 + \varepsilon\, h_1) = F(v_0, h_0) + \varepsilon\,\frac{\partial F}{\partial v}(v_0, h_0)\, v_1 + \varepsilon\,\frac{\partial F}{\partial h}(v_0, h_0)\, h_1 + O(\varepsilon^2),$$

$$G(v_0 + \varepsilon\, v_1, h_0 + \varepsilon\, h_1) = G(v_0, h_0) + \varepsilon\,\frac{\partial G}{\partial v}(v_0, h_0)\, v_1 + \varepsilon\,\frac{\partial G}{\partial h}(v_0, h_0)\, h_1 + O(\varepsilon^2). \tag{C.74}$$

Since $\Theta(-v_0) \equiv \Theta(\xi)$, $\Theta(v_0 - 1) \equiv \Theta(-\xi - \Delta)$ and using the fact that $\delta(u) = \dfrac{d\Theta(u)}{du}$ and from chain rule $\delta(-v_0) = \delta(v_0) = \dfrac{1}{v_0'}\delta(\xi)$, $\delta(v_0 - 1) = \dfrac{-1}{v_0'}\delta(\xi + \Delta)$,

$$F(v_0, h_0) = \Theta(-\xi - \Delta)\, h_0, \qquad\qquad G(v_0, h_0) = \Theta(\xi) - h_0,$$

$$\frac{\partial F}{\partial v}(v_0, h_0) = \frac{-1}{v_0'}\delta(\xi + \Delta)\, h_0, \qquad\qquad \frac{\partial G}{\partial v}(v_0, h_0) = \frac{1}{v_0'}\delta(\xi),$$

$$\frac{\partial F}{\partial h}(v_0, h_0) = \Theta(-\xi - \Delta), \qquad\qquad \frac{\partial G}{\partial h}(v_0, h_0) = -1. \tag{C.75}$$

Equation (C.70) then reduce to (neglecting higher order terms)

$$\frac{\partial v_1}{\partial t} = c\,\frac{\partial v_1}{\partial \xi} + \frac{\partial^2 v_1}{\partial \xi^2} - \frac{1}{v_0'}\delta(\xi + \Delta)\, h_0\, v_1 + \Theta(-\xi - \Delta)\, h_1,$$

$$\frac{\partial h_1}{\partial t} = c\,\frac{\partial h_1}{\partial \xi} + \left(\frac{1}{v_0'}\delta(\xi)\, v_1 - h_1\right)/\tau. \tag{C.76}$$

C.3.1 Eigenvalue problem

Let the linearized eqtn (C.76) support solutions of the form $v_1(\xi,t) = e^{\lambda t}\,\phi(\xi)$ and $h_1(\xi,t) = e^{\lambda t}\,\psi(\xi)$. This lead to the (*temporal* eigenvalue) problem

$$\lambda\,\phi = \frac{\mathrm{d}^2\phi}{\mathrm{d}\xi^2} + c\,\frac{\mathrm{d}\phi}{\mathrm{d}\xi} - \frac{1}{v_0'}\delta(\xi+\Delta)\,h_0\,\phi + \Theta(-\xi-\Delta)\,\psi,$$

$$\lambda\,\psi = c\,\frac{\mathrm{d}\psi}{\mathrm{d}\xi} + \Big(\frac{1}{v_0'}\delta(\xi)\,\phi - \psi\Big)\big/\tau, \tag{C.77}$$

where $\phi(\xi)$ and $\psi(\xi)$ are some eigenfunctions. The eigenvalue problem (C.77) of the linearized equations (C.76) can be express in a compact form as

$$\mathcal{L}\,\bar V = \lambda\,\bar V, \tag{C.78}$$

where

$$\mathcal{L} = \bar D\,\frac{\mathrm{d}^2}{\mathrm{d}\xi^2} + \bar C\,\frac{\mathrm{d}}{\mathrm{d}\xi} + \bar F, \qquad \bar V = \begin{pmatrix}\phi\\\psi\end{pmatrix}, \qquad \bar D = \begin{pmatrix}1 & 0\\0 & 0\end{pmatrix},$$

$$\bar C = \begin{pmatrix}c & 0\\0 & c\end{pmatrix}, \qquad \bar F = \begin{pmatrix}\dfrac{-1}{v_0'}\delta(\xi+\Delta)\,h_0 & \Theta(-\xi-\Delta)\\[2mm] \dfrac{1}{\tau\,v_0'}\delta(\xi) & -1/\tau\end{pmatrix}. \tag{C.79}$$

Equation (C.78) is then converted into a three first-order (ODE) equations by letting $\dfrac{\mathrm{d}\phi}{\mathrm{d}\xi} = \eta$ and $\Xi = (\phi,\,\eta,\,\psi)^{\mathrm{T}}$. Thus, we obtain a linear system in $\mathbb{C}^3$

$$\Xi' = A\,\Xi, \tag{C.80}$$

where $(') = \dfrac{\mathrm{d}}{\mathrm{d}\xi}$ and

$$A = \begin{pmatrix} 0 & 1 & 0 \\[2mm] \lambda + \dfrac{1}{v_0'}\delta(\xi+\Delta)\,h_0 & -c & -\Theta(-\xi-\Delta) \\[2mm] \dfrac{-1}{\tau\,c\,v_0'}\delta(\xi) & 0 & \dfrac{1+\lambda\tau}{\tau\,c} \end{pmatrix}, \tag{C.81}$$

$$v_0(\xi) = \begin{cases} \omega - \dfrac{\tau^2\,c^2}{1+\tau\,c^2}\,e^{\xi/\tau c}, & \xi \le -\Delta, \\[3mm] -\alpha + \alpha\,e^{-c\xi}, & \xi \ge -\Delta, \end{cases}$$

$$h_0(\xi) = \begin{cases} e^{\xi/\tau c}, & \xi \le 0, \\[2mm] 1, & \xi \ge 0, \end{cases} \tag{C.82}$$

where

$$\xi = x - c\,t, \quad \omega = 1 + \tau\,c^2\,(1+\alpha), \quad \Delta = \frac{1}{c}\,\ln\!\Big(\frac{1+\alpha}{\alpha}\Big). \tag{C.83}$$

We have three intervals (cases $i = a$, b, c) to consider. For case $i = a$, $\xi \in (-\infty, -\Delta)$ so therefore in this interval, $\Theta(-\xi - \Delta) = 1$, $\delta(\xi + \Delta) = \delta(\xi) = 0$ and $h_0 = e^{\xi/\tau c}$. Thus, the matrix A in (C.81) becomes

$$
A^a = \begin{pmatrix} 0 & 1 & 0 \\ \lambda & -c & -1 \\ 0 & 0 & \nu_1 \end{pmatrix},
\tag{C.84}
$$

and whose characteristic equation (i.e., $|\mu^a I - A^a| = 0$) gives the *spatial* eigenvalues

$$
\mu_1^a = \nu_1 = \frac{1 + \lambda \tau}{\tau c},
$$
$$
\mu_{2,3}^a = -\nu_2, \; -\bar{\nu}_2,
\tag{C.85}
$$
$$
\tag{C.86}
$$

where

$$
\nu_2 = \frac{c + \sqrt{c^2 + 4\lambda}}{2},
\tag{C.87}
$$
$$
\bar{\nu}_2 = \frac{c - \sqrt{c^2 + 4\lambda}}{2}.
\tag{C.88}
$$

Eigenvectors for case $i = a$:

The eigenvector corresponding to $\mu_1^a = \nu_1 = \dfrac{1 + \lambda \tau}{\tau c}$ is derived as follow

$$
\begin{pmatrix} \nu_1 & -1 & 0 \\ -\lambda & \nu_1 + c & 1 \\ 0 & 0 & 0 \end{pmatrix} \begin{pmatrix} v_{11}^a \\ v_{21}^a \\ v_{31}^a \end{pmatrix} = \begin{pmatrix} 0 \\ 0 \\ 0 \end{pmatrix}.
\tag{C.89}
$$

From (C.89) and for some parameter k

$$
v_{11}^a = k, \; v_{21}^a = k \, \nu_1, \; v_{31}^a = k \left(\lambda - \nu_1 (\nu_1 + c) \right).
\tag{C.90}
$$

Thus, the eigenvector is

$$
\vec{v}_1^a = \begin{pmatrix} v_{11}^a \\ v_{21}^a \\ v_{31}^a \end{pmatrix} = k \begin{pmatrix} 1 \\ \nu_1 \\ -(\nu_1^2 + c\nu_1 - \lambda) \end{pmatrix}.
\tag{C.91}
$$

Hence, taking $k = 1$,

$$
\vec{v}_1^a = \begin{pmatrix} 1 \\ \nu_1 \\ -\nu_q \end{pmatrix},
\tag{C.92}
$$

130

where $\nu_q = (\nu_1^2 + c\,\nu_1 - \lambda) = \dfrac{(1 + \lambda\,\tau)^2 + \tau\,c^2}{\tau^2\,c^2}$. For $\mu_2^a = -\nu_2$

$$
\begin{pmatrix}
-\nu_2 & -1 & 0 \\
-\lambda & -\nu_2 + c & 1 \\
0 & 0 & -\nu_2 - \nu_1
\end{pmatrix}
\begin{pmatrix}
v_{12}^a \\
v_{22}^a \\
v_{32}^a
\end{pmatrix}
=
\begin{pmatrix}
0 \\
0 \\
0
\end{pmatrix},
\tag{C.93}
$$

From (C.93) and for some parameter k

$$
v_{12}^a = k,\ v_{22}^a = -\nu_2\,k,\ v_{32}^a = 0 \Big(\text{since } \nu_1 + \nu_2 \neq 0\Big).
\tag{C.94}
$$

Thus, the eigenvector is

$$
\vec{v}_2^{\,a} =
\begin{pmatrix}
v_{12}^a \\
v_{22}^a \\
v_{32}^a
\end{pmatrix}
= k
\begin{pmatrix}
1 \\
-\nu_2 \\
0
\end{pmatrix},
\tag{C.95}
$$

hence, taking $k = 1$,

$$
\vec{v}_2^{\,a} =
\begin{pmatrix}
1 \\
-\nu_2 \\
0
\end{pmatrix}.
\tag{C.96}
$$

Similarly, for $\mu_3^a = -\bar{\nu}_2$, the eigenvector is

$$
\vec{v}_3^{\,a} =
\begin{pmatrix}
1 \\
-\bar{\nu}_2 \\
0
\end{pmatrix}.
\tag{C.97}
$$

For case $i = b$, $\xi \in (-\Delta, 0)$, and in this region, $\Theta(-\xi - \Delta) = 0$, $\delta(\xi + \Delta) = \delta(\xi) = 0$, $h_0 = \mathrm{e}^{\xi/\tau c}$. Therefore, the matrix A in (C.81) then becomes

$$
A^b =
\begin{pmatrix}
0 & 1 & 0 \\
\lambda & -c & 0 \\
0 & 0 & \nu_1
\end{pmatrix},
\tag{C.98}
$$

from which we get the *spatial* eigenvalues

$$
\mu_1^b = \nu_1 = \frac{1 + \lambda\,\tau}{\tau\,c},
$$
$$
\mu_{2,3}^b = -\nu_2,\ -\bar{\nu}_2.
\tag{C.99}
$$

Eigenvectors for case $i = b$:

The eigenvector corresponding to $\mu_1^b = \nu_1$ is derived as follow

$$
\begin{pmatrix}
\nu_1 & -1 & 0 \\
-\lambda & \nu_1 + c & 0 \\
0 & 0 & 0
\end{pmatrix}
\begin{pmatrix}
v_{11}^b \\
v_{21}^b \\
v_{31}^b
\end{pmatrix}
=
\begin{pmatrix}
0 \\
0 \\
0
\end{pmatrix}.
\tag{C.100}
$$

From (C.100)

$$
\nu_1\, v_{11}^b - v_{21}^b = 0,
$$
$$
-\lambda\, v_{11}^b + (\nu_1 + c)\, v_{21}^b = 0,
\tag{C.101}
$$

since $\nu_1^2 + c\,\nu_1 - \lambda \neq 0$ then $v_{21}^b = 0$, $v_{11}^b = 0$ and $v_{31}^b = k$ for some parameter k. Thus, the eigenvector is

$$
\vec{v}_1^b =
\begin{pmatrix}
v_{11}^b \\
v_{21}^b \\
v_{31}^b
\end{pmatrix}
= k
\begin{pmatrix}
0 \\
0 \\
1
\end{pmatrix},
\tag{C.102}
$$

hence, taking $k = 1$,

$$
\vec{v}_1^b =
\begin{pmatrix}
0 \\
0 \\
1
\end{pmatrix}.
\tag{C.103}
$$

For $\mu_2^b = -\nu_2$

$$
\begin{pmatrix}
-\nu_2 & -1 & 0 \\
-\lambda & -\nu_2 + c & 0 \\
0 & 0 & -\nu_2 - \nu_1
\end{pmatrix}
\begin{pmatrix}
v_{12}^b \\
v_{22}^b \\
v_{32}^b
\end{pmatrix}
=
\begin{pmatrix}
0 \\
0 \\
0
\end{pmatrix},
\tag{C.104}
$$

and from it we get for some parameter k

$$
v_{12}^b = k,\ v_{22}^b = -\nu_2\,k,\ v_{32}^b = 0\,(\text{since }\nu_1 + \nu_2 \neq 0),
\tag{C.105}
$$

therefore, the eigenvector is

$$
\vec{v}_2^b =
\begin{pmatrix}
v_{12}^b \\
v_{22}^b \\
v_{32}^b
\end{pmatrix}
= k
\begin{pmatrix}
1 \\
-\nu_2 \\
0
\end{pmatrix};
\tag{C.106}
$$

hence, taking $k = 1$,

$$
\vec{v}_2^b =
\begin{pmatrix}
1 \\
-\nu_2 \\
0
\end{pmatrix}.
\tag{C.107}
$$

Similarly, for $\mu_3^b = -\bar{\nu}_2$, the eigenvector will then be

$$
\vec{v}_3^{\,b} = \begin{pmatrix} 1 \\ -\bar{\nu}_2 \\ 0 \end{pmatrix}. \tag{C.108}
$$

And lastly for the case $i = c$, $\xi \in (0, +\infty)$, then $\Theta(-\xi - \Delta) = 0$, $\delta(\xi + \Delta) = \delta(\xi) = 0$ and $h_0 = 1$. Thus, the matrix A in (C.81) then becomes

$$
A^c = \begin{pmatrix} 0 & 1 & 0 \\ \lambda & -c & 0 \\ 0 & 0 & \nu_1 \end{pmatrix}, \tag{C.109}
$$

from which we get the same set of *spatial* eigenvalues as with the case $i = b$

$$
\mu_1^c = \nu_1,
$$
$$
\mu_{2,3}^c = -\nu_2, \ -\bar{\nu}_2, \tag{C.110}
$$

and so we will have the same corresponding eigenvectors

$$
\vec{v}_1^{\,c} = \begin{pmatrix} 0 \\ 0 \\ 1 \end{pmatrix}, \ \vec{v}_2^{\,c} = \begin{pmatrix} 1 \\ -\nu_2 \\ 0 \end{pmatrix}, \ \vec{v}_3^{\,c} = \begin{pmatrix} 1 \\ -\bar{\nu}_2 \\ 0 \end{pmatrix}. \tag{C.111}
$$

C.3.2 Characteristic equation

To determine the characteristic equation we rewrite the solutions to (C.80) by considering each of the three regions. Each of the solutions are written as a linear combination of the product of its corresponding eigenvectors and the exponential of its eigenvalues. That is,

$$
\begin{pmatrix} \phi_i \\ \eta_i \\ \psi_i \end{pmatrix} = \sum_j i_j \, \vec{v}_j^{\,i} \, e^{\mu_j^i \xi}, \tag{C.112}
$$

and is such that $A^i \vec{v}_j^{\,i} = \mu_j^i \vec{v}_j^{\,i}$, where $A^i = A^i(\lambda)$, $\mu_j^i = \mu_j^i(\lambda)$ for $i = a, b, c$ and $j = 1, 2, 3$.

NB: Note that $\vec{v}_2^{\,a} = \vec{v}_2^{\,b} = \vec{v}_2^{\,c}$, $\vec{v}_3^{\,a} = \vec{v}_3^{\,b} = \vec{v}_3^{\,c}$, $\vec{v}_1^{\,b} = \vec{v}_1^{\,c}$. The solutions for the three cases can be written explicitly as

$$
\begin{pmatrix} \phi_a \\ \eta_a \\ \psi_a \end{pmatrix} = a_1 \, \vec{v}_1^{\,a} \, e^{\nu_1 \xi} + a_2 \, \vec{v}_2^{\,a} \, e^{-\nu_2 \xi} + a_3 \, \vec{v}_3^{\,a} \, e^{-\bar{\nu}_2 \xi}, \tag{C.113}
$$

133

$$\begin{pmatrix} \phi_b \\ \eta_b \\ \psi_b \end{pmatrix} = b_1 \, \vec{v}_1^{\,b} \, e^{\nu_1 \xi} + b_2 \, \vec{v}_2^{\,b} \, e^{-\nu_2 \xi} + b_3 \, \vec{v}_3^{\,b} \, e^{-\bar{\nu}_2 \xi}, \tag{C.114}$$

$$\begin{pmatrix} \phi_c \\ \eta_c \\ \psi_c \end{pmatrix} = c_1 \, \vec{v}_1^{\,c} \, e^{\nu_1 \xi} + c_2 \, \vec{v}_2^{\,c} \, e^{-\nu_2 \xi} + c_3 \, \vec{v}_3^{\,c} \, e^{-\bar{\nu}_2 \xi}, \tag{C.115}$$

where $\nu_1 = \dfrac{1 + \lambda \tau}{\tau \, c}$, $\nu_2 = \dfrac{c + \sqrt{c^2 + 4\,\lambda}}{2}$, $\bar{\nu}_2 = \dfrac{c - \sqrt{c^2 + 4\,\lambda}}{2}$.

And $\vec{v}_1^{\,a}, \vec{v}_2^{\,a}, \vec{v}_3^{\,a}; \vec{v}_1^{\,b}, \vec{v}_2^{\,b}, \vec{v}_3^{\,b}; \vec{v}_1^{\,c}, \vec{v}_2^{\,c}, \vec{v}_3^{\,c}$ as given in equations (C.92) - (C.96), (C.103) - (C.108) and (C.111)

$$\vec{v}_1^{\,a} = \begin{pmatrix} v_{11}^a \\ v_{21}^a \\ v_{31}^a \end{pmatrix} = \begin{pmatrix} 1 \\ \nu_1 \\ -\nu_q \end{pmatrix}, \quad \vec{v}_1^{\,b} = \begin{pmatrix} v_{11}^b \\ v_{21}^b \\ v_{31}^b \end{pmatrix} = \vec{v}_1^{\,c} = \begin{pmatrix} v_{11}^c \\ v_{21}^c \\ v_{31}^c \end{pmatrix} = \begin{pmatrix} 0 \\ 0 \\ 1 \end{pmatrix},$$

$$\vec{v}_2^{\,a} = \begin{pmatrix} v_{12}^a \\ v_{22}^a \\ v_{32}^a \end{pmatrix} = \vec{v}_2^{\,b} = \begin{pmatrix} v_{12}^b \\ v_{22}^b \\ v_{32}^b \end{pmatrix} = \vec{v}_2^{\,c} = \begin{pmatrix} v_{12}^c \\ v_{22}^c \\ v_{32}^c \end{pmatrix} = \begin{pmatrix} 1 \\ -\nu_2 \\ 0 \end{pmatrix},$$

$$\vec{v}_3^{\,a} = \begin{pmatrix} v_{13}^a \\ v_{23}^a \\ v_{33}^a \end{pmatrix} = \vec{v}_3^{\,b} = \begin{pmatrix} v_{13}^b \\ v_{23}^b \\ v_{33}^b \end{pmatrix} = \vec{v}_3^{\,c} = \begin{pmatrix} v_{13}^c \\ v_{23}^c \\ v_{33}^c \end{pmatrix} = \begin{pmatrix} 1 \\ -\bar{\nu}_2 \\ 0 \end{pmatrix}. \tag{C.116}$$

Determination of the constants (i_j): To determine the constants $i_j : i = a, b, c;\ j = 1, 2, 3$, the solutions (C.113), (C.114) and (C.115) has to satisfy both the boundaries at $\pm\infty$ (i.e., $\xi \to \pm\infty$) and at the internal boundaries $\xi = -\Delta$ and $\xi = 0$.

Boundary conditions at $\pm\infty$: With $\lambda \geq 0 : \nu_1 > 0$, $\nu_2 > 0$, $\bar{\nu}_2 < 0$:

For the case $i = a$

$$\lim_{\xi \to -\infty} \begin{pmatrix} \phi_a \\ \eta_a \\ \psi_a \end{pmatrix}, \tag{C.117}$$

must be bounded and therefore $a_2 = 0$. Thus,

$$\begin{pmatrix} \phi_a \\ \eta_a \\ \psi_a \end{pmatrix} = a_1 \begin{pmatrix} 1 \\ \nu_1 \\ -\nu_q \end{pmatrix} e^{\nu_1 \xi} + a_3 \begin{pmatrix} 1 \\ -\bar{\nu}_2 \\ 0 \end{pmatrix} e^{-\bar{\nu}_2 \xi}. \tag{C.118}$$

134

For the case $i = b$, we can only consider the internal boundary conditions and so the solution (for the time being) is

$$\begin{pmatrix} \phi_b \\ \eta_b \\ \psi_b \end{pmatrix} = b_1 \begin{pmatrix} 0 \\ 0 \\ 1 \end{pmatrix} e^{\nu_1 \xi} + b_2 \begin{pmatrix} 1 \\ -\nu_2 \\ 0 \end{pmatrix} e^{-\nu_2 \xi} + b_3 \begin{pmatrix} 1 \\ -\bar\nu_2 \\ 0 \end{pmatrix} e^{-\bar\nu_2 \xi}. \tag{C.119}$$

However, for the case $i = c$

$$\lim_{\xi \to +\infty} \begin{pmatrix} \phi_c \\ \eta_c \\ \psi_c \end{pmatrix} \tag{C.120}$$

must be bounded and so therefore $c_1 = 0$, $c_3 = 0$. Thus

$$\begin{pmatrix} \phi_c \\ \eta_c \\ \psi_c \end{pmatrix} = c_2 \begin{pmatrix} 1 \\ -\nu_2 \\ 0 \end{pmatrix} e^{-\nu_2 \xi}. \tag{C.121}$$

Internal boundary conditions (IBCS): Let (C.80) be rewritten in terms of regular $(R1, R2)$ and singular $(S1, S2)$ functions

$$\frac{\mathrm{d}\phi}{\mathrm{d}\xi} = \eta,$$

$$\frac{\mathrm{d}\eta}{\mathrm{d}\xi} = \overbrace{\lambda\phi - c\,\eta - \Theta(-\xi - \Delta)\,\psi}^{R1(\xi)} + \overbrace{\frac{1}{v_0'}\delta(\xi + \Delta)\,h_0\,\phi}^{S1(\xi)},$$

$$\frac{\mathrm{d}\psi}{\mathrm{d}\xi} = \overbrace{\nu_1\,\psi}^{R2(\xi)} - \overbrace{\frac{1}{\tau c\,v_0'}\delta(\xi)\,\phi}^{S2(\xi)}. \tag{C.122}$$

IBCS at $\xi = -\Delta$: The trick here is to integrate the second equation from (C.122) around $\xi = -\Delta$ over a small range, $(-\Delta - \varepsilon, -\Delta + \varepsilon)$ and consider limit $\varepsilon \to 0$,

$$\lim_{\varepsilon \to 0} \int_{-\Delta - \varepsilon}^{-\Delta + \varepsilon} \frac{\mathrm{d}\eta}{\mathrm{d}\xi}\,\mathrm{d}\xi = \lim_{\varepsilon \to 0} \int_{-\Delta - \varepsilon}^{-\Delta + \varepsilon} R1(\xi)\,\mathrm{d}\xi + \lim_{\varepsilon \to 0} \int_{-\Delta - \varepsilon}^{-\Delta + \varepsilon} \frac{h_0(\xi)\,\phi(\xi)}{v_0'(\xi)} \delta(\xi + \Delta)\,\mathrm{d}\xi. \tag{C.123}$$

Its solution is

$$\lim_{\varepsilon \to 0} \left[\eta_b(-\Delta + \varepsilon) - \eta_a(-\Delta - \varepsilon) \right] \le \lim_{\varepsilon \to 0} M\,\varepsilon + \lim_{\varepsilon \to 0} \frac{h_0(-\Delta)\,\phi(-\Delta)}{v_0'(-\Delta)}, \tag{C.124}$$

hence,

$$\eta_b(-\Delta) - \eta_a(-\Delta) = \frac{h_0(-\Delta)\,\phi(-\Delta)}{v_0'(-\Delta)}, \tag{C.125}$$

135

for some bounded function M. Now from (C.116), we have

$$\eta_b(-\Delta) - \eta_a(-\Delta) = -a_1\nu_1 \ e^{-\nu_1\Delta} + a_3\bar{\nu}_2 \ e^{\bar{\nu}_2\Delta} - b_2\nu_2 \ e^{\nu_2\Delta} - b_3\bar{\nu}_2 \ e^{\bar{\nu}_2\Delta}, \quad \text{(C.126)}$$

meanwhile, from (C.82), (C.113)

$$h_0(-\Delta) = \ e^{-\Delta/(\tau c)},$$
$$v_0'(-\Delta) = -\alpha c \ e^{c\Delta},$$
$$\phi(-\Delta) = \phi_b(-\Delta) = b_2 \ e^{\nu_2\Delta} + b_3 \ e^{\bar{\nu}_2\Delta}, \quad \text{(C.127)}$$

thus,

$$\frac{h_0(-\Delta)\,\phi(-\Delta)}{v_0'(-\Delta)} = \frac{e^{-\nu\Delta}(b_2 \ e^{\nu_2\Delta} + b_3 \ e^{\bar{\nu}_2\Delta})}{-\alpha c}, \quad \text{(C.128)}$$

where $\nu = \dfrac{1 + \tau c^2}{\tau c}$. Hence, (C.125) becomes

$$a_1 \, \alpha \, c\, \nu_1 \ e^{-\nu_1\Delta} - a_3 \, \alpha \, c\bar{\nu}_2 \ e^{\bar{\nu}_2\Delta} + b_2 \ e^{\nu_2\Delta}\left(\alpha c\nu_2 - \ e^{-\nu\Delta}\right) + b_3 \ e^{\bar{\nu}_2\Delta}\left(\alpha c\bar{\nu}_2 - \ e^{-\nu\Delta}\right) = 0.$$
$$\text{(C.129)}$$

The IBCS at $\xi = -\Delta$ for regular functions are derived using the continuity conditions

$$\lim_{\xi\to-\Delta-} \phi_a = \lim_{\xi\to-\Delta+} \phi_b,$$
$$\lim_{\xi\to-\Delta-} \psi_a = \lim_{\xi\to-\Delta+} \psi_b, \quad \text{(C.130)}$$

which respectively give

$$a_1 \ e^{-\nu_1\Delta} + a_3 \ e^{\bar{\nu}_2\Delta} - b_2 \ e^{\nu_2\Delta} - b_3 \ e^{\bar{\nu}_2\Delta} = 0, \quad \text{(C.131)}$$
$$a_1 \nu_q + b_1 = 0. \quad \text{(C.132)}$$

IBCS at $\xi = 0$: In this case, we integrate the third equation from (C.122) around $\xi = 0$ over a small range, $(-\varepsilon, \varepsilon)$ and consider limit $\varepsilon \to 0$,

$$\lim_{\varepsilon\to0}\int_{-\varepsilon}^{\varepsilon} \frac{\mathrm{d}\psi}{\mathrm{d}\xi} \ \mathrm{d}\xi = \lim_{\varepsilon\to0}\int_{-\varepsilon}^{-\varepsilon} R2(\xi) \ \mathrm{d}\xi - \frac{1}{\tau c}\lim_{\varepsilon\to0}\int_{-\varepsilon}^{\varepsilon} \frac{\phi(\xi)}{v_0'(\xi)}\delta(\xi) \ \mathrm{d}\xi. \quad \text{(C.133)}$$

Its solution is

$$\lim_{\varepsilon\to0}\left[\psi_c(\varepsilon) - \psi_b(-\varepsilon)\right] \le \lim_{\varepsilon\to0} N\varepsilon - \lim_{\varepsilon\to0}\frac{1}{\tau c}\frac{\phi(0)}{v_0'(0)}, \quad \text{(C.134)}$$

hence,

$$\psi_c(0) - \psi_b(0) = \frac{-\phi(0)}{\tau c\, v_0'(0)}, \quad \text{(C.135)}$$

136

for some bounded function N. Now from (C.116), we have

$$\psi_c(0) - \psi_b(0) = 0 - b_1 = -b_1, \tag{C.136}$$

and meanwhile from (C.82), (C.115)

$$v_0'(0) = -\alpha\,c,$$
$$\phi(0) = \phi_c(0) = c_2; \tag{C.137}$$

thus,

$$\frac{\phi(0)}{\tau\,c\,v_0'(0)} = \frac{c_2}{\alpha\,\tau\,c^2}, \tag{C.138}$$

hence, (C.135) becomes

$$b_1\,\alpha\,\tau\,c^2 + c_2 = 0. \tag{C.139}$$

The IBCS at $\xi = 0$ for regular functions are also derived using the continuity conditions

$$\lim_{\xi\to0-}\phi_b = \lim_{\xi\to0+}\phi_c,$$
$$\lim_{\xi\to0-}\eta_b = \lim_{\xi\to0+}\eta_c, \tag{C.140}$$

which respectively yield

$$b_2 + b_3 - c_2 = 0, \tag{C.141}$$
$$b_2\,\nu_2 + b_3\,\bar\nu_2 - c_2\,\nu_2 = 0. \tag{C.142}$$

Thus, we have a system of six equations in terms of the undetermined arbitrary constants

$$a_1\,\alpha\,c\,\nu_1\,e^{-\nu_1\Delta} - a_3\,\alpha\,c\bar\nu_2\,e^{\bar\nu_2\Delta} + b_2\,e^{\nu_2\Delta}\Big(\alpha\,c\,\nu_2 - e^{-\nu\Delta}\Big)$$
$$+ b_3\,e^{\bar\nu_2\Delta}\Big(\alpha\,c\,\bar\nu_2 - e^{-\nu\Delta}\Big) = 0,$$
$$a_1\,e^{-\nu_1\Delta} + a_3\,e^{\bar\nu_2\Delta} - b_2\,e^{\nu_2\Delta} - b_3\,e^{\bar\nu_2\Delta} = 0,$$
$$a_1\,\nu_q + b_1 = 0,$$
$$b_1\,\alpha\,\tau\,c^2 + c_2 = 0,$$
$$b_2 + b_3 - c_2 = 0,$$
$$b_2\,\nu_2 + b_3\,\bar\nu_2 - c_2\,\nu_2 = 0. \tag{C.143}$$

The system in (C.143) with a_1, a_3, b_1, b_2, b_3, and, c_2 to be determined can be written in matrix form having a six-by-six coefficient matrix. The system has nontrivial solutions

137

if the determinant of the coefficient matrix equals zero

$$
\begin{vmatrix}
\alpha\,c\,\nu_1\,\mathrm{e}^{-\nu_1\,\Delta} & -\alpha\,c\,\bar\nu_2\,\mathrm{e}^{\bar\nu_2\,\Delta} & 0 & \left(\alpha\,c\,\nu_2 - \mathrm{e}^{-\nu\,\Delta}\right)\mathrm{e}^{\nu_2\,\Delta} & \left(\alpha\,c\,\bar\nu_2 - \mathrm{e}^{-\nu\,\Delta}\right)\mathrm{e}^{\bar\nu_2\,\Delta} & 0 \\
\mathrm{e}^{-\nu_1\,\Delta} & \mathrm{e}^{\bar\nu_2\,\Delta} & 0 & -\mathrm{e}^{\nu_2\,\Delta} & -\mathrm{e}^{\bar\nu_2\,\Delta} & 0 \\
\nu_q & 0 & 1 & 0 & 0 & 0 \\
0 & 0 & \alpha\,\tau\,c^2 & 0 & 0 & 1 \\
0 & 0 & 0 & 1 & 1 & -1 \\
0 & 0 & 0 & \nu_2 & \bar\nu_2 & -\nu_2
\end{vmatrix}
= 0.
$$

(C.144)

The solvability condition for this system leads to the characteristic equation

$$
f_e(\lambda; c, \alpha, \tau) = \alpha\,c\,(\nu_2 - \bar\nu_2)\,\mathrm{e}^{\nu\,\Delta} - 1 + \frac{\tau\,c\,(\nu_1 + \bar\nu_2)}{(1 + \lambda\,\tau)^2 + \tau\,c^2}\,\mathrm{e}^{-(\nu_1 + \nu_2 - \nu)\,\Delta} = 0, \quad (\text{C.145})
$$

where

$$
\begin{aligned}
\nu &= \frac{1 + \tau\,c^2}{\tau\,c}, & \nu_1 &= \frac{1 + \lambda\,\tau}{\tau\,c}, \\
\nu_2 &= \frac{c + \sqrt{c^2 + 4\,\lambda}}{2}, & \bar\nu_2 &= \frac{c - \sqrt{c^2 + 4\,\lambda}}{2}, \\
\Delta &= \frac{1}{c}\ln\left(\frac{1 + \alpha}{\alpha}\right). &&
\end{aligned}
$$

(C.146)

Parameters/variables/solutions relations between Hinch (2004) and Biktashev (2002) model

The relationships between parameters are given by

$$
\begin{aligned}
\tilde c &= \sqrt{\tau}\,c, \quad \tilde\lambda = \tau\,\lambda, & \beta &= \tilde c^2 = \tau\,c^2, \\
\tilde\Delta &= \frac{1}{1 + \alpha}, & \delta &= -\ln\left(1 - \tilde\Delta\right) = -\ln\left(\frac{\alpha}{1 + \alpha}\right), \\
\tau &= \frac{\tilde g}{\tilde\Delta}, & \Delta &= \frac{\delta}{c},
\end{aligned}
$$

(C.147)

and that for the variables and solutions are

$$
\begin{aligned}
v &= 1 + \frac{1}{\tilde\Delta}\,\tilde v, & v_0 &= 1 + \frac{1}{\tilde\Delta}\,\tilde v_0, & v_1 &= \frac{1}{\tilde\Delta}\,\tilde v_1, \\
\xi &= -\Delta - \frac{\beta}{c}\,\tilde\xi, &&&& \\
\phi_j &= \frac{1}{\tilde\Delta}\,\tilde\phi_j, & \eta &= \frac{-1}{c\,\tilde g}\,\tilde\eta, & \psi_j &= \tilde\psi_j, & (\text{C.148})
\end{aligned}
$$

138

for $j = a$, b, c. Meanwhile, for the yet to be determined constants and eigenvalues the relationships are

$$a_1 = \frac{1}{\tilde{\Delta}} \, e^{\frac{\delta}{\beta}(1+\tilde{\lambda})} \, \tilde{c}_1, \qquad a_2 = 0 \, \{\underline{\tilde{c}_2 = 0}\}, \qquad a_3 = \frac{1}{\tilde{\Delta}} \, e^{-\delta\mu} \, \tilde{c}_3,$$

$$b_1 = e^{\frac{\delta}{\beta}(1+\tilde{\lambda})} \, \tilde{b}_1, \qquad b_2 = \frac{1}{\tilde{\Delta}} \, e^{-\delta\sigma} \, \tilde{b}_2, \qquad b_3 = \frac{1}{\tilde{\Delta}} \, e^{-\delta\mu} \, \tilde{b}_3,$$

$$c_1 = 0 \, \{\underline{\tilde{a}_1 = 0}\}, \qquad c_2 = \frac{1}{\tilde{\Delta}} \, e^{-\delta\sigma} \, \tilde{a}_2, \qquad c_3 = 0 \, \{\underline{\tilde{a}_3 = 0}\};$$

$$\nu_1 = \frac{c}{\beta} \tilde{\nu}_1 = \frac{c}{\beta}(1 + \tilde{\lambda}), \qquad \nu_2 = \frac{c}{\beta} \tilde{\nu}_2 = c\,\sigma, \qquad \bar{\nu}_2 = \frac{c}{\beta} \tilde{\bar{\nu}}_2 = c\,\mu. \qquad \text{(C.149)}$$

C.3.3 Adjoint eigenvalue problem

We can construct the adjoint eigenvalue problem to the front model from the eigenvalue problem (C.79) Thus, the *adjoint* eigenvalue problem is

$$\mathcal{L}^+ \, \bar{W} = \mu \, \bar{W}, \qquad \text{(C.150)}$$

where

$$\mathcal{L}^+ = \bar{D}^T \frac{\mathrm{d}^2}{\mathrm{d}\xi^2} - \bar{C} \, \frac{\mathrm{d}}{\mathrm{d}\xi} + \bar{F}^T, \quad \bar{D}^T = \bar{D}, \quad \bar{W} = \begin{pmatrix} \phi^* \\ \psi^* \end{pmatrix}, \qquad \text{(C.151)}$$

and

$$\bar{F}^T = \begin{pmatrix} \dfrac{-1}{v_0'}\delta(\xi + \Delta)\,h_0 & \dfrac{1}{\tau\,v_0'}\delta(\xi) \\ \Theta(-\xi - \Delta) & -1/\tau \end{pmatrix}. \qquad \text{(C.152)}$$

Now when casted into a three ODE equations, (C.150) becomes

$$\frac{\mathrm{d}\phi^*}{\mathrm{d}\xi} = \eta^*,$$

$$\frac{\mathrm{d}\eta^*}{\mathrm{d}\xi} = \left(\mu + \frac{1}{v_0'}\delta(\xi + \Delta)\,h_0\right)\phi^* + c\,\eta^* - \frac{1}{\tau\,v_0'}\delta(\xi)\psi^*,$$

$$\frac{\mathrm{d}\psi^*}{\mathrm{d}\xi} = \frac{1}{c}\Theta(-\xi - \Delta)\,\phi^* - \frac{(1+\mu\,\tau)}{\tau\,c}\phi^*, \qquad \text{(C.153)}$$

which is then written in matrix format as

$$\Xi^{*\prime} = B\,\Xi^*, \qquad \text{(C.154)}$$

where $(') = \dfrac{\mathrm{d}}{\mathrm{d}\xi}$ and

$$B = \begin{pmatrix} 0 & 1 & 0 \\ \mu + \dfrac{1}{v_0'}\delta(\xi + \Delta)\,h_0 & c & \dfrac{-1}{\tau\,c\,v_0'}\delta(\xi) \\ \dfrac{1}{c}\Theta(-\xi - \Delta) & 0 & -\dfrac{(1+\mu\,\tau)}{\tau\,c} \end{pmatrix}. \qquad \text{(C.155)}$$

We have three intervals (cases $i = a, b, c$) to consider. For the case $i = a, \xi \in (-\infty, -\Delta)$: $\Theta(-\xi - \Delta) = 1$, $\delta(\xi + \Delta) = \delta(\xi) = 0$ and $h_0 = e^{\xi/\tau c}$. Thus, the matrix B in (C.155) becomes

$$B^a = \begin{pmatrix} 0 & 1 & 0 \\ \mu & c & 0 \\ 1/c & 0 & -\gamma_1 \end{pmatrix}, \qquad (C.156)$$

and whose characteristic equation (i.e., $|\gamma^a I - B^a| = 0$) gives the *spatial* eigenvalues

$$\gamma_1^a = -\gamma_1 = -\frac{1 + \mu\tau}{\tau c},$$

$$\gamma_{2,3}^a = \gamma_2, \bar{\gamma}_2, \qquad (C.157)$$

$$(C.158)$$

where

$$\gamma_2 = \frac{c + \sqrt{c^2 + 4\mu}}{2}, \qquad (C.159)$$

$$\bar{\gamma}_2 = \frac{c - \sqrt{c^2 + 4\mu}}{2}. \qquad (C.160)$$

Eigenvectors for case $i = a$:

The eigenvector corresponding to $\gamma_1^a = -\gamma_1 = -\dfrac{1 + \mu\tau}{\tau c}$ is derived as follow

$$\begin{pmatrix} -\gamma_1 & -1 & 0 \\ -\mu & -(\gamma_1 + c) & 0 \\ -1/c & 0 & 0 \end{pmatrix} \begin{pmatrix} w_{11}^a \\ w_{21}^a \\ w_{31}^a \end{pmatrix} = \begin{pmatrix} 0 \\ 0 \\ 0 \end{pmatrix}, \qquad (C.161)$$

and from (C.161) and for some parameter k

$$w_{11}^a = 0, \quad \text{since} \quad c \neq 0 \quad w_{21}^a = 0, \text{ and } w_{31}^a = k, \qquad (C.162)$$

thus, the eigenvector for $k = 1$

$$\vec{w}_1^a = \begin{pmatrix} w_{11}^a \\ w_{21}^a \\ w_{31}^a \end{pmatrix} = \begin{pmatrix} 0 \\ 0 \\ 1 \end{pmatrix}. \qquad (C.163)$$

For $\gamma = \gamma_2$

$$\begin{pmatrix} \gamma_2 & -1 & 0 \\ -\mu & \gamma_2 - c & 0 \\ -1/c & 0 & \gamma_1 + \gamma_2 \end{pmatrix} \begin{pmatrix} w_{12}^a \\ w_{22}^a \\ w_{32}^a \end{pmatrix} = \begin{pmatrix} 0 \\ 0 \\ 0 \end{pmatrix}, \qquad (C.164)$$

and we get from (C.164) for some parameter k

$$w_{12}^a = k, \; w_{22}^a = \gamma_2\, k, \; (\text{since } \gamma_2(\gamma_2 - c) - \mu = 0)\,, w_{32}^a = \frac{k}{c\,(\gamma 1 + \gamma 2)}. \qquad \text{(C.165)}$$

Hence, the eigenvector is (for $k = 1$)

$$\vec{w}_2^a = \begin{pmatrix} w_{12}^a \\ w_{22}^a \\ w_{32}^a \end{pmatrix} = \begin{pmatrix} 1 \\ \gamma_2 \\ \gamma_3 \end{pmatrix}, \qquad \text{(C.166)}$$

where $\gamma_3 = \dfrac{1}{c\,(\gamma_1 + \gamma_2)}$.

Similarly, for $\gamma = \bar{\gamma}_2$, the eigenvector will then be

$$\vec{w}_3^a = \begin{pmatrix} w_{13}^a \\ w_{23}^a \\ w_{33}^a \end{pmatrix} = \begin{pmatrix} 1 \\ \bar{\gamma}_2 \\ \bar{\gamma}_3 \end{pmatrix}, \qquad \text{(C.167)}$$

where $\bar{\gamma}_3 = \dfrac{1}{c\,(\gamma_1 + \bar{\gamma}_2)}$.

For case $i = b$, $\xi \in (-\Delta, 0)$, and in this region, $\Theta(-\xi - \Delta) = 0$, $\delta(\xi + \Delta) = \delta(\xi) = 0$, $h_0 = e^{\xi/\tau c}$. Therefore, the matrix B in (C.155) then becomes

$$B^b = \begin{pmatrix} 0 & 1 & 0 \\ \mu & c & 0 \\ 0 & 0 & -\gamma_1 \end{pmatrix}, \qquad \text{(C.168)}$$

from which we get the *spatial* eigenvalues, $\gamma_1^b = -\gamma_1$, $\gamma_{2,3}^b = \gamma_2, \bar{\gamma}_2$.

Eigenvectors for case $i = b$:

The eigenvector corresponding to $\gamma_1^b = -\gamma_1$ is derived as follow

$$\begin{pmatrix} -\gamma_1 & -1 & 0 \\ -\mu & -(\gamma_1 + c) & 0 \\ 0 & 0 & 0 \end{pmatrix} \begin{pmatrix} w_{11}^b \\ w_{21}^b \\ w_{31}^b \end{pmatrix} = \begin{pmatrix} 0 \\ 0 \\ 0 \end{pmatrix}, \qquad \text{(C.169)}$$

which yields

$$-\gamma_1\, w_{11}^b - w_{21}^b = 0,$$
$$-\mu\, w_{11}^b - (\gamma_1 + c)\, w_{21}^b = 0, \qquad \text{(C.170)}$$

since $\gamma_1^2 + c\,\gamma_1 - \mu \neq 0$ then $w_{21}^b = 0$, $w_{11}^b = 0$ and $w_{31}^b = k$ for some parameter k. Thus, the eigenvector is, for $k = 1$

$$\vec{w}_1^b = \begin{pmatrix} w_{11}^b \\ w_{21}^b \\ w_{31}^b \end{pmatrix} = \begin{pmatrix} 0 \\ 0 \\ 1 \end{pmatrix}. \qquad \text{(C.171)}$$

For $\gamma_2^b = \gamma_2$

$$
\begin{pmatrix}
\gamma_2 & -1 & 0 \\
-\mu & \gamma_2 - c & 0 \\
0 & 0 & \gamma_1 + \gamma_2
\end{pmatrix}
\begin{pmatrix}
w_{12}^b \\
w_{22}^b \\
w_{32}^b
\end{pmatrix}
=
\begin{pmatrix}
0 \\
0 \\
0
\end{pmatrix},
\tag{C.172}
$$

and then from (C.172) for some parameter k

$$
w_{12}^b = k, \; w_{22}^b = \gamma_2 \, k \; (\text{ since } \gamma_2^2 - c\gamma_2 - \mu = 0), w_{32}^b = 0 \; (\; \gamma_1 + \gamma_2 \neq 0). \tag{C.173}
$$

Therefore, the eigenvector for $k = 1$ is

$$
\vec{w}_2^{\,b} =
\begin{pmatrix}
w_{12}^b \\
w_{22}^b \\
w_{32}^b
\end{pmatrix}
=
\begin{pmatrix}
1 \\
\gamma_2 \\
0
\end{pmatrix}.
\tag{C.174}
$$

Similarly, for $\gamma_3^b = \bar{\gamma}_2$, the eigenvector will then be

$$
\vec{w}_3^{\,b} =
\begin{pmatrix}
1 \\
\bar{\gamma}_2 \\
0
\end{pmatrix}.
\tag{C.175}
$$

For region (i.e. case $i = c$) three, the matrix is exactly the same as that one in (C.168), that is case $i = b$, and so has the eigenvectors

$$
\vec{w}_1^{\,c} =
\begin{pmatrix}
w_{11}^c \\
w_{21}^c \\
w_{31}^c
\end{pmatrix}
=
\begin{pmatrix}
0 \\
0 \\
1
\end{pmatrix}, \;
\vec{w}_2^{\,c} =
\begin{pmatrix}
w_{12}^c \\
w_{22}^c \\
w_{32}^c
\end{pmatrix}
=
\begin{pmatrix}
1 \\
\gamma_2 \\
0
\end{pmatrix}, \;
\vec{w}_2^{\,c} =
\begin{pmatrix}
w_{13}^c \\
w_{23}^c \\
w_{33}^c
\end{pmatrix}
=
\begin{pmatrix}
1 \\
\bar{\gamma}_2 \\
0
\end{pmatrix}. \tag{C.176}
$$

C.3.4 Characteristic equation for the adjoint problem

To determine the characteristic equation, we rewrite the solutions to (C.154) taking into account each of the three regions. The solutions are written as

$$
\begin{pmatrix}
\phi_i^* \\
\eta_i^* \\
\psi_i^*
\end{pmatrix}
= \sum_j i_j \, \vec{w}_j^{\,i} \, \mathrm{e}^{\gamma_j^i \xi},
\tag{C.177}
$$

and is such that $B^i \, \vec{w}_j^{\,i} = \gamma_j^i \, \vec{w}_j^{\,i}$, where $B^i = B^i(\mu)$, $\gamma_j^i = \gamma_j^i(\mu)$ for $i = a, b, c$ and $j = 1, 2, 3$.

   NB: The solutions for the three cases can be written explicitly as

$$
\begin{pmatrix}
\phi_a^* \\
\eta_a^* \\
\psi_a^*
\end{pmatrix}
= a_1^* \, \vec{w}_1^{\,a} \, \mathrm{e}^{-\gamma_1 \xi} + a_2^* \, \vec{w}_2^{\,a} \, \mathrm{e}^{\gamma_2 \xi} + a_3^* \, \vec{w}_3^{\,a} \, \mathrm{e}^{\bar{\gamma}_2 \xi},
\tag{C.178}
$$

$$
\begin{pmatrix} \phi_b^* \\ \eta_b^* \\ \psi_b^* \end{pmatrix} = b_1^* \, \vec{w}_1^{\,b} \, \mathrm{e}^{-\gamma_1 \, \xi} + b_2^* \, \vec{w}_2^{\,b} \, \mathrm{e}^{\gamma_2 \, \xi} + b_3^* \, \vec{w}_3^{\,b} \, \mathrm{e}^{\bar{\gamma}_2 \, \xi}, \tag{C.179}
$$

$$
\begin{pmatrix} \phi_c^* \\ \eta_c^* \\ \psi_c^* \end{pmatrix} = c_1^* \, \vec{w}_1^{\,c} \, \mathrm{e}^{-\gamma_1 \, \xi} + c_2^* \, \vec{w}_2^{\,c} \, \mathrm{e}^{\gamma_2 \, \xi} + c_3^* \, \vec{w}_3^{\,c} \, \mathrm{e}^{\bar{\gamma}_2 \, \xi}, \tag{C.180}
$$

where $\gamma_1 = \dfrac{1 + \mu\,\tau}{\tau\,c}$, $\gamma_2 = \dfrac{c + \sqrt{c^2 + 4\,\mu}}{2}$, $\bar{\gamma}_2 = \dfrac{c - \sqrt{c^2 + 4\,\mu}}{2}$.

And $\vec{w}_1^{\,a}, \vec{w}_2^{\,a}, \vec{w}_3^{\,a}$; $\vec{w}_1^{\,b}, \vec{w}_2^{\,b}, \vec{w}_3^{\,b}$; $\vec{w}_1^{\,c}, \vec{w}_2^{\,c}, \vec{w}_3^{\,c}$ as given in equations (C.163), (C.166), (C.167), (C.171), (C.174), (C.175), and (C.176)

Determination of the constants (i_j): To determine the constants $i_j : i = a,\ b,\ c;\ j = 1,\ 2,\ 3$, the solutions (C.178), (C.179) and (C.180) has to satisfy both the boundaries at $\pm\infty$ (i.e., $\xi \to \pm\infty$) and at the internal boundaries $\xi = -\Delta$ and $\xi = 0$.

Boundary conditions at $\pm\infty$: With $\mu \geq 0 : \gamma_1 > 0$, $\gamma_2 > 0$, $\bar{\gamma}_2 < 0$, then for the case $i = a$:

$$
\lim_{\xi \to -\infty} \begin{pmatrix} \phi_a^* \\ \eta_a^* \\ \psi_a^* \end{pmatrix}, \tag{C.181}
$$

must be bounded and therefore $a_1^* = 0$ and $a_3^* = 0$. Therefore,

$$
\begin{pmatrix} \phi_a^* \\ \eta_a^* \\ \psi_a^* \end{pmatrix} = a_2^* \begin{pmatrix} 1 \\ \gamma_2 \\ \gamma_3 \end{pmatrix} \mathrm{e}^{\gamma_2 \, \xi}. \tag{C.182}
$$

For the case $i = b$, only the internal boundary conditions are considered, and so the solution (for the time being) is

$$
\begin{pmatrix} \phi_b^* \\ \eta_b^* \\ \psi_b^* \end{pmatrix} = b_1^* \begin{pmatrix} 0 \\ 0 \\ 1 \end{pmatrix} \mathrm{e}^{-\gamma_1 \, \xi} + b_2^* \begin{pmatrix} 1 \\ \gamma_2 \\ 0 \end{pmatrix} \mathrm{e}^{\gamma_2 \, \xi} + b_3^* \begin{pmatrix} 1 \\ \bar{\gamma}_2 \\ 0 \end{pmatrix} \mathrm{e}^{\bar{\gamma}_2 \, \xi}. \tag{C.183}
$$

For the case $i = c$:

$$
\lim_{\xi \to +\infty} \begin{pmatrix} \phi_c^* \\ \eta_c^* \\ \psi_c^* \end{pmatrix}, \tag{C.184}
$$

143

must be bounded and so therefore $c_2^* = 0$, therefore,

$$\begin{pmatrix} \phi_c^* \\ \eta_c^* \\ \psi_c^* \end{pmatrix} = c_1^* \begin{pmatrix} 0 \\ 0 \\ 1 \end{pmatrix} e^{-\gamma_1 \xi} + c_3^* \begin{pmatrix} 1 \\ \bar\gamma_2 \\ 0 \end{pmatrix} e^{\bar\gamma_2 \xi}. \tag{C.185}$$

Internal boundary conditions (IBCS): Let (C.154) be rewritten in terms of regular ($R1$) and singular ($S1$, $S2$) functions

$$\frac{\mathrm{d}\phi^*}{\mathrm{d}\xi} = \eta^*,$$

$$\frac{\mathrm{d}\eta^*}{\mathrm{d}\xi} = \overbrace{\mu\phi^* + c\,\eta^*}^{R1(\xi)} + \overbrace{\frac{1}{v_0'}\delta(\xi + \Delta)\,h_0\,\phi^*}^{S1(\xi)} - \overbrace{\frac{1}{\tau\,v_0'}\delta(\xi)\psi^*}^{S2(\xi)},$$

$$\frac{\mathrm{d}\psi^*}{\mathrm{d}\xi} = \frac{1}{c}\,\Theta(-\xi - \Delta)\,\phi^* - \frac{(1 + \mu\,\tau)}{\tau\,c}\,\psi^*. \tag{C.186}$$

IBCS at $\xi = -\Delta$: Integrating the second equation from (C.186) around $\xi = -\Delta$ over a small range, $(-\Delta - \varepsilon, -\Delta + \varepsilon)$ and consider limit $\varepsilon \to 0$

$$\lim_{\varepsilon \to 0} \int_{-\Delta-\varepsilon}^{-\Delta+\varepsilon} \frac{\mathrm{d}\eta^*}{\mathrm{d}\xi}\,\mathrm{d}\xi = \lim_{\varepsilon \to 0} \int_{-\Delta-\varepsilon}^{-\Delta+\varepsilon} R1(\xi)\,\mathrm{d}\xi + \lim_{\varepsilon \to 0} \int_{-\Delta-\varepsilon}^{-\Delta+\varepsilon} \delta(\xi + \Delta)\,\frac{h_0(\xi)\,\phi^*(\xi)}{v_0'(\xi)}\,\mathrm{d}\xi$$
$$- \lim_{\varepsilon \to 0} \int_{-\Delta-\varepsilon}^{-\Delta+\varepsilon} \delta(\xi)\frac{\psi^*(\xi)}{\tau\,v_0'(\xi)}\,\mathrm{d}\xi, \tag{C.187}$$

and its value is

$$\lim_{\varepsilon \to 0} \left[\eta_b^*(-\Delta + \varepsilon) - \eta_a^*(-\Delta - \varepsilon)\right] \leq \lim_{\varepsilon \to 0} M1\,\varepsilon + \lim_{\varepsilon \to 0} \frac{h_0(-\Delta)\,\phi^*(-\Delta)}{v_0'(-\Delta)}. \tag{C.188}$$

Hence, (C.188) reduces to

$$\eta_b^*(-\Delta) - \eta_a^*(-\Delta) = \frac{h_0(-\Delta)\,\phi^*(-\Delta)}{v_0'(-\Delta)}, \tag{C.189}$$

for some bounded function $M1$. But

$$\eta_b^*(-\Delta) - \eta_a^*(-\Delta) = -a_2^*\gamma_2\,e^{-\gamma_2\,\Delta} + b_2^*\gamma_2\,e^{-\gamma_2\,\Delta} + b_3^*\bar\gamma_2\,e^{-\bar\gamma_2\,\Delta}. \tag{C.190}$$

Meanwhile, from (C.82), (C.182)

$$h_0(-\Delta) = e^{-\Delta/(\tau\,c)},$$
$$v_0'(-\Delta) = -\alpha\,c\,e^{c\,\Delta},$$
$$\phi^*(-\Delta) = \phi_b^*(-\Delta) = b_2^*\,e^{-\gamma_2\,\Delta} + b_3^*\,e^{-\bar\gamma_2\,\Delta}, \tag{C.191}$$

144

thus,

$$\frac{h_0(-\Delta)\,\phi^*(-\Delta)}{v_0'(-\Delta)} = \frac{e^{-\gamma\Delta}(b_2^*\,e^{-\gamma_2\Delta} + b_3^*\,e^{-\bar{\gamma}_2\Delta})}{-\alpha\,c}, \tag{C.192}$$

where $\gamma = \dfrac{1 + \tau\,c^2}{\tau\,c}$. Hence, (C.189) becomes

$$a_2^*\,\alpha\,c\,\gamma_2\,e^{-\gamma_2\Delta} - b_2^*\,e^{-\gamma_2\Delta}\left(\alpha\,c\,\gamma_2 + e^{-\gamma\Delta}\right) - b_3^*\,e^{-\bar{\gamma}_2\Delta}\left(\alpha\,c\,\bar{\gamma}_2 + e^{-\gamma\Delta}\right) = 0. \tag{C.193}$$

The IBCS at $\xi = -\Delta$ for regular functions are derived using the continuity conditions

$$\lim_{\xi\to-\Delta-}\phi_a^* = \lim_{\xi\to-\Delta+}\phi_b^*,$$
$$\lim_{\xi\to-\Delta-}\psi_a^* = \lim_{\xi\to-\Delta+}\psi_b^*, \tag{C.194}$$

which respectively give

$$a_2^*\,e^{-\gamma_2\Delta} - b_2^*\,e^{-\gamma_2\Delta} - b_3^*\,e^{-\bar{\gamma}_2\Delta} = 0, \tag{C.195}$$

and

$$a_2^*\,\gamma_3\,e^{-\gamma_2\Delta} - b_1^*\,e^{\gamma_1\Delta} = 0, \tag{C.196}$$

where $\gamma_3 = \dfrac{1}{c\,(\gamma_1 + \gamma_2)}$.

IBCS at $\xi = 0$: In this case, we integrate the second from (C.186) around $\xi = 0$ over a small range, $(-\varepsilon, \varepsilon)$ and consider limit $\varepsilon \to 0$.

$$\lim_{\varepsilon\to0}\int_{-\varepsilon}^{\varepsilon}\frac{\mathrm{d}\eta^*}{\mathrm{d}\xi}\,\mathrm{d}\xi = \lim_{\varepsilon\to0}\int_{-\varepsilon}^{\varepsilon}R1(\xi)\,\mathrm{d}\xi + \lim_{\varepsilon\to0}\int_{-\varepsilon}^{\varepsilon}\delta(\xi+\Delta)\frac{h_0(\xi)\,\phi^*(\xi)}{v_0'(\xi)}\,\mathrm{d}\xi$$
$$- \lim_{\varepsilon\to0}\int_{-\varepsilon}^{\varepsilon}\delta(\xi)\frac{\psi^*(\xi)}{\tau\,v_0'(\xi)}\,\mathrm{d}\xi, \tag{C.197}$$

which evaluates to

$$\lim_{\varepsilon\to0}\left[\eta_c^*(\varepsilon) - \eta_b^*(-\varepsilon)\right] \le \lim_{\varepsilon\to0}M2\,\varepsilon - \lim_{\varepsilon\to0}\frac{\psi^*(\xi)}{\tau\,v_0'(\xi)}, \tag{C.198}$$

thus,

$$\eta_c^*(0) - \eta_b^*(0) = -\frac{\psi^*(0)}{\tau\,v_0'(0)}, \tag{C.199}$$

for some bounded function $M2$. Now from (C.185), we have

$$\eta_c^*(0) - \eta_b^*(0) = -b_2^*\,\gamma_2 - b_3^*\,\bar{\gamma}_2 + c_3^*\,\bar{\gamma}_2, \tag{C.200}$$

and from (C.82), (C.185)

$$v_0'(0) = -\alpha\,c,$$
$$\psi^*(0) = \psi_c^*(0) = c_1^*. \tag{C.201}$$

Hence, (C.189) becomes

$$b_2^*\,\alpha\,\tau\,c\,\gamma_2 + b_3^*\,\alpha\,\tau\,c\,\bar{\gamma}_2 + c_1^* - c_3^*\,\alpha\,\tau\,c\,\bar{\gamma}_2 = 0. \tag{C.202}$$

The IBCS at $\xi = 0$ for regular functions are also derived using the continuity conditions

$$\lim_{\xi \to 0-} \phi_b^* = \lim_{\xi \to 0+} \phi_c^*,$$
$$\lim_{\xi \to 0-} \psi_b^* = \lim_{\xi \to 0+} \psi_c^*,$$

(C.203)

which respectively yield

$$b_2^* + b_3^* - c_3^* = 0,$$

(C.204)

$$b_1^* - c_1^* = 0.$$

(C.205)

Thus, we have a system of six equations in terms of the undetermined arbitrary constants

$$a_2^* \alpha c \gamma_2 \, e^{-\gamma_2 \Delta} - b_2^* \, e^{-\gamma_2 \Delta} \left(\alpha c \gamma_2 + e^{-\gamma \Delta} \right) - b_3^* \, e^{-\bar{\gamma}_2 \Delta} \left(\alpha c \bar{\gamma}_2 + e^{-\gamma \Delta} \right) = 0,$$

$$a_2^* \, e^{-\gamma_2 \Delta} - b_2^* \, e^{-\gamma_2 \Delta} - b_3^* \, e^{-\bar{\gamma}_2 \Delta} = 0,$$

$$a_2^* \gamma_3 \, e^{-\gamma_2 \Delta} - b_1^* \, e^{\gamma_1 \Delta} = 0,$$

$$b_2^* \alpha \tau c \gamma_2 + b_3^* \alpha \tau c \bar{\gamma}_2 + c_1^* - c_3^* \alpha \tau c \bar{\gamma}_2 = 0,$$

$$b_2^* + b_3^* - c_3^* = 0,$$

$$b_1^* - c_1^* = 0. \quad \text{(C.206)}$$

The system in (C.206) can be written in matrix form with a six-by-six coefficient matrix whose determinant is given as

$$\begin{vmatrix} \alpha c \gamma_2 \, e^{-\gamma_2 \Delta} & 0 & -(\alpha c \gamma_2 + e^{-\gamma \Delta}) \, e^{-\gamma_2 \Delta} & -(\alpha c \bar{\gamma}_2 + e^{-\gamma \Delta}) \, e^{-\bar{\gamma}_2 \Delta} & 0 & 0 \\ e^{-\gamma_2 \Delta} & 0 & - e^{-\gamma_2 \Delta} & e^{-\bar{\gamma}_2 \Delta} & 0 & 0 \\ \gamma_3 \, e^{-\gamma_2 \Delta} & - e^{\gamma_1 \Delta} & 0 & 0 & 0 & 0 \\ 0 & 0 & \alpha \tau c \gamma_2 & \alpha \tau c \bar{\gamma}_2 & 1 & -\alpha \tau c \bar{\gamma}_2 \\ 0 & 0 & 1 & 1 & 0 & -1 \\ 0 & 1 & 0 & 0 & -1 & 0 \end{vmatrix}$$

$$= 0.$$

(C.207)

System (C.206), has non-trivial solutions only if the determinant of the coefficient matrix is zero. This lead to a characteristic equation $\left(f_e^*(\mu; c, \alpha, \tau) \right)$

$$f_e^* = \alpha c \left(\gamma_2 - \bar{\gamma}_2 \right) e^{\gamma \Delta} - 1 + \frac{1}{\tau c \left(\gamma_1 + \gamma_2 \right)} e^{-(\gamma_1 + \gamma_2 - \gamma) \Delta} = 0.$$

(C.208)

NB: Note that $\dfrac{1}{\tau\,c\,(\gamma_1 + \gamma_2)} \equiv \dfrac{\tau\,c(\gamma_1 + \bar\gamma_2)}{(1 + \mu\,\tau)^2 + \tau\,c^2}$. Hence,

$$f_e^* = \alpha\,c\,(\gamma_2 - \bar\gamma_2)\,\mathrm{e}^{\gamma\Delta} - 1 + \frac{\tau\,c\,(\gamma_1 + \bar\gamma_2)}{(1 + \mu\,\tau)^2 + \tau\,c^2}\,\mathrm{e}^{-(\gamma_1 + \gamma_2 - \gamma)\Delta} = 0, \qquad \text{(C.209)}$$

where

$$\gamma = \frac{1 + \tau\,c^2}{\tau\,c}, \qquad\qquad \gamma_1 = \frac{1 + \mu\,\tau}{\tau\,c},$$

$$\gamma_2 = \frac{c + \sqrt{c^2 + 4\,\mu}}{2}, \qquad\qquad \bar\gamma_2 = \frac{c - \sqrt{c^2 + 4\,\mu}}{2},$$

$$\Delta = \frac{1}{c}\ln\left(\frac{1 + \alpha}{\alpha}\right). \qquad\qquad\qquad\qquad\qquad\qquad \text{(C.210)}$$

Bibliography

[1] R. R. Aliev and A. V. Panfilov. A simple two-variable model of cardiac excitation. *Chaos, Solitons and Fractals*, 7(3):293–301, 1996.

[2] M. Argentina and P. Coullet. Colliding waves in a model excitable medium: Preservation, annihilation, and bifurcation. *Phys. Rev. Lett.*, 79(15):2803–2806, 1997.

[3] M. Argentina, P. Coullet, and V. Krinsky. Head-on-collisions of waves in an excitable FitzHugh-Nagumo system: a transition from wave annihilation to classical wave behavior. *J. Theor. Biol.*, 205:47–52, 2000.

[4] O. V. Aslanidi and O. A. Mornev. Soliton-like regimes and excitation pulse reflection (Echo) in homogeneous cardiac purkinje fibres: Results of numerical simulations. *J. Biol. Phys.*, 25:149–164, 1999.

[5] D. Barkley. A model for fast computer simulation of waves in excitable media. *Physica D.*, 49:61–70, 1991.

[6] R. D. Benguria and M. C. Depassier. Speed of fronts of the reaction-diffusion equation. *Phys. Rev. Lett*, 77(6):1171–1173, 1996.

[7] O. Bernus, R. Wilders, C. W. Zemlin, H. Verschelde, and A. V. Panfilov. A computationally efficient electrophysiological model of human ventricular cells. *Am. J. Physiol. Heart. Circ Physiol.*, 282(6):H2296–H2308, 2002.

[8] V. N. Biktashev. Dissipation of the excitation wavefronts. *Phys. Rev. Lett.*, 89(16):168102–1 – 168102–4, 2002.

[9] V. N. Biktashev. A simplified model of propagation and dissipation of excitation fronts. *Int. J. of Birfucation and Chaos*, 13(12):3605–3619, 2003.

[10] V. N. Biktashev and I. V. Biktasheva. *Dissipation of Excitation Fronts as a Mechanism of Conduction Block in Re-entrant Waves,*, volume 3504 of *Lecture Notes in Computer Science*, pages 283–292. Springer Berlin/Heidelberg, 2005.

[11] V. N. Biktashev and A. V. Holden. Deterministic Brownian motion in the hypermeander of spiral waves. *Physica D.*, 116(3–4):342–354, 1998.

[12] I. V. Biktasheva, R. D. Simitev, R. S. Suckley, and V. N. Biktashev. Asymptotic properties of mathematical models of excitability. *Phil. Trans. Roy. Soc. A.*, 364(1842):1283–1298, 2006.

[13] M. A. Biot. *Variational principles in heat transfer.* Oxford University Press, 1970.

[14] G. Bordyugov. *Dynamics and Stability of Pulses and Pulse Trains in Excitable Media.* PhD thesis, Technical University Berlin, Germany, 2006.

[15] T. Bountis, C. F. Starmer, and A. Bezerianos. Stationary pulses and wave front formation in an excitable medium. *Progr. Theor. Phys. Suppl.*, 139:12–33, 2000.

[16] W. E. Boyce and R. C. Diprima. *Elementary differential equations and boundary value problems.* John Wiley & Sons, Inc., eigth edition, 2005.

[17] M. Braun. *Differential equations and their applications.* Springer-Verlag New York, Inc., fourth edition, 1993.

[18] J. Brindley, V. N. Biktashev, and M. A. Tsyganov. Invasion waves in populations with excitable dynamics. *Biol. Invasions.*, 7:807816, 2005.

[19] N. F. Britton. Threshold phenomena and solitary traveling waves in a class of reaction-diffusion systems. *SIAM J. Appl. Math.*, 42(1):188–217, 1982.

[20] N. F. Britton. *Essential Mathematical Biology.* Springer Verlag London, first edition, 2003.

[21] K. J. Brown and A. A. Lacey. *Reaction-Diffusion Equations.* Oxford Science Publications, 1990.

[22] G. Cain and G. H. Meyer. *Separation of Variables for Partial Differential Equations: An Eigenfunction Approach.* Chapman & Hall/CRC, 2006.

[23] R. G. Casten, H. Cohen, and P. A. Lagerstrom. Perturbation analysis of an approximation to the Hodgkin-Huxley theory. *Quart. Appl. Math.*, 32(4):365–402, 1975.

[24] J. W. Cooley and F. A. Dodge Jr. Digital computer solutions for excitation and propagation of the nerve impulse. *Biophys. J.*, 6:583–599, 1966.

[25] M. Courtemanche, R. Ramirez, and S. Nattel. Ionic mechanisms underlying human atrial action potential properties: Insights from a mathematical model. *Am. J. Physiol. Heart. Circ Physiol*, 275:H301–H321, 1998.

[26] M. C. Cross and P. C. Hohenberg. Pattern formation outside of equilibrium. *Rev. Mod. Phys.*, 65:852–1086, 1993.

[27] P. C. Dauby, Th. Desaive, H. Croisier, and Ph. Kolh. Standing waves in FitzHugh-Nagumo model of cardiac electrical activity. *Phys. Rev. E.*, 73:021908 [1–5], 2006.

[28] J. D. Dockery. Existence of standing pulse solutions for an excitable activator-inhibitory system. *J. Dynam. Diff. Eqtns.*, 4(2):231–257, 1992.

[29] G. Duckett and D. Barkley. Modelling the dynamics of cardiac action potential. *Phys. Rev. Lett.*, 85(4):884–887, 2000.

[30] L. Edelstein-Keshet. *Mathematical models in biology.* SIAM, 2005.

[31] I. Farkas, D. Helbing, and T. Vicsek. Social behaviour: Mexican waves in an excitable media. *Nature*, 419:131–132, 2002.

[32] F. Fenton and A. Karma. Vortex dynamics in three-dimensional continuous myocardium with fiber rotation: Filament instability and fibrillation. *Chaos*, 8(1):20–47, 1998.

[33] R. A. FitzHugh. Impulses and physiological states in theoritical models of nerve membrane. *Biophys. J.*, 1:445–466, 1961.

[34] G. Flores. The stable manifold of the standing wave of the Nagumo equation. *J. Differential Equations*, 80:306–314, 1989.

[35] G. Flores. Stability analysis for the slow traveling pulse of the FitzHugh-Nagumo system. *SIAM J. Math. Anal.*, 22(2):392–399, 1991.

[36] C. J. A. Game. BVP models: An adjustment to express a mechanism of inactivation. *Biol. Cybern*, 44:223–229, 1982.

[37] G. A. Gottwald and L. Kramer. On propagation failure in one- and two-dimensional excitabe media. *Chaos.*, 14(3):855–863, 2004.

[38] I. S. Gradshteyn and I. M. Rhyzhik. *Tables of integrals, series, and products.* Academic Press, sixth edition, 2000.

[39] M. W. Green and B. D. Sleeman. On FitzHugh's nerve axon equations. *J. Math. Biol.*, 1:153–163, 1974.

[40] R. Habermann. *Elementary applied partial differential equations with Fourier series and boundary value problems.* Prentice-Hall, Inc., second edition, 1987.

[41] A. Hagberg and E. Meron. Pattern formation in non-gradient reaction-diffusion systems: the effects of bifurcations. *Nonlin.*, 7:805–835, 1994.

[42] R. Hinch. An analytical study of the physiology and pathology of the propagation of cardiac action potentials. *Progr. Biophys. Mol. Biol.*, 78:45–81, 2002.

[43] R. Hinch. Stability of cardiac waves. *Bulletin of Math. Biol.*, 66:1887–1908, 2004.

[44] A. L. Hodgkin and A. F. Huxley. A quantitative description of membrane current and its application to conduction and excitation in nerve. *J. Physiol.*, 117:500–544, 1952.

[45] I. Idris and V. N. Biktashev. Critical fronts in initiation of excitation waves. *Phys. Rev. E.*, 76(2):021906–1 – 021906–6, 2007.

[46] I. Idris, R. D. Simitev, and V. N. Biktashev. Using novel simplified models of excitation for analytic description of initiation propagation and blockage of excitation waves. In *IEEE Computers in Cardiology*, volume 33, pages 213–217, Valencia, Spain, 2006.

[47] C. K. R. T. Jones. Stability of the travelling wave solution of the FitzHugh-Nagumo system. *Trans. Amer. Math. Soc.*, 286(2):431–469, 1984.

[48] H. R. Karfunkel and F. F. Seelig. Excitable chemical reaction systems I. Definition of excitability and simulation of model systems. *J. Math. Biol.*, 2:123–132, 1975.

[49] J. P. Keener and J. Sneyd. *Mathematical Physiology*. Springer-Verlag, 1998.

[50] B. I. Khaikin and A. G. Merzhanov. Theory of thermal propagation of a chemical reaction front. *Fizika Goreniya I Vzryva*, 2:36–46, 1966.

[51] B. Krauskopf, H. M. Osinga, E. J. Doedel, M. E. Henderson, J. Guckenheimer, A. Vladimirsky, M. Dellnitz, and O. Junge. A survey of methods for computing (un)stable manifolds of vector fields. *Int. J. Birfuc. and Chaos*, 15:763–791, 2005.

[52] V. Krinsky and H. Swinney (eds). *Waves and patterns in biological and chemical excitable media*. North-Holland, Amsterdam, 1991.

[53] M. Krupa, B. Sandstede, and P. Szmolyan. Fast and slow waves in the FitzHugh-Nagumo equation. *J. Diff. Eqtns.*, 133:49–97, 1997.

[54] Y. A. Kuznetsov. *Elements of applied birfucation theory*, volume 112 of *Applied Mathematical Sciences*. Springer-Verlag New York, Inc, 1995.

[55] B. M. Levitan and I. S. Sargsjan. *Introduction to spectral theory: Selfadjoint ordinary differential operators*, volume 39 of *Translations of Mathematical monographs*. American Mathematical Society, 1975.

[56] K. Maginu. Stability of periodic travelling wave solutions of a nerve conduction equation. *J. Math. Biol.*, 6:49–57, 1978.

[57] K. Maginu. Existence and stability of periodic travelling wave solutions to Nagumo's nerve equation. *J. Math. Biol.*, 10:133–153, 1980.

[58] H. P. McKean. Nagumo's equation. *Adv. Appl. Math.*, 4:209–223, 1970.

[59] E. Meron. Pattern formation in excitable media. *Phys. Reports*, 218(1):1–66, 1992.

[60] E. Meron and P. Pelce. Model of spiral wave formation in excitable media. *Phys. Rev. Lett.*, 60(18):1880–1883, 1988.

[61] A. S. Mikhailov and V. I. Krinsky. Rotating spiral waves in excitable media: The analytical results. *Physica D.*, 9:346–371, 1983.

[62] V. Moll and S. I. Rosencrans. Calculation of the threshold surface for nerve equations. *SIAM J. Appl. Math.*, 50(5):14191441, 1990.

[63] M. R. Monica and C. K. R. T. Jones. Stability of neuron pulses composed of concatenated unstable kinks. *Phys. Rev. E.*, 63:011904[1–4], 2000.

[64] O. A. Mornev. Modification of the Biot method on the basis of the principle of minimum dissipation (with an application to the problem of propagation of nonlinear concentration waves in an autocatalytic medium). *Russian Journal of Physical Chemistry*, 72:112–118, 1998.

[65] J. D. Murray. *Mathematical Biology I: An Introduction*, volume 1. Springer-Verlag, third edition, 2002.

[66] J. D. Murray. *Mathematical Biology II: Spatial Models and Biomedical Applications*, volume 2. Springer Verlag Berlin/Heidelberg, third edition, 2003.

[67] J. Nagumo, S. Arimoto, and S. Yoshizawa. An active pulse transmission line simulating nerve axon. *Proc. IRE*, 50:2061–2070, 1962.

[68] J. C. Neu, R. S. Pressig, and W. Krassowska. Initiation of propagation in a one-dimensional excitable medium. *Physica D.*, 102:285–299, 1997.

[69] G. Nicolis and A. De Wit. Reaction-diffusion systems. http://www.scholarpedia.org/article/Reaction-diffusion_systems.

[70] D. Noble. A modification of the Hodgkin-Huxley equations applicable to Purkinje fibre action potential and pace-maker potentials. *J. Physiol.*, 160:317–352, 1962.

[71] D. Noble. The relations of Rushton's 'liminal length' for exciation to the resting and active conductances of excitable cells. *J. Physiol.*, 226(2):573–591, 1972.

[72] D. Noble. From the Hodgkin-Huxley axon to the virtual heart. *J. Physiol.*, 580(1):15–22, 2007.

[73] L. Perko. *Differential equations and dynamical systrems*. Number 7 in Text in applied Mathematics. Springer-Verlag New York, Inc., 1991.

[74] P. E. Phillipson and P. Schuster. A comparative study of the Hodgkin-Huxley and FitzHugh-Nagumo models of neuron pulse propagation. *Int. J. of Birf. and Chaos*, 15(12):3851–3866, 2005.

[75] Y. Pinchover and J. Rubinstein. *An introduction to partial differential equations*. Cambridge University Press, first edition, 2005.

[76] A. Pumir, A. Aruntunyan, V. Krinsky, and N. Sarvazyn. Genesis of ectopic waves: Role of coupling, automaticity, and heterogeneity. *Biophys. J.*, 89(4):2332–2349, 2005.

[77] D. Smitev Radostin and V. N. Biktashev. Conductions for propagation and block of excitation in an asymptotic model of atrial tissue. *Biophys. J.*, 90:2258–2269, 2006.

[78] RDEwiki. Reaction-diffusion system.
http://en.wikipedia.org/wiki/Reaction-diffusion_equation.

[79] J. Rinzel. Spatial stability of travelling wave solutions of a nerve conduction equation. *Biophys. J.*, 15:975–988, 1975.

[80] J. Rinzel and J. B. Keller. Traveling waves solutions of a nerve conduction equation. *Biophys. J.*, 13:1313–1337, 1973.

[81] W. A. H. Rushton. Initiation of the propagated disturbance. *Proc. R. Soc. B*, 124:210–243, 1937.

[82] B. Sandstede. *Stability of traveling waves*, volume 2, pages 983–1055. North-Holland, Amsterdam, 2002.

[83] L. I. Schiff. *Quantum Mechanics*. International series in pure and applied Physics. McGraw-Hill Book company, Inc, 2nd edition, 1955.

[84] A. C. Scott. The electrophysics of a nerve fiber. *Rev. Modern Phys.*, 47(2):487–535, 1975.

[85] V. Y. Sidorov, R. R. Aliev, M. C. Woods, F. Baudenbacher, P. Baudenbacher, and J. P. Wikswo. Spatiotemporal dynamics of damped propagation in excitable cardiac tissue. *Phys. Rev. Lett.*, 91(20):208104 [1–4], 2003.

[86] R. Simitev and V. N. Biktashev. *An Analytically Solvable Asymptotic Model of Atrial Excitability, in "Mathematical Modeling of Biological Systems"*, volume 2, chapter 5, pages 289–302. Birkhauster Boston, 2008.

[87] C. F. Starmer. Initiation of excitation waves.
`http://www.scholarpedia.org/article/Initiation_of_excitation_waves`.

[88] C. F. Starmer, V. N. Biktashev, D. N. Romashko, M. R. Stephanov, O. N. Makarova, and V. I. Krinsky. Vulnerability in excitable medium: Analytical and numerical studies of initiating unidirectional propagation. *Biophys. J.*, 65:1775–1787, 1993.

[89] C. F. Starmer, T. J. Colastky, and A. O. Grant. What happens when cardiac Na channels lose their function? 1-numerical studies of the vulnerable period in tissue expressing mutant channels. *Cardi-vasc. Res.*, 57:82–91, 2003.

[90] J. M. Starobin and C. F. Starmer. Boundary-layer analysis of waves propagating in an excitable medium: Medium conditions for wave-front-obstacle separation. *Phys. Rev. E.*, 54(1):430–437, 1996.

[91] J. M. Starobin, Y. I. Zilberter, and C. F. Starmer. Vulnerability in one-dimensional excitable media. *Physica D.*, 70:321–341, 1994.

[92] J. F. Stein and C. J. Stoodley. *Neuroscience: An introduction.* John Wiley & Sons Ltd, 2006.

[93] J. E. Trustcott and J. Brindley. Ocean plankton populations as excitable media. *Bull. Maths. Bios.*, 56(5):981–998, 1994.

[94] J. J. Tyson and J. P. Keener. Singular perturbation theory of traveling waves in excitable media (a review). *Physica D.*, 32:327–361, 1988.

[95] S. Wiggins. *Introduction to applied nonlinear dynamical systems and chaos*, volume 2 of *Texts in applied Mathematics.* Springer-Verlag New York, Inc., 1990.

[96] A. T. Winfree. Varieties of spirals wave behaviour: An experimentalist's approach to the theory of excitable media. *Chaos*, 1(3):303–334, 1991.

[97] J. Xian. Front propagation in heterogenous media. *SIAM REV.*, 42(2):161–230, 2000.

[98] E. Yanagida and K. Maginu. Stability of double-pulse solutions in nerve axon equations. *SIAM J. Appl. Math.*, 49(4):1158–1173, 1989.

[99] Y.B. Zel'dovich and D. A. Frank-Kamenetskii. On the theory of of uniform flame propagation. *Doklady AN SSSR*, 19:693–697, 1938.

[100] E. P. Zemskov, V. S. Zykov, K. Kassner, and S. C. Muller. Stability of travelling fronts in a piecewise-linear reaction-diffusion system. *Nonlin.*, 13(6):2063–2076, 2000.

[101] D. P. Zipes and J. Jalife. *Cardiac electrophysiology: From cell to bedside.* W B Saunders Co, 2000.

[102] V. S. Zykov. Excitable media. http://www.scholarpedia.org/article/Excitable_media.

[103] V. S. Zykov and A. T. Winfree. *Simulation of wave processes in excitable media.* Manchester University Press and New York, 1992.